# *CATALYTIC ASYMMETRIC BORYLATION OF α,β-UNSATURATED IMINES: A ROUTE TO γ-AMINO ALCOHOLS*

CALOW, ADAM,DANIEL,JAMES

# CATALYTIC ASYMMETRIC BORYLATION OF α,β-UNSATURATED IMINES: A ROUTE TO γ-AMINO ALCOHOLS

---

*A thesis submitted in partial fulfilment of the requirements*

*for the degree of*

**DOCTOR OF PHILOSOPHY**

*At the Department of Chemistry, Durham University, UK*

*Submitted by*

**Adam D. J. Calow**

*Under the supervision of*

**Professor Andrew Whiting**

*Supported by* **EPSRC**

**2015**

## Declaration

The work described in this thesis was carried out in the Department of Chemistry at Durham University (UK) between October 2011 and Janruary 2015, under the supervision of Prof. Andy Whiting. Research was conducted at the Universitat Rovira i Virgili for three months in 2012 (September-December) and one month in 2013 (July), under the supervision of Prof. M. Elena Fernández. The material contained has not been previously submitted for a degree at this or any other university. The research reported within this thesis has been conducted by the author unless indicated otherwise.

## Statement of copyright



Adam Daniel James Calow

**2015**

## Abstract

This thesis describes the asymmetric synthesis of γ-amino alcohols through the asymmetric copper-catalysed β-boration of α,β-unsaturated imines (see graphical abstract).

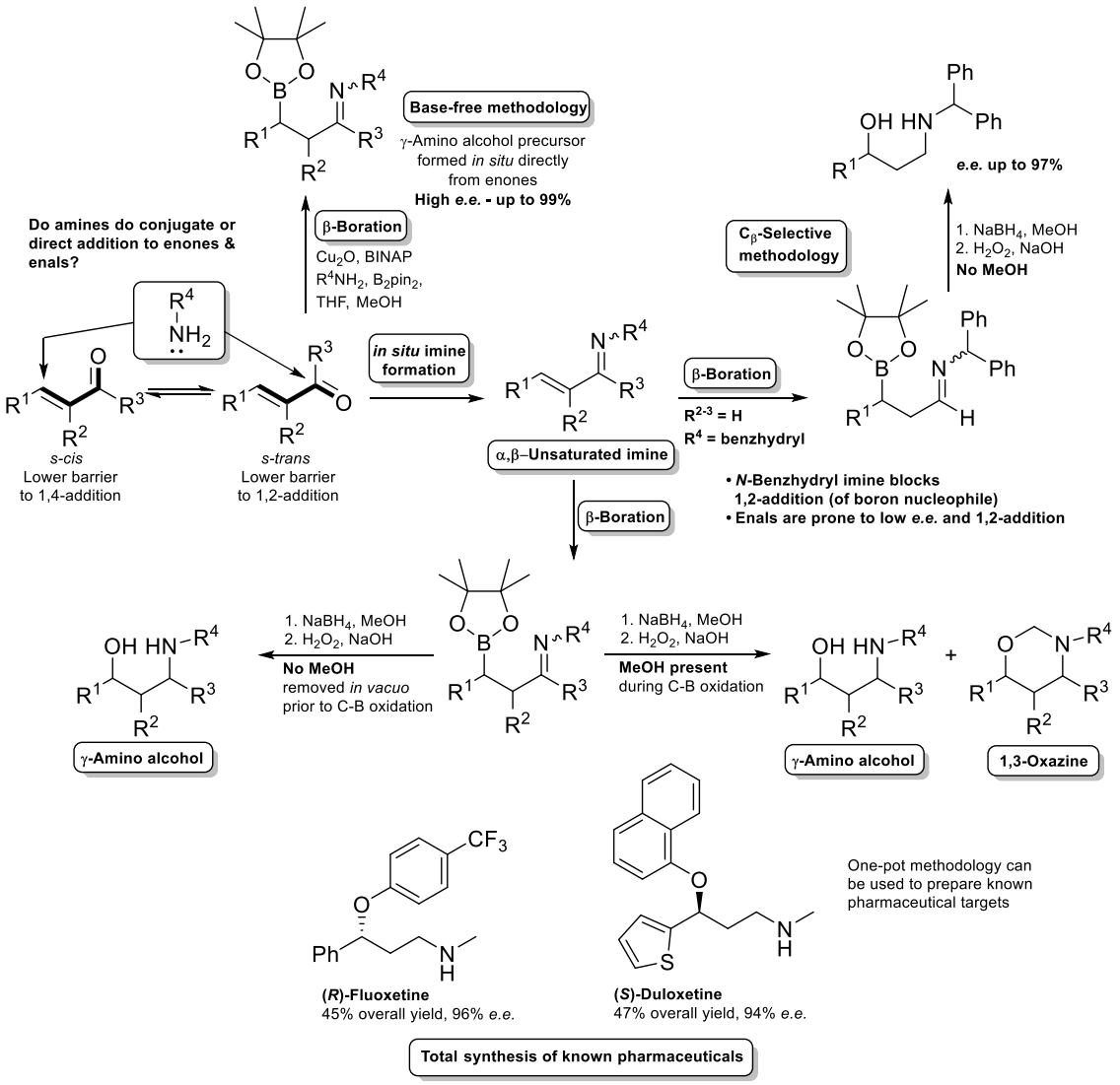


An introduction is given into the area of β-boration/borylation (or boron conjugate addition, BCA) of electron-deficient alkenes, which forms the basis of the literature review within this thesis.

The β-boration of α,β-unsaturated imines (formed *in situ* to circumvent problems with isolation) has been studied and the intermediate β-boryl imines have been

transformed to γ-amino alcohols in one-pot ('one-pot methodology'). An interesting side reaction was observed when methanol was present during the final oxidation step of the methodology. Indeed, evidence suggests that slight methanol oxidation gives rise to the formation of 1,3-oxazines (which can be made readily from γ-amino alcohols and aqueous formaldehyde) during this late stage oxidative step.

Additional *in situ* IR spectroscopy (ReactIR), $^{1}$H NMR and DFT studies were performed to understand the factors which govern direct addition-elimination *vs.* conjugate addition of primary amines to enones and enals, with the aim of using this information to prepare α,β-unsaturated imines *in situ*. It was found that most enones and enals have a kinetic preference towards the direct addition of primary amines, but enones such as methyl vinyl ketone show that the kinetic preference is towards conjugate addition. DFT calculations support this observation by showing that there is a conformational effect which favours direct- over conjugate-addition, *i.e.* enones and enals that adopt the *s-trans* conformation show a lower energy barrier of addition (kinetic preference) *via* the direct addition pathway with primary amines. Conversely, enones and enals that adopt the *s-cis* conformation show a lower energy barrier of addition (kinetic preference) *via* the conjugate addition pathway with primary amines (*i.e.* methyl vinyl ketone predominately adopts an *s-cis* conformation).

A base-free (alkoxide) β-boration methodology was developed, which allows enones to be transformed to γ-amino alcohol by the addition of a primary amine, $Cu_2O$, BINAP ligand, $B_2pin_2$ and MeOH to the starting enone, with subsequent reductive and oxidative transformations. Evidence suggests that the reaction proceeds *via* the α,β-unsaturated imine (formed *in situ*) and, in addition, the absence of the alkoxide base reduces the possibility of any alternative β-boration pathways (*e.g.* organocatalytic), leading to the highly enantioselective protocol (up to 99% *e.e.*).

Enals are prone to direct borylation under the standard β-boration-*type* methodology and low *e.e.* values. It is shown herein that the use of a sterically bulky *N*-benzyl imine auxiliary can be used (formed from the reaction between an enal and benzhydrylamine) to favour selective β-boration and, indeed, high *e.e.* can be obtained using a relatively cheap and stable DM-BINAP ligand-copper catalyst system (up to 97% *e.e.*).

The optimised one-pot methodology was applied towards the total synthesis of (*R*)-Fluoxetine in 45% yield (96% *e.e.*) and (*S*)-Duloxetine in 47% yield (94% *e.e.*), whereby the intermediate β-boryl *N*-benzhydryl imine can be readily exchanged by methylamine to form the appropriate precursor.

# Contents

## Publication list

Peer-reviewed publications produced from this thesis:

1. **Total synthesis of Fluoxetine & Duloxetine through an *in situ* imine formation/borylation/transimination and reduction approach.** A. D. J. Calow, E. Fernández and A. Whiting, *Org. Biomol. Chem*., 2014, **12**, 6121-6127.
2. **Understanding α,β-Unsaturated Imine Formation from Amine Additions to α,β-Unsaturated Aldehydes and Ketones – An Analytical and Theoretical Investigation.** A. D. J. Calow, J. J. Carbó, J. Cid, E. Fernández and A. Whiting, *J. Org. Chem.*, 2014, **11**, 5163-5172.
3. **A Selective Transformation of Enals into Chiral γ-Amino Alcohols.** A. D. J. Calow, A. Batsanov, A. Pujol, C. Solé, E. Fernández and A. Whiting, *Org. Lett.*, 2013, **15**, 4810-4813 (**Highlighted in Synfacts, see:** *Synfacts.*, 2013, **9**, 1306).
4. **Base-Free β-Boration of α,β-Unsaturated Imines Catalysed by $Cu_2O$ with Concurrent Enhancement of Asymmetric Induction.** A. D. J. Calow, C. Solé, A. Whiting and E. Fernández, *ChemCatChem*, 2013, **5**, 2233-2239.
5. **Novel transformation of α,β-unsaturated aldehydes and ketones into γ-amino alcohols or 1,3-oxazines *via* a 4 or 5 step, one-pot sequence.** A. D. J. Calow, A. S. Batsanov, E. Fernández, C. Solé and A. Whiting, *Chem. Commun.*, 2012, **48**, 11401-11403.
6. **Catalytic methodologies for the β-boration of conjugated electron deficient alkenes.** A. D. J. Calow and A. Whiting, *Org. Biomol. Chem*., 2012, **10**, 5485-5497.

## Acknowledgements

I would first like to thank Prof. Andy Whiting for giving me the opportunity to work on this project and for his unwavering support throughout. Secondly, many thanks to Prof. Elena Fernández for her enthusiasm and support during the time I spent in her laboratory (Rovira i Virgili).

Thanks go to Dr Cristina Solé and Alba Pujol Santiago for their help, dedication and for being great work colleagues in this fascinating project.

Many thanks to Dr Jessica Cid and Dr Jordi Carbó for providing the DFT calculations that accompanies the work on imine formation.

Praise must be given to the great support I have received from the services within the university. In particular the NMR, MS and crystallographic services which make research a pleasure within the department.

I would like to thank Lucas Vieira for his support, thought provoking criticism of this thesis and, in addition, highlighting my occasional use of questionable phraseology.

I would especially like to thank Jonathan Purdie for his keen-eyed proofreading of this thesis.

I would like to thank some of the members of the group, both past and present. In the order that I copied and pasted them from Andy's website, thanks must go to Dr Hayley Charville, Dr Irene Georgiou, Dr Ricardo Girling, Garr-Layy Zhou, Dr Duangduan "Nim" Chaiyaveij, Farhana Ferdousi, Hesham Raffat Shawky Haffez, Ludovic Eberlin, Enrico La Cascia, Katrina "Kate" Madden, David Chisholm, Sergey Arkhipenko and Alba Pujol (again), Dr Alexander Gehre, Dr Mona al Batal and last, but certainly not least, Dr Wade Leu.

Thanks must also go to my family for their continued support during my academic studies.

Lastly, I thank the EPSRC for funding this project and allowing me to explore many avenues of research throughout my PhD.

# Abbreviations

## Solvents

| | | |
|---|---|---|
| $CDCl_3$ | - | Deuterated chloroform |
| DCM | - | Dichloromethane |
| DMF | - | Dimethylformamide |
| DMA | - | Dimethylacetamide |
| DMSO | - | Dimethyl sulfoxide |
| $Et_2O$ | - | Diethyl ether |
| EtOAc | - | Ethyl acetate |
| THF | - | Tetrahydrofuran |

## Reagents

| | | |
|---|---|---|
| $B_2pin_2$ | - | 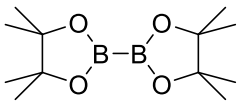 |
| $B_2neop_2$ | - | 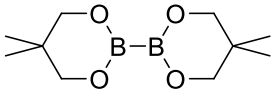 |
| $B_2cat_2$ | - | 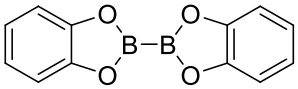 |

## Others

| | | |
|---|---|---|
| Å | - | Angstrom(s) |
| Hz | - | Hertz |
| *J* | - | Coupling constant – NMR |
| M.S. | - | Molecular sieve beads |
| m.p. | - | Melting point |
| MS | - | Mass spectrometry |
| M+ | - | Parent molecular ion |
| ASAP | - | Atmospheric Solids Analysis Probe |

| | | |
|---|---|---|
| ESI | - | Electrospray ionisation |
| HPLC | - | High performance liquid chromatography |
| LRMS | - | Low resolution mass spectrometry |
| HRMS | - | High resolution mass spectrometry |
| NMR | - | Nuclear magnetic resonance spectroscopy |
| DEPT | - | Distortionless enhancement by polarization transfer |
| COSY | - | Correlation spectroscopy |
| HSQC | - | Heteronuclear single quantum coherence |
| HMBC | - | Heteronuclear multiple-bond correlation spectroscopy |
| NOESY | - | Nuclear Overhauser Enhancement Spectroscopy |
| M | - | Molar, 1 M = 1 mol $dm^{-3}$ |
| mol | - | Mole(s) |
| $R_f$ | - | Retention factor |
| UV | - | Ultra-violet |
| ppm | - | Parts-per million |
| IR | - | Infra-red |
| ReactIR™ | - | ReactIR, trademark name for *in situ* IR spectroscopy |
| *e.e.* | - | Enantiomeric excess |
| *d.e.* | - | diastereomeric excess |
| Bn | - | Benzyl, $-CH_2Ph$ |
| Bz | - | Benzoyl, -C(O)Ph |
| Ph | - | Phenyl, -Ph |
| *i*Pr | - | *iso*-Propyl, $-CH(CH_3)_2$ |
| *tBu* | - | *tert-Butyl*, $-C(CH_3)_3$ |
| NHC | - | *N*-Heterocyclic carbenes |

*This thesis is dedicated to my Mum*

# Literature Review

# 1. Introduction

The chemistry of boron and, in particular, organoboron chemistry, is extremely diverse and ubiquitous in modern day chemistry.[1,2] During the 20th century, chemists unveiled a vast array of reactions involving boron reagents which demonstrated their utility in organic synthesis. Most notable was the 1979 Nobel Prize for Chemistry, awarded to H. C. Brown and Georg Wittig *for their development of the use of boron- and phosphorus-containing compounds, respectively, into important reagents in organic synthesis*.[3] To this day, H. C Brown is best known for his work on hydroboration and organoboron chemistry.[4]

Hydroboration methodology became of particular interest to synthetic chemists as it allowed the regioselective addition of a boron containing species to the least substituted carbon in olefinic species (*anti*-Markovnikov addition). Therefore, the functionalisation of the boron-bearing substituent led to *anti*-Markovnikov-type products, which were previously challenging to obtain. The subsequent transformation of carbon-boron bonds into C-C,[5,6] C-N,[7,8] C-O, C-X bonds and homologations.[9] Other transformations[10] have been widely explored in the literature[11-13] and, subsequently, organoboron reagents have become key reagents in synthesis.[14-16] Indeed, Akira Suzuki was awarded, along with Richard F. Heck and Ei-ichi Negishi, the 2010 Nobel prize in chemistry for his part in developing palladium-catalysed cross-coupling methodology (Suzuki-Miyaura cross-coupling), in particular using organoboron compounds.

## 1.1 β-Boration

As part of the endeavour to prepare novel organoboron species, chemists developed a process which is now commonly known as β-boration (or boron conjugate

addition, BCA).[17] This is a process by which diboron species [*e.g.* $B_2pin_2$ (pin = $OCMe_2CMe_2O$) **1**, $B_2cat_2$ (cat = 1,2-$O_2C_6H_4$) **2**, $B_2neop_2$ (neop = $OCH_2CMe_2CH_2O$) **3**, see Figure 1][18] undergo a Michael-type conjugate addition to an electron-deficient alkene **4**, leading to a 1,4-addition adduct **5** (boron enolate) which, after work-up, yields the β-boration product **6** (see Scheme 1).

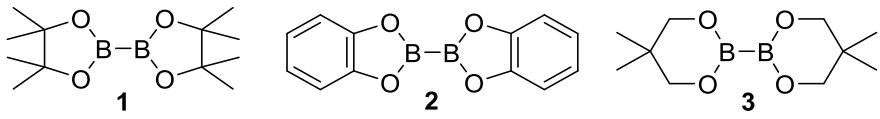


**Figure 1** Diboron species $B_2pin_2$ **1**, $B_2cat_2$ **2** and $B_2neop_2$ **3**.

The first example of this process was reported in 1997 by Marder *et al*.[19] At the time, metal-catalysed diboration of simple alkenes were becoming well-explored and, in this context, the diboration of conjugated electron-deficient alkenes seemed an attractive prospect.[20] It had been previously shown through the use of metal catalysis dramatic modifications to the chemoselectivity of boron reagents, in the presence of substrates with several functional groups (*e.g.* C=O and C=C), could be achieved. Indeed, Nöth *et al*. had demonstrated the hydroboration of simple alkenes using Wilkinson's catalyst **7** ($RhCl(PPh_3)_3$) in the presence of other functional groups (Scheme 2).[21] Later, Evans *et al*. revealed an elegant conjugate reduction methodology using Wilkinson's catalyst **7** in conjunction with catecholborane (H-Bcat) (Scheme 2).[22]

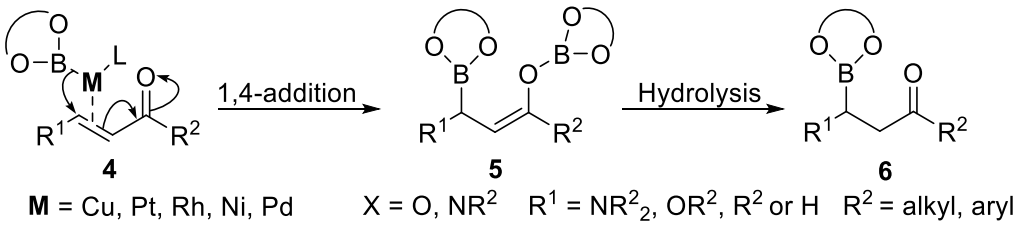


**Scheme 1** Metal-catalysed β-boration (*via* diboration).

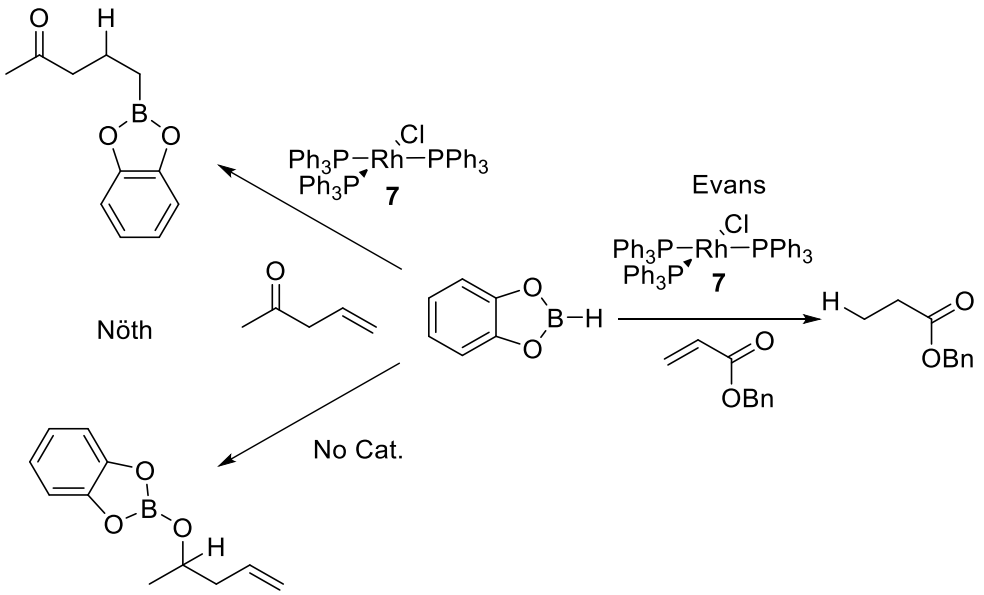


**Scheme 2** Evans' conjugate reduction and the Nöth hydroboration methodology.

Studies involving the metal-catalysed diboration of unsaturated species were becoming increasingly explored[23,24] due to the products of such reactions finding utility in cross-coupling reactions.[25] In response to the need for novel routes to organoboron reagents, Marder's team demonstrated the diboration of two α,β-unsaturated ketones (**4a** and **4b**) with $B_2pin_2$ **1** and $B_2cat_2$ **2** in the presence of a platinum catalysts, $[Pt(C_2H_4)(PPh_3)_2]$ **8** (see Scheme 3). Diboration of α,β-unsaturated ketones **4** yielded the 1,4-diboration product **5**. The addition of water resulted in the β-boration products **6** in stoichiometric conversions. It is interesting to note that there are only two examples in the literature where 1,4-diboration products of electron-deficient alkenes have been isolated and characterised, likely due to their moisture sensitivity. However, isolation of the 1,4-diboron species **5a**, **5b** and **5c**, provided valuable mechanistic insights.[19,26]

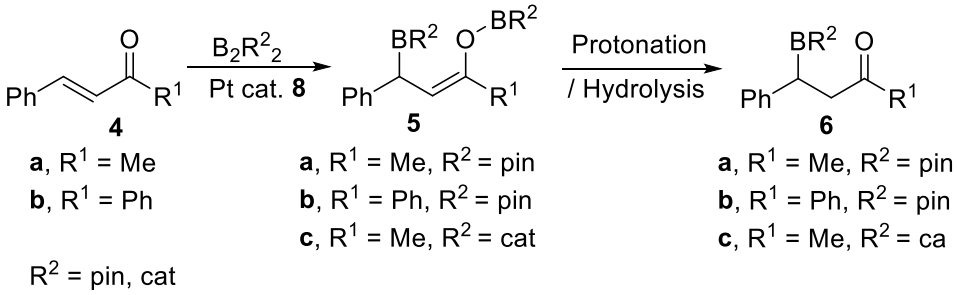


**Scheme 3** Diboration followed by aqueous work-up yields β-products **6a-c**.

These reports in 1997[19] and 2004[26] also provided a new pathway to β-hydroxy ketones (aldol-products) *via* the oxidation of boron functionalities. Marder *et al*. also noted that reactions between α,β-unsaturated ketones and chiral diboron reagents were possible developments, hinting at the potential of β-boration to be enantioselective. However, it took several years for this to be realised (2007/2008).

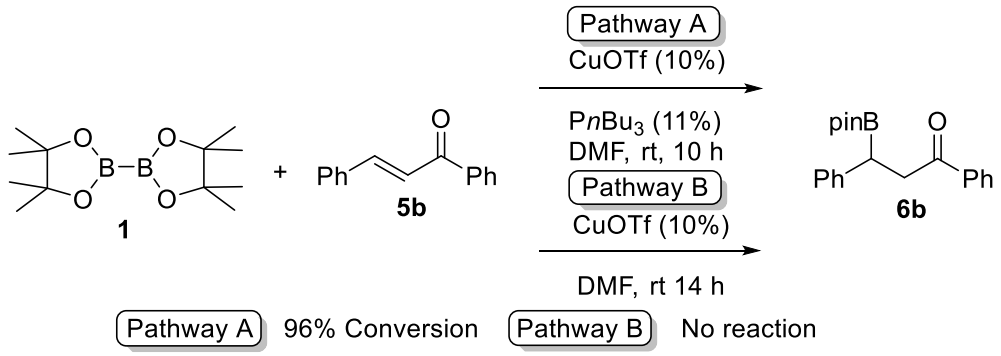


**Scheme 4** Hosomi's Cu-catalysed β-boration protocol for α,β-unsaturated species.

In 2000, Hosomi *et al*. unveiled the first example of a copper-catalysed β-boration on a series of α,β-unsaturated ketones,[27] closely followed by Miyaura *et al*.[28,29] The former report was analogous to their previous work involving the use of disilane reagents, using copper catalysis as a means of introducing silyl substituents into the β-position of electron-deficient alkenes.[30] Hosomi's group probed the utility of the copper-catalysed system (as developed for use in the disilane case[30]) in the β-boration of

chalcone **5b** with $B_2pin_2$ **1**. Their initial trials failed; however, further attempts showed that the addition of P(*n*Bu)$_3$ followed by hydrolysis gave the desired β-boration product **6b** (see Scheme 4). Hosomi *et al.* then probed the optimised reaction of this β-boration methodology using a series of enones, both cyclic and acyclic, resulting in conversions ranging from 67-96%. The reaction proceeded with just the addition of a phosphine ligand alone, albeit in low yield (7%). The role of phosphines in β-boration will be discussed later.

Miyaura *et al*. further demonstrated the utility of a copper catalysed system (stoichiometric CuCl, LiCl, KOAc in DMF)[28,29] with the β-boration of a series α,β-unsaturated esters, ketones and nitriles. Interestingly, Miyaura was the first to suggest, and provide evidence for, a boryl copper species as providing the nucleophilic source of boron in the β-boration reaction.[28] They provided evidence for this by introducing allyl chloride into their copper-boryl system; the result of which gave an allyl boronate species (Scheme 5). This result is consistent with the assumed presence of a copper-boron species, acting as a nucleophilic source of boron.[31]

The systems reported by both Hosomi and Miyaura[27,28,29] had their drawbacks due to relatively high catalyst loadings, especially in the case of Miyaura, who employed stoichiometric amounts of copper (see Scheme 5). Drawbacks aside, both reports were highly influential in the field and spawned great interest in finding other metal catalysts and more efficient reaction conditions for the β-boration process.

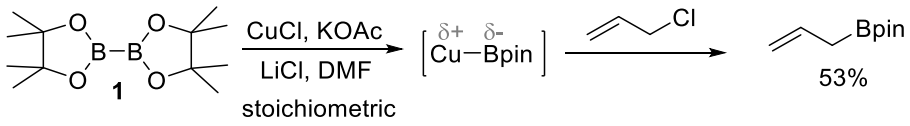


**Scheme 5** Evidence for a nucleophilic boron species presented by Miyaura *et al*.[29]

In addition to the work of Hosomi and Miyaura, Kabalka *et al*. demonstrated the use of Wilkinson's catalyst in the β-boration of electron-deficient alkenes (α,β-unsaturated esters, ketones and nitriles, see Equation 1)[32] as an approach to boronic acids for application in boron neutron capture therapy.[33] They probed the use of Wilkinson's catalyst **7** as a potential means of facilitating the β-boration reaction shown in Eqn 1. This work addressed some of the problems associated with the high catalyst loadings reported by Miyaura.[28,29] Typically only 10 mol% of Wilkinson's catalyst **7** was required compared to the stoichiometric copper catalyst loadings in the Miyaura β-boration protocol.[28,29]

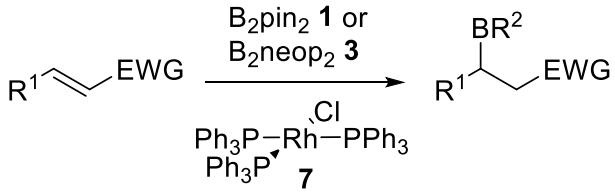


**Equation 1**

Yun *et al*. revolutionised the area by unveiling a novel methodology which enabled the β-boraton of α,β-unsaturated esters, ketones and nitriles. This methodology was achieved using a copper-based reaction system, modified with simple alcohol additives.[34] Yun *et al*. had previously developed an efficient protocol for the conjugate reduction of α,β-unsaturated nitriles [35] using copper catalysis and xanthene-type biphosphine ligands, which were key to improved activity and lower catalyst loadings. When applied to the β-boration reaction, Yun *et al.* showed that xanthene-type biphosphine ligands improved the nucleophilicity of the active copper species (copper-hydride), which resulted in an improved methodology for the chemoselective conjugate reduction of α,β-unsaturated nitriles.[35] Previous evidence[28] suggested that the

active copper species in β-boration was a nucleophilic copper-boryl species and, hence, Yun *et al*. examined whether the observed increase in nucleophilicity (as observed in the active copper-hydride case) could be applied to the active copper-boryl species in the β-boration of α,β-unsaturated species (2006).[34] They first probed the β-boration of (*E*)-ethyl crotonate **9** using a copper(I) salt, ligand and slight excess of $B_2pin_2$ **1** (Equation 2) at room temperature for over 14 hours. Their initial attempt used a copper(I) acetate salt and DPEphos **L1** (for all ligands, **L** see Figure 2) in the absence of base. GC analysis showed a conversion of 26% to **10**, which when compared to previous literature examples was poor.[27,28,32] However, by changing to copper(I) chloride with the addition of sodium *tert*-butoxide (9 mol%) the reaction improved and the yield of the β-boration product doubled to 48%. Changing the ligand from DPEphos to Xantphos (**L1** to **L2**, respectively) resulted in poor conversion to the β-boration product. Yun *et al*. had noted in their previous work on the conjugate reduction of α,β-unsaturated nitriles[35] that the addition of alcohol to their reaction improved yields dramatically.

Buchwald *et al*. had shown elsewhere that the addition of ethanol could protonate an organocopper intermediate and, hence, improve reactions yields due to improved catalytic turnover, where the suggested mechanistic pathway proceeded *via* a carbon-bound copper intermediate.[36]

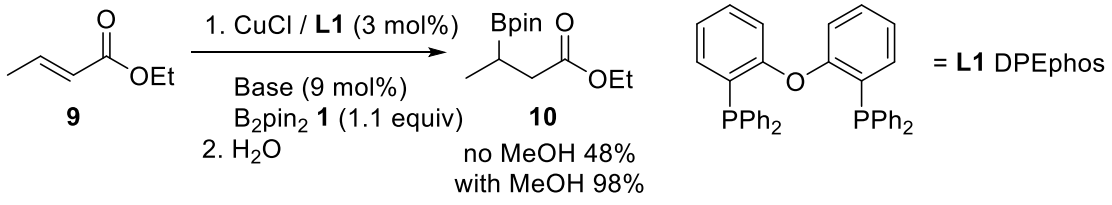


**Equation 2**

Yun *et al*. used an alcohol additive in their reaction as a means of protonation of the assumed carbon-bound copper intermediate. Indeed, they found that the addition of

*tert*-butanol or methanol dramatically improved yields in their reactions. The use of copper(I) chloride (3 mol%), Joiphos **L3** (3 mol%), sodium *tert*-butoxide (9 mol%) and methanol (2 equiv.) gave the β-boration products in up to 98% yield.

When methanol was not employed, only 48% product **10** was obtained (see Eqn 2), highlighting the importance of the alcohol additive. Next, they examined the scope of the β-boration of a series of α,β-unsaturated by probing a series of varied substrates (Table 2). It is clear from Table 2 that the system developed by Yun *et al.* was highly effective and efficient. The dramatic influence of the addition of the alcohol was clear (Table 1, Entry 3) giving higher yields compared to that obtained by Hosomi *et al*. and using a lower catalyst loading (only 3 mol%). Not only was the addition of an alcohol in the copper catalysed β-boration of electron-deficient alkenes shown to be an important step forward, but Yun *et al*. also demonstrated that this protocol had the potential to be enantioselective.[34]

**Table 1** Influence of methanol on the β-boration of electron-deficient alkenes.

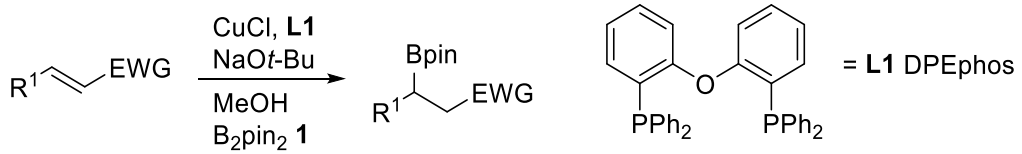


| Entry | Species | Time (h) | Yield[a,b] |
|---|---|---|---|
| 1 | 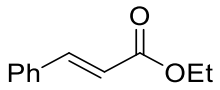 | 11 | 91 |
| 2 | 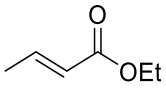 | 14.5 | 95 |
| 3 | 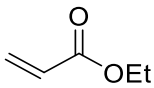 | 1.5 | 98 |
| 4 | 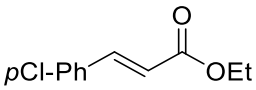 | 16 | 93 |
| 5 | 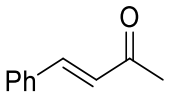 | 14 | 95 |
| 6 | 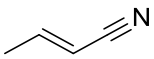 | 6.5 | 95 |

[a] Reaction conditions: CuCl (3 mol%), **L1** (3 mol%), NaO*t*Bu (9 mol%), $B_2pin_2$ **1** (1.1 equiv.), MeOH (2.2 equiv.), THF. [b] Isolated yield.

## 1.2 Asymmetric metal-catalysed β-boration

During the early development of β-boration methodology, it was suggested that this process had the potential to be enantioselective, perhaps by employing chiral diborane reagents, as suggested by Marder *et al*.[19] Interestingly, Yun *et al*. developed an enantioselective β-boration protocol, not based upon chiral diborane reagents, but on a catalytic system that employed chiral phosphine ligands.[34,37] Having shown that the copper catalysed β-boration of cinnamonitrile **11** gave the borated product **12** in high yield (95%), Yun *et al*. applied the chiral Josiphos ligand **L3** to their optimised methodology.

This was followed by C-B oxidation to yield the chiral β-hydroxy nitrile **13** with the expected complete retention of stereochemistry. This gave the product **13** 84% yield, with an observed 82% *ee* (Scheme 6).

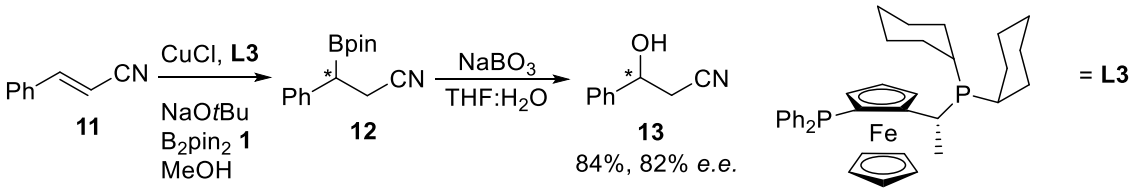


**Scheme 6** Enantioselective β-boration of cinnamonitrile **11**.

Once it had been shown that enantioselective β-boration could be achieved using chiral phosphine ligands, Yun *et al*. probed the scope of this protocol and the influence of other chiral phosphine ligands with a series of α,β-unsaturated esters and nitriles (Table 2).[38] All the ligands that were screened induced enantioselectivity; however, it is clear from looking at Table 2, that Josiphos and Mandyphos (**L3** and **L4** respectively) showed the most promise with respect to asymmetric induction.

Hence, **L3** and **L4** were employed in the enantioselective β-boration-oxidation sequence of a series of α,β-unsaturated esters and nitriles (Table 3). This protocol also resulted in high yields and high levels of enantioselectivity across a wide range of substrates (see Table 3, Entries 1-13), with **L3** providing a higher level of enantioselectivity than **L4** (see Table 3, Entries 4 *vs*. 5 and 8 *vs*. 9). Yun *et al.* also made interesting observations regarding β-substituent effects, electron withdrawing group influence and ester moiety effects on the asymmetric induction of the screened reactions.

**Table 2** Enantioselective β-boration of α,β-unsaturated esters and nitriles.

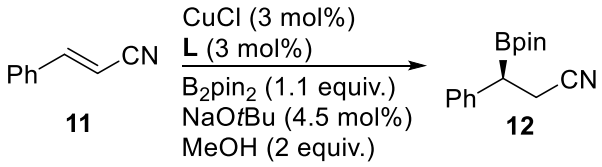


| Entry | Ligand | Yield (%)[a] | *e.e.* (%) |
|---|---|---|---|
| 1 | 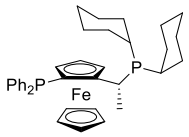 **L3** | 97 | 94 |
| 2[b] | 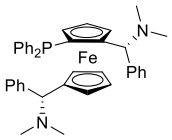 **L4** | 96 | 94 |
| 3 | 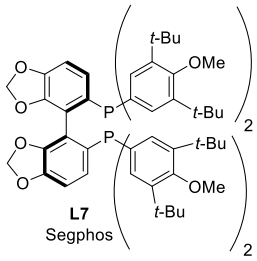 **L7** | 92 | 80 |
| 4 | 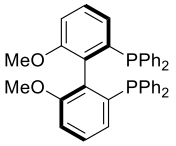 **L6** | 92 | 3 |
| 5 | 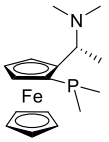 **L5** | 93 | 55 |

[a] Isolated Yield. [b] NaO*t*Bu (3 mol%).

Potential β-substituent effects on enantioselectivity can be examined by comparing entries 1-6 and 11-13 (see Table 3), where the substrates differ only by their β-substituents. The β-substituents differ in terms of both steric and electronic effects in each case and the observed *e.e.* values were remarkably similar, which suggested that the β-substituent did not have a dominant effect on the enantioselectivity of the reaction.

The nature of the electron withdrawing group (ester or nitrile in this case) was found to have an influence on the enantioselectivity (Table 2, entry 2 and Table 3, Entry 5). When the electron withdrawing group was the α,β-unsaturated nitrile, this resulted in higher enantioselectivity (94% *e.e.*) compared to the analogous ester (87% *e.e.*). Having established that the nature of the electron withdrawing group plays an important role in stereoselectivity, Yun *et al*. examined this further in the case of esters by varying the alkoxy substituent on the ester. They found that changing the alkoxy substituent (*e.g.* **14**, **15** and **16**) from a simple methoxy group to a more sterically demanding substituent (O*t*Bu) gave no observable effect on the enantioselectivity. Interestingly, Fernández *et al*. explored the nickel and palladium catalysed enantioselective β-boration of α,β-unsaturated esters,[39] having previously explored the asymmetric β-boration of α,β-unsaturated esters using a copper catalyst, furnished with chiral *N*-heterocyclic carbenes (NHC). However, they did not examine the effect of the ester moiety on the degree of asymmetric induction (see McQuade *et al*. for other work in this area).[40,41]

In light of the work by Yun *et al*.,[38] Fernández *et al*. used a nickel catalyst system to examine whether the enantioselectivity of the catalytic β-boration was indeed independent of ester variation (see Equation 3) and found that the ester moiety was influencing the enantioselectivity of the reaction. Indeed, this was observed across a range of different chiral ligand systems and the trends were similar in each case, *i.e.* from OMe to O*i*Bu, the asymmetric induction increased with greater steric bulk on the ester moiety. It is important to note that the same trend was also observed in the palladium-catalysed system, also developed by Fernández *et al*.[40]

**Table 3** Enantioselective β-boration/oxidation of α,β-unsaturated species.

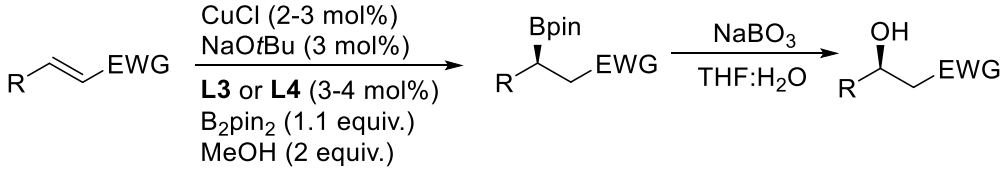


| Entry | Substrate | Yield (%)[a] | *e.e.* (%)[b] | Entry | Substrate | Yield (%)[a] | *e.e.* (%)[b] |
|---|---|---|---|---|---|---|---|
| 1 | 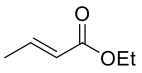 | 94[c] | 90 (*R*) | 8 | 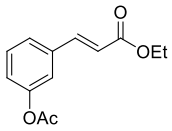 | 95[c] | 87 |
| | | | | 9 | | 89[d] | 84 |
| 2 | 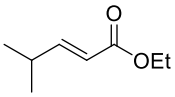 | 92[c] | 91 (*S*) | | | | |
| | | | | 10 | 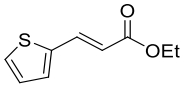 | 93[c] | 82 |
| 3 | 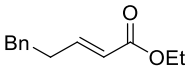 | 97[c] | 89 | | | | |
| 4 | 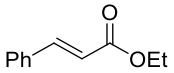 | 93[c] | 90 (*S*) | | | | |
| 5 | | 94[d] | 87 (*S*) | 11 | 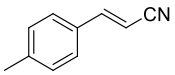 | 94[c] | 90 (*S*) |
| 6 | 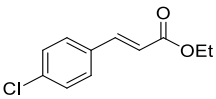 | 90[c] | 91 (*S*) | 12 | 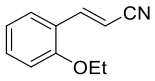 | 90[c] | 92 |
| 7 | 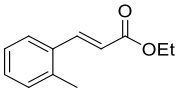 | 87[c] | 88 | 13 | 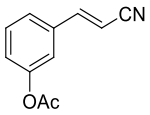 | 94[d] | 91 |

[a] Isolated yield of β-boration product. [b] *e.e.* of the oxidised product. [c] CuCl (2 mol%), NaO*t*Bu (3 mol%), **L3** (4 mol%). [d] CuCl (3 mol%), NaO*t*Bu (3 mol%), **L4** (3 mol%).

The work by Yun *et al*. was highly influential as it established for the first time a protocol for enantioselective β-boration that could be applied to a broad range of substrates. It also suggested that a varied range of β-substituent can be tolerated, as judged by the observed enantioselectivity in these reactions. That being the case, Yun *et al*. explored the β-boration of α,β-unsaturated amides as this was another way of

gauging the influence of the electron withdrawing group, and to expand the substrate scope of this protocol (see Equation 5).[42]

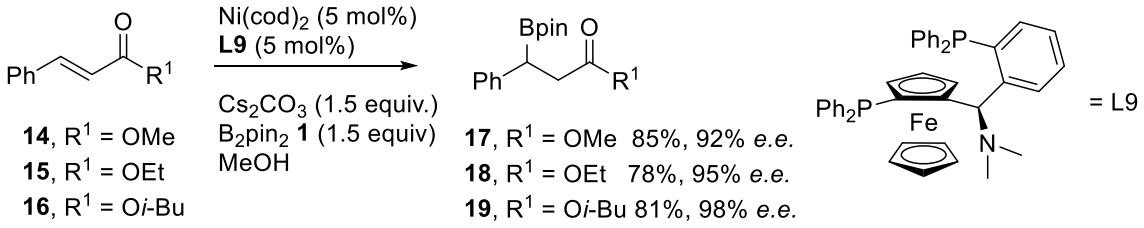


**Equation 3**

Nishiyama *et al*. examined the effect of the ester on enantioselectivity and found an inverse trend to that reported by Fernández *et al.*[43] The rhodium-catalysed β-boration had been reported previously;[32] however, an asymmetric protocol for β-boration had yet to be established. Nishiyama developed a rhodium catalyst that employed a chiral bisoxazolinylphenyl ligand to induce enantioselectivity in the β-boration (see Equation 4). Indeed, Nishiyama *et al*. found that by increasing the steric bulk of the ester moiety, a decrease in enantioselectivity was observed. Moreover, with different rhodium-bisoxazolinylphenyl systems, the same trend of decreased enantioselectivity with more sterically demanding esters was observed. [43]

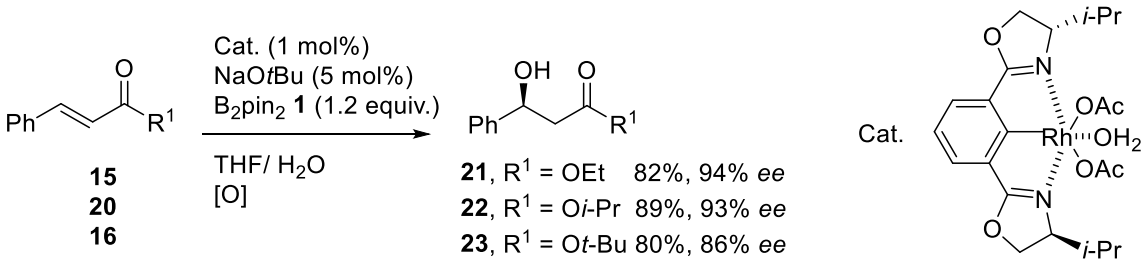


**Equation 4**

Oshima *et al*. had previously developed an efficient nickel catalysed protocol for the β-boration of α,β-unsaturated esters and amides.[44] Yun *et al.* extended their previously established enantioselective boration protocol from α,β-unsaturated esters and nitriles to the analogous α,β-unsaturated amides. The previous protocol could not be directly applied due to the α,β-unsaturated amides being poorer Michael acceptors compared to the analogous α,β-unsaturated esters and nitriles which resulted in conversions as low as 23%. Unlike their previous examples involving the enantioselective β-boration of α,β-unsaturated esters and nitriles, the system for the α,β-unsaturated amides is limited to a few substrate variants.

Nishiyama *et al*. also reported a route to α,β-unsaturated amides *via* a chiral rhodium-bisoxazolinylphenyl system,[43] giving the borated amide in good yield and excellent *e.e.* (see Equation 6). This was only limited to selected substrates. Indeed, this has recently been expanded to encompass more substrates, such as α,β-unsaturated amides, ketones and esters.[45] Interestingly, Molander *et al*. also reported a method of β-borating α,β-unsaturated amides using tetrahydroxydiborane.[46] Indeed, they managed to develop the asymmetric system several years later.[47]

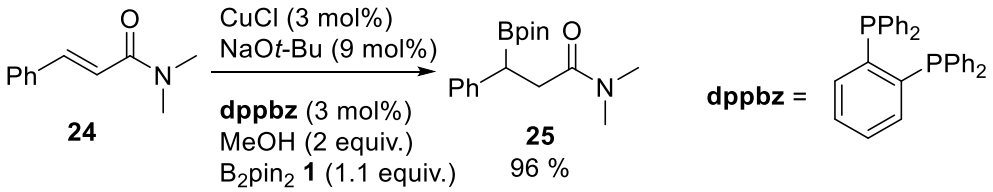


**Equation 5**

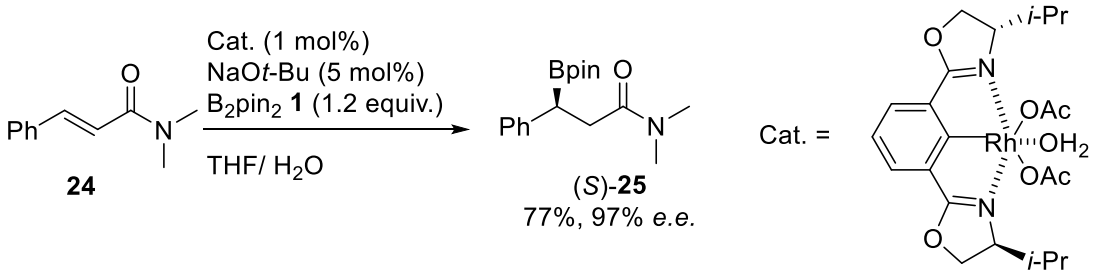


**Equation 6**

Exploration into the metal-catalysed enantioselective β-boration of α,β-unsaturated esters, nitriles and amides is both fascinating and complex. It offers great insight into the mechanistic pathways that underpin these reactions. However, points of disagreement regarding what influences enantioselectivity have arisen. It is clear that the electron withdrawing group (ester, nitrile or amide) does play a dominant role in asymmetric induction; however, the β-substituent and ester moiety effects also play a subtle role in asymmetric induction, a role that is not fully understood and a point upon which different groups disagree.[38,40,43] It is, therefore, important to examine in depth both the metal-catalysed β-boration and enantioselective β-boration of α,β-unsaturated ketones and imines.

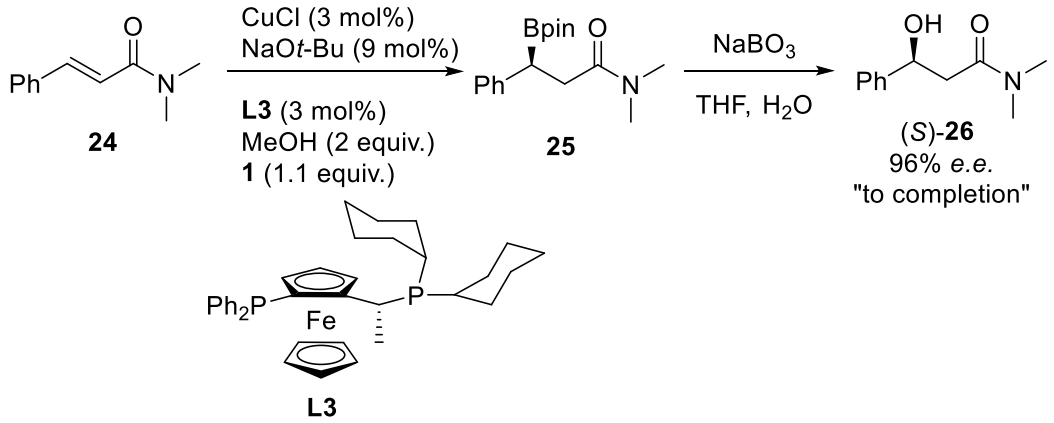


**Scheme 7** Yun's enantioselective β-boration/oxidation sequence of α,β-unsaturated amides.

The inherent low reactivity of the copper catalysed protocols of Hosomi and Miyaura *et al*.[24,25,27] meant that asymmetric induction was a challenge, even with the use of chiral phosphine ligands. This allowed the exploitation of potential enantioselective pathways in the β-boration of α,β-unsaturated ketones.[34] This was explored by Yun *et al*. on the enantioselective β-boration of acyclic α,β-unsaturated ketones.[48] The crucial role of methanol was demonstrated in the β-boration of two analogous α,β-unsaturated species (**4a** and **15**, see Equation 7). They combined two α,β-unsaturated carbonyl species and reacted them in parallel, as a means of examining the reactivity of the α,β-unsaturated ketone **4a** relative to the previously explored α,β-unsaturated ester **15**.

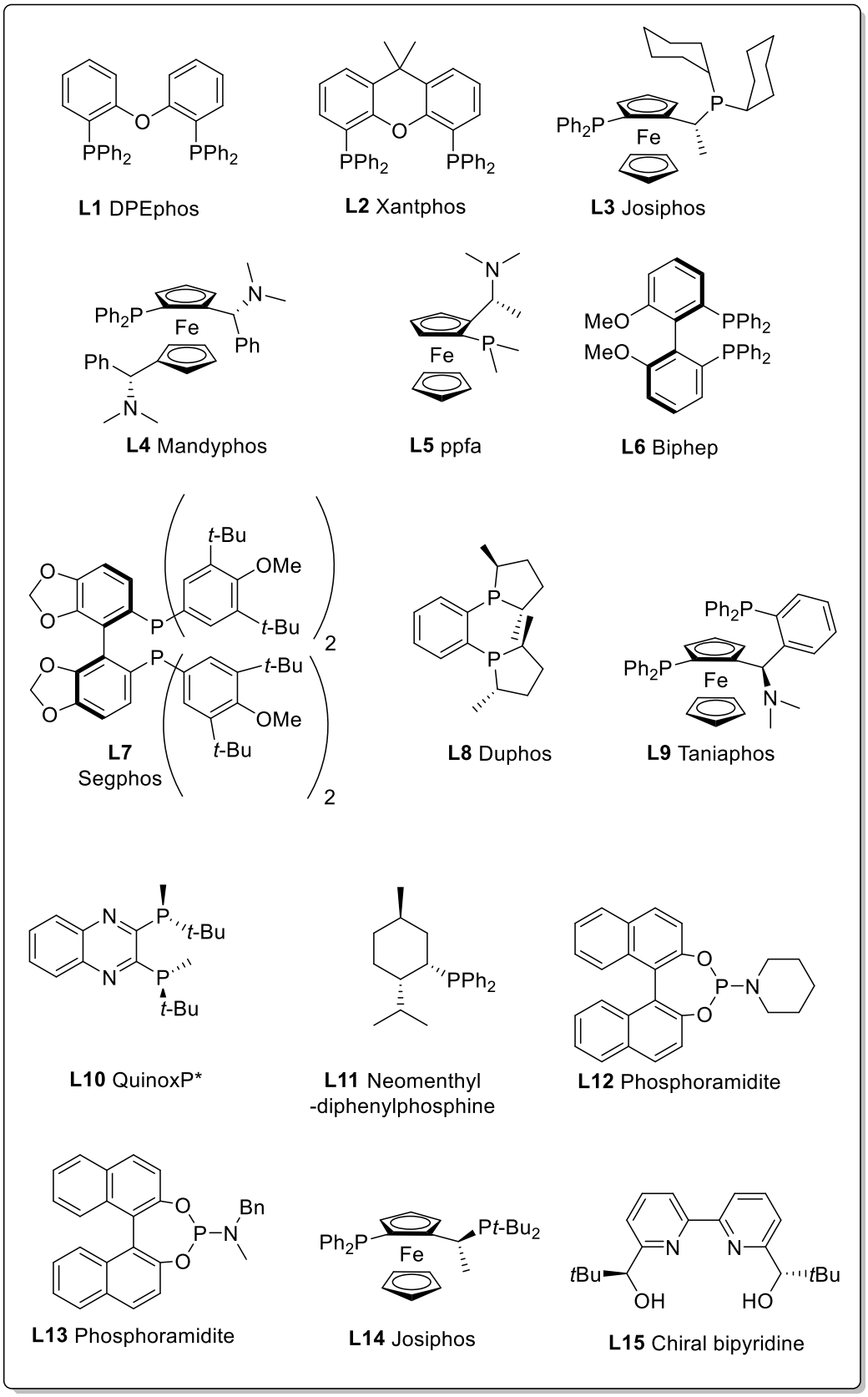


**Figure 2** Ligands **L** employed in catalytic β-boration of electron-deficient alkene.

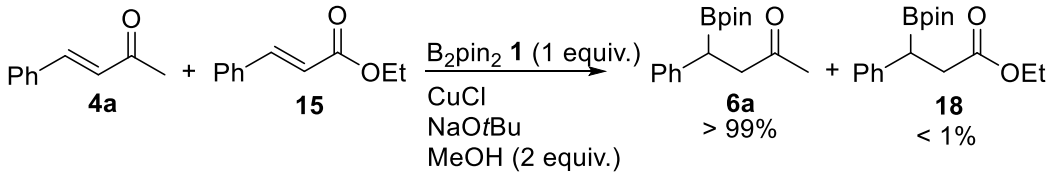


**Equation 7**

Interestingly, they found that under these conditions, the β-boryl ketone **6a** was formed in near quantitative conversion, whereas the analogous ester **18** was formed in very low yields (<1%). The above reaction (Equation 7) was achieved without the presence of a ligand and, hence, Yun examined whether asymmetry could be induced using chiral phosphine ligands. The use of these chiral ligands (**L3** and **L4**) in the presence of alcohol additives (methanol, *iso*propanol or *tert*-butanol) in varying amounts (1-2 equiv.) resulted in excellent conversions (92-100%) and moderate to good levels of asymmetric induction (37-80% *e.e.*). Interestingly, even without the addition of alcohol additives, high levels of asymmetric induction were achieved (56-77% *e.e.*). However, the alcohol free reactions did not proceed to completion and poorer yields were typically observed (18-54%).

Having established and gained an understanding of the parameters which influence both enantioselectivity and conversion, Yun *et al*. expanded this methodology further by probing various substrates using both **L3** or **L4** and different alcohol additives (see Table 4). In light of the experimental evidence outlined in Table 4, Yun *et al*. observed that methanol was the more effective alcohol additive, typically leading to greater levels of conversion and improved enantioselective control. Again, as in the case of α,β-unsaturated esters and nitriles,[38] the β-substituent induced subtle changes on the degree of conversion and enantioselectivity of the reaction. Even though it is worth noting that β-substituents do indeed influence these parameters, it is difficult to deduce with any high degree of certainty if there is any trend between β-substituents and

enantioselectivity. This is due to the limited number of substituents (differing in subtle steric and mesomeric properties) probed by Yun *et al*. It is clear that **L3** is certainly more influential in enantioselective induction when compared to **L4**.

**Table 4** Enantioselective β-boration with various substrates, ligands and alcohol additives.

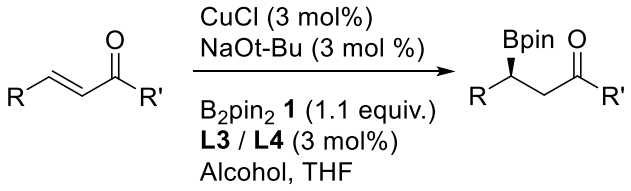


| Entry | Substrate | Ligand | Alcohol | Yield (%)[a] | *e.e.* (%)[b] |
|---|---|---|---|---|---|
| 1 | 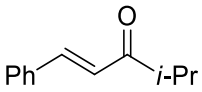 | **L3** | *i*PrOH | 94 | 95 |
| 2 | | **L3** | MeOH | 97 | 89 |
| 3 | | **L4** | MeOH | 93 | 93 |
| 4 | 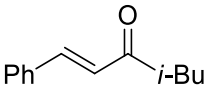 | **L3** | MeOH | 89 | 81 |
| 5 | | **L4** | MeOH | 91 | 88 |
| 6 | 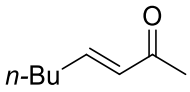 | **L3** | MeOH | 93 | 90 |
| 7 | | **L4** | MeOH | 86 | 30 |
| 8 | 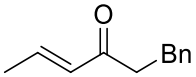 | **L3** | MeOH | 95 | 90 |
| 9 | | **L3** | *i*PrOH | 90 | 88 |
| 10 | | **L4** | MeOH | 96 | 30 |
| 11 | 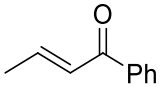 | **L3** | MeOH | 97 | 97 |
| 12 | 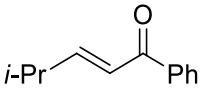 | **L3** | MeOH | 94 | 97 |
| 13 | 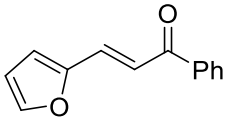 | **L3** | MeOH | 72 | 91 |
| 14 | | **L3** | *i*PrOH | 72 | 9 |
| 15 | 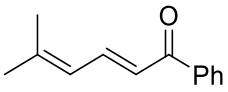 | **L3** | MeOH | 93 | 96 |
| 16 | | **L3** | *i*PrOH | 70 | 95 |

[a]Isolated yield. [b] Deduced from the corresponding β-hydroxy ketone.

β,β-Disubstituted electron-deficient alkenes are particularly challenging in terms of asymmetric synthesis. This is due to the increased difficulty in enantio-differentiation between β,β-disubstituents on conjugate addition, when compared to regular mono-β-substituted species (large steric difference between β-substituent and hydrogen). To address this, Shibasaki *et al*. presented a communication in 2009 which reported a highly efficient and enantioselective methodology for the β-boration of β,β--disubstituted enones (see Scheme 8).[49]

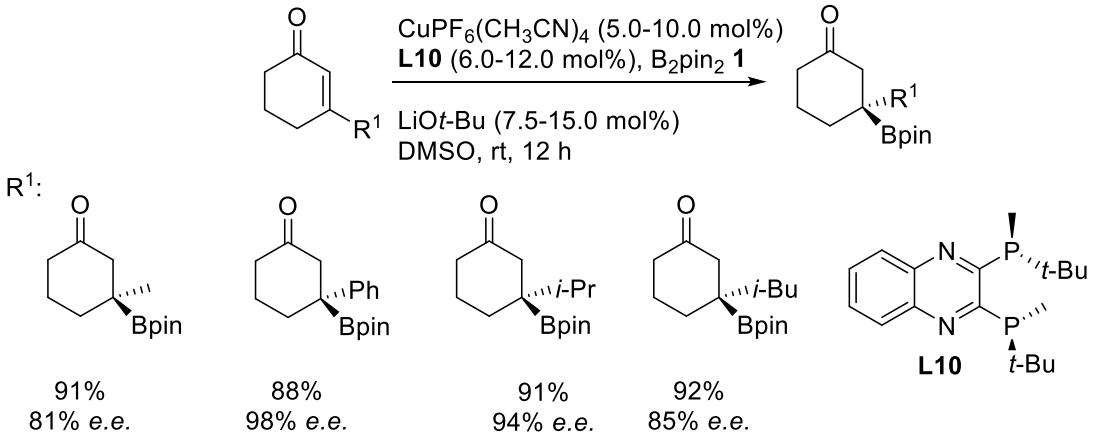


**Scheme 8** β-Boration to cyclic β,β-disubstituted α,β-unsaturated species.

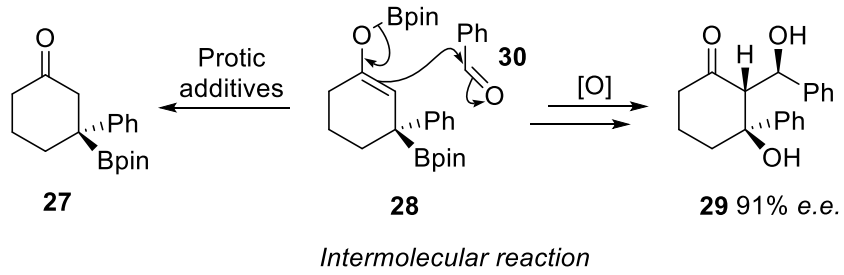


**Scheme 9** Aldol product formed *via* intermediate enolate.

Interestingly, their optimised protocol did not require alcohol additives and made use of an unexplored (in boron conjugate addition) chiral diphosphine ligand **L10**. The substrate scope of their system was probed on cyclic α,β-unsaturated ketones (Scheme 8). All substrates were obtained in excellent *e.e.* and high yield, 70-98% and 80-99%,

respectively. Shibasaki *et al*. demonstrated the potential for a stereoselective aldol-type reaction between the diboron intermediate **28** and benzaldehyde **30**. This was possibly due to the lack of protic additives quenching the intermediate boron enolate (Scheme 9). The lack of alcohol additives (*e.g.* MeOH)[34] provided a greater scope of application of the reaction. Not only was it possible to introduce one boron substituent enantioselectively, but also this showed that multiple stereocentres could be controlled in one-pot. This work overcame some limitations associated with the conjugate addition of boron to β,β-disubstituted α,β-unsaturated species.[50] Both Hoveyda *et al*. and Shibasaki *et al.* demonstrated that the intermediate enolate can serve as a suitable nucleophile which carbonyl-containing electrophiles can be reacted with and, thus, functionalising the $C_\alpha$-position stereoselectively (intermolecular reaction). The analogous intramolecular reaction was exploited by Lam *et al*., which resulted in the formation of highly cyclic products, with high stereocontrol and functionality.[51]

Not content with a protocol limited to the boration of cyclic β,β-disubstitueted α,β-unsaturated species, Shibasaki *et* al. developed a protocol for the corresponding acyclic β,β-disubstituted α,β-variants (also shown by Yun *et al*.[50]) using an adaptation of their protocol for cyclic species.[52] This produced some excellent results, with reaction conversions ranging from 71-95%, with equally high levels of stereocontrol (90-99% *e.e.*). A representative example of this is shown in Equation 8.

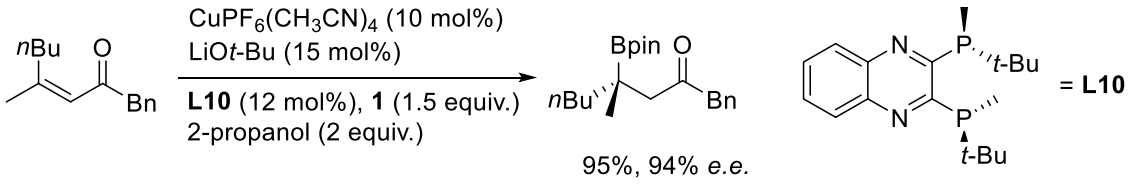


**Equation 8**

Most of the literature regarding β-boration is based on the conjugate addition of boron to activated alkenes, typically activated by a carbonyl electron-withdrawing

moiety, namely amides, ketones and esters.[53] Alkenes activated by nitriles are present in the literature, but α,β-unsaturated imines are under-explored. α,β-Unsaturated imines are can be challenging to prepare and purify.[54-56] However, they offer scope for boron conjugate addition (functionalisation at the β-carbon), and *via* exploitation of the imine functionality leading to 1,3-difunctionalisation.[57]

**Table 5** Enantioselective β-boration of α,β-unsaturated imines.

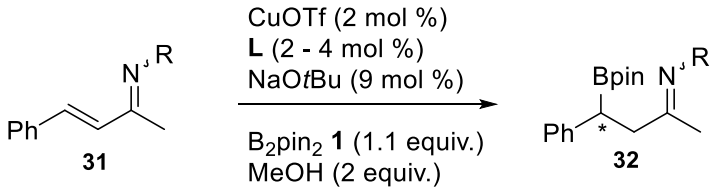


| Entry | R | Ligand | Conversion (%)[a] | *e.e.* (%) |
|---|---|---|---|---|
| 1 | Ph | 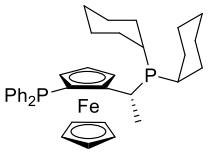 **L3** | 61 | 63 |
| 2 | Ph | 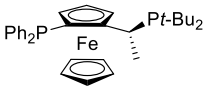 **L14** | 66 | 30 |
| 3 | Ph | 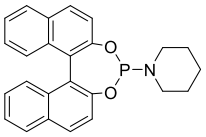 **L12** | >99 | 95 |
| 4 | Bn | **L3** | >99 | 91 |
| 5 | Bn | **L14** | >99 | 77 |
| 6 | Bn | **L12** | >99 | 75 |

[a] Deduced using $^1$H NMR analysis.

In addition, the previous examples of enantioselective β-boration, and the elegant methods for substrate controlled asymmetric reduction,[58] offered considerable potential for controlling multiple stereocentres in simple organic species. To this end, Fernández

and Whiting *et al*. examined whether α,β-unsaturated imines (*e.g.* **31**) could serve as a suitable platform for a novel asymmetric route to γ-amino alcohols.[59, 60] Other asymmetric routes to γ-amino alcohols exist;[61] however, Fernández and Whiting *et al*. explored the previously established methods of boron conjugate addition, more specifically the asymmetric variant, as a means of enantioselectively introducing a boryl substituent at the β-position of the α,β-unsaturated imine substrate (see Table 5).

Drawing on the expertise of Whiting *et al*.,[63] the resulting β-boryl imine (*e.g.* **32**) species would be ideally placed for remote asymmetric reduction.[62,63] This potential, coupled with established methods for the stereospecific oxidation of boron-containing substituents was an intriguing concept that needed to be explored. Hence, Fernández and Whiting *et al.* examined this concept by the asymmetric copper-catalysed β-boration of α,β-unsaturated imines **31** to give **32** (see Table 5 and Scheme 10).[59] This involved the screening of multiple chiral phosphine ligands as a means of devising an efficient protocol for the preparation of chiral β-boryl imines.

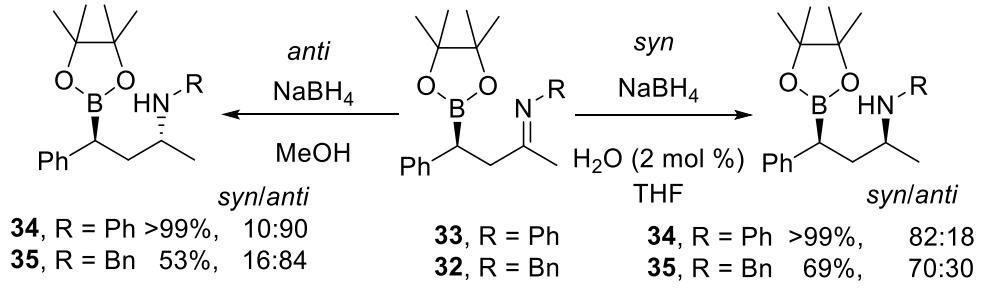


**Scheme 10** Tuneable diastereocontrol by solvent modification.

All the ligands that were screened did indeed induce asymmetry, and moreover, some of the ligands gave the β-boryl imines in excellent conversion and *e.e.* (Table 5). Next, they turned their attention to the asymmetric reduction of the imine functionality. They observed an intramolecular Lewis acid-base interaction (B-N) indirectly by $^{11}B$ NMR spectroscopy (Scheme 11) which offered potential for the exploitation of

previously established reduction methodologies.[62,63] Indeed, on screening various reducing agents and proton sources, they discovered a means of asymmetrically reducing the imino functionality, and by solvent modification, could tune the selectivity between *syn*- and *anti*-diastereoisomer formation (Scheme 10). This protocol was achieved in a one-pot synthesis, by which the β-boration, imine reduction and boronate oxidation could be carried out consecutively. This methodology brought together asymmetric conjugate boration and remote asymmetric induction, and fashioned a protocol to access γ-amino alcohols with high levels of stereocontrol across multiple stereocentres. Shortly after this, the protocol was extended to the preparation of γ-hydroxy alcohols and a wider substrate base for the previously established γ-amino alcohols.[64]

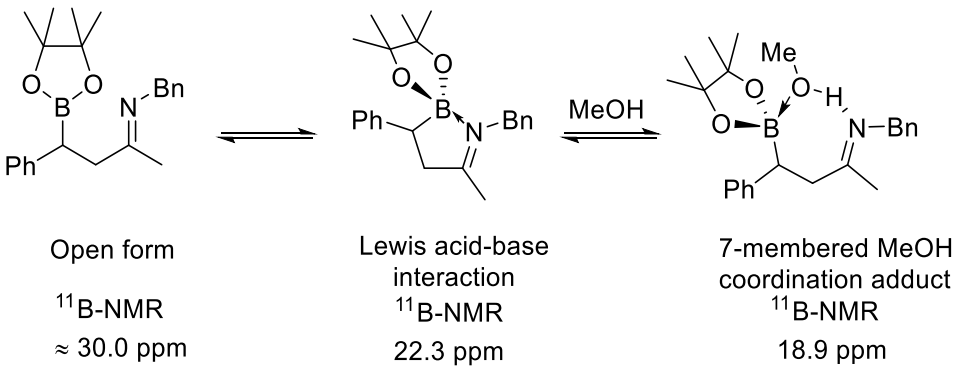


**Scheme 11** $^{11}$B NMR evidence for intramolecular Lewis acid-base interaction.[60]

## 1.3 Asymmetric organocatalytic β-boration

Enantioselective transition metal-catalysed β-boration has received a wealth of attention in the literature due to the efficiency, in both conversion and high levels of asymmetric induction, especially in copper-catalysed systems. However, organocatalysis[65] has had a renaissance in recent years, in part due to the work of Barbas and List *et al.*[66] and MacMillan *et al.*[67] Such methods have proved highly

creative, moreover, they not only offer improvements on existing metal-catalysed systems, but also novel modes of activation and catalysis can be achieved from such systems (see the work of Jørgensen *et al*.).[68] It is perhaps no surprise that such organocatalytic protocols have been developed and applied to the β-boration of electron-deficient alkenes.

The first efficient example of an organocatalytic β-boration methodology was reported by Hoveyda *et al*. in 2009.[69] Hoveyda developed the first procedure for the β-boration of both cyclic and acyclic α,β-unsaturated ketones. This breakthrough made use of an organic system consisting of *N*-heterocyclic carbenes (NHCs) in substoichiometric loadings. It should be noted that Sadighi *et al*. had previously isolated a NHC-copper-Bpin species,[70] and had demonstrated its use in the formation of β-boryl-alkyl complexes (*via* alkene insertion to the NHC-copper-Bpin adduct).[71]

To explain the observed organocatalytic behaviour of the NHCs,[69] Hoveyda *et al*. postulated the *in situ* interaction between the Lewis acidic diboron (*e.g.* 1) species and the nucleophilic (Lewis base) NHC (see Scheme 13). Furthermore, it was suggested that this resulted in a nucleophilic boron species (see Scheme 13) that could undergo conjugate addition to the α,β-unsaturated ketones (Equation 9, mechanistic considerations will be discussed in section 1.5).

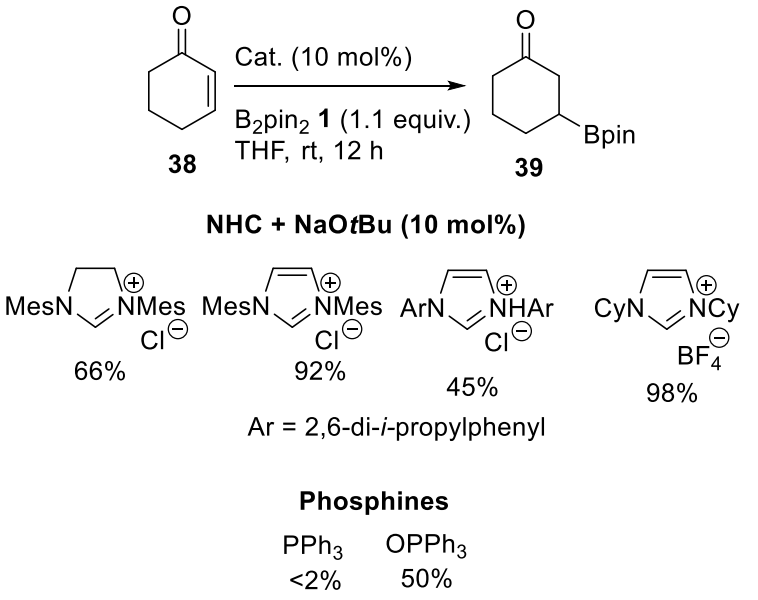


**Scheme 12** The examined catalytic species in the β-boration of cyclic enones.

Hoveyda *et al*. examined this by taking cyclic α,β-unsaturated ketones and probing the β-boration of this species with various NHC and phosphine salts. Surprisingly, addition of the catalytic species to a solution of the α,β-unsaturated ketones and diboron reagent resulted in moderate to excellent yields of the β-boration products (45-98%, see Scheme 12). Moreover, this protocol was applied to both *endo*- and *exo*-cyclic α,β-unsaturated ketones, giving excellent yield (88-98%). This protocol could even be extended to cyclic α,β-unsaturated esters showing equally excellent yields (95%). Interestingly, the catalytic activity of phosphine oxide gave the corresponding β-boryl ketone in moderate yield (50%) without the presence of a transition metal or NHC to facilitate boration. This had been observed before by Hosomi, but the overall conversion was considerably poorer (7%).[27] The importance of this protocol, and the implications for a metal-free variant for a symmetric and asymmetric protocol were clear.

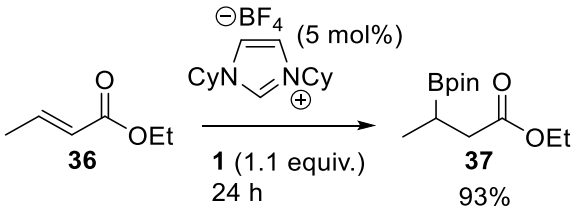


**Equation 9**

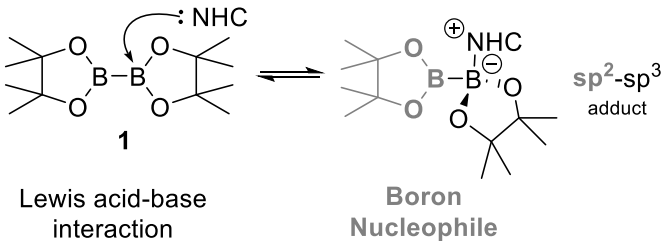


**Scheme 13** Hoveyda's proposed nucleophilic adduct in the β-boration of electron-deficient alkenes.[69]

The introduction of a non-metal-catalysed protocol for the β-boration of α,β-unsaturated species was a useful contribution to the area. It raised questions regarding the mechanistic understanding of these types of processes, especially the role the phosphine ligands (see Scheme 12). This research was probed further by Fernández and Gulyás *et al*. who, in 2010, introduced the first organocatalytic enantioselective β-boration of α,β-unsaturated species.[72] This has subsequently been explored by Hoveyda *et al*. using chiral NHCs.[73] Fernández *et al*. knew from the early work of Hosomi *et al*. that phosphines in the absence of transition metal salts had the ability to facilitate boron conjugate addition to α,β-unsaturated species. Moreover, chiral phosphine ligands had been shown in numerous examples to induce enantioselectivity with respect to the β-boration of prochiral activated alkenes in the presence of transition metal salts.[74,] First, they probed the ability of various achiral phosphines, bases and

alcohols, with the aim of facilitating β-boration of ethyl crotonate **36** (some are highlighted in Table 6).

**Table 6** Probing the catalytic potential of phosphines.

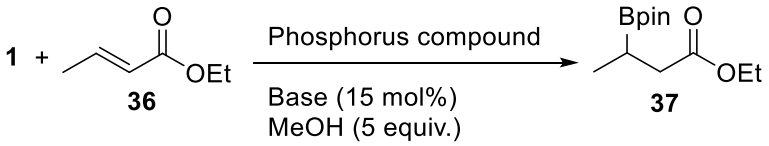


| Entry | Phosphorus compound | Base | Alcohol | Conversion (%)[a] |
|---|---|---|---|---|
| 1 | $PPh_3$ | - | MeOH | 0 |
| 2 | $PPh_3$ | $Cs_2CO_3$ | | 12 |
| 3 | $PPh_3$ | $Cs_2CO_3$ | *i*PrOH | 49 |
| 4 | $PPh_3$ | $Cs_2CO_3$ | MeOH | 99 |
| 5 | $OPPh_3$ | $Cs_2CO_3$ | MeOH | 21 |
| 6 | DPPF | $Cs_2CO_3$ | MeOH | 39 |

[a] Deduced using GC analysis, confirmed using $^1$H NMR spectroscopy.

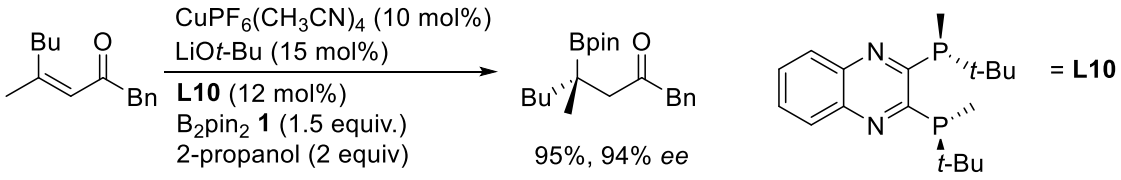


**Equation 10**

Surprisingly, a variety of phosphorus compounds facilitated β-boration of ethyl crotonate in reasonable to excellent yields (Table 6, Entries 3 & 4). The addition of base was found to be crucial for the β-boration, and of the bases that were explored (CsF, NaO*t*Bu, $K_2CO_3$ and $Cs_2CO_3$) $Cs_2CO_3$ was the most successful. Perhaps more surprisingly is the relatively poor performance of $OPPh_3$ in the β-boration. Previously, Hoveyda *et al*. had been unsuccessful in demonstrating the catalytic potential of $PPh_3$ in

β-boration, but had succeeded in demonstrating the potential of $OPPh_3$ (Scheme 12).[69] The addition of $OPPh_3$ to their system resulted in the 50% conversion to the β-boration product. It is surprising, therefore, that $OPPh_3$ performed significantly poorer than the corresponding phosphine, $PPh_3$, in the Fernández *et al*. system.[72] Now that the non-metal-catalysed protocol had been optimised for ethyl crotonate, Fernández *et al*. aimed to explore the asymmetric potential of this reaction through the use of chiral phosphine ligands.[72] This was done by probing a series of chiral ligands in the β-boration ethyl crotonate **36** (Table 7).

**Table 7** Probing chiral phosphine ligands in the development of an asymmetric organocatalytic β-boration protocol.

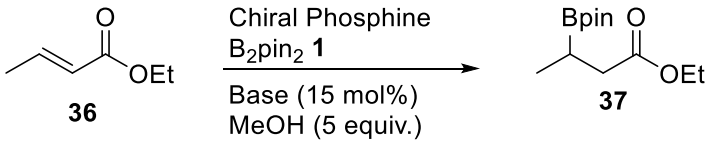


| Entry | Phosphine | Base | Conversion (%)[a] | *ee* (%) |
|---|---|---|---|---|
| 1 | 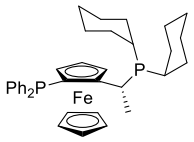 **L3** | $Cs_2CO_3$ | 99 | 75 (*S*) |
| 2 | 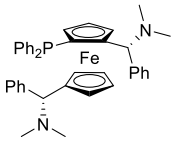 **L4** | $Cs_2CO_3$ | 58 | < 5 |
| 3 | 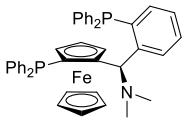 **L9** | $Cs_2CO_3$ | 64 | 72 (*S*) |
| 4 | 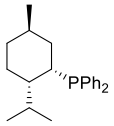 **L11** | $Cs_2CO_3$ | 74 | < 5 |
| 5 | 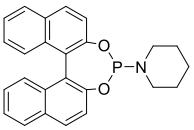 **L12** | $Cs_2CO_3$ | 53 | 7 (*R*) |
| 6 | 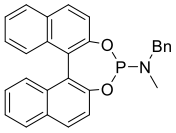 **L13** | $Cs_2CO_3$ | 54 | 35 (*S*) |
| 7 | 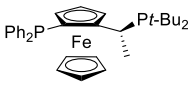 **L14** | $Cs_2CO_3$ | 94 | 88 (*S*) |
| 8 | **L14** | NaO*t*Bu | 59 | 55 (*S*) |
| 9 | **L14** | CsF | 72 | 89 (*S*) |

[a] Deduced using GC analysis, confirmed using $^1$H NMR.

Initially, **L11** was examined as a potential ligands for inducing enantioselectivity in the reaction. High conversions were observed with this phosphine, but it only provided minimal enantioselectivity (< 5%, Table 7, Entry 4). The phosphoramidites (**L12-13**) on the other hand gave poorer conversions, but did indeed induce enantioselectivity in the process. However, the more effective phosphines at inducing enantioselectivity proved to be the Taniaphos (**L9**) and the Josiphos (**L3-14**) type species (see Table 7, Entries 1, 3 and 7).

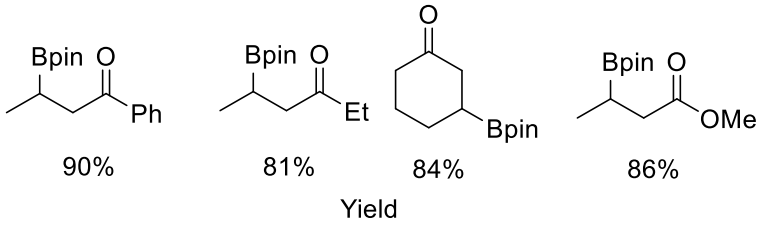


**Figure 3** Products of Fernández *et al*.'s organocatalytic β-boration protocol.[72]

This demonstrated for the first time that asymmetric β-boration need not be carried out using a metal catalyst with chiral ligands; on the contrary, chiral phosphine ligands, base and a suitable alcohol additive alone, proved sufficient to provide enantioselectivity in the conjugate addition of boron to α,β-unsaturated species. However, this protocol was limited to ethyl crotonate **36** and, hence, Fernández *et al*. needed to demonstrate that this procedure could also be applied to a various other substrates.[72] This was explored using the same substrates as explored in the racemic case. This protocol was found to be applicable to a wide rangeof substrates and proved highly effective in terms of both conversion and enantioselectivity. The Josiphos ligand **L14** proved to be the most successful phosphine species, some of these results are highlighted in Figure 3. Both cyclic and acyclic α,β-unsaturated ketones and esters were explored, the β-boration products of which showed reasonable to high levels of enantiopurity (36-83%). The utility of the process was clearly demonstrated by the

encouraging results. However, more importantly it raised questions regarding the underlying mechanistic principles of the reaction. It is not clear whether the phosphine acts either as a ligand or a catalytically active species in the β-boration of α,β-unsaturated species. Building on their previous work, Fernández and Gulyás *et al*. explored their newly devised non-metal-catalysed route to the β-boration of α,β-unsaturated species, and examined the role of iron as an additive as a means of assisting this process.[75] This case will be discussed later (section 1.5), as it provides mechanistic insight to the process of boron conjugate addition.

As previously mentioned, organocatalysis has had a renaissance in recent years. A tremendous amount of work has been published on the use of secondary amines and their roles in the catalytic activation of α,β-unsaturated aldehydes and ketones (iminium activation) towards conjugate addition.[68] To this end, Córdova *et al*. presented their work in 2012 on the organocatalytic β-boration of enals, catalysed by a combination of Lewis base (to activation the diboron reagent) and secondary amines (to activate the substrate), see Figure 4.[76]

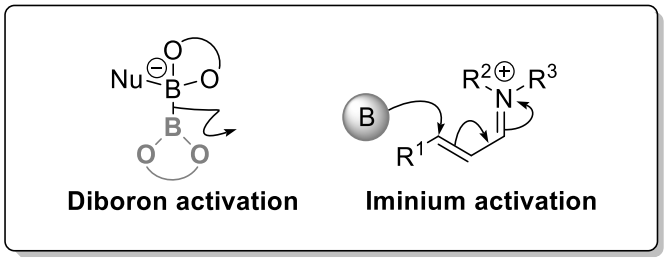


**Figure 4** Organocatalytic modes of activation in the β-boration reaction.[76]

The initial products were trapped *in situ* by phosphorous ylides to generate homoallyl boronates (this will be discussed later). They had previously reported a copper-catalysed enantioselective protocol, whereby enantioselectivity was achieved through the use of a chiral secondary amine additive.[77]

## 1.4 β-Boration in aqueous media

Transition metal catalysis often requires anhydrous, oxygen-free conditions to prevent catalytic degradation. But in recent years, water has become an attractive medium in which to do chemistry, not just because of its huge abundance and environmentally benign properties, but also because of its influence on chemical reactions.[78]

**Table 8** Influence on solvent selection in Kobayashi's aqueous methodology.[79]

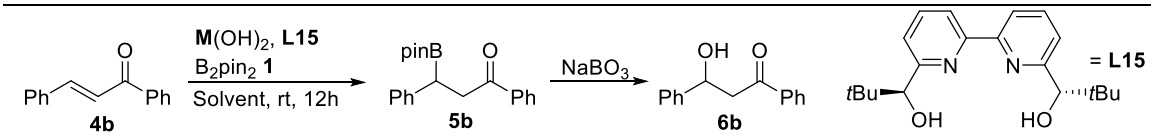


| Entry | M | Solvent | Additive | **L** | Yield (%) | *e.e.* (%) |
|---|---|---|---|---|---|---|
| 1 | Cu | $H_2O$ | - | DBA | 88 | 0 |
| 2 | Zn | $H_2O$ | - | DBA | 64 | 0 |
| 3 | Cu | $H_2O$ | - | **L15** | 83 | 81 |
| 4 | Zn | $H_2O$ | - | **L15** | 17 | 46 |
| 5 | Cu | $H_2O$ | - | **L15** | 79 | 36 |
| 6 | Cu | $H_2O$ | - | **L15** | 80 | 37 |
| 7 | Cu | THF | - | **L15** | 0 | 0 |
| 8 | Cu | Toluene | - | **L15** | 0 | 0 |
| 9 | Cu | DCM | - | **L15** | 0 | 0 |
| 10 | Cu | DMF | - | **L15** | Trace | 0 |
| 11 | Cu | DMSO | - | **L15** | 0 | 0 |
| 12 | Cu | MeOH | - | **L15** | 17 | 29 |
| 13 | Cu | EtOH | - | **L15** | 1 | 0 |
| 14 | Cu | $H_2O$ | - | **L15** | 84 | 80 |
| 15 | Cu | $H_2O$ | Pyridine | **L15** | 72 | 70 |
| 16 | Cu | $H_2O$ | AcOH | **L15** | 93 | 89 |
| 17 | Cu | $H_2O$ | TFA | **L15** | 93 | 86 |
| 18 | Cu | $H_2O$ | $PhCO_2H$ | **L15** | 86 | 81 |
| 19 | Cu | $H_2O$ | $B(OH)_3$ | **L15** | 94 | 87 |
| 20 | Cu | $H_2O$ | AcOK | **L15** | 90 | 81 |
| 21 | Cu | $H_2O$ | AcOH | **L15** | 95 | 99 |

Entries: 1-13, $M(OH)_2$ = 10 mol%; 14-21 $M(OH)_2$ = 10 mol% = 5 mol%. Optimised conditions for Entry 21 uses **L15** (6 mol%) at 5 ºC for 12 h.

It is, therefore, interesting to report the findings of Kobayashi *et al.* who reported the first copper-catalysed enantioselective protocol for the β-boration of α,β-unsaturated carbonyls in aqueous media.[79] It is important to note that in the same year Santos *et al.* reported the first copper-catalysed β-borylation under aqueous conditions.[80]

This procedure offered great potential due to the ready availability of the copper (II) salt precursor, chiral bipyridine **L15** and water (with some additives, see Table 8). Indeed, they demonstrated that this could be applied to α,β-unsaturated amides, esters and ketones. Moreover, the more challenging β,β-disubstituted enones could be β-borylated in high *e.e.* (93-97%) and conversion. In addition, they examined the regioselectivity of this protocol by examining a α,β,γ,δ-unsaturated ketone in with their methodology. To their delight, they found that this resulted in high regioselectivity, producing mainly the 1,4-addition product **6b** (96%) with excellent enantioselectivity (*e.e.* 89%).

Subsequent studies by Kobayashi *et al*. into the 1,4- *vs* 1,6-addition regiocontrol in α,β,γ,δ-unsaturated species was carried out.[81,82] It should be noted that work has been carried out in this area by Breistein, Córdova and Ibrahem *et al.*[77] Initially, they found that acyclic α,β,γ,δ-unsaturated ketones proceed to give predominately the 1,4-addition product. However, the behaviour of cyclic α,β,γ,δ-unsaturated ketones (*e.g.* **40**) was different, depending on the counter ion of the Cu(II) salt (see Scheme 14).

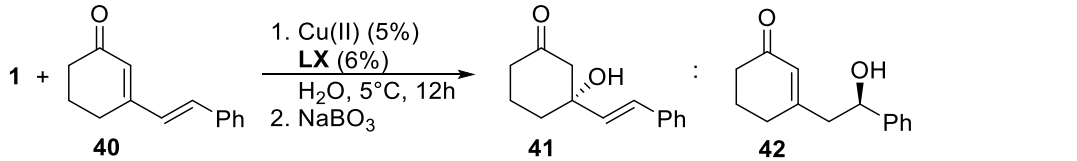


| | | | |
|---|---|---|---|
| $Cu(OH)_2$ | 1 | 99 | *e.e.* 76% |
| $Cu(OAc)_2$ | 99 | 1 | *e.e.* 91% |
| $CuSO_4$ | 56 | 44 | *e.e.* 14% : 1% |

**Scheme 14** 1,4- *vs* 1,6-addition to cyclic α,β,γ,δ-unsaturated ketones.

Indeed, modification of the counter ion, from hydroxide to acetate, allowed for the selective β-boration (1,4-addition) to γ-boration (1,6-addition), respectively. Kobayashi *et al*. rationalised this by a simple observation of the reaction. Specifically, a switch from homogeneous in, the case of $Cu(OAc)_2$, and heterogeneous with $Cu(OH)_2$. Further research was carried out in this area to elucidate the nature and mechanism of this reaction.[82] However, this will not be discussed here.

## 1.5 Mechanistic considerations

Marder *et al*. introduced the first example of 1,4-diboration to activated alkenes[19,83] which after hydrolysis, gave the corresponding β-boration product. Indirect evidence for 1,4-diboron species has been shown by other groups. Indeed, they utilised the presumed 1,4-addition intermediate for the formation of aldol products. However, the formation of such species (e.g. 5, Scheme 3) was thought to rely upon the presence of a nucleophilic boryl species, either if the reaction proceeds through an $S_N2$ or $S_N2'$ type mechanism.[84] Indeed, this idea was put forward by Miyaura *et al*., and substantiated with experimental evidence (Scheme 5).[28] It is interesting to note that nucleophilic boron species have since been reported and isolated.[31]

The initial copper-catalysed examples of conjugate boration were plagued by high catalyst loadings. The methodology of Yun *et al*. involved the use of protic additives, *i.e.* alcohols (see Table 2 and Scheme 15),[34] led them to speculate upon a plausible mechanism and suggested that a diphosphine-ligated copper-boronate species,[70] similar to the copper-boronate species suggested by Miyaura,[28] was key to the conjugate addition of the α,β-unsaturated carbonyl compounds. Furthermore, this results in either a C-bound copper intermediate or an O-bound copper enolate. Yun *et al*. suggested that the equilibrium between the C-bound and the O-bound copper intermediates was favoured towards the C-bound system and, accordingly, it would be

this species that the alcohol additive would protonate. This suggested that this copper alkoxide was the active species involved in regenerating the active copper-boronate species. Yun *et al*. also provided evidence, in the form of isotopic labelling, for the protonation of the enolate intermediate, as shown in Equation 11.

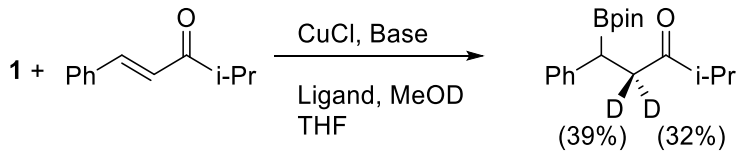


**Equation 11**

Moreover, such enolates can be trapped out by the addition of halogen electrophiles to form α-halo ketones during the β-boration process.[85]

The groups of Marder and Lin *et al*. jointly carried out extensive DFT studies to try and elucidate some aspects of the underlying mechanistic workings of such reactions.[86] As part of this endeavour, studies involving olefinic insertion to copper-boron bonds have been made[87] and, hence, led to the DFT study of the copper-catalysed boron conjugate addition of activated alkenes (namely α,β-unsaturated carbonyl containing species).[88] Their findings support a mechanism similar to that outlined in Scheme 16 by which boration results in the formation of a C-bound copper intermediate which could be protonated by the alcohol forming a ligated copper alkoxide. Such a process provides a barrier-less (as calculated by DFT methods) metathesis between such species and the diboron regent. This work substantiated the suggested mechanistic pathway proposed by Yun.[34]

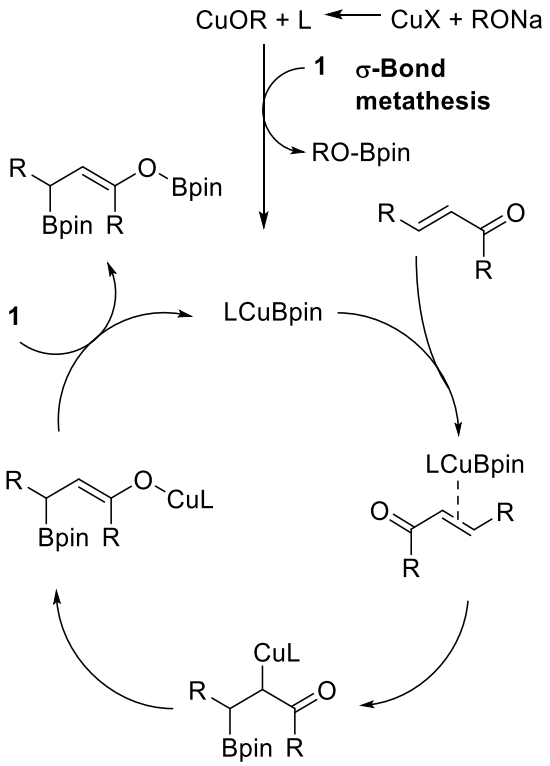


**Scheme 15** Mechanism of the copper-catalysed β-boration of α,β-unsaturated species.

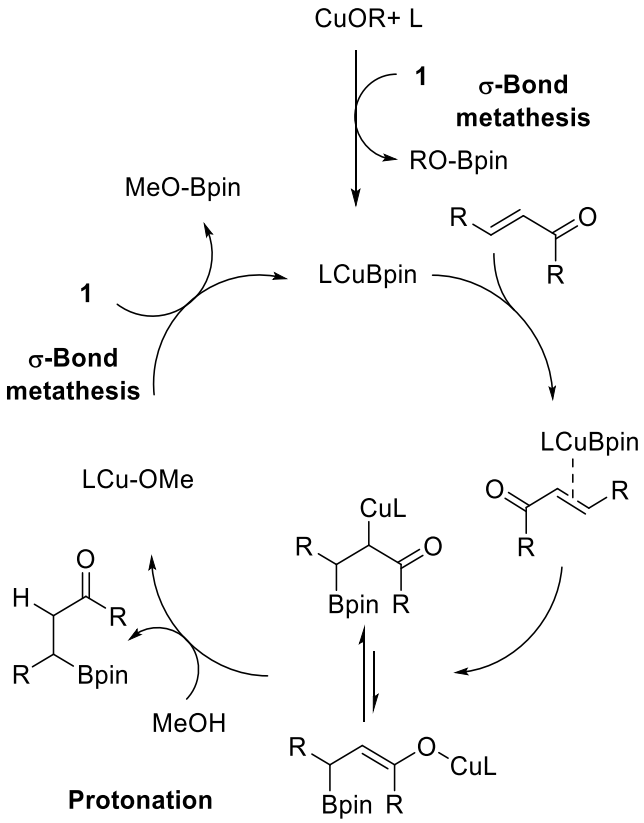


**Scheme 16** Mechanism for the copper-catalysed β-boration of α,β-unsaturated species as supported by Marder *et al*.'s DFT calculations.[88]

Marder and Lin *et al*. have, in addition to their work on the copper-catalysed β-boration, performed DFT calculations on the platinum-catalysed system.[89] Their initial calculations suggest that, unlike the copper-boron bond, in which electron density is located on boron (thus explaining the nucleophilicity), the platinum atom polarizes the platinum-boron bond towards itself, thus generating an electropositive boryl moiety. Subsequently, one cannot invoke a nucleophilic mechanism involving a catalytic platinum-boron species in the β-boration reaction. They have indeed shown, by DFT calculations and experimental observations, that the probable mechanism for the platinum catalysed protocol occurs in three distinct steps (see Scheme 17). The initial step in the reaction involves the oxidative addition of the diboron compound to the platinum(0) species **43**. This intermediate is calculated to exhibit pseudo-trigonal-bipyramidal geometry **44**. Secondly, the conjugate addition of the electron rich platinum onto the β-carbon of the α,β-unsaturated carbonyl, acrolein, and the σ-bond formation between the carbonyl oxygen and the axial boryl moiety, leading to the formation of a square planar platinum species **45**. After this, re-coordination of the carbon-carbon double bond (in acrolein) to the platinum, this results in the regeneration of a pseudo-trigonal-bipyramidal complex **46**. Finally, reductive elimination results in the 1,4-addition adduct, with the boryl units on the oxygen (of the enolate) and the β-carbon **47**. In addition, interesting computational work by Carbó and Fernández *et al*. (in the same year) supported this idea of an electrophilic mechanism.[90]

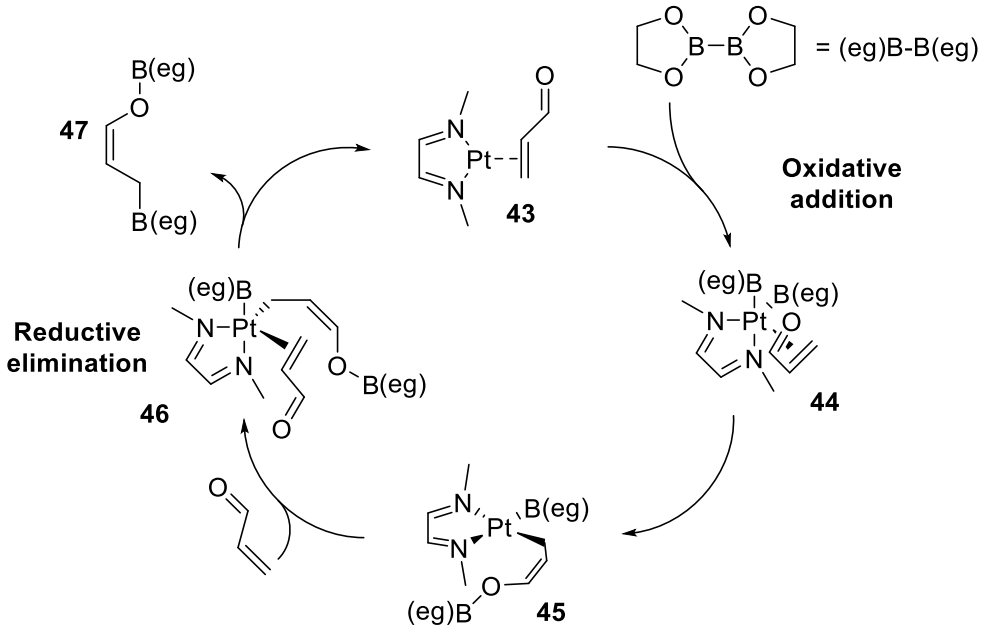


**Scheme 17** Mechanism of the platinum-catalysed β-boration of α,β-unsaturated species.

This is, therefore, consistent with the electrophilicity of the boryl ligands under platinum catalysis. Furthermore, it is consistent with the observed experimental phenomena by Marder *et al.*[19]

In light of this,[89] the mechanistic explanation appears complete; however, the organocatalytic variants of metal-catalysed boron conjugate addition cannot be understood in this mechanistic framework and brings into question the role of the reagents in such reactions. Hoveyda put forward a plausible concept by which the NHC species can generate a nucleophilic diboron adduct by the polarisation of the boron-boron bond to form an $sp^2$-$sp^3$ type species (Scheme 13). Such species have since been isolated by Marder and Lin *et al.*[91] Hoveyda suggested that this adduct can react with the electrophilic β-carbon of the activated alkenes. However, Marder and Lin *et al.* also note that from their spectroscopic observations ($^{11}$B NMR), the association between the NHC and $B_2pin_2$ **1** was weak in solution, which casts doubt on this adduct being involved in the boron conjugate addition process. An interesting side note in Hoveyda's

methodology[69] is the trapping of enolate intermediates with aldehydes to form aldol like products (analogous to the work of Shibasaki *et al*., see Scheme 11).[57] Unlike the copper-catalysed protocol, as reported by Shibasaki, the aldol products were equally formed with high levels of enantio- and diastero-control. However, under Hoveyda's organocatalysis the *syn*-diastereoisomer was the dominant isomer, unlike the copper-catalysed systems which have been reported to give the *anti*-diastereoisomer.[49,85]

Perhaps more interesting (as highlighted in Scheme 12) is that a phosphine oxide alone in the presence of $B_2pin_2$ **1** can facilitate boron conjugate addition (activation by the nucleophilic oxide coordinating to the diborane species). The ability of phosphines to be active in the metal free conjugate addition was noted by Hosomi *et al*.,[27] but like Hoveyda *et al*., Hosomi did not explore this, despite the 50% conversion to the borylated species (in the case of Hoveyda).

The organocatalytic β-boration, facilitated by phosphines, was probed by Fernández *et al*. to explore the underlying mechanism of such reactions.[72] They suggested that the acid-base interaction between the nucleophilic phosphine forms a nucleophilic adduct which, similarly to that reported by Hoveyda *et al*.,[73] can undergo conjugate addition. This mechanism was deemed consistent with the observed NMR evidence (see Scheme 18), and in particular the loss of the two $^{11}B$ signals (this suggests the presence of a $sp^2$-$sp^3$ diboron adduct, *e.g.* see Scheme 13) on addition of the activated alkene. Assuming the organocatalytic variant proceeded through this sort of mechanism, Fernández *et al*. examined the influence of Lewis acidic iron salt additives as a means of activating [92] the Michael acceptor towards conjugate addition. Interestingly, in all the examples they examined, carbonyl containing species (esters and ketones) underwent increased conversions when the additive was employed.

Intriguingly, the analogous α,β-unsaturated imines only accommodated conjugate boration in the presence of the iron additives (see Scheme 19 for a representative example).

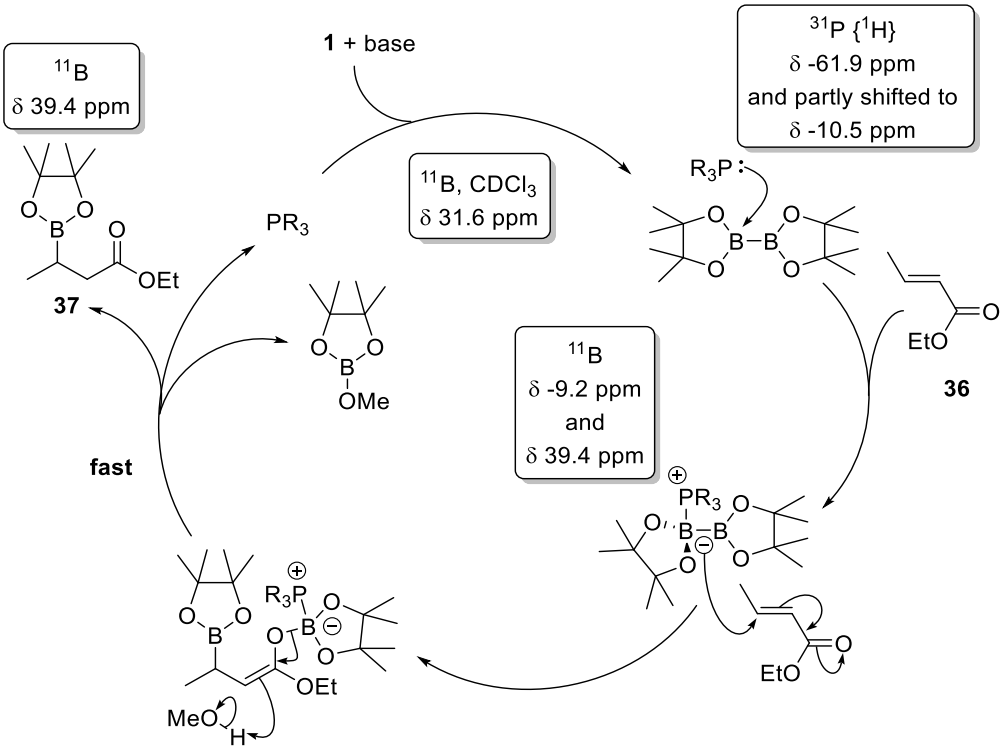


**Scheme 18** Spectroscopic evidence for the proposed organocatalytic route as described by Fernández *et al*.

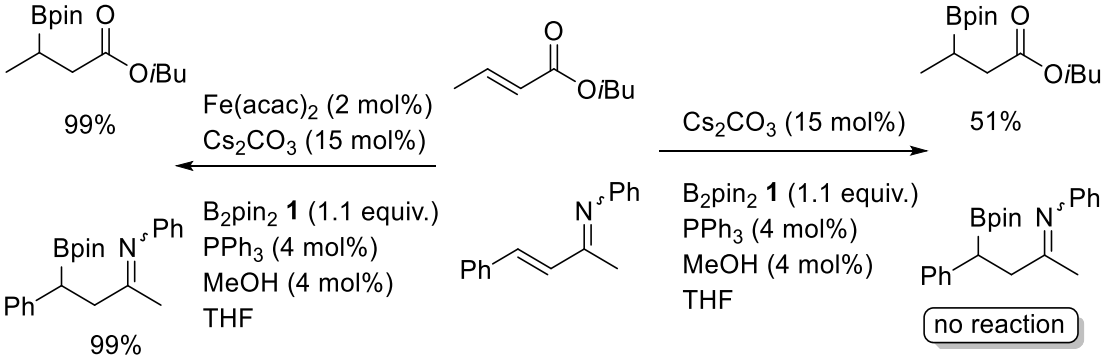


**Scheme 19** Comparison between the influence of iron additives on the β-boration of α,β-unsaturated esters and imines.

This is perhaps unexpected given that α,β-unsaturated imines have been shown previously to be more reactive to nucleophilic diboron adducts than the analogous α,β-unsaturated carbonyl containing species.[59,60] In light of this, it would be interesting to examine the effect of introducing metal salts on other organocatalytic systems, such as that developed by Hoveyda *et al*., because this suggests that activation of the carbonyl should aid conjugate boration when conversions are particularly low.

Still, alternative theories have been put forward to suggest the roll of the phosphines in the organocatalytic β-boration. Indeed, Fernández *et al.* reported other computational and experimental data[93] which shows that the phosphines can undergo a 1,4-addition to the α,β-unsaturated carbonyl compound (analogous to the Baylis-Hillman reaction[94]) which leads to the formation of an ion-pair intermediate (when in the presence of MeOH and the diboron compound 1) which  to explain the catalytic behaviour of such systems.

## 1.6 Summary

The area of boron conjugate addition (β-boration) is not only fascinating, but serves as a valuable synthetic utility for the preparation of simple organic building blocks that represent key structural moieties in many biologically active species and materials. Since the first examples appeared, transition metals have played a crucial role in facilitating this process. Platinum,[19] rhodium,[95] palladium and nickel[40] have all been shown to facilitate boron conjugate addition, but perhaps due to the work of Yun *et al*., and use of alcohol additives, copper is now the most used catalytic system in the area.[53] Recently, some groups have developed alternative methods by which β-boration can be achieved by organocatalytic means and they have obtained some excellent results. Such methodologies have not yet displayed results to rival their metal-catalysed equivalents;

however, it is likely that these organocatalytic routes will develop with the use of additives, resulting in more sustainable chemical processes.[96]

A number of mechanistic theories[88] have been put forward that aim to explain the metal-catalysed methodologies. In addition, mechanistic theories have been putforward to explain the the organocatalytic reaction. Further developments are likely to be made in order to satisfactorily explain all the observed results.[91] To this end, further research is likely to be focused not only on developing new borylation systems, especially organocatalytic protocols and new asymmetric methods, but also on further mechanistic interpretations.

# Results & Discussion

## 2.0 Project aims

The ability to control multiple stereocentres in the design and preparation of simple molecular architectures is still a major challenge to organic chemists.[97] Indeed, this problem becomes more apparent when considering the necessity of simple chiral molecules and, more specifically, their role as precursors in the preparation of pharmaceuticals.[98]

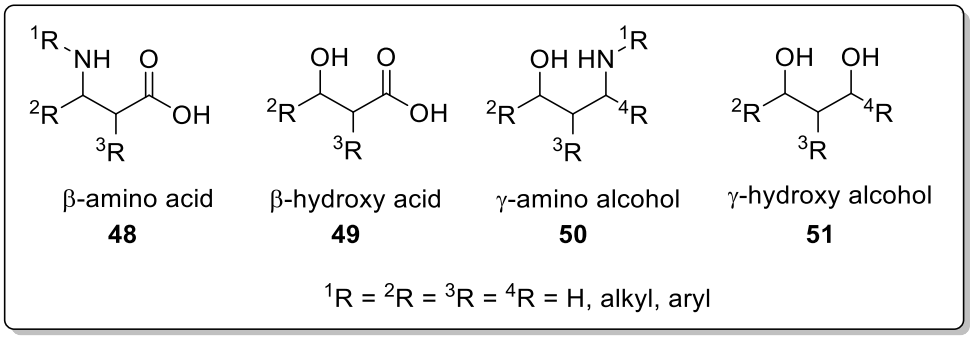


**Figure 5** Molecules of interest throughout this thesis.

β-Amino acids **48**,[99] β-hydroxy acids **49**,[100] γ-amino alcohols **50**[101] and γ-hydroxy alcohols **51**[102] (Figure 5) have received attention in the literature[103,104,105] due to their utility in catalysis, as top-selling pharmaceuticals and precursors to complex natural products. However, a low-cost, sustainable, asymmetric route to such species is still a challenge due to the potential obstacle of controlling up to three contiguous stereocentres.

The aim of this project was to develop a simple, sustainable, synthetic methodology for the preparation of chiral β-amino acids **48**, β-hydroxy acids **49**, γ-amino alcohols **50** and γ-hydroxy alcohols **51** (*i.e.* 1,2,3-trifunctional materials). The initial aim involved the utilisation of asymmetric β-boration technology on prochiral activated alkenes, α,β-unsaturated imines. Subsequent transformations would thus yield the desired targets.

## 2.1 γ-Amino alcohols

γ-Amino alcohols **50** and their derivatives are found in some of the world's top-selling pharmaceuticals (Figure 6), for example: Fluoxetine and Duloxetine (also known as Prozac and Cymbalta, respectively). These γ-amino alcohol derivatives are utilised medically as antidepressants,[106] with Fluoxetine belonging to the selective serotonin reuptake inhibitor (SSRI)[107] class of antidepressants, and Duloxetine belonging to the serotonin-norepinephrine reuptake inhibitor (SNRI)[108] class (see Venlafaxine[109]). It is interesting to note that the total sales of Fluoxetine peaked at 2.2 billion US Dollars in 1998[110] and, according to IMS Health, sales of Duloxetine reached 5.8 billion US Dollars in 2012, making it one of the top-ten selling drugs worldwide.[111] Tramadol,[112] used to treat moderate to severe pain (also see Ciramadol[113]), is another example of γ-amino alcohols being utilised for medical applications.

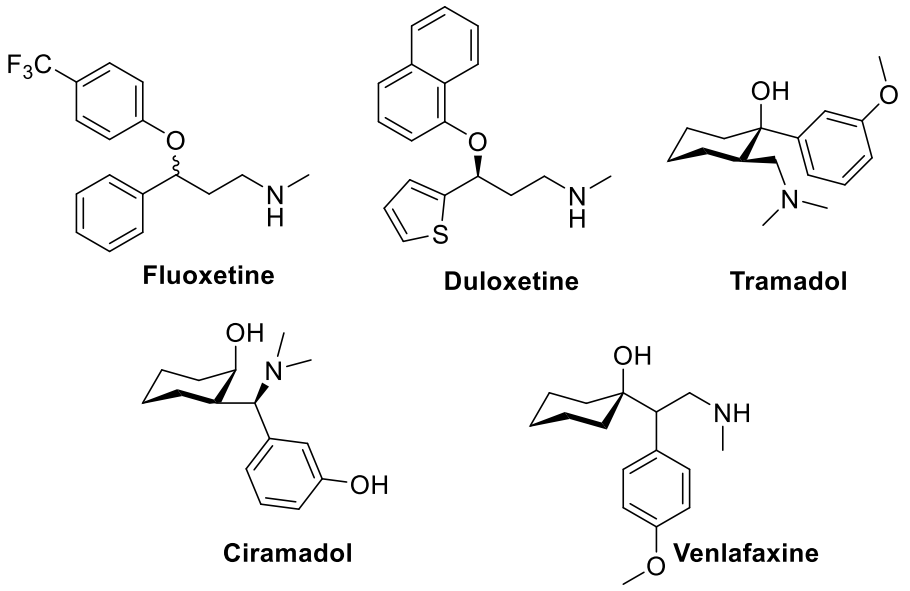


**Figure 6** γ-Amino alcohol-based pharmaceuticals.

Various approaches towards the synthesis of γ-amino alcohols exist in the literature.[114] Indeed, Scheme 20 shows several named reactions which can potentially serve as routes towards the synthesis of γ-amino alcohols.

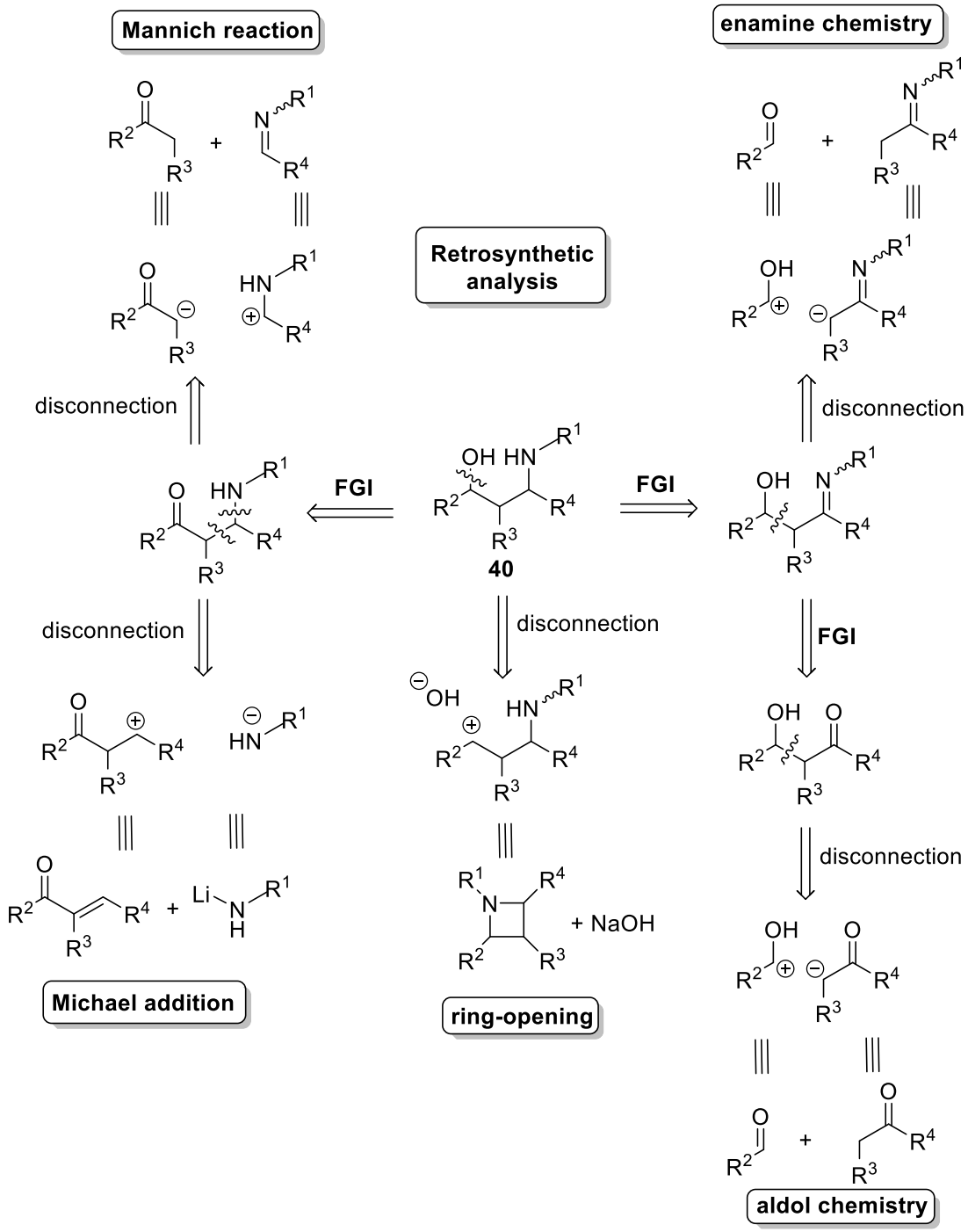


**Scheme 20** Retrosynthetic analysis of γ-amino alcohols **40**.

In the context of metallo-emamine chemistry, Ellman *et al*.[58] employed chiral *N*-sulfinyl imines **54** for the preparation of β-hydroxy *N*-sulfinyl imines **55**, which allowed for the selective preparation of either the *anti*- or *syn*-diastereoisomers (see Scheme 21).

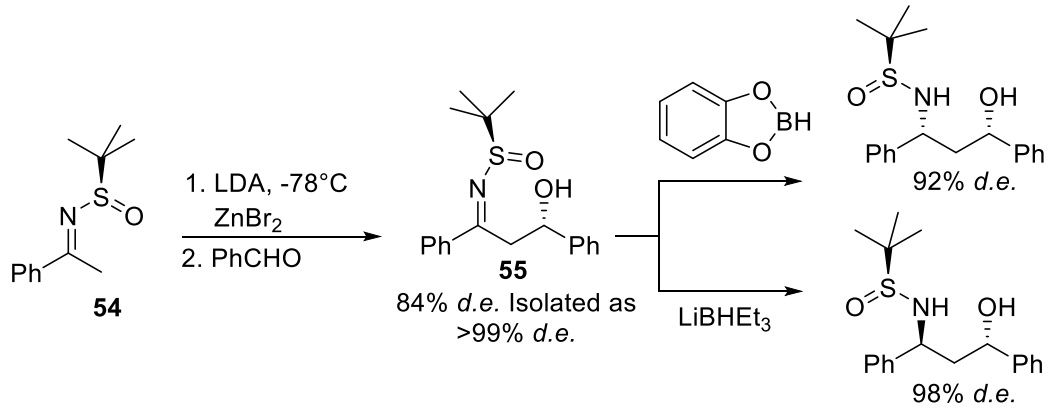


**Scheme 21** Ellman's *N*-sulfinyl imine chiral auxiliary approach to the synthesis of γ-amino alcohols.

Other examples in the literature include the selective ring-opening of *N*-tosylazetidines with alcohols in the presence of Lewis acids.[115]

One of the most common methods for the synthesis of γ-amino alcohols are based on asymmetric hydrogenation.[116] Indeed, Zhang *et al*. reported the asymmetric synthesis of γ-amino alcohols through the asymmetric hydrogenation of β-amino ketones (see Equation 12).[61] This was later expanded to encompass the control of multiple stereocentres, in a highly enantio- and diastereoselective synthesis of γ-amino alcohols from β-ketoenamides.

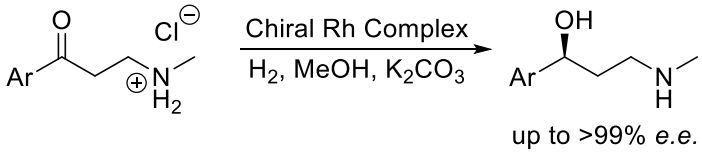


**Equation 12**

In addition to asymmetric hydrogenation, the Mannich reaction serves as a useful tool for the synthesis of β-amino ketones (Scheme 20).[117] Such species are complimentary intermediates, in the context of asymmetric hydrogenation, for the synthesis of γ-amino alchols (see Equation 12 and Scheme 21).

It should be mentioned that Davies *et al*. have produced a plethora of work on asymmetric conjugate addition of chiral lithium amides[118] to α,β-unsaturated esters and amides.[119] Indeed, such studies have resulted in this methodology being employed in the total synthesis of natural products.[120] It is clear from looking at the intermediates[121] of such reactions that this methodology could be applied to the synthesis of γ-amino alcohols through the derivatisation of the product β-amino esters.[122]

### 2.1.1 Developing a one-pot route towards γ-amino alcohols

In 2009, Fernández *et al*. introduced a protocol for the preparation of β-hydroxyl imines.[59] This was later expanded to the enantio- and diastereoselective synthesis of γ-amino alcohols[60] and γ-hydroxy alcohols[64] in collaboration with Whiting *et al*. An asymmetric route to these difunctional species required the technology to control multiple stereocentres. This was achieved by three key steps in the methodology (see Table 5 and Scheme 10):

- Enantioselective copper-catalysed β-boration of α,β-unsaturated imines;
- Substrate controlled asymmetric reduction of the imine functionality;
- C-B oxidation with retention of stereochemistry.

This protocol is highly useful for the preparation of γ-amino alcohols and γ-hydroxy alcohols where $^{4}R$ = Ph, Ar, etc. (see Figure 5). This is due to the relative ease in preparing α,β-unsaturated imines from the analogous enals or enones due to the β-carbon being less susceptible to Michael addition. In turn, this results in the direct

1,2-addition-elimination of a primary amine to the carbonyl, which gives the resulting imine (see Scheme 22).

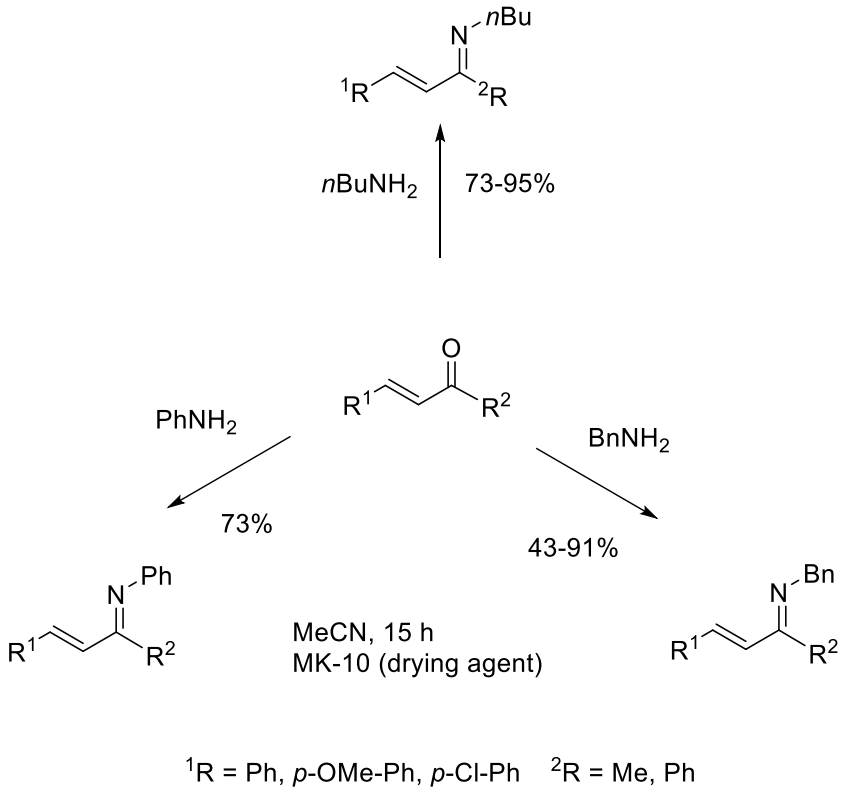


**Scheme 22** Preparation of α,β-unsaturated imines *via* 1,2-addition to the analogous carbonyl compound.

However, the purification of such species is problematic due to the susceptibility of the imino-group (C=N) to being readily hydrolysed to the parent carbonyl compound. In addition, if these species are to be utilised synthetically, bulky substituents throughout the structure may not be desired. Also, bulky substituents on the β-carbon of these β-unsaturated imines would render this methodology useless in the preparation of the analogous β-amino acids and β-hydroxy acids, due to the inability of secondary or tertiary alcohols to be oxidised to the carboxylic acid level. It was, therefore, clear that the first challenge to overcome was the preparation of a versatile array of α,β-unsaturated imines (species where $^{1}$R = H, Me, see Scheme 22) and, in this process,

the development of a simple method for the purification for such species.

α,β-Unsaturated imines are becoming increasingly explored in recent years.[123,124] Indeed, they have even found a place in the preparation of pharmaceuticals.[125,126] However, routes towards the preparation of α,β-unsaturated imines are limited. The conventional method of 1,2-addition-elimination to the parent carbonyl compound (using an appropriately nucleophilic amine) is a common method.

Interestingly, Schomaker *et al.* demonstrated a method by which α,β-unsaturated imines can be prepared from the coupling of allylic alcohols and an amine under Rh-catalysis.[127] Other groups have demonstrated the synthesis of such species *via* the aza-Wittig reaction (see Scheme 23).[128,129]

Having examined the literature for suitable methodologies for the preparation of α,β-unsaturated imines, it seemed logical to prepare such desired α,β-unsaturated imines *via* the aza-Wittig reaction (see Scheme 23).[130] However, this would have involved handling potentially explosive azides, in addition to the additional two steps (alkyl azide synthesis followed the *in situ* preparation of the desired iminophosphorane) to the reaction protocol. Assuming that this methodology would proceed as planned, problems associated with the purification of such species were anticipated and other pathways had to be considered. Fortunately, alternative routes to α,β-unsaturated imines are present in the literature. Indeed, such species are employed in the preparation of dihydropyridines and pyridines, as shown by Ellman *et al.* (see Scheme 24).[131] The α,β-unsaturated imines employed in the named example were specifically the species with non-bulky R-substituents at the $C_\beta$ position (**56**-**58**).

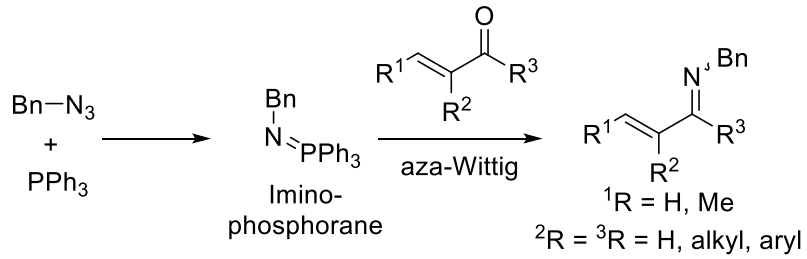


**Scheme 23** Planned route to α,β-unsaturated imines *via* the aza-Wittig reaction.

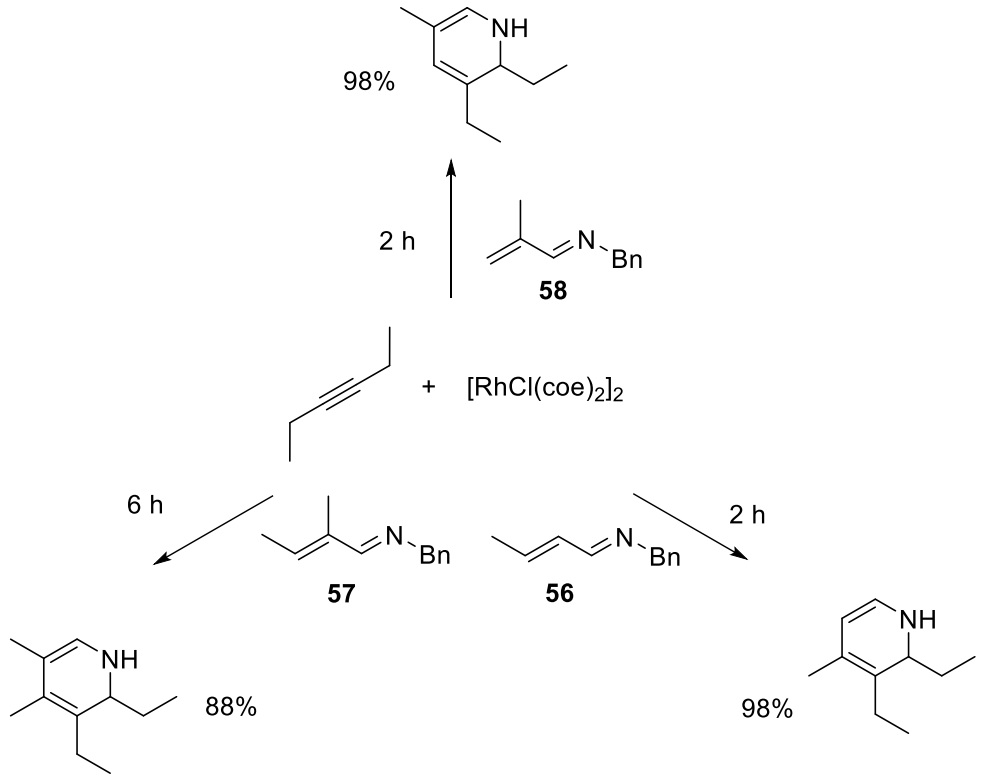


**Scheme 24** Preparation of dihydropyridines, as demonstrated by Ellman *et al*.

This paper[131] described the preparation of the desired α,β-unsaturated imines *via* a simple 1,2-addition to the analogous α,β-unsaturated carbonyl species (see Scheme 25).[132]

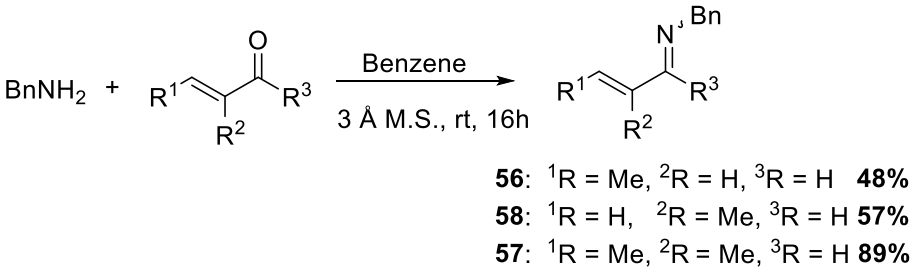


**56**: $^{1}$R = Me, $^{2}$R = H, $^{3}$R = H **48%**
**58**: $^{1}$R = H, $^{2}$R = Me, $^{3}$R = H **57%**
**57**: $^{1}$R = Me, $^{2}$R = Me, $^{3}$R = H **89%**

**Scheme 25** Method for preparing α,β-unsaturated imines.

Hence, the preparation of such species was examined with minor changes to the reaction conditions (toluene was employed instead of benzene); the results of which are shown in Scheme 26.

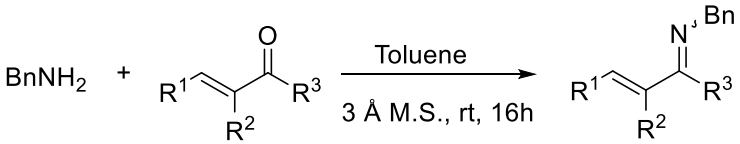


**4a**: $^{1}$R = Ph, $^{2}$R = H, $^{3}$R = Me
**59**: $^{1}$R = Me, $^{2}$R = H, $^{3}$R = H
**60**: $^{1}$R = H, $^{2}$R = Me, $^{3}$R = H
**61**: $^{1}$R = Me, $^{2}$R = Me, $^{3}$R = H

**62**: $^{1}$R = Ph, $^{2}$R = H, $^{3}$R = Me **22%**
**56**: $^{1}$R = Me, $^{2}$R = H, $^{3}$R = H **7%**
**58**: $^{1}$R = H, $^{2}$R = Me, $^{3}$R = H **34%**
**57**: $^{1}$R = Me, $^{2}$R = Me, $^{3}$R = H **21%**

**Scheme 26** Results from the preparation and isolation of α,β-unsaturated imines.

Disappointingly, the desired species were difficult to purify due to apparent decomposition and polymerisation, even by using Kugelröhr distillation. It was therefore considered whether it was necessary to purify these species. Moreover, could these species be prepared *in situ* and be utilised effectively in their crude form?[133]

Reductive amination is a common functional group transformation by which the addition of an amine to a carbonyl containing species (aldehydes or ketones) results in the formation of an imine. The resulting imine can subsequently be reduced (typically in a one-pot procedure) to yield the analogous amine. The reductive amination of α,β-unsaturated species has also been explored.[134] As previously stated, the addition of

amines to α,β-unsaturated carbonyls can result in either 1,4- or 1,2-addition depending on the given nucleophile/electrophile. If α,β-unsaturated imines are to be utilised, an effective way of gauging which species undergoes 1,2- and not 1,4-addition needed to be acquired. Allylic amines are typically more stable due to their reduced ability to undergo hydrolysis when compared to their analogous α,β-unsaturated imines. Indeed, reductive amination was considered to be a good way of gauging which substrate proceeded through 1,2-addition (and thus indirect evidence of α,β-unsaturated imine formation). The reductive amination of crotonaldehyde **59** and tiglic aldehyde **61** (low isolated yield of the parent imine) led to the formation of the analogous allylic amines in moderate to high yields (47 and 88%, respectively, see Scheme 27). Unsurprisingly, the reductive amination of cinnamaldehyde proceeded likewise (74%, see Scheme 27). Both of these results were consistent with the presence of the intermediate α,β-unsaturated imine species, as prepared by both Ellman *et al.*[131,132] and Fernández *et al.*[60,64]

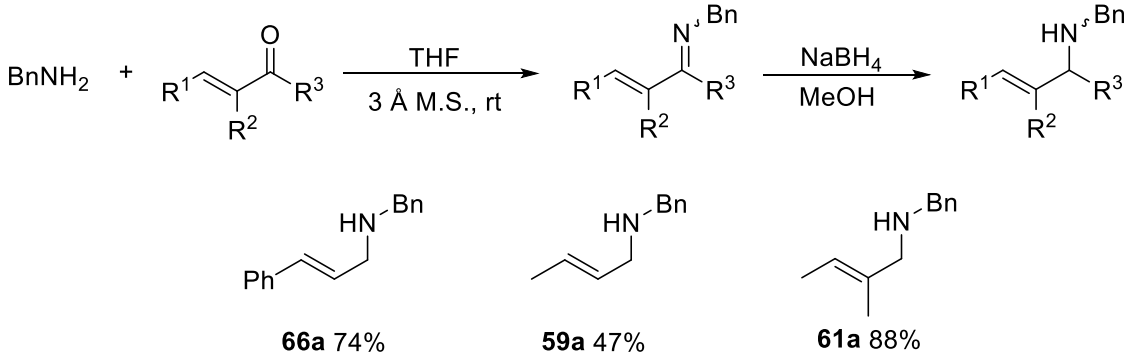


**Scheme 27** Reductive amination of α,β-unsaturated imines

It was disappointing to discover that methyl vinyl ketone proceeded through 1,4-addition, as the α,β-unsaturated imines of such species were ideal substrates for the devised methodology. This proved to be an effective way of gauging which species proceeded through the α,β-unsaturated imine intermediate. Information regarding the kinetics of the formation of α,β-unsaturated imines is limited. Therefore, investigation

by *in situ* IR Spectroscopy (ReactIR[135]) of the reaction between benzylamine and a series of α,β-unsaturated aldehydes (enals) and ketones (enones) was carried out as a means of:

- Understanding 1,2- *vs.* 1,4-addition of amines to enals or enones;
- Following the kinetics of imine formation (reaction times);
- Determining which substrates were applicable to this methodology.

The results obtained from the ReactIR experimentation will not be discussed here in detail (see section 2.2 for a full discussion). However, in summary, 1,2-addition-elimination of benzylamine to the examined α,β-unsaturated aldehydes and ketones proceeds to completion in the order of a few hours. This is significantly quicker when compared to the results reported in the literature (overnight/24 hours).[131] Moreover, these results suggested that it might not be necessary to isolate such species at all. These results suggested that it could be possible to develop a four-step, one-pot reaction protocol whereby the desired α,β-unsaturated imines are generated *in situ*, and can subsequently undergo the previously established three-steps towards γ-amino alcohol **26** synthesis (see Scheme 10). The first experiment that established this as a possibility was the copper-catalysed β-boration, reduction sequence of the α,β-unsaturated imine **58** (formed *in situ* from benzylamine and methacrolein **60**, see Scheme 28).

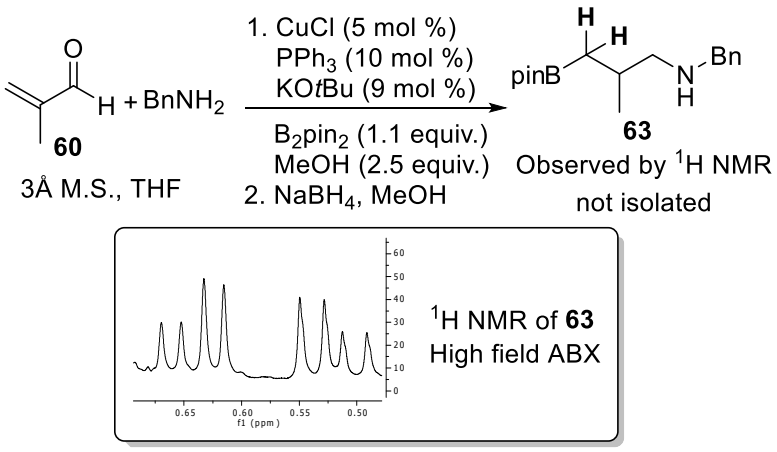


**Scheme 28** Probing the four-step, one-pot reaction on methacrolein **60**.

This reaction was conducted in the presence of 3 Å-molecular sieves to aid imine formation and prevent any possible imine hydrolysis due to water generation. It is important to note that the use of 4 Å-molecular sieves was examined; however, 4 Å-molecular sieves exhibit methanol scavenger properties[136] Hence due to this, 4 Å molecular sieves could inhibit the β-boration step due to methanol absorption and as noted in the introduction, methanol is essential for catalysis. The reaction was stopped before the final oxidation step (see Scheme 28). The ability to oxidise C-B bonds is well documented and,[2] therefore, the synthesis of γ-amino boron esters **63** would have been an appropriate probe in assessing the reaction. Interestingly, the reaction proceeded as predicted (as observed by $^{1}$H & $^{11}$B NMR, see Scheme 28); however, the products proved difficult to purify by chromatographic means and, therefore, it was difficult to optimise this protocol on this particular substrate.

Next, attention was turned to enone **4a** as a suitable substrate on which to optimise this potential four-step, one-pot protocol. The results of this optimisation are summarised in Table 9.

Perhaps as expected, an increase in the conversion of **4a** to **64** with increased catalyst loading was observed (Entries 1-5, Table 9). Conversely, a decrease in the

conversion of **4a** to **64** is observed when catalyst loadings are increased beyond 5% (Entry 7). This at first may seem counterintuitive; however, this can be rationalised by assuming that higher catalyst loadings favour Pathway A, as shown in Scheme 29. Indeed, it has been shown in the literature that the β-boration of α,β-unsaturated imines is faster, under the copper-catalysed system, when compared to that of the analogous carbonyl compound.[59]

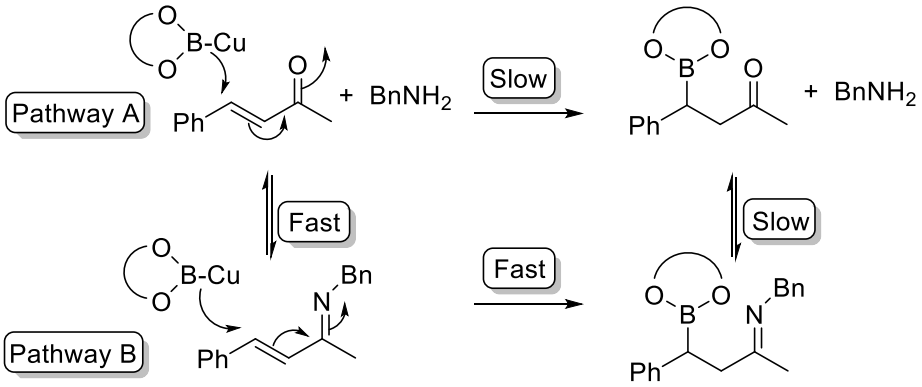


**Scheme 29** Competing pathways in one-pot reaction; Michael *vs.* direct addition of benzylamine.

**Table 9** Optimisation of the one-pot methodology.

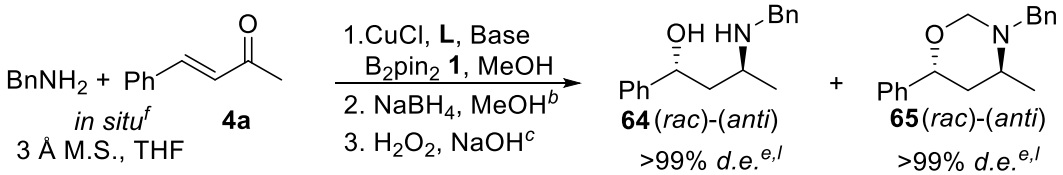


| Entry | CuCl (%) | **L** (%) | Base (%) | t[d] (h) | Conv.[e] (%) **64** | Conv.[e] (%) **65**[k] | Yield (%) **64** | Yield (%) **65** |
|---|---|---|---|---|---|---|---|---|
| 1 | 1 | $PPh_3$ (2) | KO*t*Bu (20) | 24 | 37 | 30 | 17 | 32 |
| 2 | 3 | $PPh_3$ (6) | KO*t*Bu (9) | 24 | 42 | 29 | 40 | - |
| 3 | 5 | $PPh_3$ (10) | KO*t*Bu (18) | 24 | 63 | 27 | 62 | - |
| 4 | 5 | $PPh_3$ (10) | KO*t*Bu (18) | 48 | 62 | 36 | 56 | - |
| 5 | 5 | P(*n*Bu)$_3$ (10) | KO*t*Bu (18) | 18 | 63 | 34 | 63 | - |
| 6[g] | 5 | P(*n*Bu)$_3$ (10) | NaO*t*Bu (18) | 18 | >95 | 0 | 90 | - |
| 7 | 10[j] | $PPh_3$ (20) | KO*t*Bu (36) | 24 | 40 | 27 | 25 | - |
| 8[h] | 5 | $PPh_3$ (10) | NaO*t*Bu (15) | 18 | 52 | 34 | - | 30 |
| 9[i] | 5 | $PPh_3$ (10) | NaO*t*Bu (15) | 18 | 44 | 54 | - | 51 |

[a] Reactions carried out on a 1-1.5 mmol scale. [b] $NaBH_4$ (3 equiv.), MeOH (excess). [c] 1 : 1, NaOH : $H_2O_2$ (THF), 1 h reflux. [d] Reaction time for 1h, benzylamine and Cu–B cat. in one-pot. [e] Determined by $^1$H NMR. [f] Imines were formed *in situ* (1 : 1 amine : α,β-unsaturated carbonyl, 3 Å M.S., THF, 6 h) and transferred to Cu–B cat (18 h). [g] MeOH removed prior to oxidation (*via* vacuum). [h][O] NaOH, $H_2O_2$ (1 : 1, 20 equiv.), MeOH (10 ml), 4 h reflux. [i][O] NaOH, $H_2O_2$ (1 : 1, 40 equiv.), MeOH (15 ml), 4 h reflux. [j] High catalyst loadings favour β-boration of the a,b-unsaturated carbonyl without formation of imine. [k]**65** was confirmed by the reaction of **64** with $CH_2O$ (1.1 equiv.) in THF, rt, 4.5 h (74% yield). [l] *anti*-Diastereoisomer had previously been confirmed.[60]

Furthermore, increasing reaction times to from 24 to 48 hours resulted in no significant change in the overall conversion to γ-amino alcohol **64** (Entries 3 and 4, Table 9). This was repeated several times and still the reaction appeared to plateau at 62-63% conversion to **64**. After extensive chromatographic purifications, small amounts of allylic amine (<5%) were isolated, indicating no β-boration of the α,β-unsaturated imine (imine is reduced to the allylic amine on addition of $NaBH_4$).

More importantly, perhaps, was the isolation of a significant side product. This would ultimately lead to the optimisation of the one-pot methodology.

The side product was identified and found to be the cyclic 1,3-oxazine **65**. It was considered that methanol, under the oxidising conditions of the one-pot methodology, could perhaps form formaldehyde, which could be trapped by the γ-amino alcohol **64** to complete the cyclic 1,3-oxazine **65**. This was probed by simple changes to the experimental procedure in which methanol was removed from the system (*via* rotary evaporation) prior to the oxidation. Then, THF, NaOH and $H_2O_2$ was added to the resulting crude mixture and subsequently heated to reflux for one hour. This resulted in the high conversion of **4a** to the γ-amino alcohol **64** (>95%), but more importantly, no formation of the 1,3-oxazine **65** (Entry 6, Table 9). The formation of the 1,3-oxazine **65** can be forced by increasing the quantity of methanol, NaOH and $H_2O_2$ during the oxidation step, leading to 54% conversion to **65** (see Entry 9, Table 9).

### 2.1.2 1,3-Oxazine formation

The formation of the 1,3-oxazine **65** was highly unexpected. Indeed, there is limited literature regarding the transformation of methanol to formaldehyde, or equivalents thereof, under these conditions. Although, it should be noted that boric acid-catalysed oxidations are known (hydrogen peroxide used as an oxidant)[137, 138] and have been used to oxidise organic sulfides.[139] In addition, Punniyamurthy *et al*. have examined the copper(II)-catalysed C-H bond oxidation of saturated hydrocarbons using hydrogen peroxide.[140] This methodology was applied to the oxidation of primary alcohols which, upon the addition of (2,2,6,6-tetramethyl-piperidin-1-yl)oxyl (TEMPO) and oxygen ($O_2$), gave the corresponding aldehydes in good yield.[141]

With regards to the methanol oxidation (to formaldehyde), it is important to comment on some of the early reports of the preparation of formaldehyde[142] from methanol *via* the process of catalytic[143] or thermal dehydrogenation.[144] Hoffmann was able to prepare formaldehyde by passing methanol vapour over platinum wire, thus providing the first unambiguous preparation of formaldehyde.[145] Crucially, early reports on the thermodynamics of such processes discussed the thermal dehydration of methanol to formaldehyde at temperatures ranging from 200 to 450 ºC, noting that they consider this to be an equilibrium process (see Equation 13).[146]

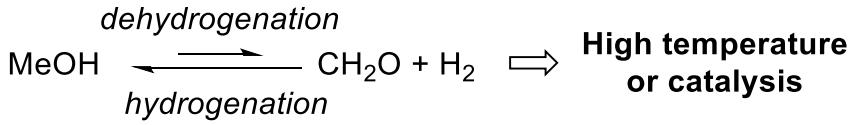


**Equation 13**

Moreover, they found that the equilibrium could be favoured towards formaldehyde under high temperature (450 ºC). Nevertheless, appreciable proportions of formaldehyde were formed *via* this method at lower temperatures (2.4% at 200 ºC).

In the case of the one-pot methodology, formation of 1,3-oxazine **65** occurs during the oxidation step (due to the presumed presence of formaldehyde), still in the presence of methanol, hydrogen peroxide, copper salts and various boronate-type species, all of which are being heated together at reflux (not dissimilar to previous reports).[139,141] Despite methanol being identified as the formaldehyde precursor, the species responsible for dehydration/oxidation of methanol is still not resolved, but it is perhaps not implausible that such conditions can generate formaldehyde in small concentrations, thus leading to the iminium intermediate (Scheme 30) being trapped (equilibrium process) to form the resulting 1,3-oxazine **65**. See appendix for an investigation into the copper, peroxide and boric acid-catalysed oxidation of primary alcohols to aldehydes.

When 1,3-oxazine **65** was first isolated, it is important to note that this species did not display the typical characteristics of γ-amino alcohols. More specifically, when γ-amino alcohols are subjected to purification by column chromatography, due to the basicity of the amine functionality and the acidity of the silica gel (stationary phase), these compounds, like other amine containing species, tend to streak during purification (also observed *via* TLC), leading to poor resolution and longer elution times, which was not the case with the 1,3-oxazine **65**.

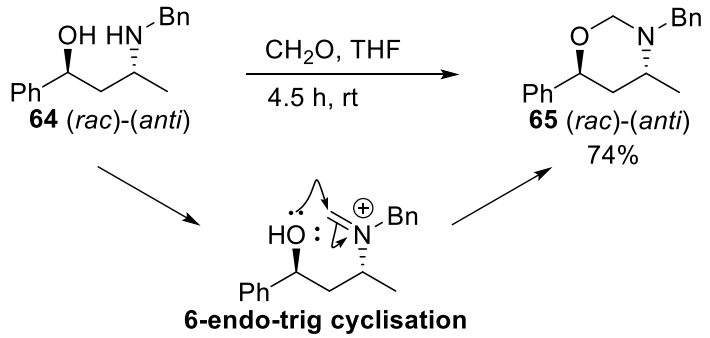


**Scheme 30** 1,3-Oxazine **65** formation from the parent γ-amino alcohol **64**.

When one compares the $^{1}$H NMR spectra of the 1,3-oxazine **65** and γ-amino alcohol **65**, it is clear that they are extremely similar, leading to the suspicion that the 1,3-oxazine **65** could, at first glance, be a diastereoisomer of γ-amino alcohol **64**. However, the $^{1}$H NMR of the 1,3-oxazine **65** contains an additional AB-splitting pattern (compare Figure 7 and Figure 8). In addition, $^{13}$C NMR and DEPT-135 (See Figure 9) experimentation revealed the presence of an additional $CH_2$-carbon (δ 83.7 ppm). This, in tandem with IR spectroscopy (no visible OH and NH stretches), CHN-analysis and mass spectrometry suggested, beyond reasonable doubt, that the 1,3-oxazine **65** had indeed formed in the reaction mixture.

The presence of **65** was further confirmed experimentally by the addition of aqueous formaldehyde solution to γ-amino alcohol **64** which, after 4.5 hours, resulted in

the formation of 1,3-oxazine **65** (74% isolated yield, Scheme 30) despite the lack of drying agents or additives (to promote the loss of water in the cyclisation step).[147] See Appendix 1 for additional COSY, HMBC, HSQC and NOESY NMR experiments that aided the elucidation of structure **65**.

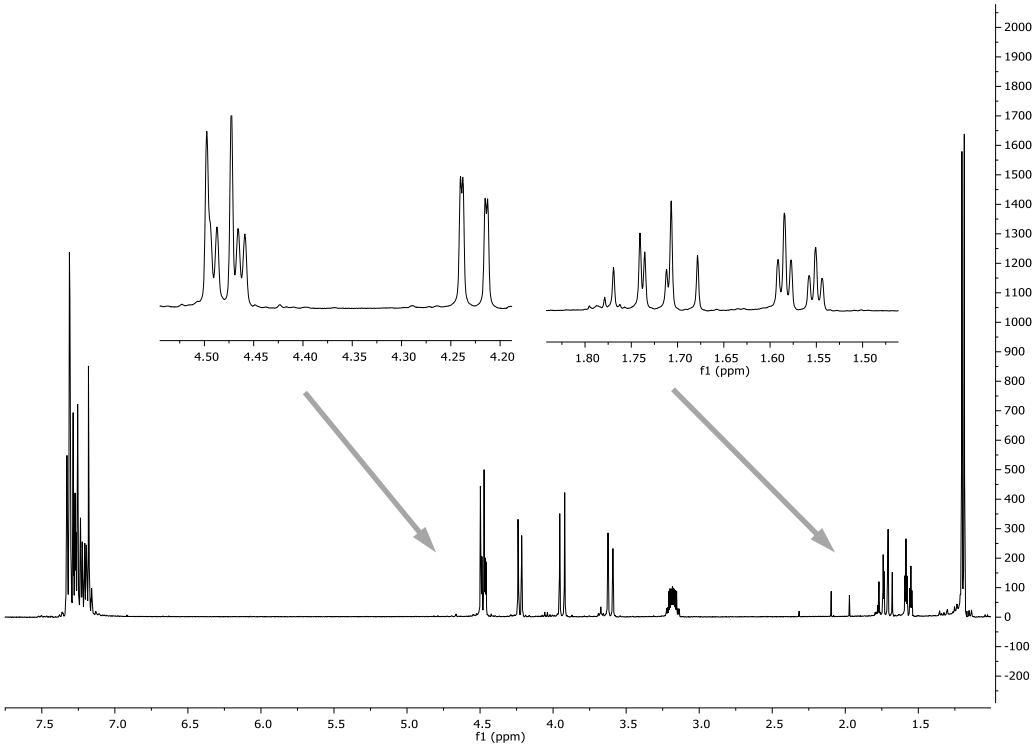


**Figure 7** $^{1}$H NMR Spectrum of the 1,3-oxaxine **65**, showing similar splitting to that of compound **64**. Characteristic AB-splitting pattern for the N-C$\underline{H_2}$-O is observed between 4.50-4.20 ppm, with unresolved $^{4}J$-coupling in the peak at 4.23 ppm.

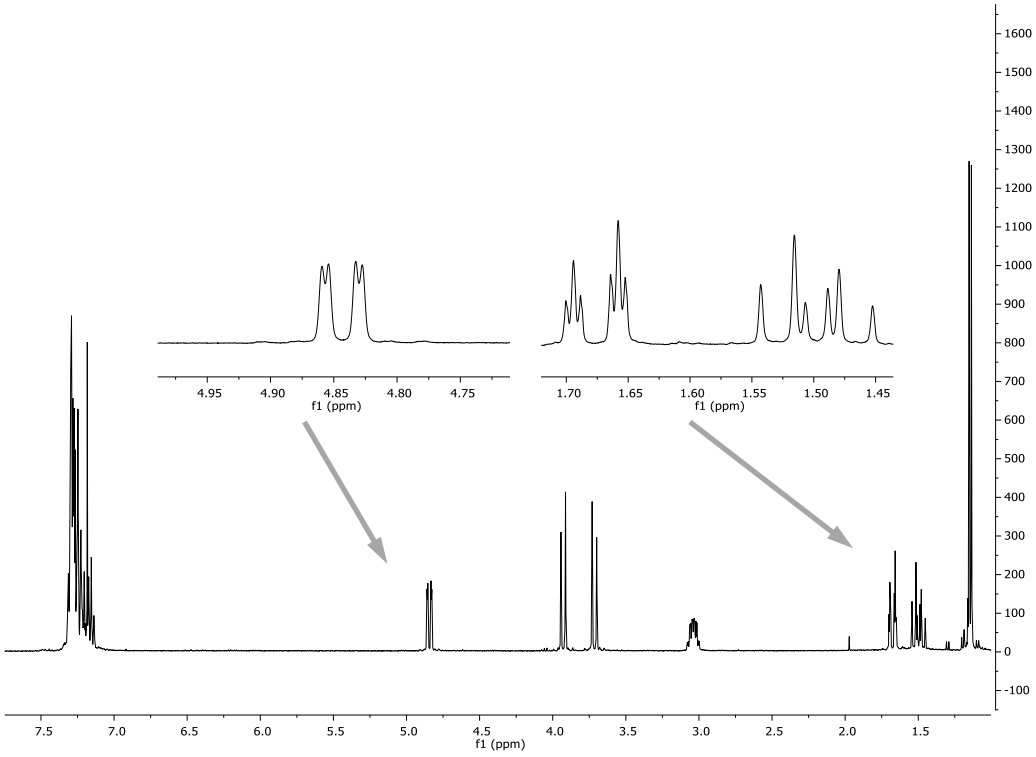


**Figure 8** $^{1}$H NMR Spectrum of the γ-amino alcohol **64**, isolated as a single *anti*-diastereoisomer.

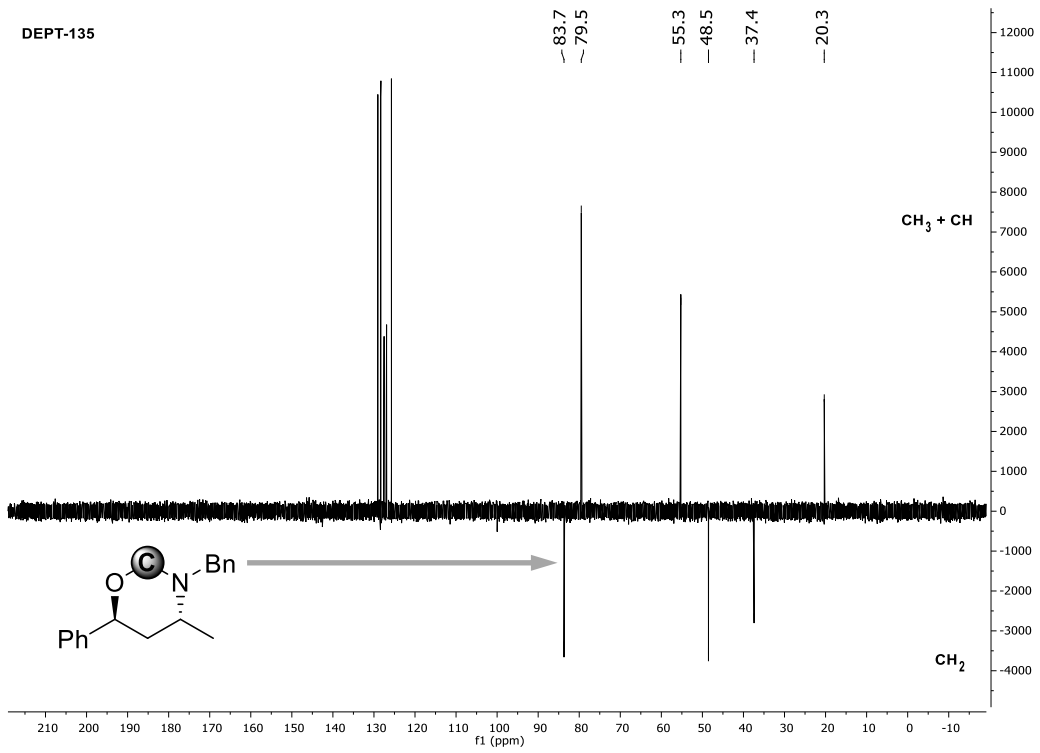


**Figure 9** $^{13}$C NMR DEPT-135 Analysis on compound **65**: $CH_2$ appear negative; $CH_3$ and CH appear positive (quaternary carbons are not visible).

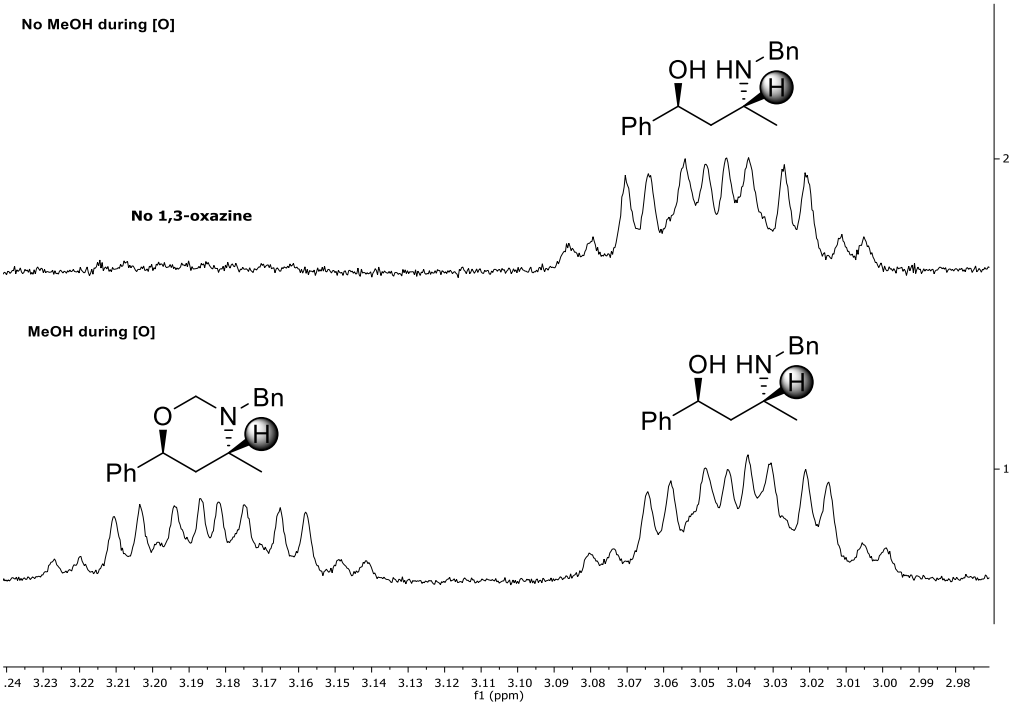


**Figure 10** $^{1}$H NMR spectrum of the crude reaction mixture of Entry 3 (bottom) and Entry 6 (top), Table 9 (multiplet of the C-H highlighted in the above structures).

After the structure of the 1,3-oxazine **65** had been confirmed, retrospective examination of the $^{1}$H NMR spectrum of the crude reaction mixtures (shown in Table 9) allowed for the ratios of the 1,3-oxazine **65** and the γ-amino alcohol **64** to be determined. This was achieved by integration of the signal of the hydrogen atom α-to the amino group (in each respective species), as shown in Figure 10. Clearly, when methanol was present during the oxidation step, a mixture of the 1,3-oxazine **65** and γ-amino alcohol **65** was observed. But more importantly, when methanol was removed prior to the final oxidation, no 1,3-oxazine **65** was formed, leading to the clean formation of the γ-amino alcohol **64**.

### 2.1.3 Substrate scope

Once it had been identified that 1,3-oxazines **65** were forming as side products in the one-pot methodology, steps were taken to minimise this reaction which, to great success, resulted in the formation of the γ-amino alcohol **64** in high yield (90%, see Table 9, Entry 6 – see section 2.11).

The next challenge was to probe the substrate scope of this reaction methodology. This was achieved by screening several enals and enones under these optimised conditions (see Entry 6, Table 9); the results are outlined in Table 10. This screening proved successful, showing that a broad range of substrates could be β-borylated in good conversion and, for some γ-amino alcohols that were difficult to isolate *via* flash column chromatography, derivatisation to the 1,3-oxazine was advantageous due to their increased water solubility and ease of purification. The γ-amino alcohol **74** obtained from α-methyl cinnamaldehyde **73** was isolated as a solid, and the crystal structure of this structure was obtained (see Figure 11).

However, some enals suffered from poor conversion (*e.g.* α-methyl cinnamaldehyde **73**) to the respective γ-amino alcohol (Entry 6). Retrospectively, it was concluded that this is due to competitive 1,2- *vs* 1,4-borylation (see sections 2.3 and 2.4).

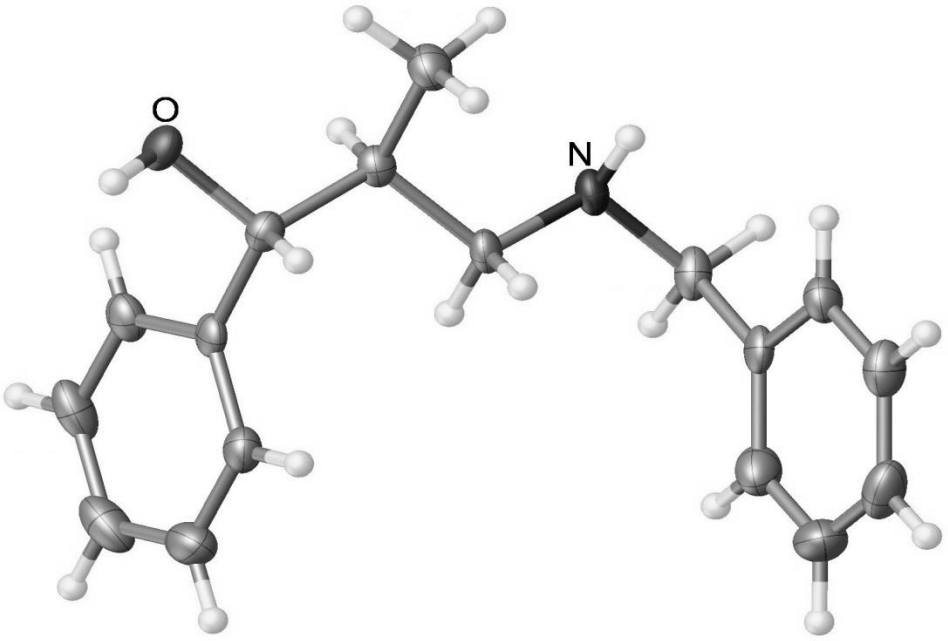


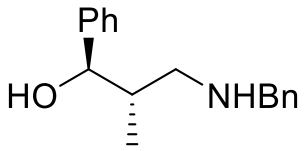


(*rac*)-(*anti*)-**74**

**Figure 11** Olex2[13] thermal ellipsoid plot (50% probability) of **74**.

**Table 10** Substrate screening of the one-pot methodology.

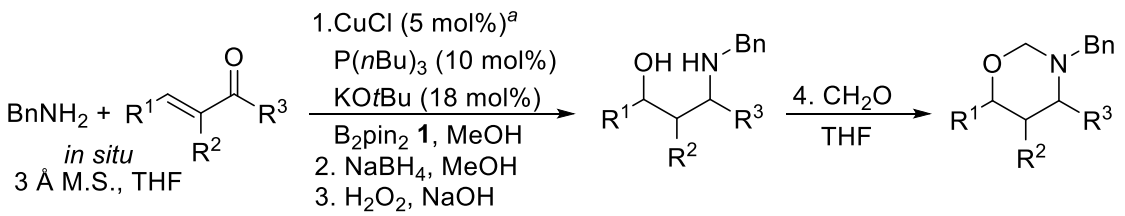


| | | Conversion[b] (isolated yield) (%) | | *d.e.*[b] (%) | |
|---|---|---|---|---|---|
| Entry | Substrate | Amino alcohol | Oxazine | Amino alcohol | Oxazine |
| 1[h] | 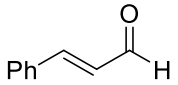 **66** | 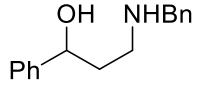 **67** 63 (58) | - | - | - |
| 2 | 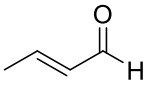 **59** | - | 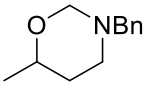 **79** (50) | - | - |
| 3[h] | 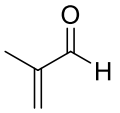 **60** | 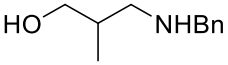 **69** 82 (64)[g] | - | - | - |
| 4[d] | 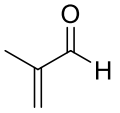 **60** | - | 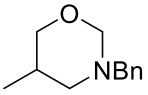 **70** (75) | - | - |
| 5 | 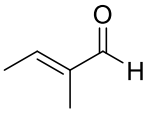 **61** | 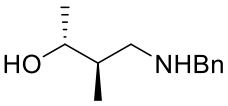 **71** 79 (71) | 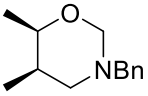 **72** 63 (28) | *rac-anti* >99 | *rac-anti* >99 |
| 6 | 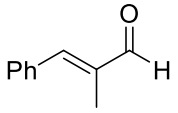 **73** | 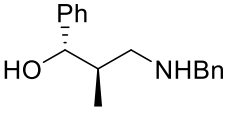 **74** 37 (20) | - | *rac-anti* >99 | - |
| 7[e] | 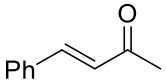 **4a** | 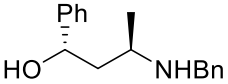 **64** 95 (90) | 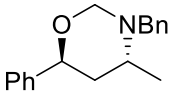 **65** (74) | *rac-anti* >99 | *rac-anti* >99 |
| 8 | 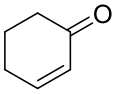 **75** | 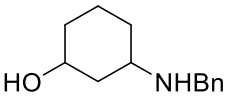 **76** 63 (58) | - | 40 | - |
| 9 | 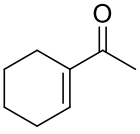 **77** | - | 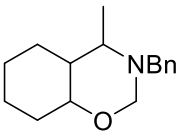 **78** (42) | | 95 |

1 mmol scale: [a] See Entry 6, Table 9 for standard conditions. [b] Determined by $^1$H NMR of isolated amino alcohol/oxazine. [c] See experimental. [g] 64%-inseparable impurity. [d] Standard conditions, except $PPh_3$ (10 mol%) used as ligand. [e]Standard conditions except NaO*t*Bu (18 mol%) is used as base.

### 2.1.4 Stereochemical analysis

Now that the potential of this one-pot methodology had been demonstrated, the next logical step was to investigate the enantio- and diastereoselective potential of this reaction. Curiously, in the examples shown in Table 10, high levels of diastereoselectivity were observed in the transformation of prochiral enals and enones into the chiral γ-amino alcohols and 1,3-oxazines. This is not surprising for substrates showing 1,3-difuctionalisation, as this had been previously observed. However, when enals are α,β-disubstituted, one major diastereoisomer is observed (>99% *d.e.* on isolation).

Analysis of the 1,3-oxazine **72**, derived from tiglic aldehyde **61**, allowed for the determination of the relative stereochemistry. By fusing the γ-amino alcohol in the form of a 1,3-oxazine ring, it was assumed that the oxazine formed the thermodynamically favoured chair conformation with the nitrogen lone pair in the equatorial position,[148] as observed in previous solution-state $^{1}$H NMR studies.[149] Furthermore, this had also been observed in the solid state by other groups,[150] and from research within this thesis (see Figure 38), even when a bulky benzhydryl (-$CHPh_2$) substituent was attached to nitrogen. The observed $^{3}J$ coupling between two neighbouring hydrogen atoms (adjacent to the methyl substituents) suggested that the two hydrogen atoms exhibited a synclinal relationship, as determined by the relatively weak $^{3}J$ coupling value of 3.1 Hz (see Figure 12 and Figure 13). This suggested that the major diastereoisomer displays one axial and one equatorial methyl substituent and, therefore, the presence of the *anti*-diastereoisomer can be assumed (in >99% *d.e.*). Furthermore, the X-ray crystal structure of **74** confirms the presence of the *anti*-diastereoisomer.

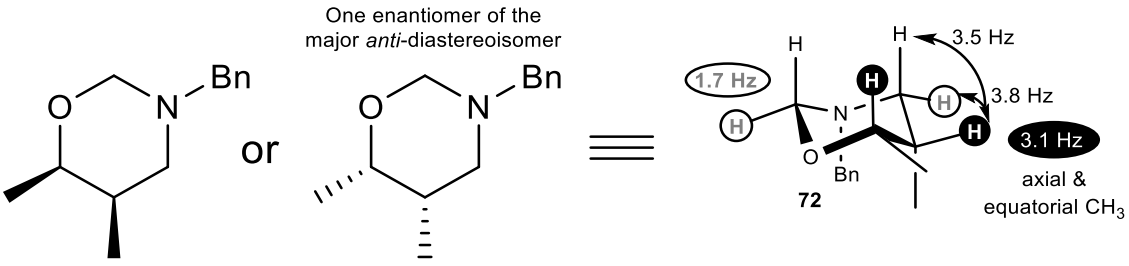


**Figure 12** 3D-representation of **72** showing coupling between H-atoms.

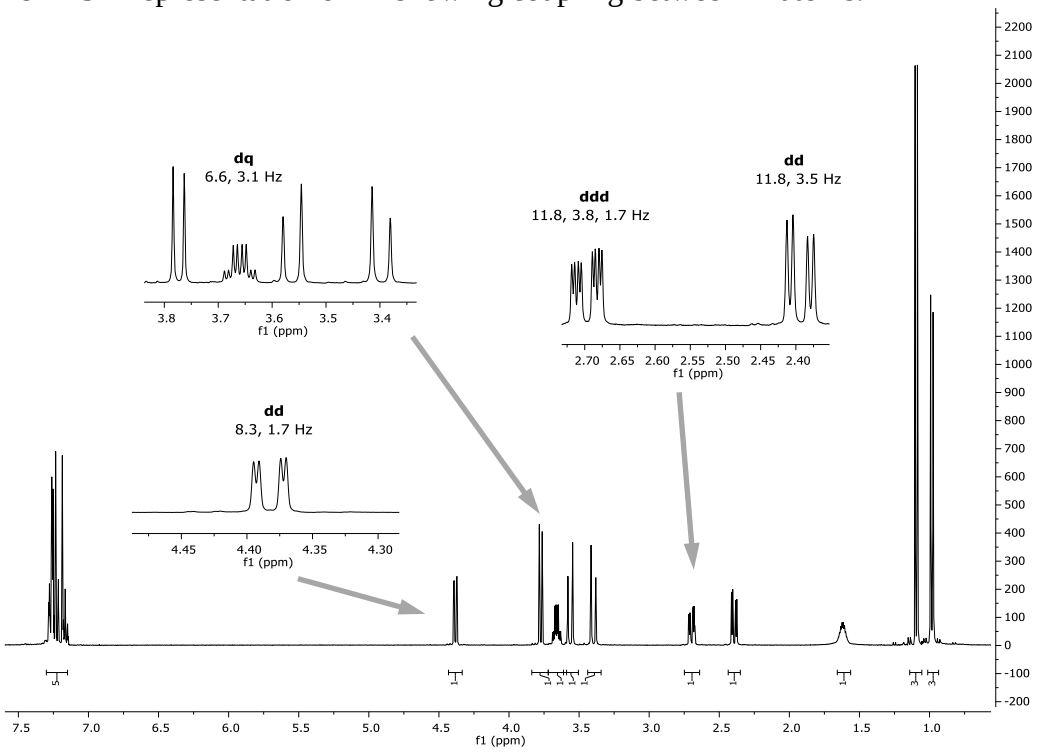


**Figure 13** $^{1}$H NMR spectrum shows >99% *anti*-diastereoisomer of **72**.

### 2.1.5 Summary of one-pot methodology

In summary, the formation of α,β-unsaturated imines *in situ* from enals and enones allowed for the development of a one-pot methodology to γ-amino alcohols. Novel side reactions were observed, leading to 1,3-oxazine formation, which could be promoted or inhibited through the respective addition or removal of methanol in the final C-B bond oxidation step of this methodology. This was then applied to a broad range of cyclic and linear enones and enals, and the stereochemistry of the major diastereoisomers were deduced where possible. ReactIR studies were crucial because they gave information regarding the formation of the α,β-unsaturated imines (this is discussed in section 2.2).

## 2.2 *In Situ* IR spectroscopy - making α,β-unsaturated imines

The DFT Calculations in section 2.2 were carried out by Jordi Carbó and Jessica Cid, at the University of Rovira i Virgili, Tarragona, Spain (2013 to 2014).

### 2.2.1 Background

The addition of nucleophiles to conjugated electron-deficient alkenes (*e.g.* α,β-unsaturated aldehydes, amides, esters and ketones) is one of the most important C-C and C-heteroatom bond forming reactions in organic synthesis.[151-153] However, due to the possibility of conjugate (1,4-) *vs.* direct (1,2-) addition products, a thorough understanding of the factors that govern these competing pathways is required.

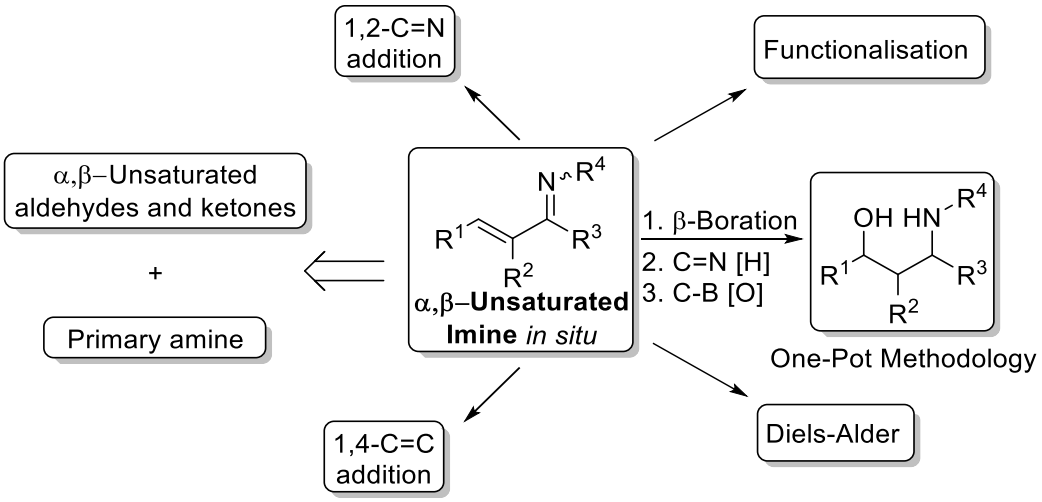


**Scheme 31** α,β-Unsaturated imines formed *in situ* are a useful platform for one-pot, sequential functionalisation.

Previously (see section 2.1), routes to γ-amino alcohols[60] were developed through the utilisation of α,β-unsaturated imines. Such species offer large scope for synthesis, due to α,β-unsaturated imines being prochiral with regards to both conjugate (1,4-addition to C=C) and direct (1,2-addition to C=N) addition. In the endeavour to prepare α,β-unsaturated imines, a lack of kinetic and mechanistic data in the literature

regarding the relative 1,2- *vs* 1,4-addition of primary amines to α,β-unsaturated aldehydes and ketones (enals and enones, respectively) was observed. This was surprising given the pre-existing data regarding the kinetic and mechanistic studies on the aza-Michael reaction[154-156] and studies on imine formation (from aldehydes and ketones).[157-163]

Other groups[164,165] have utilised α,β-unsaturated imines in synthesis[128,166,167] and, indeed, have reported their preparation *via* aza-Wittig chemistry,[168] simple condensation and catalytic methods.[56] In this context, it seemed rational to use a combination of *in situ* IR spectroscopy (ReactIR), NMR and DFT calculations as tools to understand the addition of primary amines to α,β-unsaturated aldehydes and ketones (1,2- *vs* 1,4-addition), and the relative rates of reactions thereof. In particular, ReactIR is a highly useful and relatively non-invasive method of analysis which makes it an ideal tool for this task. Indeed, groups have monitored air-sensitive catalytic processes[169] and even low-temperature lithiations[170] using such technology.[171]

### 2.2.2 1,2- *vs* 1,4-Addition of amines to enones and enals

Initially it was suspected that the addition of a primary amine (see Scheme 31 - $R^4$-$NH_2$, where $R^4$ = alkyl, aryl) to enals or enones would result in a mixture of 1,2- and 1,4-addition products. Indeed, it is typically considered that the 1,2-addition product is the kinetic product and the 1,4-addition product is the thermodynamic product due to the reversibility of the 1,2-addition step *via* hydrolysis.[172] This was investigated by the addition of benzylamine **80** to crotonaldehyde **59**, methacrolein **60** and methyl vinyl ketone **81** (whereby the position of the methyl substituent is varied across the conjugated C=C-C=O system) with and without 3Å-molecular sieve (3 Å M.S.) beads, at 25 ºC as shown in Table 11. Surprisingly, exclusive 1,2- (Entries 1 to 4, Table 11) or

1,4-addition (Entries 4 and 5, Table 13), irrespective of whether 3 Å M.S. were present in the reaction mixture, was observed. However, it should be noted that in the case of methacrolein **60** the reaction time was significantly longer when compared to the reaction where 3 Å M.S. were employed, leading to the 1,2-addition product (see Figure 14-16 for typical ReactIR data), but more importantly, no 1,4 addition products were observed. 1,2-Addition-elimination can be clearly deduced as shown by Figure 14. This highlights the reaction profile showing the loss of methacrolein **60** (C=O, 1703 $cm^{-1}$) and the concomitant gain of the α,β-unsaturated imine **58** (C=N, 1622 $cm^{-1}$). In conjunction, Figure 15 gives the IR spectrum between 1820-1580 $cm^{-1}$, overlaying three spectra at separate time intervals, t = 0, 10 and 80 min; therefore, showing that the total loss of the starting C=O stretch and the rise of the C=N asymmetric and symmetric stretches, with no observable 1,4-addition products at higher wavenumber. Finally, Figure 17 shows the ReactIR graphical output, showing the intensity of the stretch (arbitrary units, AU) *vs* wavenumber ($cm^{-1}$), over time.

**Table 11** 1,2- or 1,4-Addition of $BnNH_2$ **80** to crotonaldehyde **59**, methacrolein **60** and methyl vinyl ketone **81**?

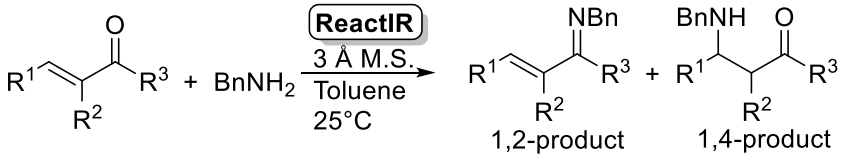


| Entry | Substrate 1- | Additive | Primary product | Time, t (min) | $I_{C=O\ 1/2}$ (min) |
|---|---|---|---|---|---|
| 1 | 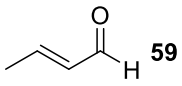 **59** | 3 Å M.S. | 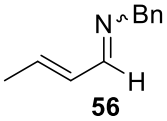 **56** | 135 | 5 |
| 2[a] | | - | | 76 | 5 |
| 3 | 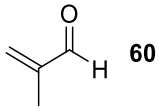 **60** | 3 Å M.S. | 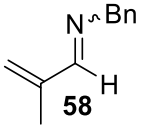 **58** | 80 | 11 |
| 4[a] | | - | | 444 | 85 |
| 5 | 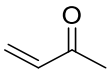 **81** | 3 Å M.S. | 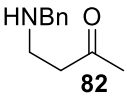 **82** | 85 | 6 |
| 6[a] | | - | | 82 | 14 |

Conditions: Enone/enal (2 mmol) was added to a stirring solution of toluene (8 mL) and 3 Å molecular sieve beads (oven-dried at 250 ºC for >48 h prior to use). $BnNH_2$ (2 mmol) was added and the reaction monitored by ReactIR. Reaction vessel was submerged in an oil bath and the temperature was maintained at 25 ºC. [a] No 3 Å M.S.

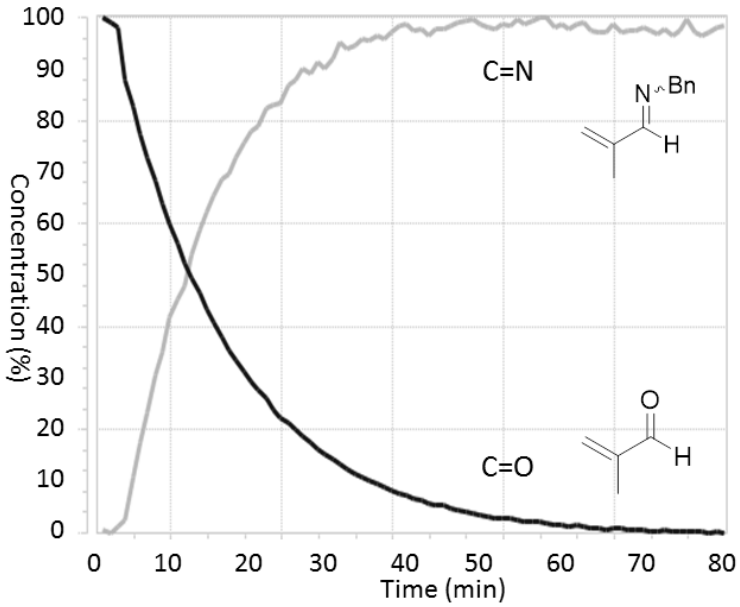


**Figure 14** Data from Entry 3, Table 11: Reaction profile showing the loss of **60** (1703 $cm^{-1}$) and the concomitant formation of **58** (1622 $cm^{-1}$).

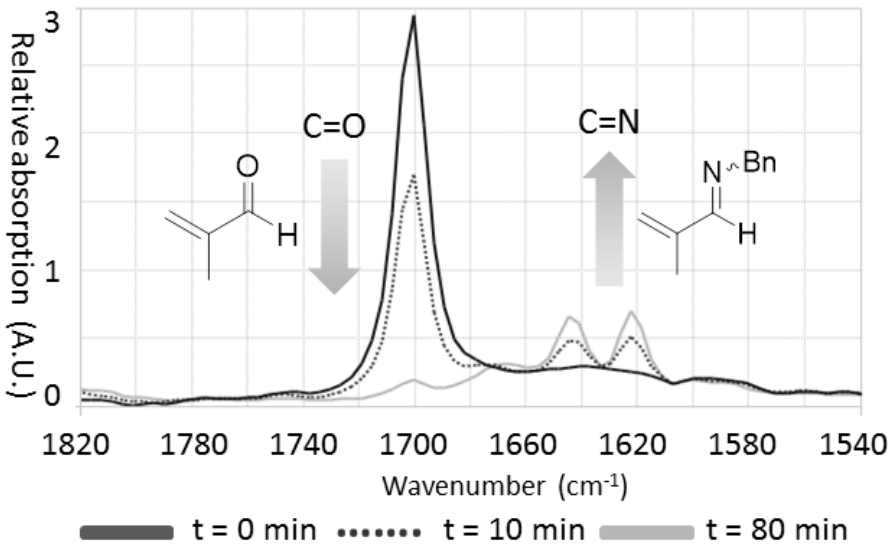


**Figure 15** Data from Entry 3, Table 11: Superimposed IR spectra at t = 0, t= 10 and t = 80 min, showing the loss of C=O **60** (1703 $cm^{-1}$) and gain of the $C=N_{asym+sym}$ **58** (1640 and 1622 $cm^{-1}$, respectively).

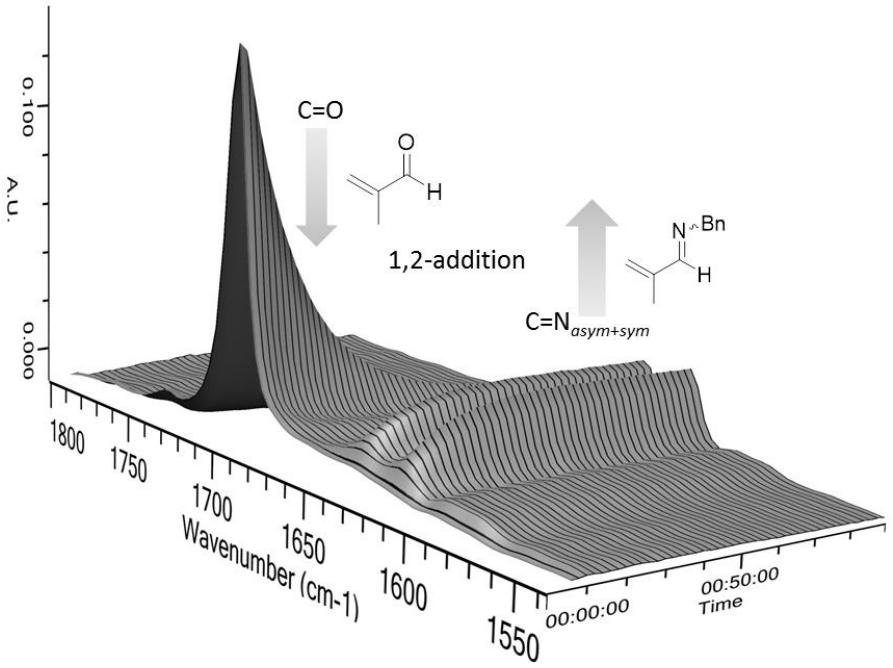


**Figure 16** Data from Entry 3, Table 11: ReactIR graphical output showing the reaction profile over time (1 sample $min^{-1}$).

Furthermore, even when 3 Å molecular sieves were employed, such as in the case of methyl vinyl ketone **81**, no 1,2-addition product was observed (Table 11, Entries 5 and 6), just 1,4-addition. This suggested that, in this case, the 1,4-addition product was the kinetic product of the reaction. One possible explanation around this is to assume the facile and rapid hydrolysis of the imine species (by the water generated from condensation), thus providing the free benzylamine **80** to proceed *via* 1,4-addition. This is unlikely given that this was not observed in the case of crotonaldehyde **59** and methacrolein **60** when no 3 Å molecular sieves were added to the reaction mixture. Again, this can be easily deduced using ReactIR. Figure 17 shows the reaction profile whereby the rapid loss of methyl vinyl ketone **81** (at 1686 $cm^{-1}$) and the concomitant gain of the β-amino ketone (secondary amine) **82** at higher wavelength (observed at 1719 $cm^{-1}$). β-Amino ketone **82** was consumed again, presumably due to addition of β-amino ketone (secondary amine) to methyl vinyl ketone **81**, due to increased nucleophilicity of the secondary amine when compared to the starting amine **80** and, therefore, was observed by the loss of the C=O stretch at 1719 $cm^{-1}$. Indeed, when studied in parallel with the ReactIR graphical output (Figure 18), 1,4-addition is clearly observed.

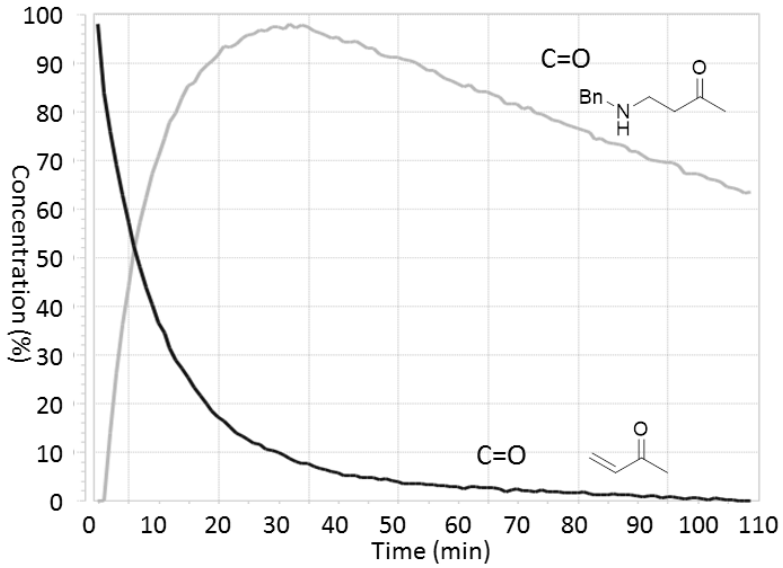


**Figure 17** Data from Entry 5, Table 11: Reaction profile showing the rapid loss of **81** (1686 $cm^{-1}$) and the concomitant gain of **82** (1719 $cm^{-1}$), followed by the loss of **82** (1719 $cm^{-1}$), consistent with 1,4-addition, with further self-addition of species **82**.

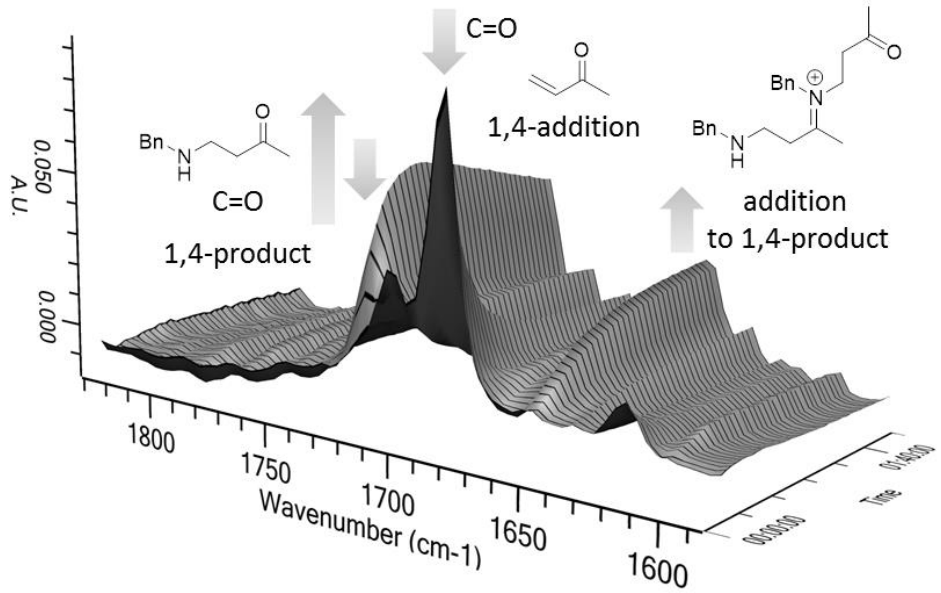


**Figure 18** Data from Entry 5, Table 11: Reaction profile showing the rapid loss of **81** (1686 $cm^{-1}$) and the concomitant gain of **82** (1719 $cm^{-1}$), followed by the loss of **82** (1719 $cm^{-1}$), consistent with 1,4-addition, with further self-addition of species **82**.

### 2.2.3 $^{1}$H NMR Validation of ReactIR

In order to validate the ReactIR results shown in Table 12, additional parallel *in situ* NMR experiments in $d_8$-toluene were conducted for the reactions between crotonaldehyde **59**, methacrolein **60** and methyl vinyl ketone **81** with benzylamine, both with and without 3 Å M.S. These results are shown in Table 12 and Figure 19, 20 and 21, which is complimentary to Table 11 (ReactIR *vs.* NMR investigation).

**Table 12** $^{1}$H NMR study into the validation of Table 11.

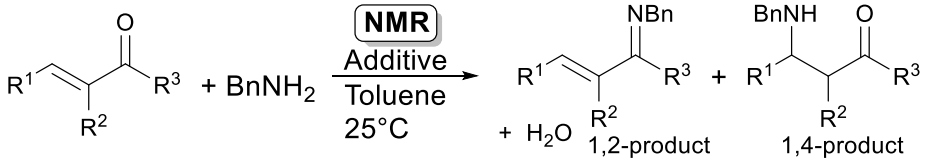


| Entry | Substrate | Additive | Time (min) | Conversion (%) | |
|---|---|---|---|---|---|
| | | | | 1,2-product | 1,4-product |
| 1 | 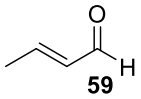 **59** | 3 Å M.S. | 310 | (90) | 0 |
| 2 | | - | 360 | (90) | 0 |
| 3 | 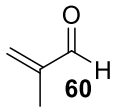 **60** | 3 Å M.S. | 1320 | (86) | 0 |
| 4 | | - | 1320 | (67) | 0 |
| 5 | 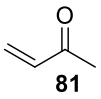 **81** | 3 Å M.S. | 140 | 0 | (>99) |
| 6 | | - | 140 | 0 | (>99) |

Enal or enone (0.18 mmol) was added to an NMR tube (Norell® Standard Series™ 5 mm x 178 mm NMR tubes) containing d8-toluene (0.7 mL) with/without 3 Å M.S. beads (filled 0.7-0.8 mm up the tube, M.S. beads oven-dried at 250 ºC for >48 h prior to use), and flushed with Argon and sealed. On the acquisition of the first spectrum, benzylamine (0.18 mmol) was added and the next spectrum was acquired in <5 min. Subsequent $^{1}$H NMR spectra were recorded over time with intermittent shaking of the NMR tube to aid mixing.

The results shown in Table 12 broadly corroborate the findings by ReactIR. Methyl vinyl ketone **81**, underwent exclusive 1,4-addition with primary amines, indicating that, for this substrate, the 1,4-addition pathway is the kinetic pathway. In addition, methacrolein **60** and crotonaldehyde **59** appeared to undergo exclusive 1,2-addition, suggesting that in these cases the kinetic pathway is the 1,2-additon route. Moreover, the presence of 3 Å-molecular sieves did not change the overall reaction outcome, but in some cases, the presence of 3 Å molecular sieves appeared to drive the reaction to near completion (presumably due to the removal of water), as shown in the case of methacrolein **60** (see Entries 3 and 4, Table 12). This was achieved by running *in situ* NMR tube experiments in deuterated solvent (toluene-d8), and monitoring the reaction progress over time.

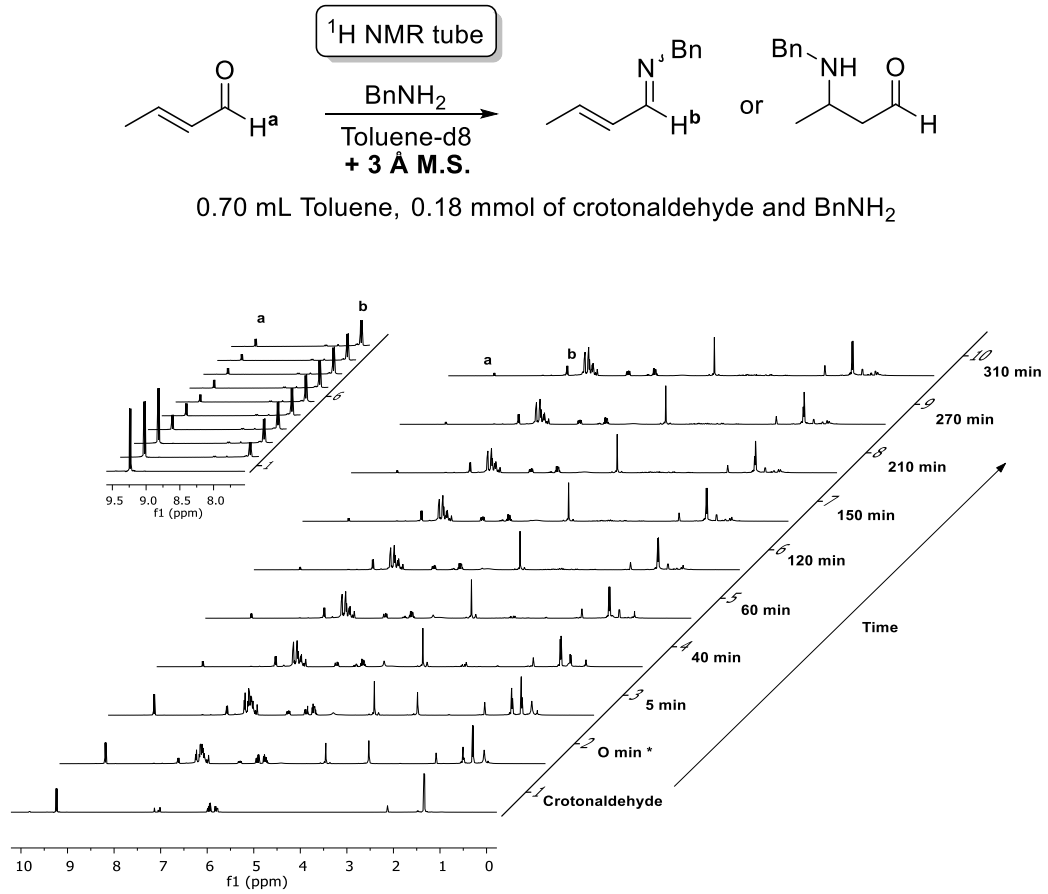


**Figure 19** NMR-Tube experiment: *In situ* monitoring by $^{1}$H NMR spectroscopy of the reaction between crotonaldehyde **59** and $BnNH_2$ in toluene-d8, with 3 Å M.S. * Initial measurement (0 min) is artificial, due to time lapse from submitting NMR experiment and data acquisition (+/-3 min). All subsequent measurements are relative to the 0 min spectrum.

This method has major advantages over taking aliquots and concentrating *in vacuo*, because this limits the probability of degradation of products (especially the hydrolysis of the imine and subsequent 1,4-addition, leading to conjugate addition products).

It should be noted that the reactions appear to take slightly longer in the $^{1}H$ NMR experiments. This can be exemplified by comparing the reaction of crotonaldehyde **59** and benzylamine in the presence of 3 Å M.S. Indeed, when monitored by ReactIR the reaction takes approximately 2.3 hours (Entry 1, Table 11), whereas in the NMR tube the reaction takes 5.2 hours (Entry 1, Table 12) to proceed to near completion.

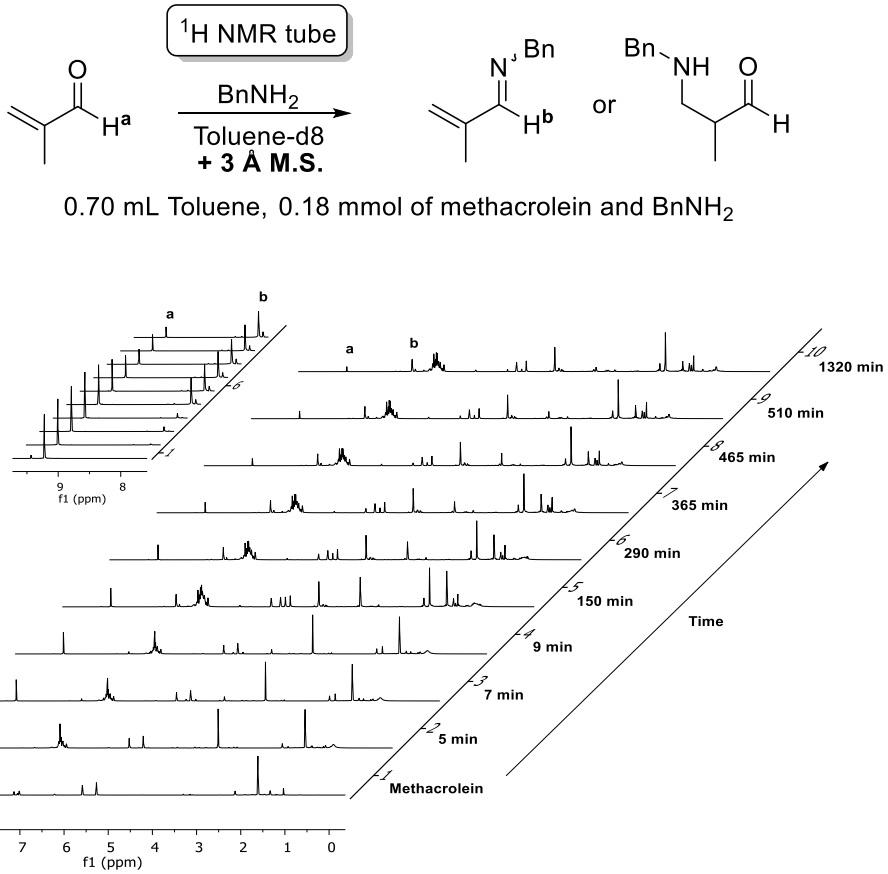


**Figure 20** NMR-Tube experiment: *In situ* monitoring by $^{1}H$ NMR spectroscopy of the reaction between methacrolein **60** and $BnNH_2$ in toluene-d8, with 3 Å M.S.

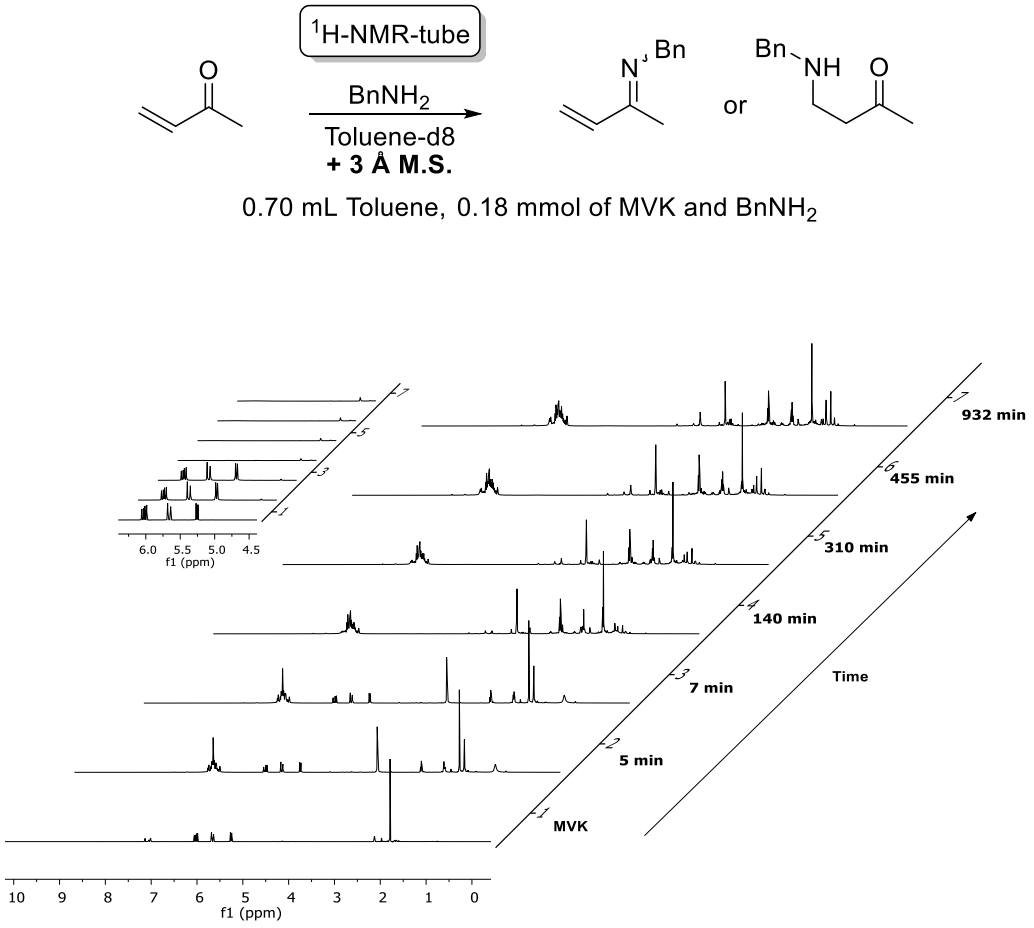


**Figure 21** NMR tube experiment: *In situ* monitoring by $^{1}$H NMR spectroscopy of the reaction between methyl vinyl ketone and $BnNH_2$ in toluene-d8, with 3 Å M.S.

Moreover, this was found to be consistent with direct experience of using such imines in synthesis, whereby the longer reaction times in the NMR tube can probably attributed to relatively poor mixing, when compared to the experiments using ReactIR. ReactIR experiments were conducted in a two-necked round-bottom flask where stirring was efficiently achieved. Indeed, this is an additional advantage of ReactIR experiments in general, *i.e.* they can be carried out in the same reaction vessel, scale, stirrer bar, etc., as one would carry out any typical experiment. This method can, therefore, be considered more representative and reliable compared with the experiments conducte din the NMR-tube.

### 2.2.4 Using different solvents and amines

The role of the amine and solvent selection (polar or non-polar) on the selectivity and rate of reaction with the three previously investigated substrate (methacrolein **60**, crotonaldehyde **59** and methyl vinyl ketone **81**), was investigated; *i.e.* using amines benzylamine **80**, aniline **83** and *n*-butylamine **84** in a non-polar solvent (toluene) and a polar solvent (acetonitrile).

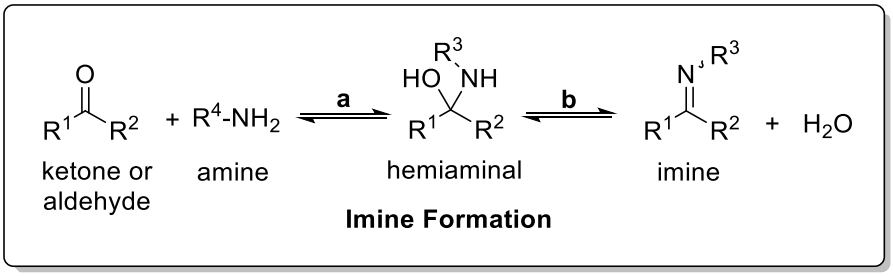


**Scheme 32** Two rate-determining steps (pH dependent) of imine formation: a) addition of the amine to the C=O; b) collapse of the hemiaminal intermediate to give the product imine *via* the loss of water.

When comparing Table 13 and Table 14, the first thing to note is that all the reactions proceed to completion in <24 h when the reactions are carried out in toluene, whereas the reactions in acetonitrile, in some cases, took >24 h (when aniline **83** was used). However, irrespective of whether the solvent was non-polar (toluene) or polar (acetonitrile), according to Table 11, the reactions proceeded with the same selectivity as one would expect, that is crotonaldehyde **59** and methacrolein **60** underwent 1,2-addition irrespective of the amine and methyl vinyl ketone **81** reacted exclusively in a 1,4-fashion with all the amines. In particular, the reaction between aniline **83** and crotonaldehyde **59** is interesting due to the rapid consumption of crotonaldehyde **59** and the formation of imine **85**, where the C=O stretch $t_{1/2}$ = 9 min (Entry 1, Table 13). However, the reaction did not proceed to completion until 6 h later (Figure 22).

**Table 13** Probing the effects of amine nucleophilicity in toluene.

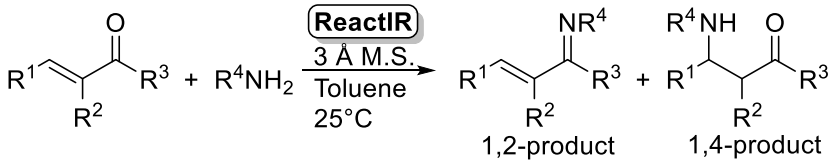


| Entry | Substrate | Amine | Major product | | Time, t (min) | $I_{C=O\ 1/2}$ (min) |
|---|---|---|---|---|---|---|
| | | | 1,2- | 1,4- | | |
| 1 | 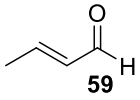 **59** | $PhNH_2$ **83** | **85** | | 365 | 9 |
| 2 | 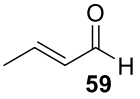 **59** | $BnNH_2$ **80** | **56** | | 135 | 5 |
| 3 | 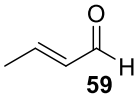 **59** | *n*$BuNH_2$ **84** | **86** | | 96 | 5 |
| 4 | 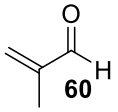 **60** | $PhNH_2$ **83** | **87** | | 632 | 16 |
| 5 | 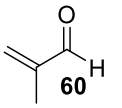 **60** | $BnNH_2$ **80** | **58** | | 80 | 11 |
| 6 | 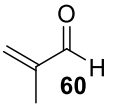 **60** | *n*$BuNH_2$ **84** | **88** | | 87 | 10 |
| 7 | 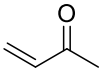 **81** | $PhNH_2$ **83** | | **89** | 601 | 50 |
| 8 | 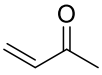 **81** | $BnNH_2$ **80** | | **82** | 85 | 6 |
| 9 | 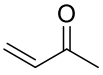 **81** | *n*$BuNH_2$ **84** | | **90** | 55 | 3 |

Standard conditions (see Table 11).

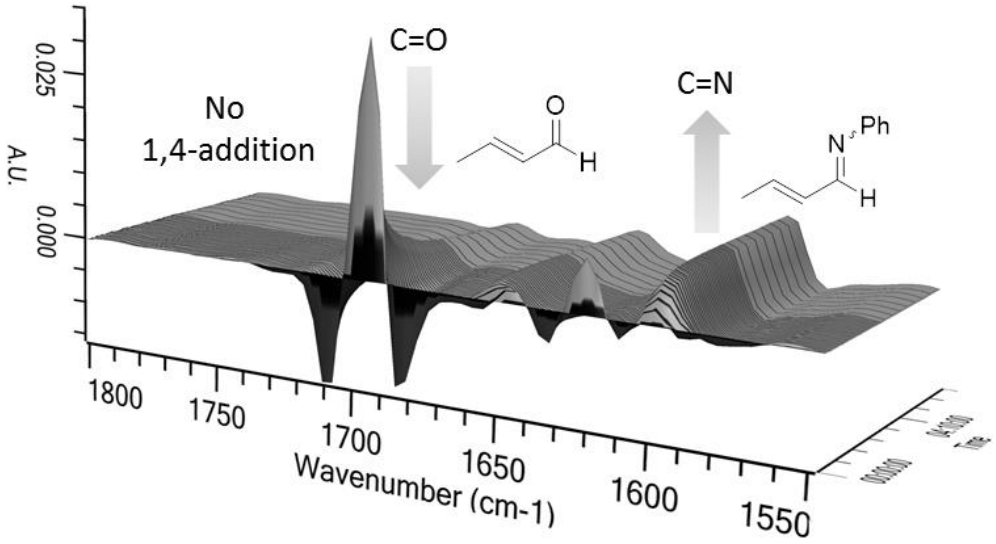


**Figure 22** Graphical output of Entry 1, Table 13 showing the rapid loss of the C=O stretch for **49** and the rise of the C=N stretch of **85** on addition of **83**. Processing - 2nd derivative base-line function was applied.

**Table 14** Probing the effects of amine nucleophilicity in acetonitrile.

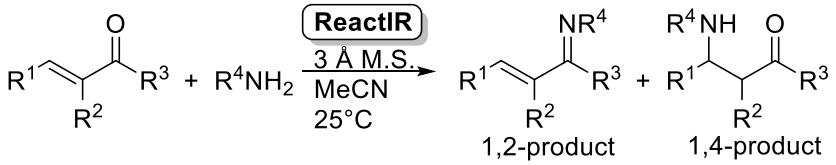


| Entry | Substrate | Amine | Primary product 1,2- | Primary product 1,4- | Entry | $I_{C=O\ 1/2}$ (min) |
|---|---|---|---|---|---|---|
| 1 | 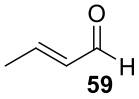 **59** | $PhNH_2$ **83** | **85** | | >1440 | 57 |
| 2 | 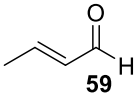 **59** | $BnNH_2$ **80** | **56** | | 178 | 5 |
| 3 | 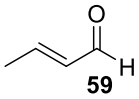 **59** | *n*$BuNH_2$ **84** | **86** | | 296 | 4 |
| 4 | 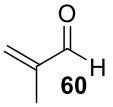 **60** | $PhNH_2$ **83** | **87** | | >1440 | 42 |
| 5 | 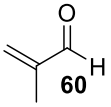 **60** | $BnNH_2$ **80** | **58** | | 174 | 14 |
| 6 | 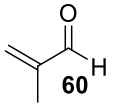 **60** | *n*$BuNH_2$ **84** | **88** | | 145 | 12 |
| 7 |  **81** | $PhNH_2$ **83** | | **89** | >1440 | 474 |
| 8 |  **81** | $BnNH_2$ **80** | | **82** | 84 | 9 |
| 9 |  **81** | *n*$BuNH_2$ **84** | | **90** | 46 | 3 |

Standard conditions, except acetonitrile is used as solvent (See Table 11).

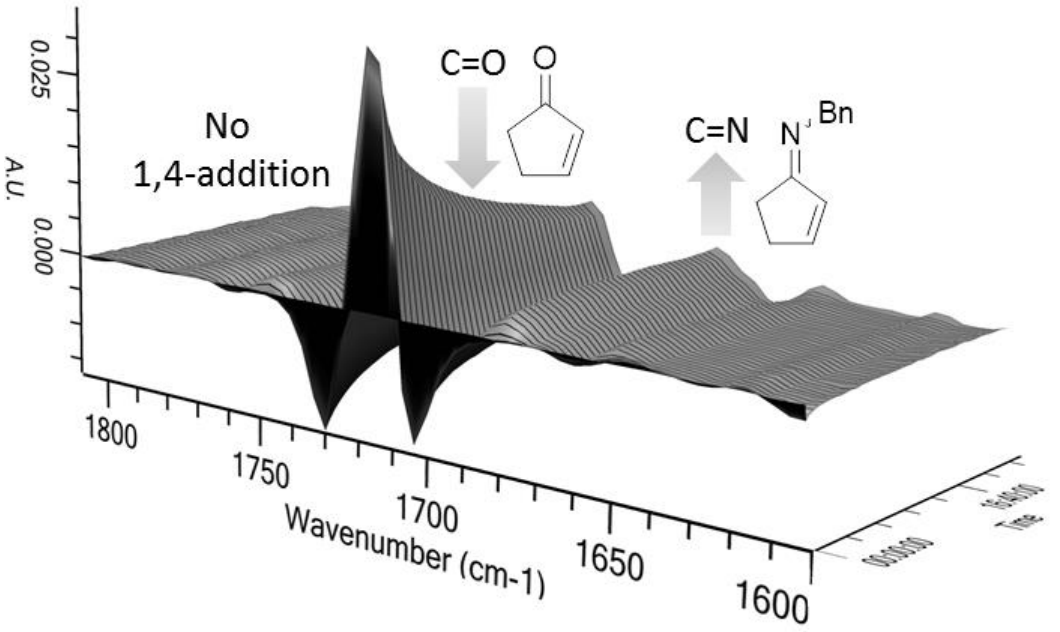


**Figure 23** Graphical output of Entry 2, Table 15. Addition of **80** to **91** results in the slow formation of **94**, but no 1,4-addition products were observed. Processing - 2nd derivative base-line function was applied.

Furthermore, it was generally found that imine formation appears to mirror the loss of the enal/enone, thus suggesting that the rate determining step is the addition of the amine, and not the collapse of the hemiaminal intermediate (Scheme 32). This is consistent with previous kinetic studies on imine formation in neutral media.[173]

Next, three cyclic enones cyclopentenone **91**, cyclohexenone **75** and 3-methyl-2-cyclohexeonone **92** with benzylamine **80** and aniline **83** were investigated, utilising toluene as solvent (see Table 15). It was assumed, given the exclusive 1,4-addition observed in the case of methyl vinyl ketone **81**, and the increased ring strain of the α,β-unsaturated conjugated system would result in the same 1,4-addition pathway as observed with the previous methyl vinyl ketone **81**. Surprisingly, 1,2-addition was observed in all cases.

**Table 15** Cyclic enones: 1,2- or 1,4- addition with primary amines?

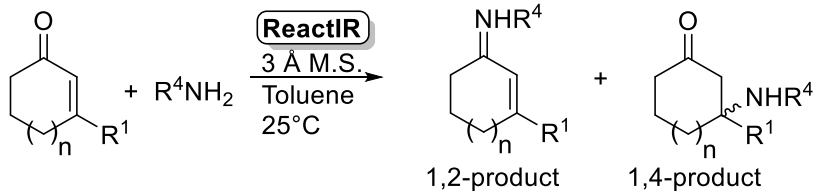


| Entry | Substrate | Amine | Primary product 1,2- | Primary product 1,4- | Time, t (h) | $I_{C=O\ 1/2}$ (h) |
|---|---|---|---|---|---|---|
| 1 | 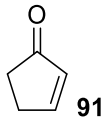 **91** | $PhNH_2$ | **93** | | >24 | 17.4 |
| | | **83** | | | | |
| 2 | | $BnNH_2$ | **94** | | >24 | 4.0 |
| | | **80** | | | | |
| 3 | 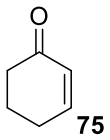 **75** | $PhNH_2$ | **95** | | >>24 | 7.4 |
| | | **83** | | | | |
| 4 | | $BnNH_2$ | **96** | | >24 | 3.5 |
| | | **80** | | | | |
| 5 | 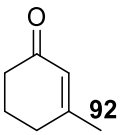 **92** | $PhNH_2$ | **97** | | >>24 | -[a] |
| | | **83** | | | | |
| 6 | | $BnNH_2$ | **98** | | >24 | 18.8 |
| | | **80** | | | | |

Conditions: Enone (2 mmol) was added to a stirring solution of toluene (8 mL) and 3 Å molecular sieve beads (oven-dried at 250 ºC for >48 h prior to use). Amine (2 mmol) was added and the reaction was monitored by ReactIR. Reaction vessel was submerged in an oil bath and the temperature was maintained at 25 ºC. [a] Peak intensity = 35% after 24 h.

However, reactions required >24 h for completion, but the time taken for the C=O to reach 50% for cyclopentenone **91** and cyclohexenone **75** was surprisingly low, given the relatively long reaction time, especially in the cases with benzylamine **80** (See Figure 23). In particular, 3-methyl-2-cyclohexeonone **92** is significantly less reactive, with the reaction only reaching 35% conversion to the α,β-unsaturated imine **98** after 24 h.

This study was continued by examining other linear enones and enals. In particular, the role and influence of substituents on the alkene, namely α,β-disubstituted enals *vs.* β-substituted enals, was examined. This was achieved by comparing cinnamaldehyde **66** and α-methylcinnamaldehyde **73**, and the methyl analogues crotonaldehyde **59** and tiglic aldehyde **61**. In both cases the β-substituted enals reacted significantly faster with benzylamine **80** and aniline **83**. Remarkably, the reaction between cinnamaldehyde **66** and benzylamine **80** was complete in <10 min, with the $t_{1/2}$ being approximately 1 min, as shown in the three superimposed IR spectra at t = 0, 1 and 9 min, respectively (see Figure 24).

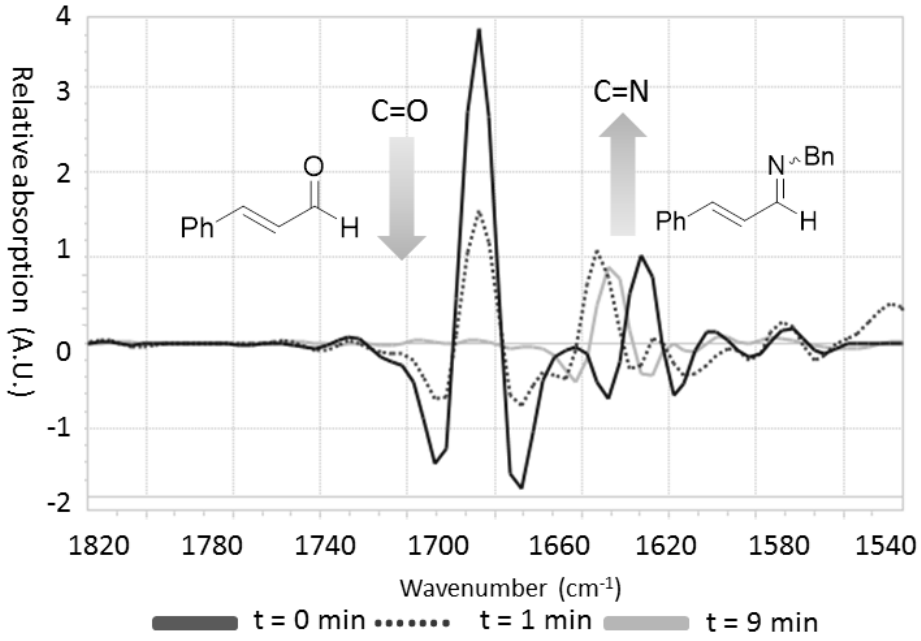


**Figure 24** Superimposed IR spectra at t = 0, t = 1, t = 9 min, showing the loss of **66** (C=O, 1685 $cm^{-1}$) and the shift of the C=C in **66** (from 1630 to 1644 $cm^{-1}$) on the addition of **80**. The concomitant formation of the product C=N **101** stretch (1641 $cm^{-1}$) can be observed (Entry 2, Table 16). Processing - 2$^{nd}$ derivative base-line function was applied.

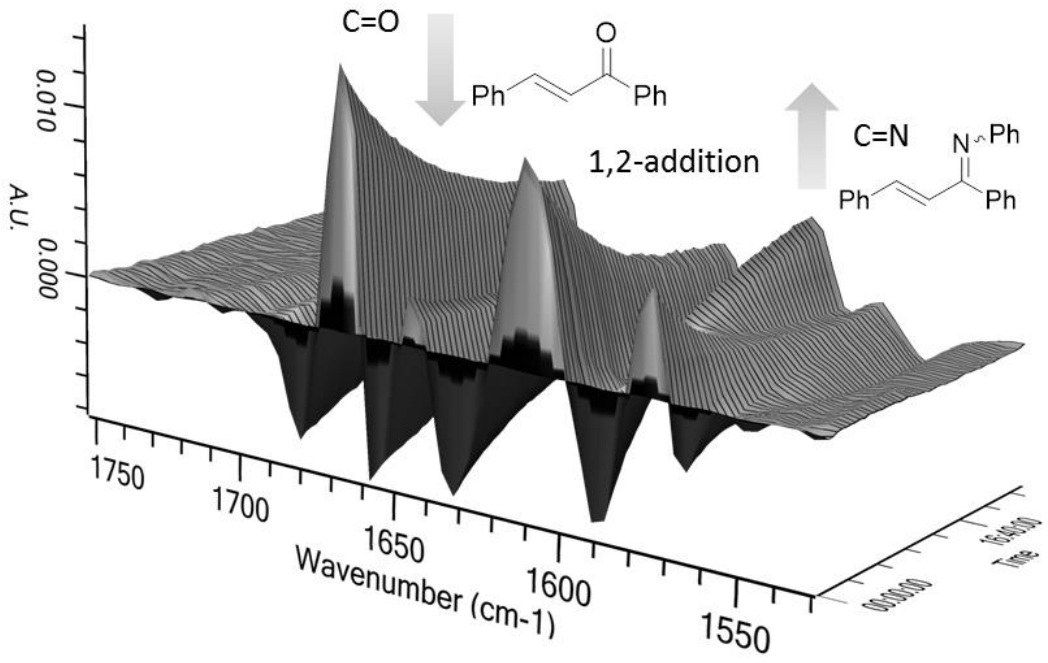


**Figure 25** Graphical output of Entry 11, Table 16. Addition of **83** to **4b** results in the slow formation of **105**, but no 1,4-addition products are observed. Processing - 2nd derivative base-line function was applied.

To conclude the series of enones, pentenone **101**, chalcones **4b** and **4a** were reacted with the amines, benzylamine **80** and aniline **83** in toluene with oven-dried 3 Å M.S. sieve beads (at 25 ºC), as shown in Table 5. It is important to note, that enones underwent predominantly 1,2-addition with the benzylamine **80** and aniline **83**. Indeed, the relatively poor nucleophile aniline **83** reacted with chalcone **1l** to give the 1,2-addition product, imine **107**, as shown in Fig. 6 (with no trace of 1,4-addition). Pentenone **99** was particularly unreactive in comparison with the other chalcones **4a** and **4b**; however, no 1,4-addition product was observed under these conditions.

**Table 16** Probing substituent effects of enals and enones.

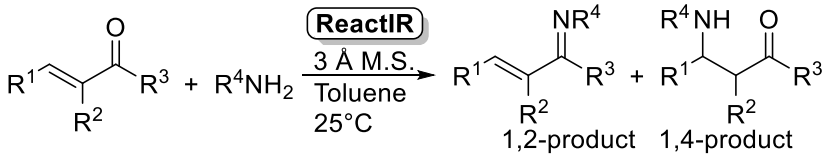


| Entry | Substrate | Amine | Primary product 1,2- | Primary product 1,4 | Time, t (min) | $I_{C=O\ 1/2}$ (min) |
|---|---|---|---|---|---|---|
| 1 | 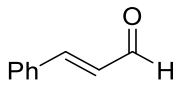 **66** | $PhNH_2$ **83** | **100** | | 78 | 7 |
| 2 | | $BnNH_2$ **80** | **101** | | 9 | 1 |
| 3 | 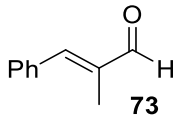 **73** | $PhNH_2$ **83** | **102** | | 220 | 25 |
| 4 | | $BnNH_2$ **80** | **103** | | 202 | 24 |
| 5 | 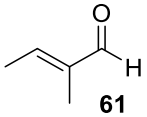 **61** | $PhNH_2$ **83** | **104** | | 545 | 28 |
| 6 | | $BnNH_2$ **80** | **57** | | 233 | 29 |
| 7 | 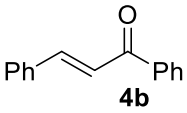 **4b** | $PhNH_2$ **83** | **105** | | >1440 | -[a] |
| 8 | | $BnNH_2$ **80** | **106** | | >1440 | 165 |
| 9 | 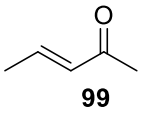 **99** | $PhNH_2$ **83** | **107** | | >1440 | 139 |
| 10 | | $BnNH_2$ **80** | **108** | | >1440 | 115 |
| 11 | 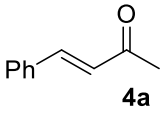 **4a** | $PhNH_2$ **83** | **109** | | >1440 | 517 |
| 12 | | $BnNH_2$ **80** | **110** | | >1440 | 108 |

Conditions: Enone/enal (2 mmol) was added to a stirring solution of toluene (8 mL) and 3 Å molecular sieve beads (oven-dried at 250 ºC for >48 h prior to use). Amine (2 mmol) was added and the reaction was monitored by ReactIR. Reaction vessel was submerged in an oil bath and the temperature was maintained at 25 ºC. [a] Peak intensity = 55% after 24 h.

### 2.2.5 DFT Study (by Jordi Carbó and Jessica Cid).

In order to understand the origin of the observed selectivity in the addition of amines to the enals and enones, DFT calculations (B3LYP functional) were carried out on representative substrates (*i.e.* crotonaldehyde **59**, methyl vinyl ketone **81**, cyclopentenone **91** and pentenone **99**) using $MeNH_2$ as a model of a simple primary alkyl amine. These calculations indicated that the kinetic preference for the 1,2- *vs.* 1,4-addition pathway depends on the conformational effects operating upon the α,β-unsaturated aldehydes and ketones. When the C=C and C=O bonds are *s-trans* to each other, the 1,2-addition pathway shows lower energy barriers and in contrast, when they are *s-cis,* the 1,4-addition pathway is preferred (see Figure 26 and Table 17). Indeed, one should note literature examples which suggest that the stereochemistry involved in the addition of crotyl magnesium chloride to enones is also notably dependent upon the enone conformation.[174]

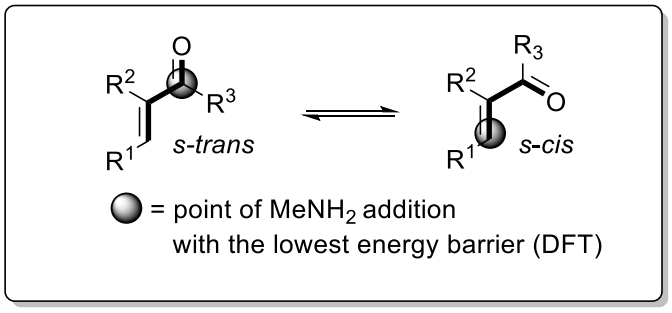


**Figure 26** The effects of conformational change on the barrier to addition of alkyl amines on enones and enals.

**Table 17** NBO orbital energies of $\pi^*_{C=O}$ and $\pi^*_{C=C}$ (in eV); and energy barriers ($\Delta E^{\neq}$ in kcal.mol$^{-1}$) for the 1,2- and 1,4-addition of $MeNH_2$ to α,β-unsaturated aldehydes and ketones; and NBO second-order perturbative donor-acceptor interaction between the $C_\alpha$ lone pair and the $\pi^*_{C=O}$ orbital at the transition state for 1,4-addition (kcal.mol$^{-1}$).

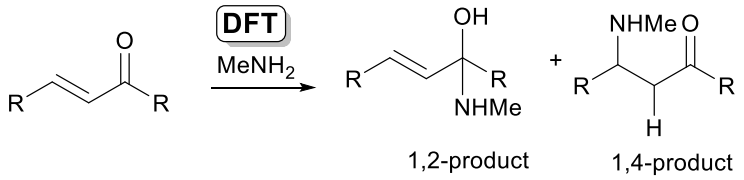


| | $\pi^*_{C=O}$ | $\Delta E^{\neq}(1,2)$ | $\pi^*_{C=C}$ | $\Delta E^{\neq}(1,4)$ | $\Delta\Delta E^{\neq}$ | Comment |
|---|---|---|---|---|---|---|
| **59** 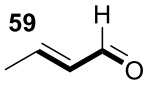 *s-trans* | **0.42** | **33.0** | **0.82** | **38.8** | **+5.8** | Large $\Delta\Delta E^{\neq}$ between 1,2- & 1,4-pathways which show a preference for 1,2-addition. |
| 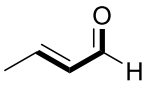 *s-cis* | 0.41 | 30.3 | 1.10 | 29.0 | -1.2 | Small $\Delta\Delta E^{\neq}$ between 1,2- & 1,4-pathways, but shows a small preference for 1,4-addition. |
| **81** 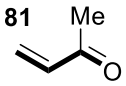 *s-trans* | 0.57 | 35.5 | 0.86 | 37.4 | +1.8 | Small $\Delta\Delta E^{\neq}$ between 1,2- & 1,4-pathways, but show small preference for 1,2-addition. |
| 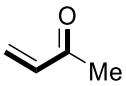 *s-cis* | **0.63** | **33.6** | **0.98** | **27.1** | **-6.5** | Large $\Delta\Delta E^{\neq}$ between 1,2- & 1,4-pathways which show a large preference for 1,4-addition. |
| **99** 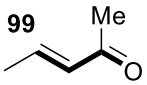 *s-trans* | 0.74 | 36.7 | 1.18 | 41.4 | +4.7 | Both *s-cis* & *s-trans* show the same trend in conformational preference for 1,2- *vs.* 1,4-addition, but $\Delta\Delta E^{\neq}$ for each conformation is very large, indicating a potential driving force for each pathway, that is presumably dependent on solution state conformation. |
| 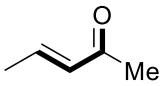 *s-cis* | **0.78** | **34.7** | **1.30** | **30.4** | **-4.3** | |
| **91** 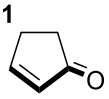 *s-trans* | **0.80** | **38.2** | **1.02** | **38.9** | **+0.7** | Fixed *s-trans* conformation shows a kinetic preference to 1,2-addition. |

Calculations were performed with Gaussian09 (B3LYP functional) and the basis set was the 6-31g(d,p).

The predominance for 1,2- over 1,4-addition in the *s-trans* conformation can be explained from the relative energy of the acceptor π*-orbitals.[175] The origin of this effect is due to the fact that the energies of the $\pi^*_{C=O}$ orbitals are lower than those of the $\pi^*_{C=C}$ orbitals, suggesting that the electrophilic carbon of the carbonyl group is more reactive than that of the C=C double bond in the *s-trans* conformation. Indeed, for *s-trans* conformers, a linear correlation between the computed energy barriers and the energies of the $\pi^*_{C=O}$ and $\pi^*_{C=C}$ orbitals was observed (see Figure 27). In contrast, when *s-cis* conformers are considered, no correlation between the activation barriers and the energies of the π-antibonding orbitals was observed.

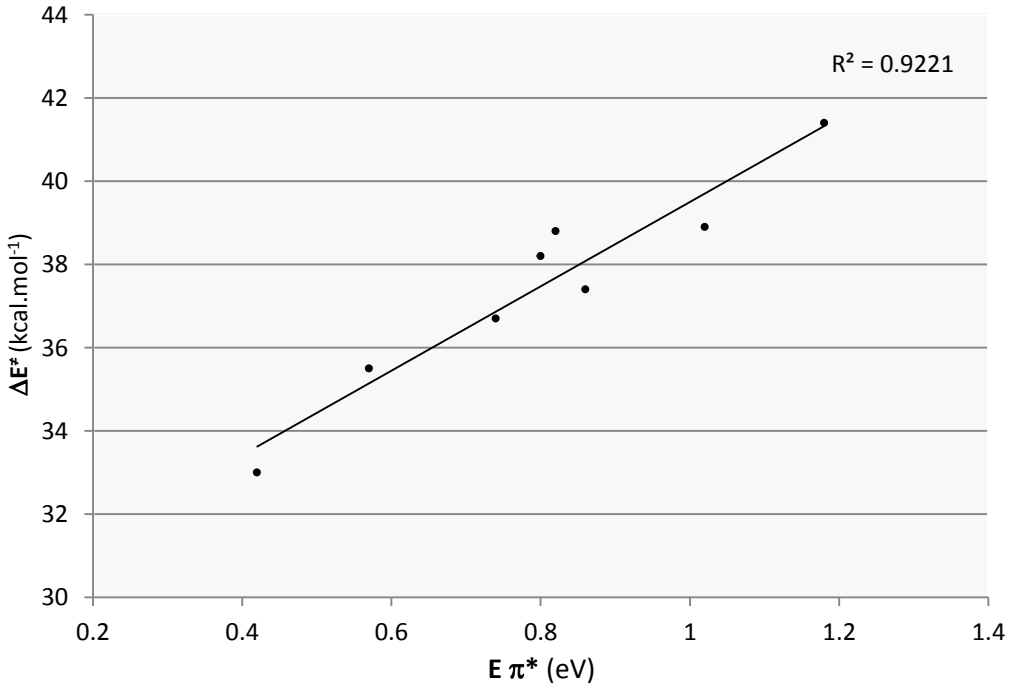


**Figure 27** Correlation between the computed energy barriers and the energies of the C=C and C=O π* orbitals in the *s-trans* isomers.

In the *s-cis* conformation, the energy barriers for 1,4-addition pathway ($\Delta E^{\neq}(1,4)$) are lowered significantly (~10 kcal.mol$^{-1}$), with respect to those of the *s-trans* forms (see Table 17).

Analogously, calculations have shown that the *s-cis* conformation of α,β-unsaturated aldehydes is more reactive towards the addition of dienes.[176] Houk *et at.* attributed the larger reactivity to the greater electrophilicity of the *s-cis* conformer and also suggested that secondary orbital interactions between the carbonyl and the diene play a key role in controlling stereoselectivity.[177]

Herein, the NBO analysis shows that the reactivity is not consistent with the lower energy of the $\pi^*_{C=C}$ orbitals. Instead, we find a clear correlation with a greater intramolecular $n(C_\alpha) \rightarrow \pi^*_{C=O}$ interaction in the transition state (see Table 17). The developing negative charge at the α-carbon is better delocalized through the $\pi^*_{C=O}$ orbitals when the C=O and (reacting) C=C bonds are *s-cis*. For example, in the 1,4-addition TS of methyl vinyl ketone **81**, the NBO $n(C_\alpha) \rightarrow \pi^*_{C=O}$ interaction energies (68 and 75 kcal.mol$^{-1}$) correlate with energy barriers of 37.4 and 27.1 kcal.mol$^{-1}$ for *s-trans* and *s-cis*, respectively. Indeed, the HOMO of the transition states have a strong contribution *via* this interaction, that is, a bonding combination of the p-orbitals of the α-C-atom and the π* orbitals of C=O moiety (see Figure 30). It is important to note that in this TS, the axis of the forming C-H bond is bent towards the C=O moiety in an *s-cis* form, whereas, it is bent towards the C(O)-Me in the *s-trans* form, generating two different stereo-configurations (see Figure 30). In summary, electronic effects play a major role in determining the kinetic pathway of amine additions to enones and enals. That is, conformational change from the *s-trans* to the *s-cis* conformers results in reversing the relative reactivity of the C=C and C=O functional groups.

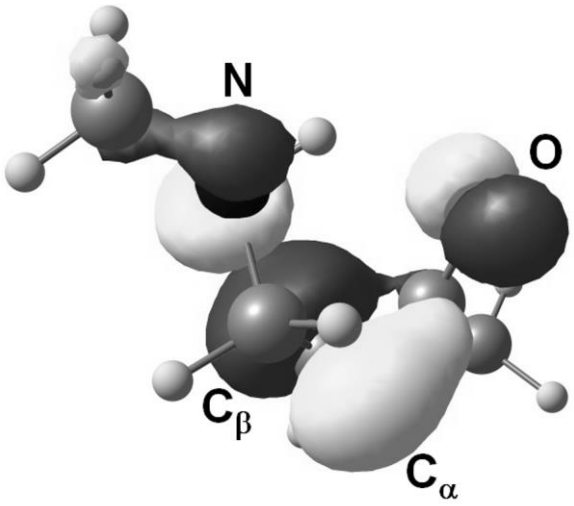


**Figure 28** Representation of the $p_{C\alpha}$-$\pi^*_{C=O}$ interaction in the HOMO orbital for the transition state of the 1,4-addition in the *s-cis* isomer of **81**.

For crotonaldehyde **59**, the *s-trans* conformation is thermodynamically favoured over the *s-cis* conformation by 1.3 kcal.mol$^{-1}$, thereby selectively leading to the kinetically preferred 1,2-addition imine product (see Figure 29 for the main geometric parameters involved in the computed TS).

The computed relative stabilities agree with the results of the high-level calculation[178] and experiments,[179] in which the *s-trans* conformers are favoured by 2.1 and 1.7 kcal mol$^{-1}$, respectively. In addition, vibrational spectroscopic studies showed that only the *s-cis* conformation exists in solution (in small quantities),[179] indicting that only the *s-trans* reaction pathway is operative. For the aliphatic ketones, such as methyl vinyl ketone **81** and pentenone **99**, the additional alkyl group most likely induces steric repulsion with the double bond, destabilizing the *s-trans* conformer which results in shifting the equilibrium towards the *s-cis* conformer. In turn, this is more stable by 0.3 and 0.7 kcal mol$^{-1}$, respectively for **81** and **99**. In the case of **81**, spectroscopic studies revealed that both the *s-cis* and *s-trans* conformations existed.[180,181] Indeed, the energy difference between them is reduced to less than 1 kcal mol$^{-1}$.[182]

Thus, the reaction is likely to proceed through the lowest energy transition states available and that means the *s-cis* pathway. These systems of course, contrast with the cyclic enones. Since they can only adopt the *s-trans* conformation, the kineticically preferred reaction pathway becomes the 1,2-addition process. Although the energy difference for cyclopentenone **91** is quite small, it follows the same trend as the other *s-trans* conformer substrates (see Table 18).

**Table 18** Energy analysis for the 1,2- and 1,4-addtion of $MeNH_2$ to enones and enals [energy barrier ($\Delta E^{\neq}$) and reaction energy ($\Delta E$) in kcal.mol$^{-1}$].

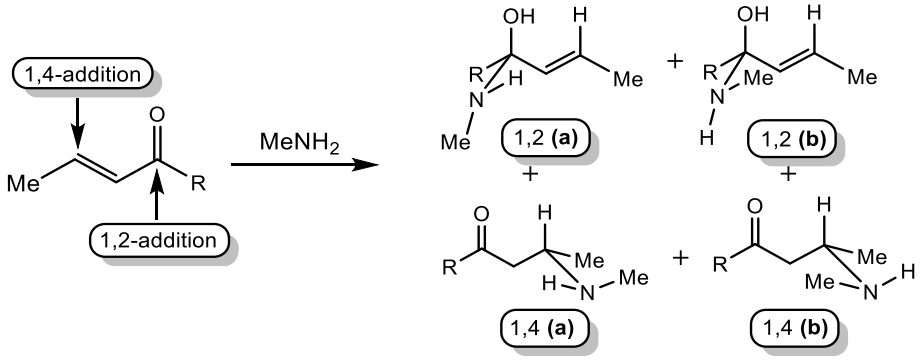


| | $\Delta E^{\neq}$ (1,2a) | $\Delta E$ (1,2a) | $\Delta E^{\neq}$ (1,2b) | $\Delta E$ (1,2b) | $\Delta E^{\neq}$ (1,4a) | $\Delta E$ (1,4a) | $\Delta E^{\neq}$ (1,4b) | $\Delta E$ (1,4b) |
|---|---|---|---|---|---|---|---|---|
| 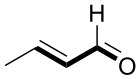 | 33.0 | -4.3 | 33.8 | -2.8 | 38.8 | -9.4 | 37.4 | -10.7 |
| 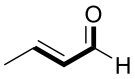 | 30.3 | -4.9 | 31.2 | -4.3 | 29.0 | -14.3 | 30.3 | -12.2 |
| 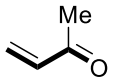 | 35.5 | -1.3 | 35.5 | -0.8 | 37.4 | -16.9 | 37.5 | -15.5 |
| 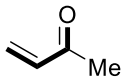 | 33.6 | -1.0 | 33.4 | -0.6 | 27.1 | -16.0 | 30.2 | -18.3 |
| 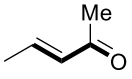 | 36.7 | 0.0 | 36.6 | 0.6 | 41.4 | -11.1 | 40.1 | -12.4 |
| 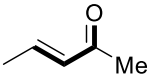 | 34.7 | 0.6 | 34.6 | -0.4 | 30.4 | -14.6 | 32.1 | -11.6 |
|  | 38.2 | 2.2 | 38.9 | 2.5 | 38.9 | -12.3 | 40.1 | -12.4 |

Comparing the different substrates, it was observed that the computed overall energy barriers for the preferred reaction pathways follow the order: aliphatic ketone < aldehydes < cyclic ketones. This is in line with experimental results and supports the idea that the nucleophilic amine addition is the rate-determining step under these non-acidic conditions. As expected, and in all cases, the 1,4-products are thermodynamically favoured over the hemi-aminal intermediates resulting from the 1,2-addition mode.

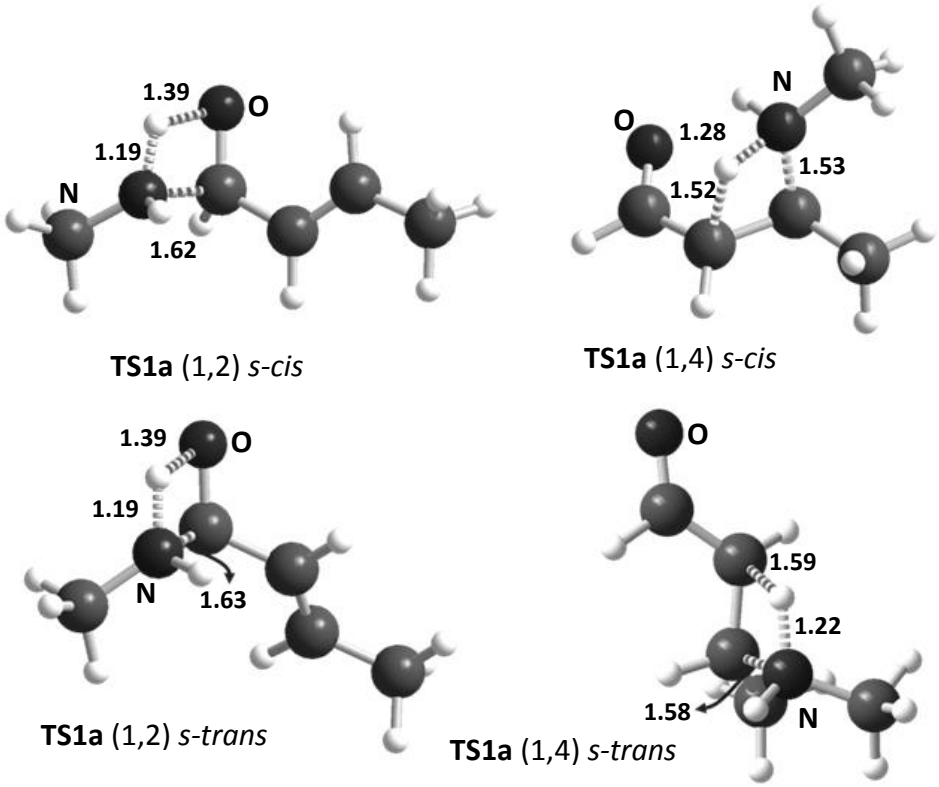


**Figure 29** Molecular structures and geometric parameters of the transition states for the 1,2- and 1,4-addition of $MeNH_2$ to crotonaldehyde **59**. Distances in Å.

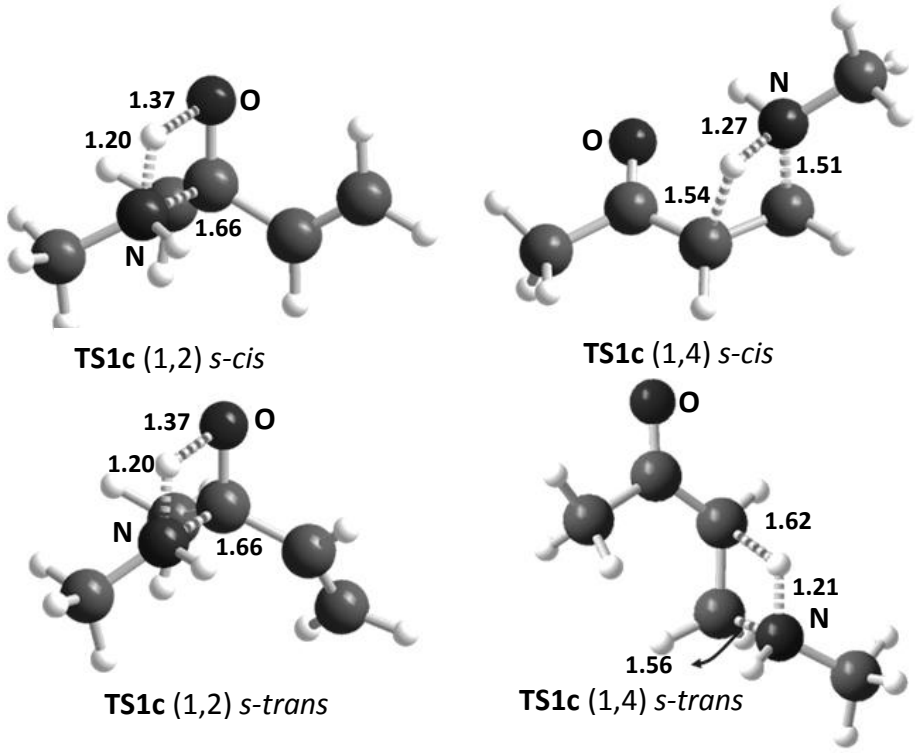


**Figure 30** Molecular structures and geometric parameters of the transition states for the 1,2- and 1,4-addition of $MeNH_2$ to methyl vinyl ketone **81**. Distances in Å.

Thus, not only is the 1,2-addition product kinetically controlled, but also, the 1,4-addition product is observed for methyl vinyl ketone **81**, which is kinetically preferred as a direct consequence of the conformation change that occurs.

Upon expanding the scope of the substrates examined by the DFT calculations, we were surprised to find that the other linear enones prefer to give the 1,2-addition products. This supports the results obtained from the ReactIR and *in situ* $^1$H NMR studies. Following on from methyl vinyl ketone **81** to pentenone **99**, the calculated barriers showed the same pattern as previously identified; however, for the 1,4-addition to C=C, they were found to be somewhat higher for pentenone **99** (*i.e.* by around 3 kcal.mol$^{-1}$) than methyl vinyl ketone **81**, as expected for a substrate with an electron-donating substituent on the C=C (**1j**).

To understand the origin of selectivity on the addition of amines to enals and enones, DFT calculations were performed (B3LYP functional) on representative substrates (crotonaldehyde **59**, methyl vinyl ketone **81**, cyclopentenone **91** and pentenone **99**) using methylamine as a model of primary alkyl amines. Calculations indicated that the kinetic preference for 1,2- or 1,4-addition pathway depends on the conformation of the α,β-unsaturated aldehydes and ketones(*s-cis* or *s-trans*). When the C=C and C=O bonds are *s-trans* to each other the 1,2-addition pathway shows lower energy barriers, while when they exhibit a *s-cis* relationship the 1,4-addition pathway is favoured (see Table 17). The energy of the $\pi^*_{C=O}$ orbitals is lower than that of the $\pi^*_{C=C}$ orbitals suggesting that the electrophilic carbon of the carbonyl group is more reactive than the one of the C-C double bond. Indeed, for *s-trans* isomers, a linear correlation between the computed energy barriers and the energy of the $\pi^*_{C=O}$ and $\pi^*_{C=C}$ orbitals (see Figure 27) was identified. On the other hand, for the *s-cis* conformation the conjugative effects seem to increase the electrophilicity of the olefinic (C=C) group significantly, inverting the relative reactivity of the two functional groups (see Table 17). In fact when *s-cis* isomers are considered, there is no observed correlation between the activation barriers and the energies of the $\pi^*$-orbitals. This supports the idea that the inversion of the selectivity in *s-cis* isomers involves additional electronic effects related to conjugation.

### 2.2.6 Imine study conclusions

The relative reactivity of enones and enals with primary amines have been examined by looking into the competitive 1,2- *vs.* 1,4-addition pathway using a combination of *in situ* IR spectroscopy (ReactIR), NMR and DFT calculations.

*In situ* IR spectroscopy (ReactIR) revealed that enones and enals undergo either

1,2- (to C=O) or 1,4-addition (to C=C) with primary amines (with or without the addition of 3 Å M.S.). This, therefore, suggested that the formation of α,β-unsaturated imines (formed through 1,2-addition to C=O) is under kinetic control for all enals and most enones. However, compounds such as methyl vinyl ketone showed exclusive 1,4-addition, suggesting that 1,4-addition products, *i.e.* β-amino ketones, are kinetically favoured in this case.

A ReactIR investigation, conducted in parallel with a series of $^{1}$H NMR experiments, allowed for confirmation of the results, with regards to the validity of the observations made by ReactIR. Indeed, *in situ* NMR appeared to validate such methods with great success.

In collaboration Jordi Carbó and Jessica Cid, attention was turned to a theoretical explanation for the observations made by ReactIR and $^{1}$H NMR. Indeed, DFT calculations clearly indicate that the selectivity in these addition reactions is governed entirely by conformational and stereoelectonic effects: *s-trans* conformations kinetically favour 1,4-additions; *s-cis* conformations kinetically favour 1,2–additions, and substitution effects can cause conformational swap over due to steric effects.

The rationalisation of the interplaying effects involved in preparing α,β-unsaturated imines from enals and enones makes the preparation and utilisation of the resulting α,β-unsaturated imines *in situ* more predictable. The clean and selective formation of such imines *in situ* has already proven highly valuable for reacting with boryl nucleophiles,[183] and it is expected that these results offer the potential for wider applications in synthesis.

## 2.3 Base-free β-boration

This section (2.3) was carried out with Dr Cristina Solé at the Universitat Rovira i Virgili for three months in 2012 (September-December), under the supervision of Prof M. Elena Fernández.

### 2.3.1 Discovering 1,2-boration of α,β-unsaturated imines.

It was previously shown that the preparation of α,β-unsaturated imines *in situ* could be utilised as suitable platforms for β-boration and other sequential transformations (see section 2.1). In addition, it had been previously observed that the combination of a chiral ligand (usually a phosphine), copper-salt and base, with the appropriate additive (alcohol), allows for the asymmetric β-boration of α,β-unsaturated carbonyls and their analogues (see section **1** for a complete review of this area).

**Table 19** Asymmetric β-boration of α,β-unsaturated aldimines.

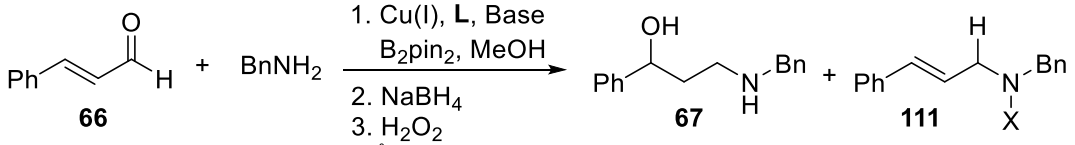


| Entry | **L** (%) | Conv. **66** (%)[a] | Conv. **111** (%)[a] | *e.e.* **67** (%)[b] |
|---|---|---|---|---|
| 1 | $PPh_3$ (6) | 83 | 17 | - |
| 2 | 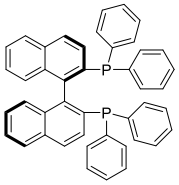 **L16** (3) | 26 | 74 | 0 |
| 3 | 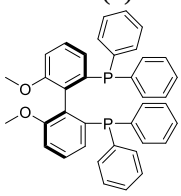 **L6** (3) | 14 | 86 | 11 |
| 4 | 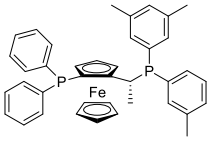 **L19** (3) | 31 | 69 | 0 |
| 5 | 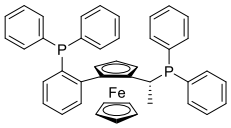 **L18** (3) | 14 | 86 | 7 |
| 6 | 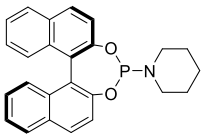 **L12** (6) | 12 | 88 | 0 |
| 7 | 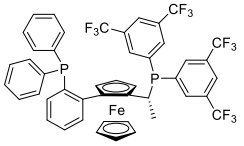 **L22** (3) | 22 | 78 | 5 |

0.25 mmol Scale: **66**: CuCl (3%), **L** (3-6%), NaO*t*Bu (20%), 3 Å M.S. (250 mg) and THF (1.3 mL) were stirred for 15 min under argon. $B_2pin_2$ (1.1 equiv.) is added under argon. After 10 min, enal and amine (0.25 mmol) are simultaneously added to the prepared catalyst mixture, followed by the addition of MeOH (2.5 equiv.). The resulting mixture is stirred under argon for 16 h. After 16 h, $NaBH_4$ (3 equiv.) and MeOH (0.5 mL) was added, and allowed to stir for 3 h. All the solvent was removed under vacuum and replacd with THF (2 mL). Oxidation was achieved by the addition of $H_2O_2$ (3 equiv.) and NaOH (3 equiv.) solutions to give the resulting γ-amino alcohol.[a] Determined by $^1$H NMR analysis. [b]Determined by chiral HPLC-UV.

The investigation of the potential asymmetric β-boration of α,β-unsaturated imines was initially probed on the *in situ*-formed α,β-unsaturated imine **101**, derived from the reaction between cinnamaldehyde **66** and benzylamine **80**. This was achieved by probing different ligands, as shown in Table 19.

Curiously, ligands that usually perform well in such asymmetric β-borations, performed particularly poorly (see Entries 2-6, Table 19) in this case, in both enantioselectivity and conversion of the starting enal to the target β-boryl imine. It is important to note that these results were repeated several times and, indeed, the reaction outcome was the same.

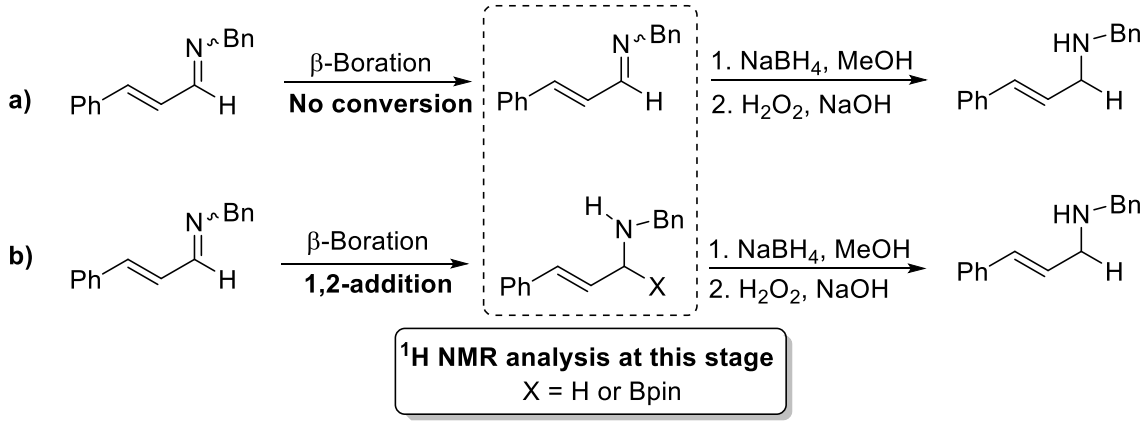


**Scheme 33** Two extreme scenarios of the one-pot methodology: a) No β-boration, with sequential reduction and oxidation gives the allylic amine product **111**; b) Total 1,2-boration of the C=N, with sequential reduction and oxidation gives the allylic amine product.

To investigate the observed inefficiency of the reaction shown in Table 19, $^{1}$H NMR spectra were acquired after the β-boration step in each example (Entries 1-7, Table 19). Surprisingly the presence of allylic species, identified by the characteristic olefinic H-peaks; however, no (H)C=N-peak, observed in crude reaction mixture was unexpected, because this had not been previously observed in such imine systems. However, due to late-stage $^{1}$H NMR analysis, after the subsequent transformations in

this one-pot methodology, such as the reduction of the imine (C=N) functionality and the oxidation of the C-B to the analogous secondary alcohol, these transformations prevented such allylic species being identified. Indeed, it is not possible to distinguish between poor conversion (β-boration, with subsequent reduction to give the allylic amine) and competitive 1,2-boration, because they yield the same allylic amine product (see Scheme 33).

Due to the observed 1,2-boron addition in α,β-unsaturated aldimines, it was decided that it would be more appropriate to examine the asymmetric β-boration of α,β-unsaturated imines derived from enones (not susceptible to 1,2-addition).

### 2.3.2 *In situ* or preformed imines?

When it was first observed that α,β-unsaturated imines, formed *in situ* (see section 2.1), allowed for the formation of the corresponding β-boryl imine, it was uncertain whether this had implications on the asymmetric β-boration process, when compared to that of the asymmetric β-boration of preformed α,β-unsaturated imines.

With the aim of increasing our understanding the asymmetric β-boration of *in situ* (enone and amine added directly to pre-catalyst solution) *vs.* preformed α,β-unsaturated imines was compared and the results are compiled in Table 20. Interestingly, it was found that α,β-unsaturated imines, formed *in situ*, gave comparable conversion to the β-boryl imine. However, significant differences were observed in the enantioselectivity of the reaction. In particular, when the phosphoramidite **L12** was employed, a significant difference in enantioselectivity was observed between *in situ* (*e.e.* 89%) and preformed (*e.e.* 13%) α,β-unsaturated imines (Entries 2 and 8, Table 20, respectively).

**Table 20** Investigating *In situ vs.* preformed imine methodology.

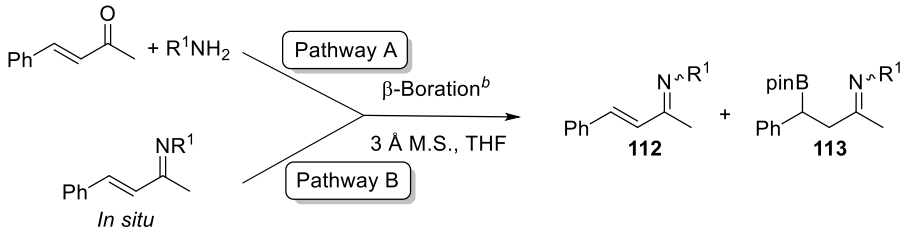


| Entry | L (%) | $R^1$ | Pathway A / B[a] | Conversion (%)[c] | | *e.e.* (%)[d] |
|---|---|---|---|---|---|---|
| | | | | **112** | **113** | **113** |
| 1 | 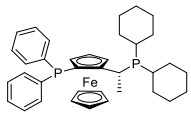 **L3** | Bn | A | 0 | >99 | 33 |
| 2 | 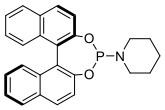 **L12** | Bn | A | 0 | >99 | 89 |
| 3 | 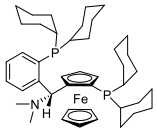 **L21** | Bn | A | 35 | 65 | 69 |
| 4 | 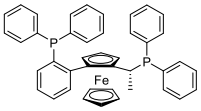 **L18** | Bn | A | 24 | 76 | 76 |
| 5 | 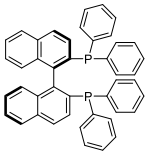 **L16** | Bn | A | 0 | >99 | 56 |
| 6 | 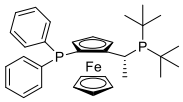 **L20** | Bn | A | 0 | >99 | 37 |
| 7 | **L3** | Bn | B | 12 | 88 | 52 |
| 8 | **L12** | Bn | B | 0 | >99 | 13 |
| 9 | **L21** | Bn | B | 10 | 90 | 31 |
| 10 | **L18** | Bn | B | 0 | >99 | 31 |
| 11 | **L16** | Bn | B | 0 | >99 | 23 |
| 12 | **L20** | Bn | B | 0 | >99 | <5 |

[a]Pathway A: Enone and amine (0.25 mmol, 1:1) were added to catalyst. Pathway B: α,β-Unsaturated imine was formed from the corresponding enone and amine (0.25 mmol, 1:1) over night in the presence of 3 Å M.S., THF, and a was transferred to catalyst without further purification. [b] Assuming 0.25 mmol of substrate. CuOTf (2%), **L** (2%, bidentate or 4% monodenate), NaO*t*-Bu (9%), $B_2pin_2$ (1.1 equiv.), MeOH (2.5 equiv.), 3 Å M.S. (250 mg), THF (1.5 mL). [c] Determined by $^1$H NMR spectroscopy. [d] Determined by chiral-HPLC.

This result was hard to explain at this point, but this inspired further studies into the role of copper, and the presence of free amine in the β-boration catalytic process.

### 2.3.3 Why use copper(I) chloride?

Ma *et al*. recently (2012) reported an interesting and highly enantioselective protocol for the β-boration of α,β-unsaturated *N*-acyloxazolidinones, in which the enantioselectivity was achieved using a chiral bicyclic 1,2,4-triazolium salt.[184] This was later expanded to a full manuscript, highlighting that this protocol is applicable to scale-up.[185] Unlike most β-boration methodologies, they utilised $Cu_2O$ instead of CuCl. With this in mind, various copper-salt and amine combinations were undertaken in the *in situ*-imine formation/β-boration sequence (see Table 21).

In the context of developing cheaper and more sustainable chemical process, attention was turned to streamlining this process by removing the alkoxide base (normally required in copper-catalysed β-boration, see Scheme 16) and using the readily available BINAP **L16** ligand.

**Table 21** Probing the influence of amine concentration on *e.e.* and conversion.

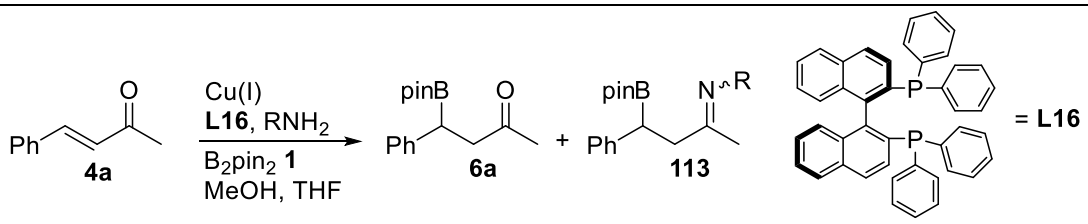


| Entry | Cu(I) | $RNH_2$ (%) | Conv. (%)[a] | | *e.e.* (%)[b, f] | |
|---|---|---|---|---|---|---|
| | | | **6a** (%) | **113** (%) | **6a** (%) | **113** (%) |
| 1 | CuCl | - | - | - | - | - |
| 2 | CuCl | $BnNH_2$ (10) | 21 | 3 | 21 (*S*) | nd |
| 3 | CuCl | $BnNH_2$ (25) | 32 | 3 | 22 (*S*) | nd |
| 4 | CuCl | $BnNH_2$ (50) | - | 36 | - | 89 (*S*) |
| 5 | CuCl | $BnNH_2$ (100) | - | 71 | - | 85 (*S*) |
| 6 | $Cu_2O$ | - | - | - | - | - |
| 7 | $Cu_2O$ | $BnNH_2$ (10) | 37 | 6 | 16 (*S*) | 99 (*S*) |
| 8 | $Cu_2O$ | $BnNH_2$ (25) | 32 | 21 | 22 (*S*) | 99 (*S*) |
| 9 | $Cu_2O$ | $BnNH_2$ (50) | 11 | 46 | nd | 95 (*S*) |
| 10 | $Cu_2O$ | $BnNH_2$ (100) | - | 99 | - | 95 (*S*) |
| 11[c] | $Cu_2O$ | $BnNH_2$ (100) | - | 99 | - | 93 (*S*) |
| 12[d] | $Cu_2O$ | $BnNH_2$ (100) | - | 99 | - | 95 (*S*) |
| 13[e] | CuO | $BnNH_2$ (100) | - | 71 | - | 73 (*S*) |
| 14 | $Cu_2O$ | *n*$BuNH_2$ (100) | - | 99 | - | 27 (*S*) |

Reaction conditions: substrate (0.25 mmol), CuCl (3 mol%) or $Cu_2O$ (1.5 mol%), **L16** (3 mol%), $B_2pin_2$ (1.1 equiv.), MeOH (2.5 equiv.), THF (1 mL), 25 °C, 16 h. [a] Conversion and selectivity calculated from consumed substrate determined by $^1H$ NMR spectroscopy. [b] *e.e.* Calculated by using HPLC–UV spectroscopy as an average of two results. [c] $Cu_2O$ (1.5 mol%), **L16** (6 mol%). [d] $Cu_2O$ (3 mol%), **L16** (6 mol%). [e] CuO (3 mol%), **L16** (6 mol%). [f] *e.e.* Calculated based on the hydrolysed imine (parent ketone) as determined by HPLC–MS.

Firstly, it was observed that no reaction occurs in the absence of amine, regardless of the fact that enone **4a** is a common Michael acceptor in such β-boration reactions (Entries 1 and 6, Table 21), but when the amine loading is increased (0-100%), β-boration is achieved.

The combined conversion to either the β-boryl ketone **6a** or the β-boryl imine **113** is greater than that of the added amine. Indeed, when benzylamine (10%) is employed, the combined conversion to **6a** and **113** is greater than 24%, when a 10%

loading of amine was added (10%). This suggests that the free amine plays a role in the catalytic process. It is important to note the recent advances in amine catalysis, and their role in activating enals and enones towards potential nucleophiles.[186]

When $Cu_2O$ was utilised as the copper source in the β-boration reaction (Table 21), the reaction efficiency was notably better than CuCl. Indeed, when stoichiometric benzylamine was added, the reaction gave complete conversion to the β-boryl imine **113** (>99%, see Entry 10, Table 21). This is in contrast to that of CuCl which gave a poorer conversion to the β-boryl imine **113** (71%, see Entry 5, Table 21). Furthermore, $Cu_2O$ performed better than CuCl in not just efficiency, but also allowed for the enantioselective synthesis of **113** in 95% *e.e.* (%, see Entry 10, Table 21). It was also noted that on increased amine loading, the enantioselectivity of the catalytic process decreased from 99% *e.e.* to 95% (on increasing amine loadings from 10-100%). It should be noted that CuO showed comparable activity to that of CuCl, but with diminished enantioselectivity (see Entry 13, Table 21).

Once it had been established that the presence of free amine in the *in situ* imine formation/β-boration reaction does indeed play an important role in both the catalytic efficiency (judged by conversion to the product β-boryl imine) and enantioselectivity, the β-boration of the preformed α,β-unsaturated imine was probed. This was carried out using various copper salt and base combinations (see Table 22). $Cu_2O$ proved highly efficient in the catalytic β-boration. However, it should be noted that the enantioselectivity was slightly less than (87%, see Entry 1, Table 22) previously observed when free amine was present (95%, see Entry 10, Table 21). Interestingly, when $(MeCN)_4CuPF_6$ was employed both the conversion and enantioselectivity was comparable to when $Cu_2O$ was employed (see Entry 6, Table 22).

**Table 22** Choosing the right copper-source.

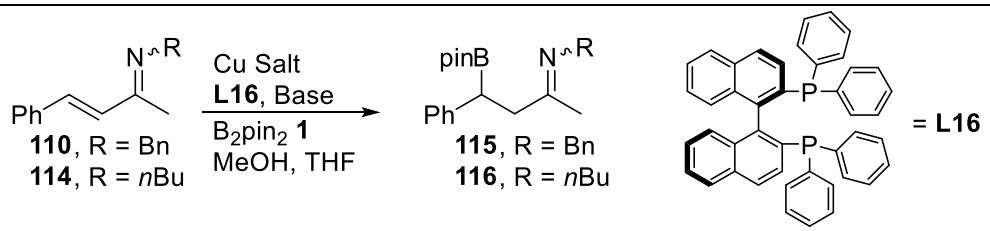


| Entry | Imine **110**/**114** | Cu (3%) | Base (%) | Conv. **115**/**116** (%)[a] | *e.e.* **115**/**116** (%)[b,c] |
|---|---|---|---|---|---|
| 1 | **110** | $Cu_2O$ | - | >99 | 87 |
| 2 | **110** | CuCl | - | - | - |
| 3 | **110** | CuCl | $BnNH_2$ (10) | - | - |
| 4 | **110** | CuCl | $CsCO_3$ (10) | 99 | 0 |
| 5 | **110** | CuCl | NaO*t*Bu (10) | 99 | 0 |
| 6 | **110** | $(MeCN)_4CuPF_6$ | - | 99 | 85 |
| 7 | **110** | CuO | - | 15 | 69 |
| 8 | **114** | $Cu_2O$ | - | 99 | 7 |
| 9 | **114** | $(MeCN)_4CuPF_6$ | - | 99 | 8 |
| 10 | **114** | CuCl | - | - | - |

Reaction conditions: a,b-unsaturated imine (0.25 mmol), CuCl (3 mol%)/**L16** (6 mol%), $(CH_3CN)_4CuPF_6$ (3 mol%)/**L16** (6 mol%) or $Cu_2O$ (1.5 mol%)/**L16** (3 mol%), $B_2pin_2$ (1.1 equiv.), MeOH (2.5 equiv.), THF (1 mL), 25 °C, 16 h. [a] Conversion calculated from consumed substrate determined by $^1H$ NMR spectroscopy. [b] *e.e.* Calculated by using HPLC-UV spectroscopy as an average of two results. [c] *e.e.* Calculated based on the hydrolysed imine (the parent ketone) by using HPLC–MS.

On screening various copper-ligand-base combinations, some interesting observations were made, particularly in the utilisation of $Cu_2O$ instead of CuCl, and the presence of free-amine when carrying out a tandem imine-formation/β-boration. In this context, alternative metal-salts were investigated to examine their catalytic activity in the β-boration reaction. Disappointingly, $Ag_2O$ and FeO were found to be inactive (see Entry 1-2, Table 23). It is important to note that the control reaction, in which no metal salt was utilised, is shown in Entry 3, Table 23. Furthermore, no activity was observed under these conditions, therefore excluding any potential organocatalytic (see Scheme 13 for organocatalytic activation of diboron regents towards conjugate addition) routes as being responsible for the observed β-boration.

**Table 23** Probing other metals in the β-boration reaction.

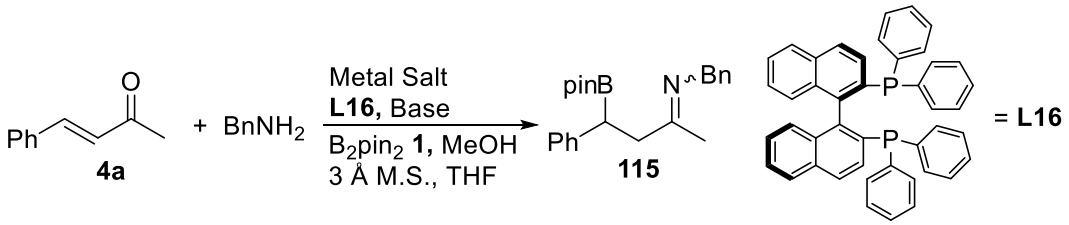


| Entry | Metal Salt (%) | Conv. **115** (%)[a] | *e.e.* **115** (%)[b] |
|---|---|---|---|
| 1 | $Ag_2O$ | 0 | 0 |
| 2 | FeO | 0 | 0 |
| 3 | No Metal | 0 | 0 |

Assuming 0.25 mmol of substrate: Metal salt(0-3%), **L** (3%), 3 Å M.S. (250 mg) and THF (1.300 mL) were stirred for 15 min under argon. $B_2pin_2$ (1.1 equiv.) is added under argon. After 10 min, enone and benzylamine (0.25 mmol, 1:1) are simultaneously added to the prepared catalyst mixture, followed by the addition of MeOH (2.5 equiv.). The resulting mixture is stirred under argon for 16 h. [a] Determined by $^1$H NMR analysis. [b]Determined by chiral HPLC-UV.

### 2.3.4 Scope of base-free methodology

Previous investigations on the base-free β-boration were conducted on chalcone derivatives (*e.g.* **4a** and **4b**, see previous section 2.3.3). Indeed, it was desirable to understand whether this process was general and, therefore, could be applied to a broad range of substrates. This was investigated (see Table 24) on a series of linear enones (Entries 1-12, Table 24), chalcone derivatives (Entries 13-20, Table 24) and a cyclic enone (Entries 21- 24, Table 24) with a selection of chiral ligands (Figure 31). Indeed, this methodology was highly successful, resulting in the β-boration of linear and cyclic enones (see Table 24) to the β-boryl imine. It should be noted that key intermediates towards the synthesis of enantio- and diastereomerically enriched γ-amino alcohol within the Whiting and Fernández groups.[64]

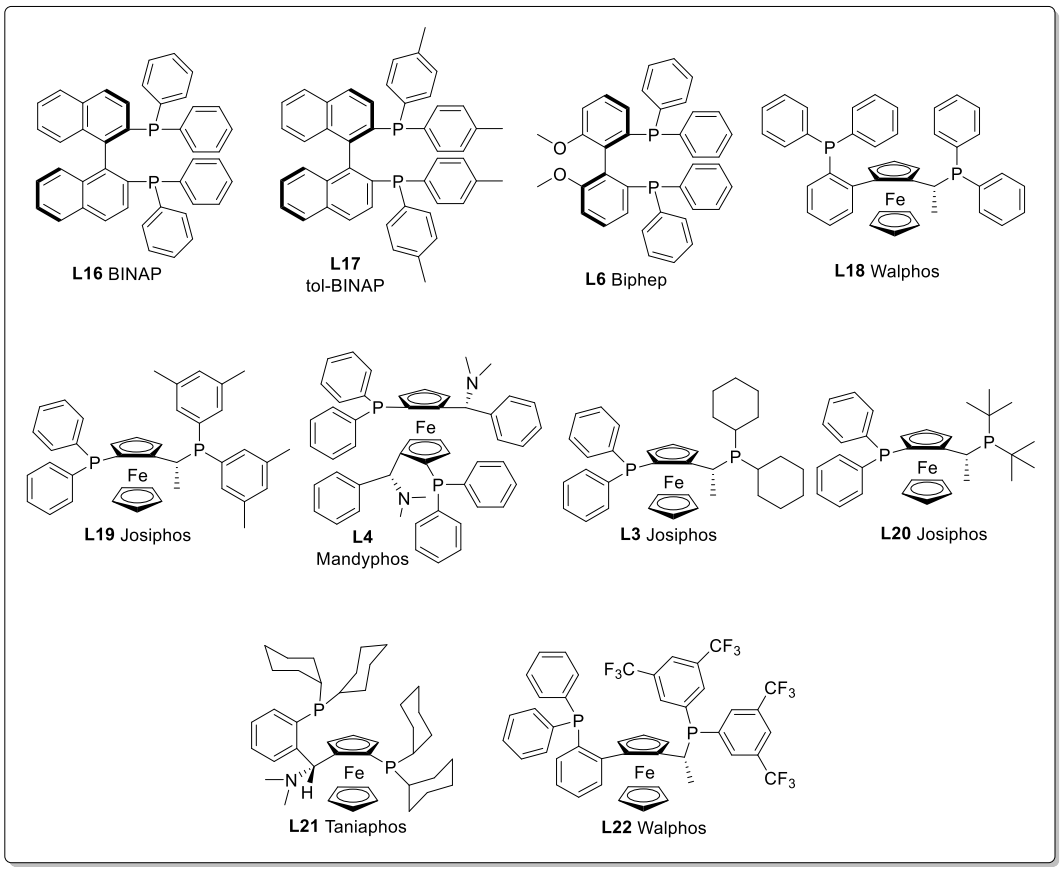


**Figure 31** Chiral ligands **L**.

**Table 24** Investigating the substrate scope of the base-free methodology.

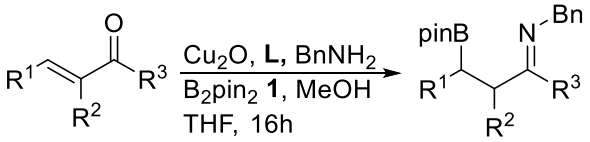


| Entry | Substrate | **L** (%) | Conv. (%)[a] | *e.e.* (%)[b,c] |
|---|---|---|---|---|
| 1 | 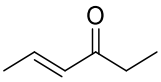 | **L16** | 55 | 66 |
| 2 | | **L17** | 63 | 61 |
| 3 | | **L6** | 68 | 50 |
| 4 | | **L19** | 54 | 80 |
| 5 | 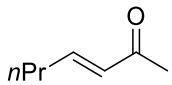 | **L16** | 70 | 62 |
| 6 | | **L17** | 93 | 60 |
| 7 | | **L6** | 90 | 64 |
| 8 | | **L19** | 52 | 73 |
| 9 | 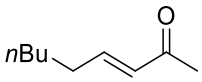 | **L16** | 71 | 70 |
| 10 | | **L17** | 77 | 66 |
| 11 | | **L6** | 58 | 64 |
| 12 | | **L19** | 64 | 92 |
| 13 | 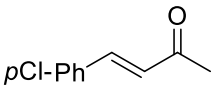 | **L16** | 99 | 48 |
| 14 | | **L17** | 99 | 47 |
| 15 | | **L6** | 99 | 58 |
| 16 | | **L4** | 99 | 35 |
| 17 | 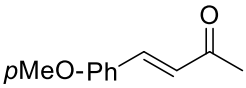 | **L16** | 67 | 86 |
| 18 | | **L17** | 71 | 82 |
| 19 | | **L6** | 85 | 49 |
| 20 | | **L4** | 99 | 35 |
| 21 | 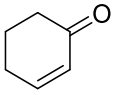 | **L16** | 99 | 39[d] |
| 22 | | **L17** | 99 | 65[d] |
| 23 | | **L6** | 97 | 30[d] |
| 24 | | **L18** | 20 | 92[d] |

Conditions: a,b-unsaturated imine (0.25 mmol), $Cu_2O$ (3 mol%), **L** (6 mol%), $B_2pin_2$ (1.1 equiv.), MeOH (2.5 equiv.), THF (1.3 mL), 25 $^oC$, 16 h. [a] Conversion calculated from consumed substrate determined by $^1H$ NMR spectroscopy; isolated yield in parentheses. [b] *e.e.* Calculated by using HPLC–UV spectroscopy as an average of two results. [c] *e.e.* Calculated based on the hydrolysed β-borated ketone by using HPLC–MS. [d] CuCl (3 mol%), NaOtBu (3 mol%), **L** (3 mol%).

### 2.3.5 Mechanism of base-free β-boration

The mechanism of copper-catalysed β-boration has been discussed previously (Scheme 16). Generally, the presence of a base (usually an alkoxide) is required to form a copper alkoxide species which, on addition of a suitable diboron reagent (*e.g.* $B_2pin_2$) and ligand, readily undergoes σ-bond metathesis with the diboron compound to form the active ligated-copper-boryl nucleophilic species.

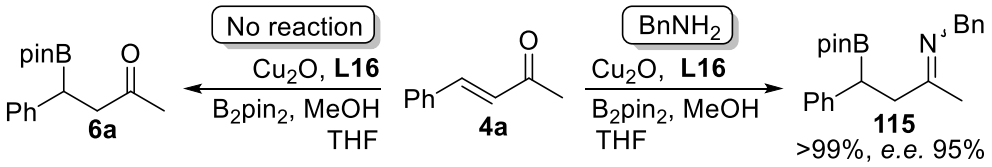


**Scheme 34** Base free β-boration (with and without amine additives).

Initial observations showed that enone **4a** was unreactive in the $Cu_2O$ base-free system. The addition of an amine resulted in quantitative transformation of enone **4a** to the β-boryl imine **115** (see Scheme 34). Furthermore, the preformed imine is reactive under these conditions; however, the enantioselectivity is slightly lower under these conditions (87% *e.e.*, see Entry 1, Table 22), thus suggesting a beneficial effect as a result of free amine in the catalytic system.

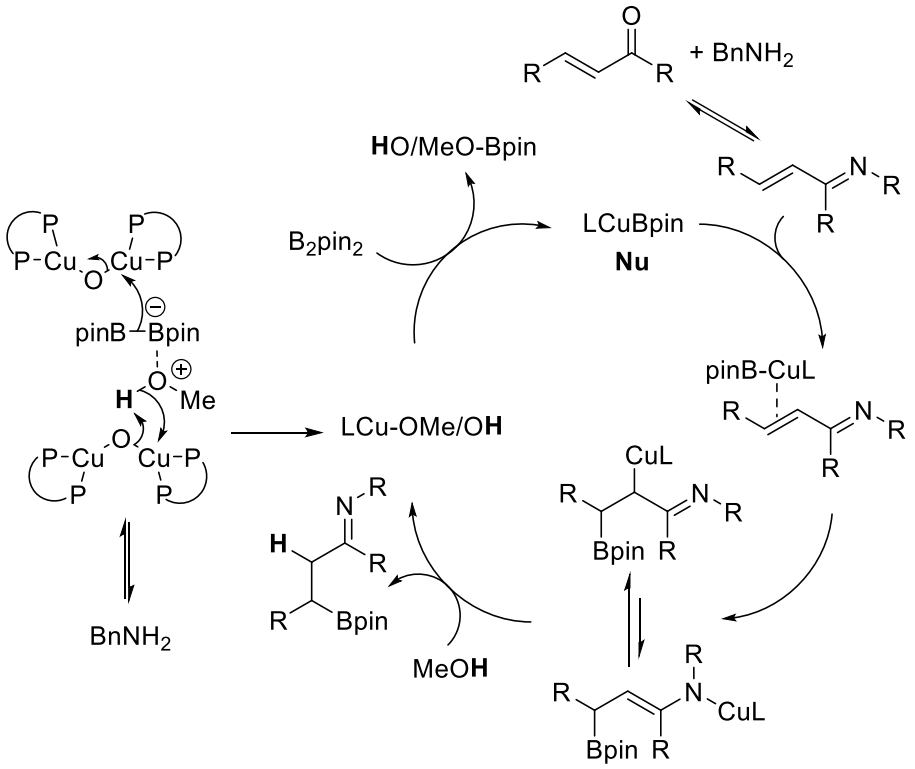


**Scheme 35** Proposed mechanism of the base-free β-boration methodology.

Mechanistic elucidation is challenging in such complex catalytic system and, indeed, can be often difficult to elucidate.[187, 188] Nevertheless, it is clear that:

- Enone **4a** is unreactive under these conditions;
- α,β-unsaturated imine **110** is reactive under these conditions;
- forming imine **110** *in situ*, thus providing a large surplus of free amine, results in higher enantioselectivity (to **115**) than that of the preformed imine.

Therefore a mechanism or catalytic cycle must accommodate these observations. Indeed, it is suggested in Scheme 35 that $Cu_2O$ can undergo σ-bond metathesis to form the copper methoxide (or hydroxide) species. Moreover, this process might be facilitated by free-amine, available through dynamic equilibria, coordinating to copper and therefore aiding σ-bond metathesis and improving catalytic activity. Such copper

alkoxides or hydroxides are accepted catalytically active species in the copper-catalysed β-boration reaction (see Scheme 16).

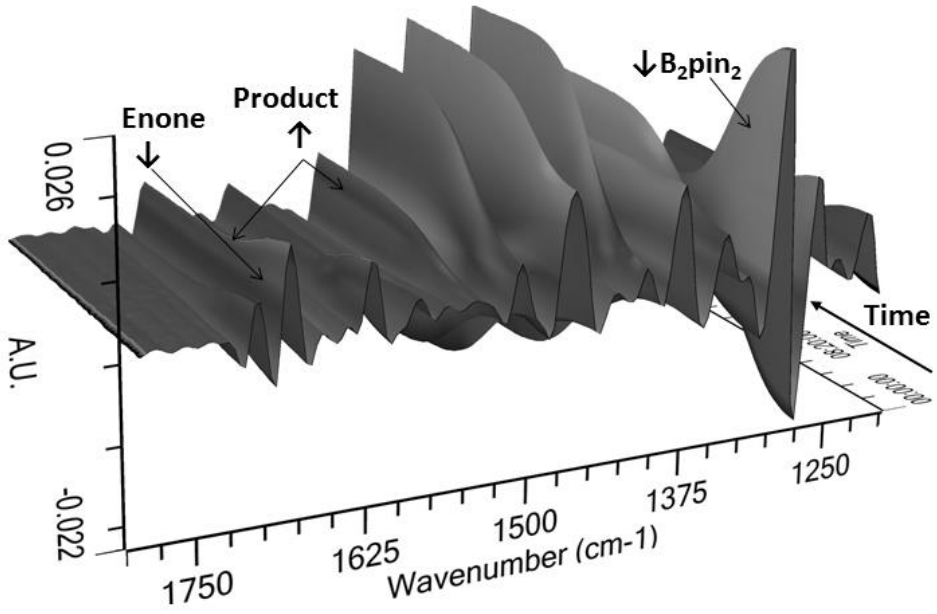


**Figure 32** Monitoring the base-free β-boration by ReactIR.

Further mechanistic studies were conducted using *in situ* IR spectroscopy (see Figure 32). It was clear from this analysis that the reaction appears to proceed through one primary pathway. Indeed, the loss of enone **4a** (C=O stretch) appeared to mirror the concurrent rise in the product imine **115** (following C=N). This was deemed consistent with the formation of imine **110** followed by β-boration, and not β-boration of enone **4a** (with subsequent imine formation of **6a**).

### 2.3.6 Summarising the base-free methodology

Through aiming to develop the analogous asymmetric one-pot methodology, as introduced in Section 2.1, it was identified that α,β-unsaturated imines, derived from enals, are susceptible to 1,2-addition of the nucleophilic copper-boryl nucleophile. This was only a minor problem when such species are ligated with $PPh_3$ and, therefore, was not identified earlier. However, on the application of chiral phosphine ligands, 1,2-addition became the predominant reaction pathway, presumably through increased nucleophilicity of the copper-boryl adduct. This forced a change in project direction. This change in direction allowed for the exploration and development of a base-free β-boration methodology. Moreover, this allowed for a direct comparison between forming imines *in situ* and preforming them, with their subsequent transformation *in situ*. This allowed for a more streamlined, efficient and highly enantioselective process to be developed, which gives access to chiral γ-amino alcohols, based on previous derivatisation methods within the group(s).[60,64] It became apparent that a methodology, limited in application to enones, would be a major disadvantage. Controlling and, indeed, stopping 1,2-addition was investigated. This will be discussed in the following section (2.4).

## 2.4 Selective transformation of enals into γ-amino alcohols

The addition of copper-boryl nucleophiles to α,β-unsaturated aldimines, when modified with chiral phosphines, proceed *via* a 1,2-addition pathway (see section 2.3). This section deals with: 1) the 1,2-addition pathway; 2) the nature of the R-group (C=N-R) attached to the nitrogen of the imine functionality and; 3) overcoming such 1,2-addition *via* the use of *N*-benzhydryl derived aldimines.

### 2.4.1 The problem with 1,2-addition

The addition of boron nucleophiles to prochiral electron-deficient alkenes has been described previously (section 1). However, it has been noted in the literature that α,β-unsaturated aldehydes suffer from competitive 1,2-boron addition[73] and, therefore, the synthesis of β-boryl aldehydes is a challenge (see Figure 33a). Indeed, it should be noted that Sadighi *et al*. unambiguously demonstrated the insertion of an aldehyde into a copper-boron bond, ultimately leading to the 1,2-diboron product (C- and O-bound boryl units).[189] Moreover, evidence for such species was obtained in solution and the solid state (X-ray crystallography of NHC-Cu-Bpin species).[70]

Previously, preformed copper-alkoxide catalysts have proved to efficiently interact with $B_2pin_2$ **1** *via* σ-bond metathesis, which demonstrated an improved selectivity (1,2- *vs* 1,4-addition) in the β-boration of α,β-unsaturated aldehydes.[190] However, the asymmetric induction of the $C_\beta$-B bond formation was originally afforded in modest *e.e.* when chiral *N*-heterocyclic carbene (NHCs) modified copper-salts were used. The direct activation of $B_2pin_2$ with chiral NHCs favoured the formation of enantioenriched mixtures of β-boryl aldehydes with *e.e.* values up to 90%, despite large amounts of base and MeOH (30 mol% and 60 equiv. respectively) being required.[73]

Moreover, this methodology was limited to β-aryl substituted α,β-unsaturated aldehydes. Alternative approaches to promote the selective 1,4-boryl addition to enals were postulated on the basis of iminium intermediates, both in copper-mediated-reactions[77] and organocatalytic reactions.[76]

Alternative approaches to promote the 1,4-addition pathway (β-boration) in enals were proposed on the basis of using iminium intermediates, both in copper-mediated[77] and organocatalytic reactions.[76] However, only when CuOTf/$PPh_3$ catalysed the reaction in the presence of a chiral proline-derived co-catalyst could the resulting β-borated product be formed with moderate to high *e.e.* (up to 95%), as proved by conversion of the β-boryl aldehyde intermediates into enantioenriched mixtures of homoallylboronates (through Wittig chemistry).[76] The use of an organic acid as an additive (2-fluorobenzoic acid) was required in order to accelerate the catalytic cycle of the iminium ion formation, hence providing the selective 1,4-addition product in this process.

### 2.4.2 Stopping 1,2-boration of α,β-unsaturated aldimines

To access γ-amino alcohols using one-pot protocols, through organoboron intermediates,[8] a highly selective copper-catalysed β-boration of *in situ* formed enone and enal-derived α,β-unsaturated imines, with subsequent C=N reduction and C-B oxidation was developed (see this section, 2.4).[9] Furthermore, the four steps were efficiently carried out without isolation of intermediates, allowing for the overall high mass recovery. In addition, the substrate scope was open to β-alkyl and β-aryl substituted α,β-unsaturated aldehydes (see upcoming sections).

Focus was turned to the enantioselective version of this straightforward methodology to establish a new protocol to induce enantioselectivity in the β-borylation

step through the use of chiral phosphine ligands, *i.e.* to modify the copper-catalytic system (see Figure 33c).

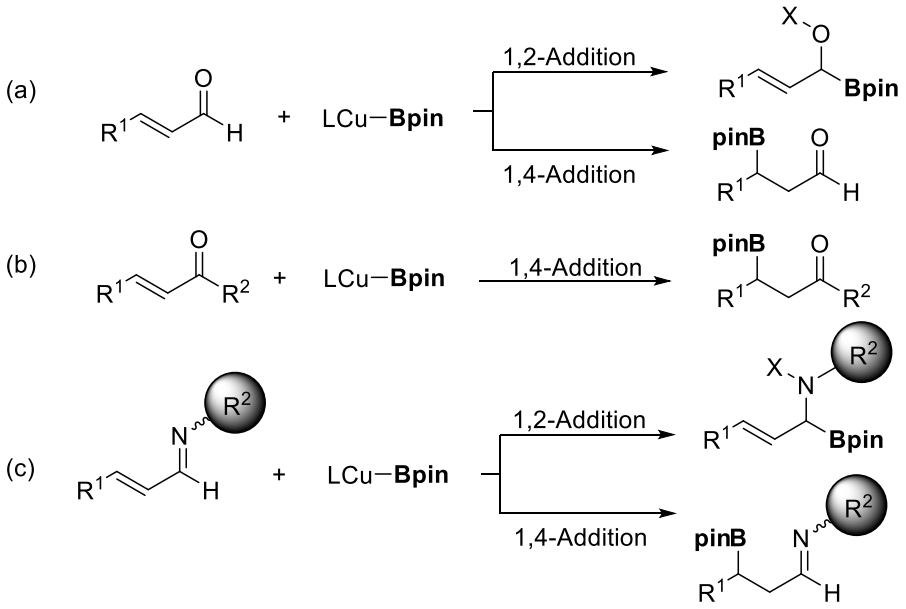


**Figure 33** Competitive 1,2- *vs* 1,4-addition in different electron-deficient alkenes.

The advantage of using α,β-unsaturated aldimines as borylation substrates is based on the complete selectivity on the 1,4-addition as a result of steric hindrance of C=NR bond versus C=O (Table 25). Indeed, a comparative study of the selective β-boration of 2-hexenal **116** and the β-boration of the corresponding imines formed *in situ* by condensation with benzhydrylamine ($Ph_2CHNH_2$), benzylamine, *p*MeO-benzylamine and *n*-butylamine. Subsequent hydrolysis of the β-borated imines (Scheme 36) thus provided the β-borated aldehyde with higher selectivity than the direct β-boration of 2-hexenal **116**. In the β-boration of the α,β-unsaturated imine formed from *n*-butylamine, the selectivity dropped significantly, which is consistent with the reduced steric hindrance around the C=N bond (Table 25, Entry 5).

**Table 25** Controlling 1,2- *vs* 1,4-boration with the use of sterically bulky amines.

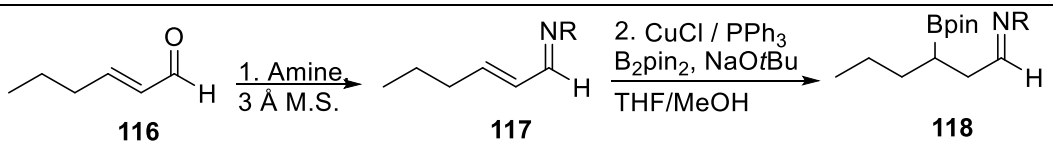


**116** **117** **118**

| Entry | Amine | Conv. **118** (%)[b] |
|---|---|---|
| | - | |
| 1 | | 63 |
| 2 | *p*MeO-Ph-$NH_2$ | 99 |
| 3 | $BnNH_2$ | 99 |
| 4 | $Ph_2CHNH_2$ | 99 |
| 5 | *n*$BuNH_2$ | 75 |

[a] 0.25 mmol scale reaction: 2.00 mmol (1:1, amine: enal) was stirred in THF (8 mL) and 3 Å M.S. (2.0 g) for 16 h, after which a 1 mL aliquot was transferred to a Schlenk-tube (under Ar) containing Cu(I) salt (3 mol%), $PPh_3$ (6 mol%), NaO*t*Bu (9 mol%) and $B_2pin_2$ (1.1 equiv.). After 5 min, MeOH (2.5 equiv.) was added to the solution and the reaction was stirred 6 h. [b] Determined by $^1$H NMR.

It was found that benzhydrylamine provided sufficient steric hindrance to guarantee the complete selective β-boration of 2-hexenal **116**. For that reason, attention was turned to β-aryl and β-alkyl substituted enals to explore the viability of this methodology. Furthermore, the *in situ* formation of imine **119**, derived from cinnamaldehyde **66** and benzhydrylamine, could be monitored using ReactIR (see Figure 34 and Table 26). Indeed, it should be noted that if this reaction is conducted in IPA, a white precipitate (imine **119**) forms throughout the reaction [see work of Alba Pujol, Whiting & Fernández group(s), from 2013]. Taking an aliquot of the suspension and adding several drops of toluene results in the formation of a clear, colourless suspension which, upon slow and gradual evaporation yielded a pale yellow, crystalline solid. This crystal was of sufficient purity to allow for the crystal structure (see Figure 35) to be acquired.

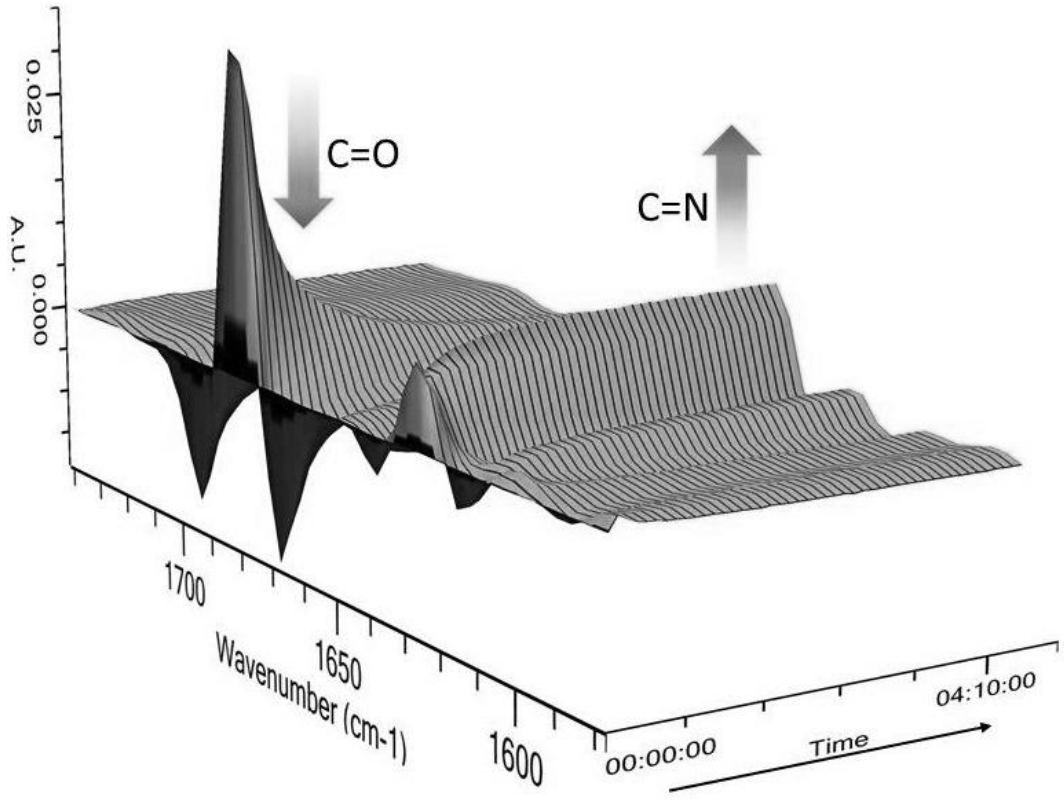


**Figure 34** ReactIR graphical output showing the reaction between **66** and benzhydrylamine to give the α,β-unsaturated imine **119**.

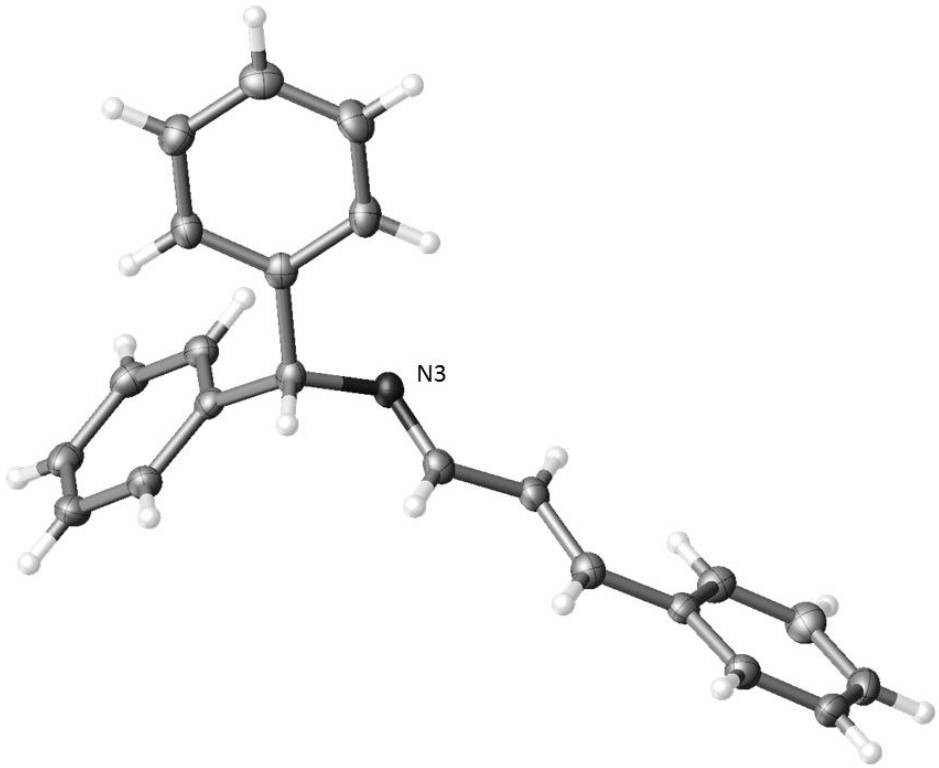


**Figure 35** X-ray crystal structure of α,β-unsaturated imine **119**.

**Table 26** ReactIR studies on imine formation.

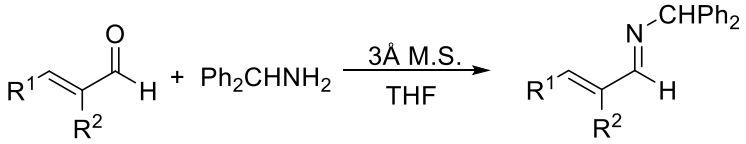


| Entry | Substrate | Product | t / min (h) | $t_{1/2}$/ min |
|---|---|---|---|---|
| 1 | 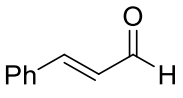 **66** | 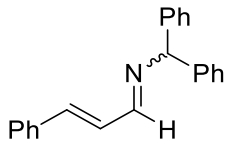 **119** | 270 (4.5) | 22 |
| 2 | 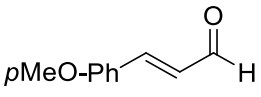 **120** | 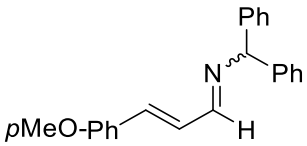 **121** | 300 (5) | 54 |
| 3 | 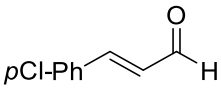 **122** | 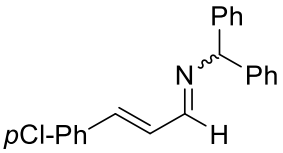 **123** | 480 (8) | 55 |
| 4 | 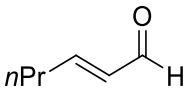 **116** | 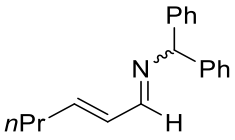 **124** | 420 (7) | 28 |
| 5 | 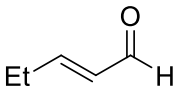 **125** | 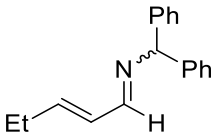 **126** | 480 (8) | 30 |
| 6 | 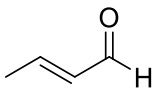 **59** | 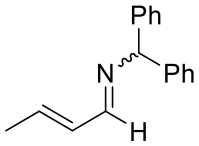 **127** | 300 (5) | 29 |

Conditions: Enal (1 mmol) was added to a stirring solution of THF (4 mL) and 3 Å-molecular sieve pellets. Amine (1 mmol) was added to the stirring solution and the reaction was monitored by ReactIR until the complete loss of the C=O stretch had been observed.[a] Time for total loss of C=O and the emergence of the new species.

### 2.4.3 Highly enantioselective β-boration

The next challenge of this methodology was to examine a series of chiral ligands (see Figure 36) in the β-borylation of imine **119** (formed *in situ*).

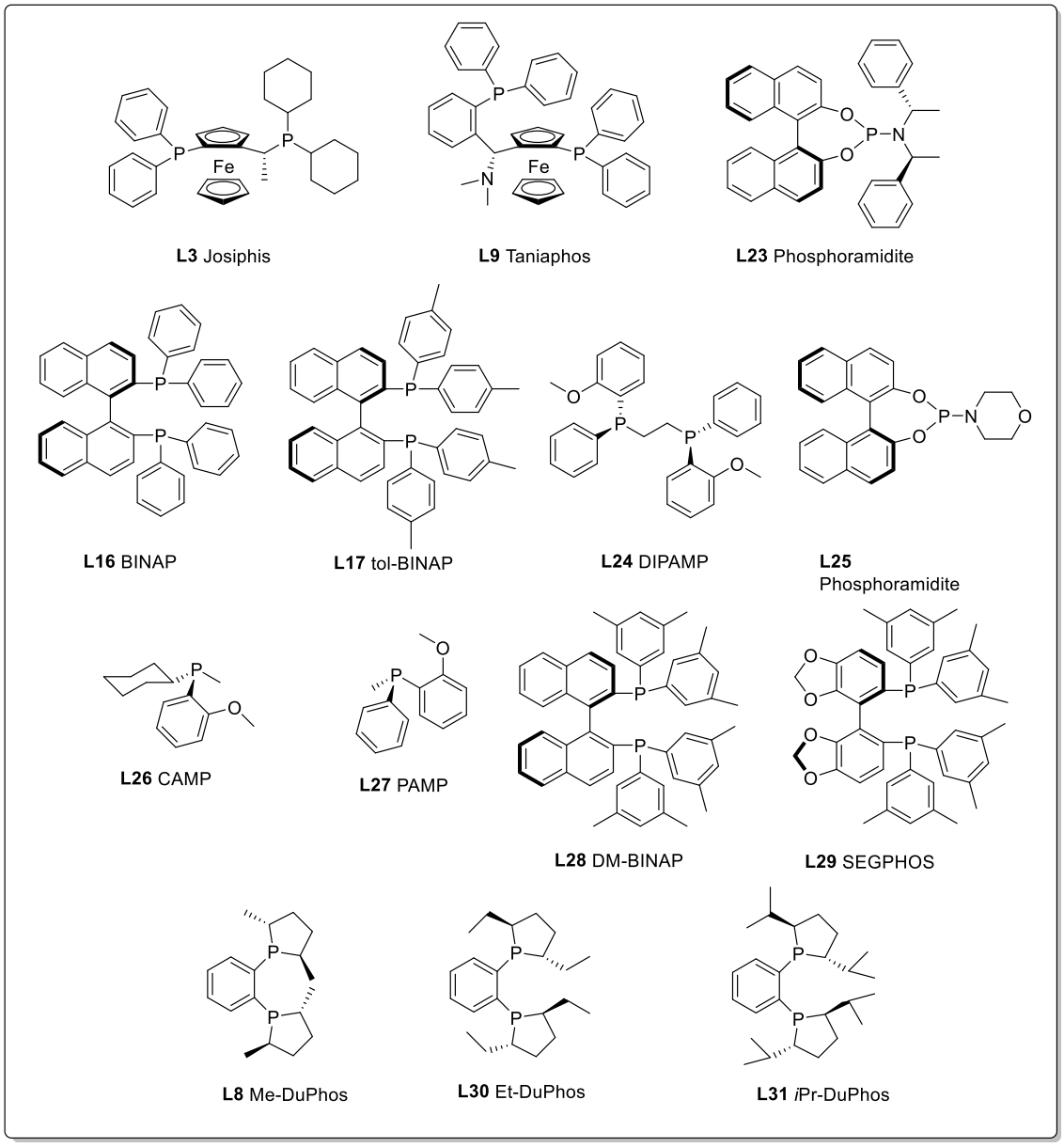


**Figure 36** Chiral Ligands, **L**.

**Table 27** Screening chiral ligands in the enantioselective preparation of **128**.

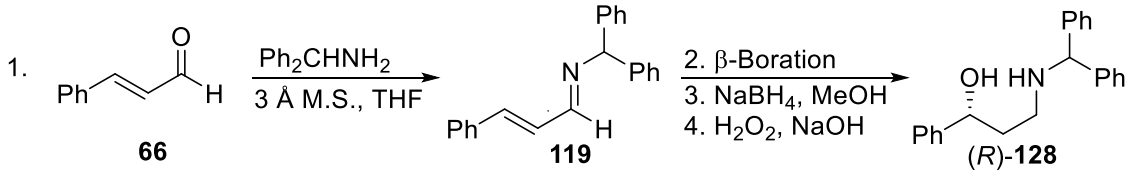


| Entry | L (%) | Cu(I) (%) | Base (%) | Conv. **128** (%)[a] | I.Y. **128** (%)[b] | *e.e.* **128** (%)[c] |
|---|---|---|---|---|---|---|
| 1 | $PPh_3$ (6) | CuCl (3) | NaO*t*Bu (9) | 82 | 62 | - |
| 2 | **L16** (3) | CuCl (3) | NaO*t*Bu (9) | 85 | 53 | 72 |
| 3 | **L16** (3) | $Cu_2O$ (1.5) | - | 0 | - | - |
| 4 | **L17** (3) | CuCl (3) | NaO*t*Bu (9) | >95 | 64 | 71 |
| 5 | **L17** (3) | $Cu_2O$ (1.5) | - | 0 | - | - |
| 6 | **L24** (3) | CuCl (3) | NaO*t*Bu (9) | 62 | 32 | 5 |
| 7 | **L25** (6) | CuCl (3) | NaO*t*Bu (9) | 60 | 28 | 17 |
| 8 | **L28** (3) | CuCl (3) | NaO*t*Bu (9) | >95 | 50 | 97 |
| 9 | **L29** (3) | CuCl (3) | NaO*t*Bu (9) | >95 | 45 | 80 |
| 10 | **L8** (3) | CuCl (3) | NaO*t*Bu (9) | 54 | 52 | 14* |
| 11 | **L30** (3) | CuCl (3) | NaO*t*Bu (9) | >95% | 86 | 58 |
| 12 | **L31** (3) | CuCl (3) | NaO*t*Bu (9) | 27 | -[d] | 97 |

0.50 mmol Scale reaction: 2.00 mmol (1:1, benzhydrylamine: cinnamaldehyde) was stirred in THF (8 mL) and 3 Å M.S. (2.0 g) for 6 h, after which a 2 mL aliquot of *in situ*-formed imine **119** was transferred to a Schlenk-tube (under argon) containing Cu(I) salt, **L**, base and $B_2pin_2$ (1.1 equiv.). After 5 min MeOH (2.5 equiv.) was added to the solution and the reaction was stirred overnight. $NaBH_4$ (1.50 mmol) was added, followed by the drop-wise addition of MeOH (1 mL). The mixture was stirred for 3h, followed by the removal of solvent under reduced pressure. THF (3 mL) was added to the resulting residue, followed by NaOH (0.30 mL, w/v 20%) and $H_2O_2$ (0.13 mL, w/v 35%), and the solution was heated to reflux for 1 h. After standard work-up procedures and column chromatography, a white solid was obtained. [a] Determined by $^1H$ NMR analysis. [b] Isolated yield. [c] Determined by Chiral HPLC on the resulting *O*/*N*-diacetate. [d] Converted to the *O*/*N*-diacetate and isolated before HPLC.

It was observed that under these conditions, conversions up to >95% to the γ-amino alcohol **128**) could be achieved and, moreover, up to 97% *e.e.* in the case of the BNAP derivative, DM-BINAP **L28** (see Table 27, Entry 8).

It should be noted that compound **128** is initially formed as a viscous, colourless oil. However, this compound, upon standing, yields a white amorphous solid. The addition of this amorphous solid to anhydrous hexanes resulted in a white cloudy suspension. The addition of several drops of anhydrous diethyl ether, in tandem with heating, resulted in the formation of a colourless clear solution. This was allowed to cool and slowly evaporate (through a capillary tube) overnight at room temperature, which resulted in the formation of several spots of crystalline **128** (see Figure 37).

Evidence of intramolecular hydrogen bonding was observed in the solid state. It was previously mentioned (Section 2.1) that no N-H or O-H signals are typically observed in the $^{1}$H NMR spectrum (*e.g.* see Figure 8) of such γ-amino alcohols. It was suspected that these signals are present, but highly diffuse, and therefore not visible, due to intramolecular hydrogen bonding.

The derivatisation of **128** into the analogous 1,3-oxazine **129** (by the addition of formaldehyde solution) resulted in the formation of a solid compound which allowed for the absolute stereochemistry to be determined by copper-source X-ray crystallography (see Figure 38).[191]

It is important to note at this stage that ligands **L3**, **L9**, and **L23** (*e.g.* Josiphos and Taniaphos class of ligands) were examined due to their previous success in the asymmetric catalytic β-boration (see section 1.2). However, on inspection of the crude NMR after the β-borylation step, catalytic β-borylation was found to be <5%, <5% and 16% respectively, for the ligands **L3**, **L9** and **L23** (in the system shown in Table 27). It is not clear why this is, but these results were repeated and the outcome was consistent with the previous observation. No competitive 1,2-addition was observed, just small amounts of β-borylated product and the starting imine **119**.

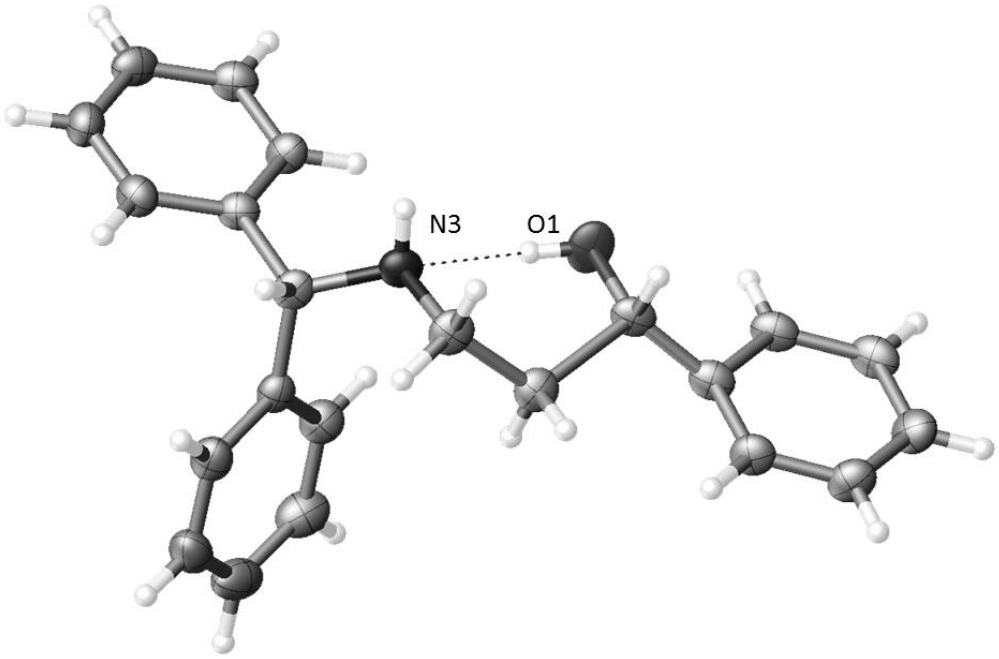


**Figure 37** X-Ray structure γ-amino alcohol **128** – solid state evidence for intramolecular hydrogen bonding.

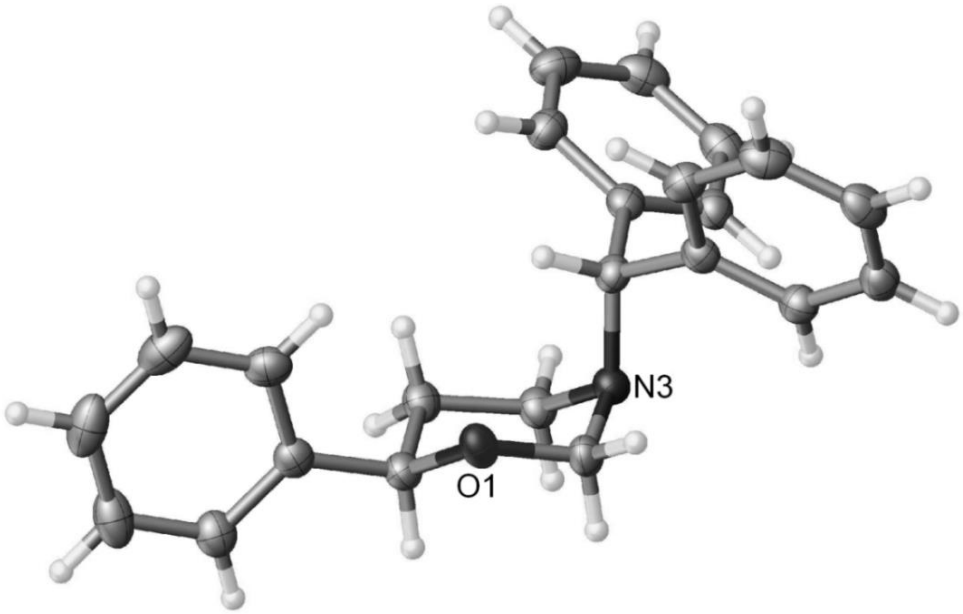


**Figure 38** X-Ray structure of 1,3-Oxazine **129** – used to determine the absolute stereochemistry of **128**.

### 2.4.4 Analysis of *e.e.* and absolute stereochemistry results

Section 2.4.3 showed that the major enantiomer in all cases of copper-catalysed β-borylation was that of the (*R*)-**128** (see Table 27), when using (*R*)-enantiomers of BINAP **L16** (including analogues thereof). This was confirmed by copper-source X-ray analysis of an enantiopure sample of the 1,3-oxazine **129**, as shown in Figure 38. It should also be noted that this absolute stereochemical outcome was consistent with previous experiments conducted on other analogous systems.[64]

It is clear from looking at Table 27 that the BINAP-type ligands perform the best in terms of catalytic turnover (judged by conversion to the desired product **128**) and enantioselectivity. Indeed, ligands with axial chirality (through restricted bond rotation about the biphenyl C-C bond axis) seem to perform the best.

Of the ligands that were examined, (*R*)-DM-BINAP **L28**, (*R*)-DM-SEGPHOS **L29** and the DuPhos **L31** ligands performed the best. If one examines the BINAP ligands (*R*)-BINAP **L16**, (*R*)-tol-BINAP **L17** and (*R*)-DM-BINAP **L28**, the only difference is the substitution on the phenyl ring attached to the phosphorous atom. Furthermore, in the case of **L17** a *para*-methyl substituent appears to have no significant effect on enantioselectivity, but the conversion to the product **128** was slightly higher when compared to **L16** (>95 when using **L17** and 85% when using **L16**). However and perhaps unpredictably, two *meta*-methyl substituents on the phenyl ring gave equally high conversions, but significantly greater enantioselectivity (97%, Entry 8, Table 27). Again, (*R*)-SEGPHOS **L29** has two *meta*-methyl substituents present on the phenyl ring, which results in 80% *e.e.* of the product **128** (see Entry 9, Table 27).

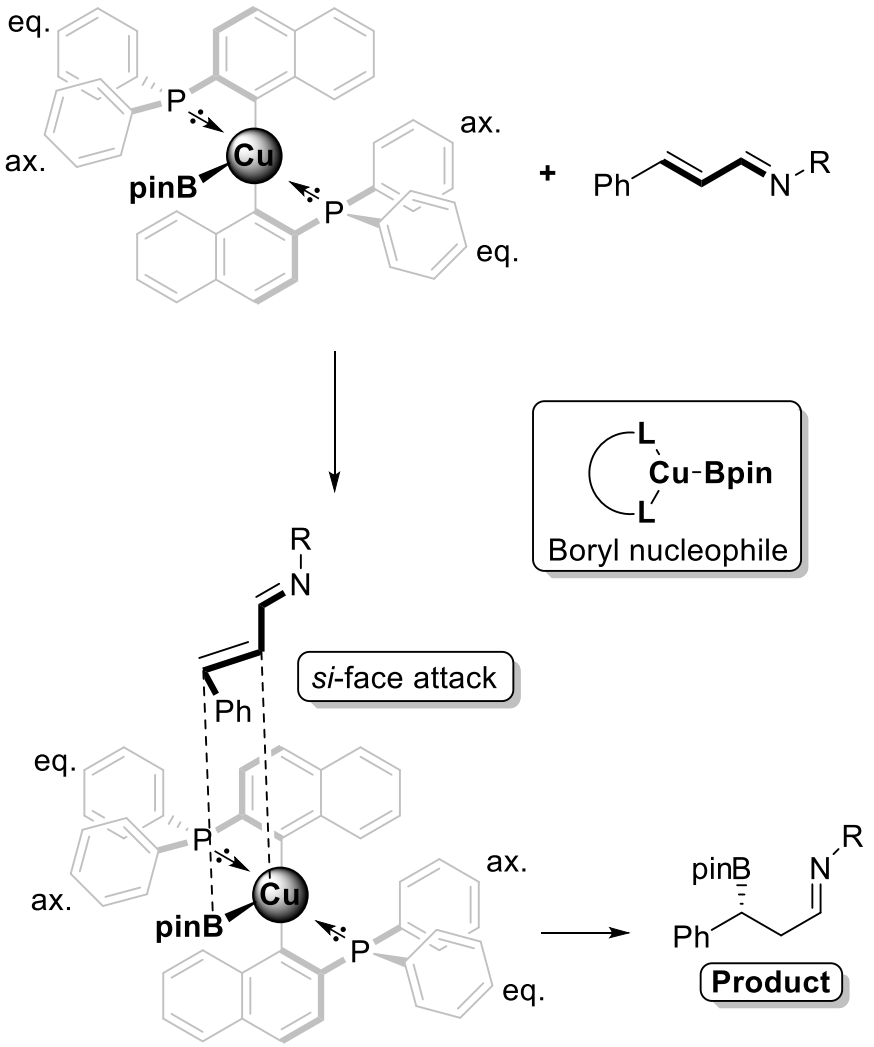


**Figure 39** Proposed model to explain absolute stereochemical outcome.

Trying to explain the absolute stereochemical outcome is particularly difficult because sophisticated models of the copper-phosphine ligated boryl-nucleophile do not exist and, indeed, no crystal structures have been obtained to date (the acquisition of such crystal structures may shed light on this). This is perhaps additionally problematic due to the ability of copper to exist in trigonal, tetrahedral and more exotic geometries in solution.[192,193] Therefore, the active catalytic species in this section is just speculative and needs further investigation.

One might initially suspect that *P*-chiral ligands,[194] such as the DIPAMP ligand **L24**, might perform the best due to the chiral motif being in close contact to that of the copper-boryl moiety. However, experimentally this was found to perform particularly poorly in terms of asymmetric induction (5% *e.e.*, Entry 6, Table 27).

By considering previous models of BINAP-metal complexes (Pt, Rh, Cu etc),[195,196] models were considered to explain the absolute stereochemical outcome observed in these transformations (see Figure 39). The first thing to note is the relative distance of the phosphine ligand to the site of nucleophilic attack ($C_\beta$). Therefore, if high levels of enantio-differentiation (between β-substituents) are to be achieved, the chiral information, derived from the axial chirality on BINAP, has to be transferred through space to influence selectivity upon β-borylation. Indeed, Figure 39 shows how the phenyl substituents on phosphorous impose through space, transferring this chiral information from the axial binapthyl motif. More specifically, the phenyl substituents on phosphorous exhibit axial and equatorial arrangements and could, under this model, allow for levels of enantioselectivity on β-borylation. This is explained by assuming that the β-aryl substituent faces away from the imposing axial phenyl during the suggested transition state on β-boration. This could explain why the observed enantioselectivities with ligands (*R*)-BINAP **L16** and (*R*)-tol-BINAP **L17** are similar, possibly due to the *para*-methyl in **L17** not imposing significant conformational change on such copper-ligand complexation. However, it can be imagined that the addition of two *meta*-methyl substituents on the phenyl rings may impose rigid axial and equatorial arrangements due to the increased steric influence about the phenyl rings. Therefore, one can deduce that **L28** is more effective due to its ability to communicate the chiral information through space due to the greater steric effects of the two *meta*-methyl substituted phenyl rings.

Pregosin *et al.* have examined the influence of *meta*-substituents on the phenyl rings of BINAP analogues.[197] Indeed, they named the higher enantioselectivity associated with such ligands, in comparison to the non-*meta*-substituted ligands, 'the 3,5-dialkyl *meta*-effect'. They attribute this to the increased conformational rigidity of the axial and equatorial phenyl rings (on the ligand), imposed by the *meta*-substituents, due to steric repulsion. This is consistent with the high levels of *e.e.* observed in the case of (*R*)-DM-BINAP **L28**. It should be noted that higher levels of *e.e.* when using (*R*)-DM-BINAP **L28**, in comparison to (*R*)-BINAP **L16** and (*R*)-tol-BINAP **L17**, have been observed in the literature, especially when performing asymmetric hydrogenations.[198]

### 2.4.5 Probing the substrate scope

Due to the low cost and ready availability of (*R*)-DM-BINAP **L28**, this methodology was applied to the optimised one-pot reaction, probing a variety of enals with varying β-substituents (alkyl and aryl), as shown in Table 28. Indeed, as part of this investigation a series of β-alkyl and β-aryl enals were transformed into the analogous γ-amino alcohols in excellent conversion and *e.e.*, which were all readily determined by derivatisation to the analogous *O*/*N*-diacetates (see Table 29 and Figure 40 for a representative chromatogram showing the resolution of enantiomers by chiral HPLC). The levels of enantioselectivity were found to be greater for β-aryl enals, when compared to that of β-alkyl enals. This is could be due to greater enantiodifferentiation between aryl- *vs.* H- β-substituents, when compared to alkyl- *vs.* H- β-substituents. This is additionally consistent with the speculated model in Figure 39.

**Table 28** Substrate scope of the selective transformation of enals into chiral amino γ-alcohols.

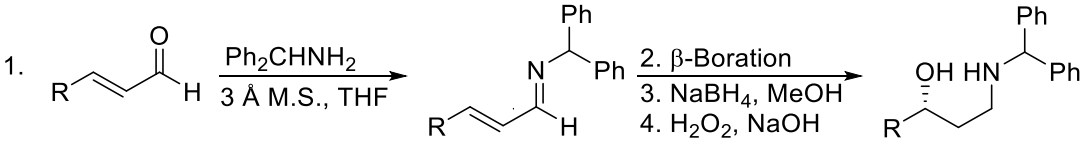


| Entry | Substrate | L | γ-Amino alcohol product | Conv. (%)[a] | I.Y. (%)[b] | *e.e.* (%)[c,d] |
|---|---|---|---|---|---|---|
| 1 | 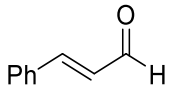 **66** | $PPh_3$ | 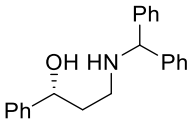 **128** | >82 | 62 | - |
| 2 | | **L28** | | >95 | 50 | 97 |
| 3 | 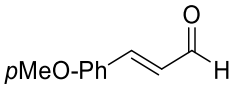 **120** | $PPh_3$ | 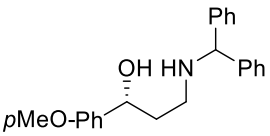 **130** | >95 | 61 | - |
| 4 | | **L28** | | >95 | 90 | 90 |
| 5 | 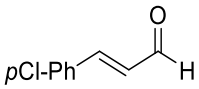 **122** | $PPh_3$ | 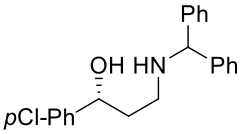 **131** | >95 | 71 | - |
| 6 | | **L28** | | >95 | 59 | 90 |
| 7 | 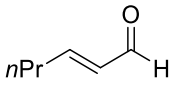 **116** | $PPh_3$ | 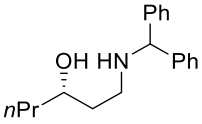 **132** | >95 | 50 | - |
| 8 | | **L28** | | >95 | 59 | 87 |
| 9 | 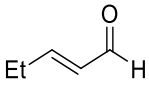 **123** | $PPh_3$ | 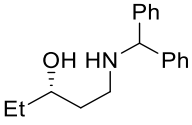 **133** | 79 | 42 | - |
| 10 | | **L28** | | >95 | 65 | 76 |
| 11 | 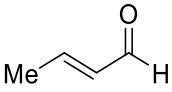 **59** | $PPh_3$ | 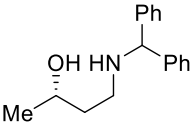 **134** | >95 | 78 | - |
| 12 | | **L28** | | >95 | 88 | 80 |

0.50 mmol Scale reaction: 2.00 mmol (1:1, benzhydrylamine: enal) was stirred in THF (8 mL) and 3 Å M.S. (2.0 g) for 6 h, after which a 2 mL aliquot of *in situ*-formed imine was transferred to a Schlenk-tube (under argon) containing Cu(I) salt, L, base and $B_2pin_2$ (1.1 equiv.). After 5 min MeOH (2.5 equiv.) was added to the solution and the reaction was stirred overnight. $NaBH_4$ (1.50 mmol) was added, followed by the drop-wise addition of MeOH (1 mL). The mixture was stirred for 3 h, followed by the removal of solvent under reduced pressure. THF (3 mL) was added to the resulting residue, followed by NaOH (0.30 mL, w/v 20%) and $H_2O_2$ (0.13 mL, w/v 35%), and the solution was heated to reflux for 1 h. After standard work-up procedures and column chromatography, a white solid was obtained. [a] Determined by $^1H$ NMR analysis. [b] Isolated yield. [c] Determined by Chiral HPLC on the resulting O/N-diacetate. [d] Converted to the O/N-diacetate and isolated before HPLC.

**Table 29** Making *O*/*N*-diacetate for *e.e.* determination.

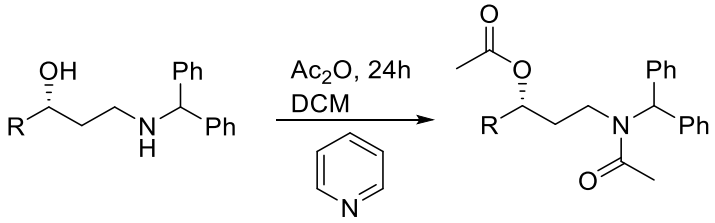


| Entry | γ-Amino alcohol | R | *O*/*N*-diacetate yield (%) | | *e.e.* (%)[a] |
|---|---|---|---|---|---|
| 1 | 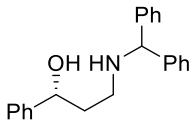 **128** | Ph | **135** | 88 | 97 |
| 2 | 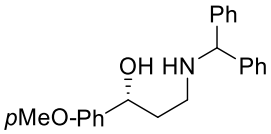 **130** | *p*MeO-Ph | **136** | 31 | 90 |
| 3 | 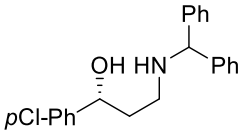 **131** | *p*Cl-Ph | **137** | 45 | 90 |
| 4 | 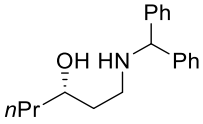 **132** | *n*Pr | **138** | 70 | 87 |
| 5 | 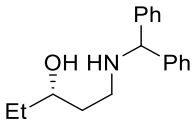 **133** | Et | **139** | 84 | 76 |
| 6 | 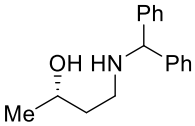 **134** | Me | **140** | 51 | 80 |

Assuming the reaction was carried out on a 0.2 mmol Scale: γ-Amino alcohol (0.2 mmol), DCM (3 mL), acetic anhydride (0.5 mL) and pyridine (0.5 mL) were combined under argon and stirred overnight. After an acid-base wash the resulting *O*/*N*-diacetate was purified by column chromatography. [a] Determined using Chiral-HPLC by comparison with the racemic standard of each *O*/*N*-diacetate compound.

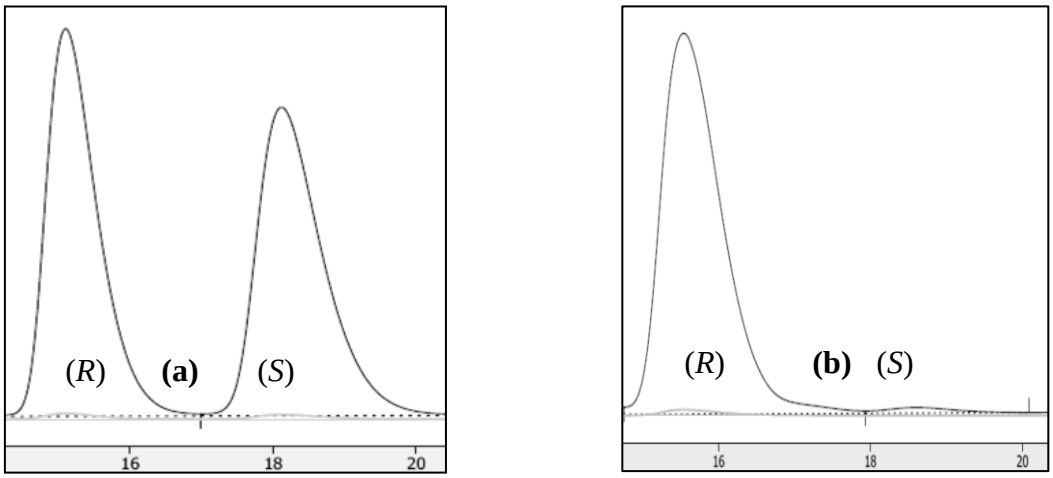


**Figure 40** Chromatogram showing: (a) racemic diacetate **135** of compound **128** (Table 27, Entry 1); (b) enantioenriched diacetate **135** of compound **128** (Table 27, Entry 8).

### 2.4.6 Access to β-boryl aldehydes

In addition to accessing γ-amino alcohols, β-boryl aldehydes (*e.g.* **142**) can be obtained in good yield by simple hydrolysis of the intermediate β-boryl imine **141** (see Scheme 36). In this context, the *N*-benzhydryl groups acts as an appropriate auxiliary to favour 1,4-addition (through steric effects), which can then undergo facile deprotection by hydrolysis.

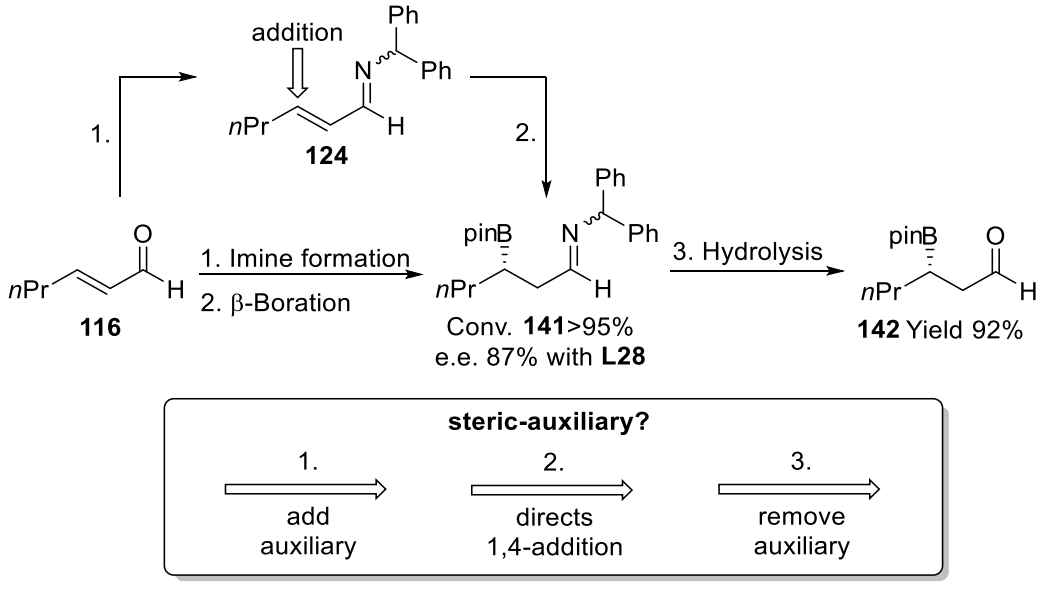


**Scheme 36** Hydrolysis of imine **141** to give β-boyl aldehyde **142**.

### 2.4.7 Implications for future synthesis

This methodology proved highly effective for the preparation of novel γ-amino alcohol compounds. The implication for future applications were clear. Section 2.5 demonstrates the potential application of such methodologies by the synthesis of some top-selling pharmaceuticals.

## 2.5 Preparation of some pharmaceuticals

With the novel one-pot methodology in hand (see section 2.4), attention was turned towards the real-world application of this methodology in the synthesis of some pharmaceuticals. It was first introduced in section 2.1 that γ-amino alcohols are found in some of the World's top-selling pharmaceuticals and, therefore, Fluoxetine and Duloxetine were deemed as suitable targets for the one-pot methodology.

### 2.5.1 Origin and medical applications of Fluoxetine

Fluoxetine (also known as Prozac), developed by Eli Lilly, first appeared in the literature in 1974.[199] In the late 1980s, it was approved for medical use and it became one of the world's most widely prescribed antidepressant, used to treat major depressive disorder (MDD), obsessive-compulsive disorder and other conditions.[200,201] Fluoxetine belongs to the selective serotonin reuptake inhibitor (SSRI) class of anti-depressants. Despite Fluoxetine been sold as the racemate, each individual enantiomer has differing potency with regards to serotonin reuptake inhibition, but are relatively similar [(*S*)-Fluoxetine > (*R*)-Fluoxetine]. However, (*S*)-norfluoxetine (primary metabolite *via* *N*-demethylation) shows significantly greater activity when compared to the (*R*)-enantiomer.[202]

### 2.5.2 Total synthesis of Fluoxetine

Over the years, many groups have been interested in the total synthesis of Fluoxetine. Indeed, groups have reported the synthesis of Fluoxetine using classical chemistry, exemplifying traditional (now) methods of asymmetric synthesis. For example, Brown *et al*. reported the synthesis of Fluoxetine by the asymmetric reduction of ketones using stoichiometric chiral diisopinocamphenylchloroborane.[203] In addition, Sharpless *et al*. installed the chiral centre by asymmetric epoxidation of allylic alcohols with subsequent transformations (*e.g.* epoxide ring-opening).[204] Corey *et al.* attempted the synthesis of Fluoxetine though asymmetric hydrogenation chemistry. Indeed, this was achieved using chiral oxazaborolidine (CBS reduction) in combination with borane to reduce prochiral ketones, which served as a chiral precursor to the synthesis of Fluoxetine. [205] Furthermore, asymmetric aldol chemistry has been demonstrated by Shibasaki *et al.* towards this end.[206] Due to the highly significant work of Noyori *et al*. on asymmetric hydrogenation,[207,208] such adapted protocols have found applications in the synthesis of Fluoxetine by Noyori *et al*.[209] and others.[210] It should be mentioned at this stage that Yun *et al*. have demonstrated a formal synthesis of Fluoxetine by borylation chemistry on α,β-unsaturated amides (see Scheme 37).[42]

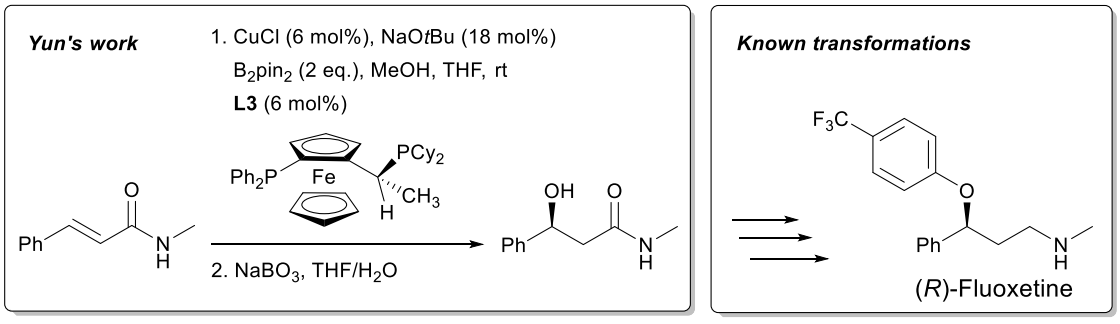


**Scheme 37** Yun's formal synthesis of fluoxetine.[42]

Looking at the γ-amino alcohol **128**, one can clearly see through retrosynthetic analysis that **128** is a suitable precursor to Fluoxetine (see Scheme 38). Indeed, by disconnecting the aryl the (C-O bond cleavage to give **143**) and the *N*-methyl substituent (C-N bond cleavage, to give **144**), one arrives at precursor **144** to Fluoxetine. Furthermore, **144** can be obtained *N*-benzhydryl deprotection of the γ-amino alcohol **128**.

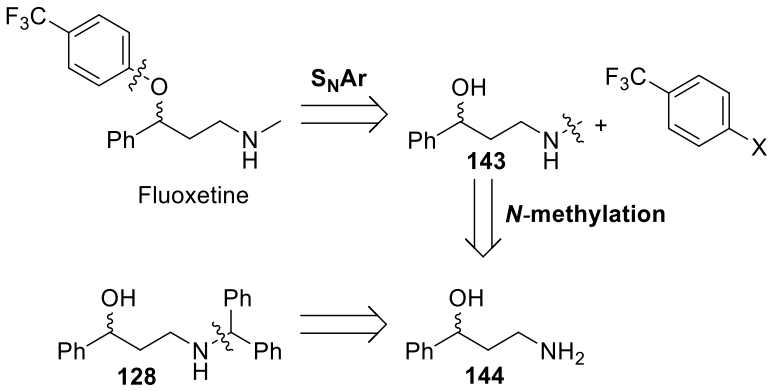


**Scheme 38** Retrosynthetic analysis of Fluoxetine

### 2.5.3 Benzhydryl reductive deprotection approach

Initially, *N*-benzhydryl deprotection was attempted using previously established and well documented methods for *N*-benzyl deprotection (Pathway A, Scheme 39).[211]

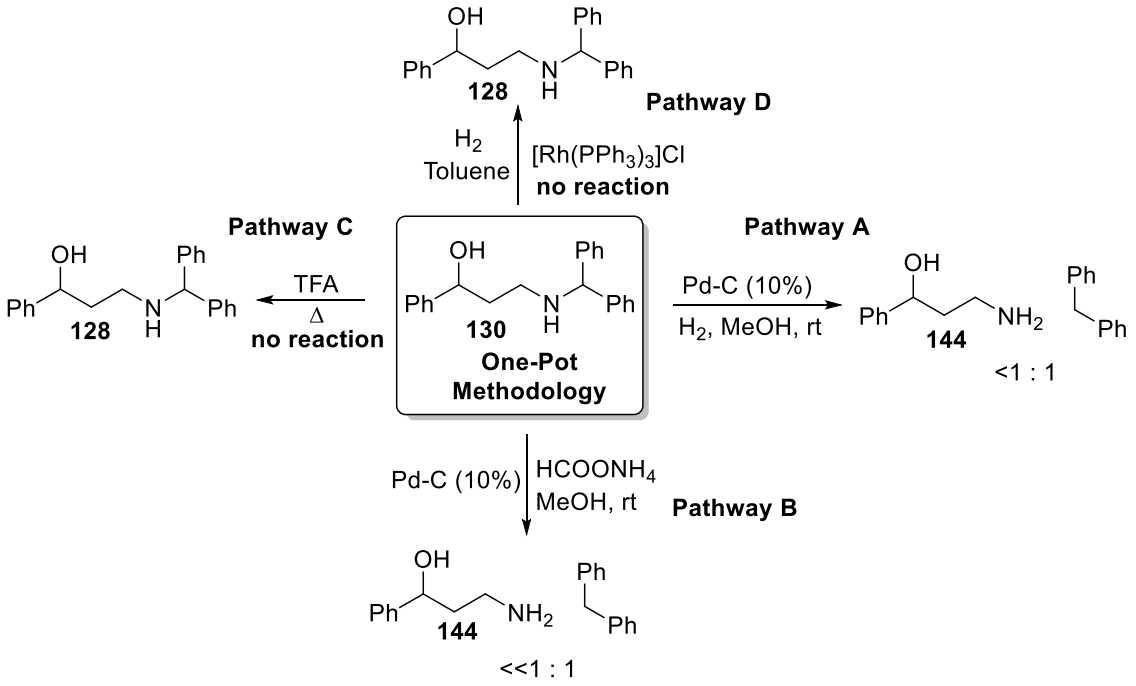


**Scheme 39** Examined methods of *N*-benzhydryl deprotection.

Unsurprisingly, subsequent *N*-benzhydryl deprotection (*via* C-N bond cleavage) was achieved under palladium-catalysed hydrogenation. However, on inspection of the crude $^{1}$H NMR spectrum, it was observed that the resulting products of C-N bond cleavage, diphenylmethane and the primary amine **144**, were present in a ratio that was not 1:1. Furthermore, additional inspection revealed that under these conditions, C-O bond hydrogenolysis of the benzylic hydroxyl-group was a significant competing side reaction, thus explaining to lack of 1:1 stoichiometry of the primary amine **144** and diphenylmethane.[212] On repeating this reaction multiple times, a range of conversions (20-50%) were observed to compound **144**, due to the relative difficulty controlling the

quantity of gaseous hydrogen delivery. It should be noted that C-O bond hydrogenolysis is documented in the literature.[213, 214]

Transfer hydrogenation was examined (Pathway B, Scheme 39),[215] due to the benefit and relative ease in delivering a stoichiometric quantity of hydrogen in the form of ammonium formate (easy to weigh, and decomposes to give hydrogen on heating). However, despite limiting the quantity of hydrogen, C-O bond hydrogenolysis of the benzylic hydroxyl group was still observed (this was attempted at longer and shorter reaction times).

Alternative methods (not based on metal-catalysed hydrogenation) of benzhydryl deprotection were attempted (Pathway C, Scheme 39).[216] In particular, stirring in trifluoroacetic acid (at room and elevated temperature) was attempted, but such attempts resulted in a lack of C-N bond cleavage and, indeed, quantitative recovery of the γ-amino alcohol **128** was achieved. Final attempts were made at *N*-benzhydryl deprotection using Wilkinson's catalyst (Pathway C, Scheme 39), but this method proved futile, resulting in the quantitative recovery of the γ-amino alcohol **128**. This final attempt led to a change in approach to cleave the benzhydryl substituent.

Attention was turned away from hydrogenolysis as several variants on this methodology. On examining the literature, novel oxidative methods for benzyl deprotection (through C-N bond cleavage) were found.[217] Indeed, such methods are based on employing $O_2$, DMSO and KO*t*Bu as suitable reagents for deprotection.

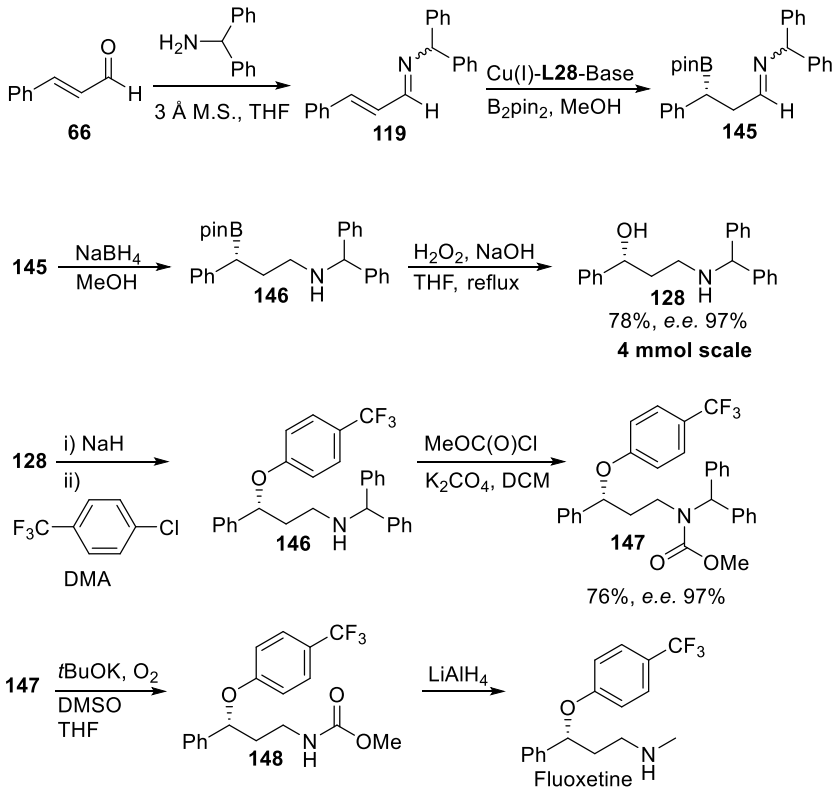


**Scheme 40** Novel methods towards Fluoxetine through oxidative benzhydryl deprotection.

Derivatisation of **128**, first to the aryl ether **146** and then towards the carbamate **147** was achieved in 76% isolated yield (Scheme 40). By forming the carbamate **147**, the pKa of the C-H (on the benzhydryl substituent) is presumably lowered and can be deprotonated, under equilibrium-type conditions, by *tert*-butoxide. The resulting anion (which can be delocalised across the N-C=O system) can be trapped by molecular oxygen. The resulting peroxide intermediate can react with dimethyl sulfoxide (DMSO), which results in the cleavage of the benzhydryl substituent (see Scheme 41). Clear and quantitative cleavage of the benzhydryl substituent (lost as benzophenone, $Ph_2CO$) was achieved.[218,219] However, such conditions appeared to be too forcing, as observed by significant side-products in the reaction (see previous literature).[220]

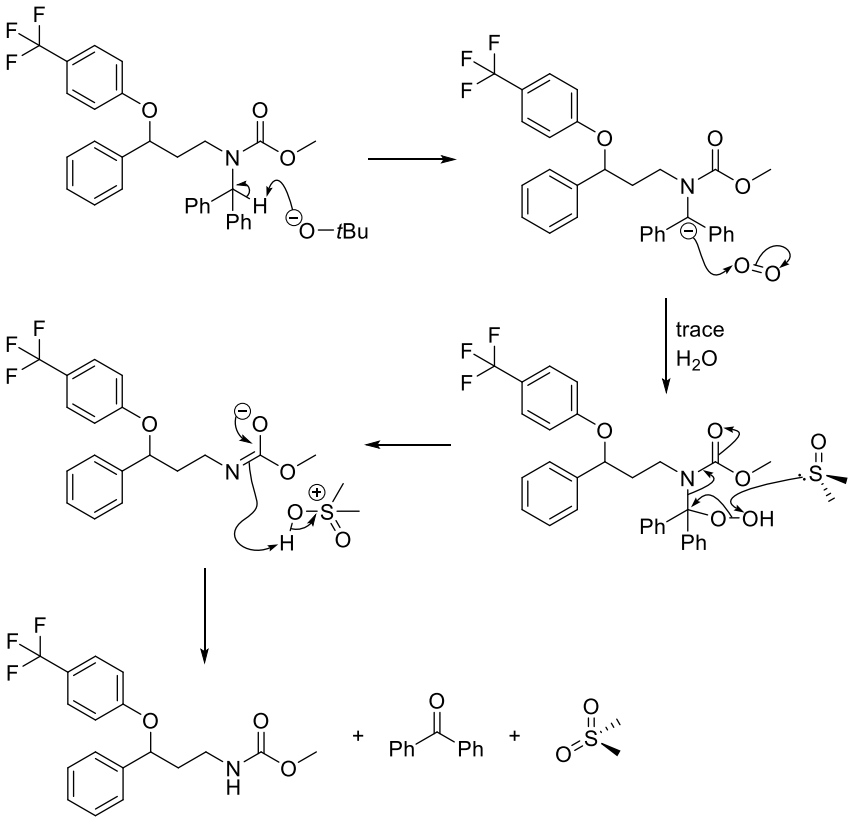


**Scheme 41** Mechanism of the oxidative $O_2$, KO*t*Bu, DMSO deprotection methodology.

## 2.5.4 Transimination approach

It was previously mentioned (in section 2.4.5) that a β-boryl *N*-benzhydryl imine could be hydrolysed to form the resulting β-boryl aldehyde. Indeed, it was considered if benzhydryl deprotection, in the form of facile imine hydrolysis on the addition of water, would be an advantageous alternative to the late stage benzhydryl deprotection. In the context of the one-pot methodology, this was examined by hydrolysis of the β-boryl imine **145** to the aldehyde **149** (see Scheme 42). It should be noted that attempts were made to purify **149**, but they failed due to compound instability on silica gel column chromatography. Furthermore, cinnamaldehyde was recovered, presumably *via* an elimination-type mechanism.

It should be noted that Córdova *et al*. also found that this aldehyde **149** degraded on purification to give the starting cinnamaldehyde **66** (see Scheme 42).[77]

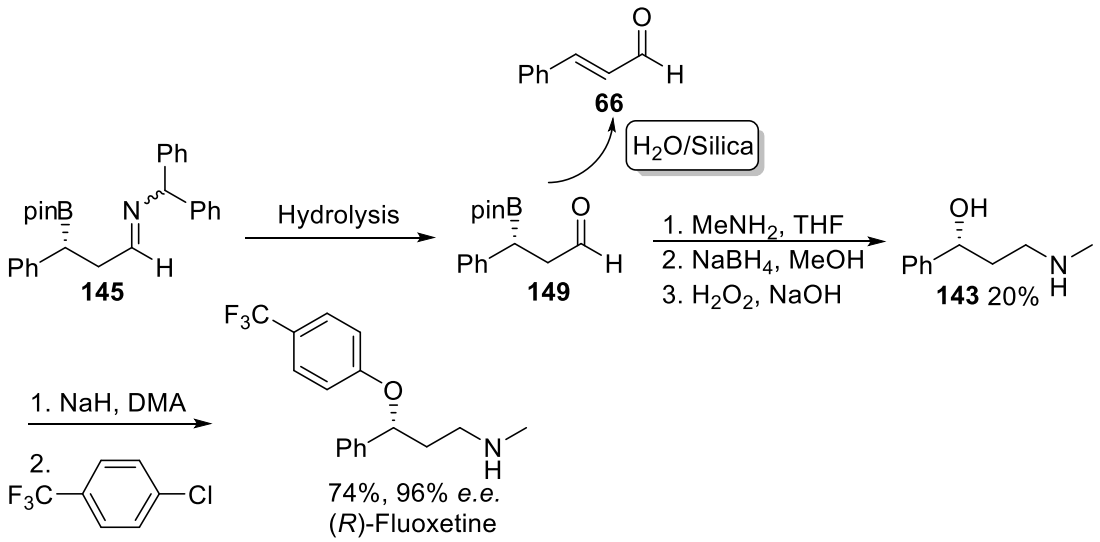


**Scheme 42** Hydrolysis and reductive amination approach to Fluoxetine.

This can be partially circumvented by hydrolysis of the imine **145** to aldehyde **149**, with subsequent transformations by reductive amination. Finally, oxidation of the C-B bond to give the Fluoxetine precursor **143** was achieved in 20% isolated yield. Next, the addition of NaH to **143** resulted in the *in situ* generation of the analogous Na-alkoxide of **143** which, on addition of 4-chlorobenzotrifluoride at elevated temperature (100 $^{o}$C, 3 h), gave Fluoxetine in 74% isolated yield (see Scheme 42).

Despite success in preparing the known pharmaceutical Fluoxetine, the overall yield was relatively low (15%). This was attributed to the known and documented instability of the β-boryl aldehyde intermediate **149**.[77] Intrigued by recent reports on transimination (also known as imine-metathesis[221]), it was considered whether treating the β-boryl imine **145** with an excess of methylamine would result in the formation of *N*-methyl imine **150**, thus by-passing the unstable intermediate aldehyde. More specifically, would the equilibrium between *N*-benzhydryl imine **145** and *N*-methyl

imine **150** (on addition of methylamine) lie towards **150**, as a result of the difference in the nucleophilicity of methylamine and benzhydrylamine (kinetic) or a difference in the stability (thermodynamic) of each respective imine product (see Scheme 43)? Hence, transimination was considered and subsequently examined as a suitable method towards Fluoxetine.[222]

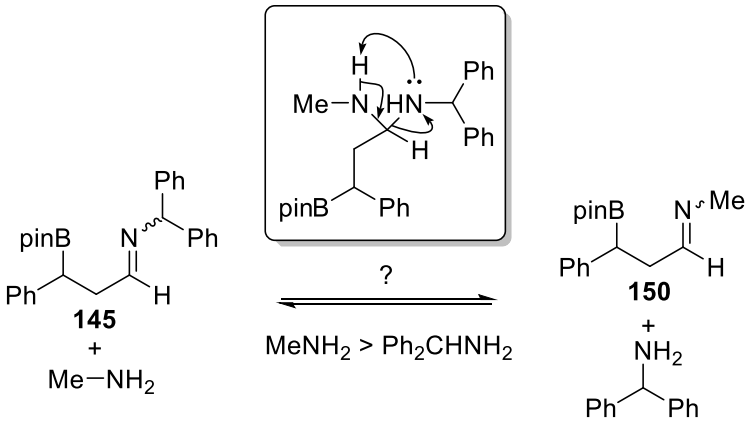


**Scheme 43** Transimination - a suitable method to form *N*-methyl imine **150**?

Continuing with the established one-pot methodology, imine **145** was treated with excess methylamine (4 equiv.), with subsequent *in situ* reduction using $NaBH_4$/MeOH. Subsequently, all the solvent was removed (this was to prevent MeOH oxidation to formaldehyde) and replaced with THF, $H_2O_2$ and NaOH, which on heating to reflux, gave the known precursor to Fluoxetine, γ-amino alcohol **143** [54% yield when using $PPh_3$ and 61% when using (*R*)-DM-BINAP **L28**, see Scheme 44]. This was achieved in five steps, all of which were in conducted in one pot.

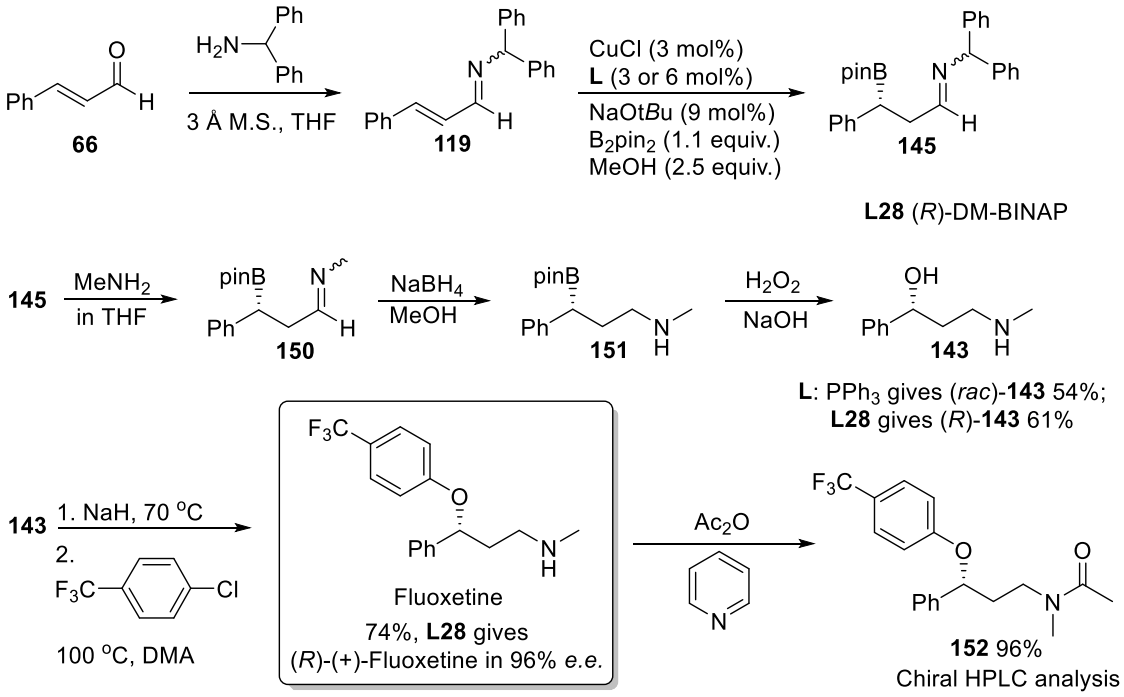


**Scheme 44** Transimination approach to the synthesis of Fluoxetine; (*R*)-Fluoxetine is prepared in 96% *e.e.*, with an overall yield of 45%.

Finally, nucleophilic aromatic substitution gave Fluoxetine in 74% yield, with an overall yield of 45% (derivatisation was required to measure the *e.e.*). It had been noted previously that the ligand **L28** could achieve high enantioselectivity on this system **66** (97% *e.e.*). It was, therefore, important to confirm that this high enantioselectivity was maintained after these transformations.

In order to measure the *e.e.* of Fluoxetine, it was first acetylated under standard conditions to give the *N*-acetate **152** in high yield (96%). This allowed for the baseline resolution of each constituent enantiomer, as shown in Figure 41. The enantioenriched sample was measured under these conditions and the *e.e.* of **152** was found to be 96%. This is within experimental error (+/- 1%) of 97%, as previously measured by derivatisation of **128** to **135**. In addition, to confirm the absolute stereochemistry (independently confirmed in section 2.4), the optical rotation of Fluoxetine was

measured and found to be $[\alpha]_D^{22}$ = +3.5 (1.0, $HCCl_3$). This is consistent with the literature value of (*R*)-Fluoxetine in 96% *e.e.*, which was found to be $[\alpha]_D^{20}$ = +3.8 (0.9, $HCCl_3$).[223]

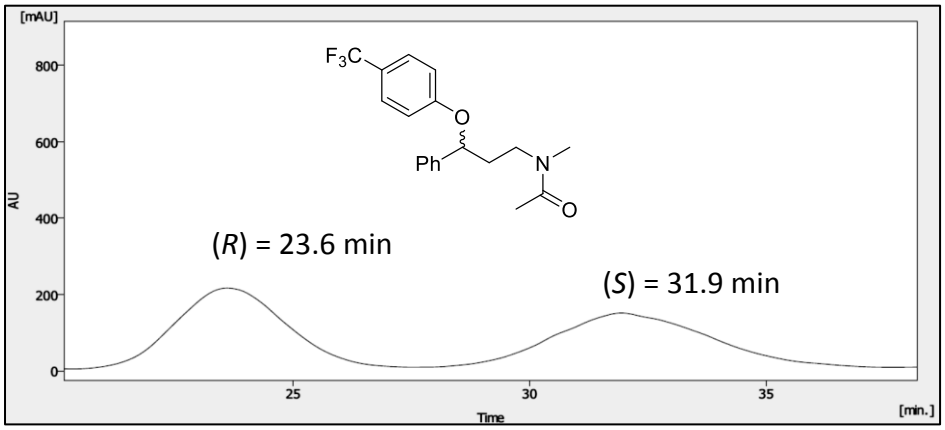


**Figure 41** Chiral HPLC of (*rac*)-**152** showing base-line resolution of each enantiomer.

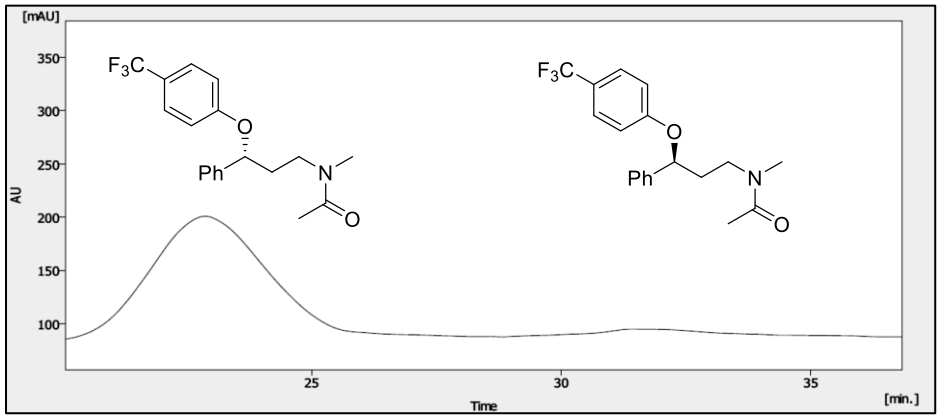


**Figure 42** Chiral HPLC chromatogram of (*R*)-**152** showing a 98:2 ratio of the major and minor (respectively) enantiomers, thus giving 96% *e.e.* overall.

### 2.5.5 Summary of the total synthesis of Fluoxetine

The total asymmetric synthesis of Fluoxetine was achieved in 96% *e.e.*, with an overall yield of 45%. This was achieved by an *in situ* imine formation/asymmetric borylation/transimination approach. Novel conditions for the chiral separation of the *N*-acetate **152** (of Fluoxetine) were achieved, showing good baseline resolution (approximately 2 min) under chiral HPLC. With these results optimised for the cinnamaldehyde **66** system, attention was turned towards to asymmetric synthesis of (*S*)-Duloxetine (marketed as a single enantiomer).

### 2.5.6 Duloxetine

Duloxetine (also known as Cymbalta) is top-selling pharmaceutical, marketed by Eli Lilly. Sales figures acquired by IMS Health show peak sales of Duloxetine at 5.8 billion US Dollars in 2012.[111] Duloxetine belongs to the serotonin-norepinephrine reuptake inhibitor (SNRI) class of drugs and, indeed, is used to treat major depressive disorder (MDD) and general anxiety disorder (GAD) and other conditions.[224] Unlike Fluoxetine, Duloxetine is marketed as a single (*S*)-enantiomer. Therefore, the synthesis of Duloxetine required the successful transformation of prochiral material to the (*S*)-enantioenriched Duloxetine drug. This was attempted using the optimised methodology from the synthesis of Fluoxetine.

## 2.5.7 Synthesis of the starting β-thiophenyl enal

The first step towards the synthesis of Duloxetine was the preparation of the starting β-thiphenyl enal **156** (with respect to the one-pot methodology). This was attempted by forming the acid chloride **154** of the commercially available carboxylic acid **153**, which was achieved by heating **153** to reflux with oxalyl chloride in DCM (Scheme 45). Without isolating the intermediate acid chloride **154**, *N*,*O*-dimethylhydroxylamine and TEA was added and allowed to react overnight, which resulted in the formation of the Weinreb amide **155** in good yield (85%) over two steps.[225]

Weinreb amides (*e.g.* **155**) can be selectively reduced to the analogous aldehyde, due to the stable tetrahedral intermediate species, which prevents total reduction to the allylic alcohol. [226,227] Indeed, this methodology has been applied in total synthesis before, highlighting the diversity and applicability of this methodology.[228]

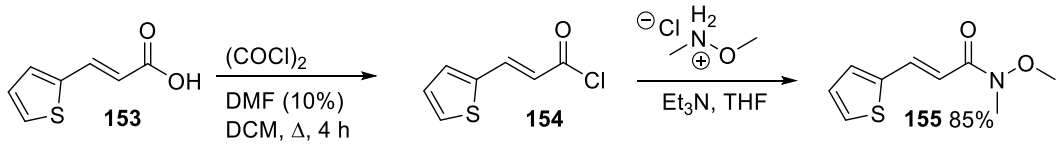


**Scheme 45** Synthesis of the Weinreb amide **155** from the carboxylic acid **153**.

The selective reduction (-10 °C) of the Weinreb amide **155** to the aldehyde **156** using DIBAL-H[229] was attempted (Scheme 46), but yielded only 11% of the desired aldehyde. Analysis of the crude NMR showed significant proportions of allylic aldehyde **157**. It should be noted, that literature examples exist which report the synthesis of enal **156** by the reduction of carboxylic acid **153** to the allylic alcohol **157** using DIBAL-H which, in turn, was oxidised under Dess-Martin[230] conditions.

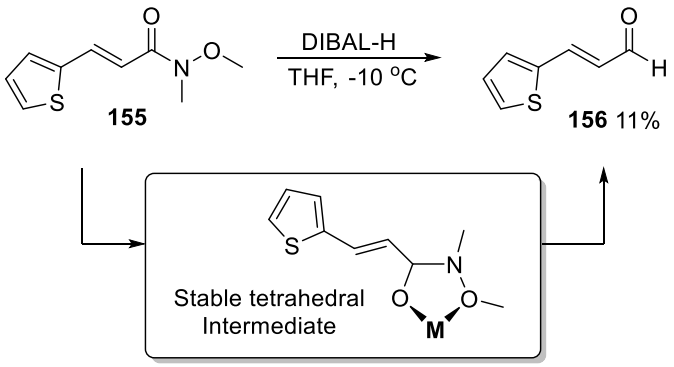


**Scheme 46** Selective reduction of the Weinreb amide **155** to enal **156**.

An analogous methodology was attempted, whereby the carboxylic acid **153** was over-reduced (using three equiv. of DIBAL-H) to the allylic alcohol **157**. Indeed, inspection of the crude NMR spectrum showed that this was highly successful and the allylic alcohol **157** was oxidised without further purification under Swern oxidation conditions (see Scheme 47).[231] This yielded the enal **156** in 37% yield over two steps (**156** obtained by column chromatography). Despite the relatively low yield, this methodology was practically simple, due to the relative simplicity of work-up, washing and final purification.

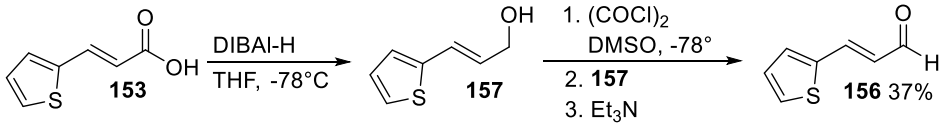


**Scheme 47** Swern oxidation of the allylic alcohol **157** to enal **156**.

### 2.5.8 Transimination approach to the synthesis of Duloxetine

Once enal **156** had been prepared, **156** was subjected to the optimised methodology (*in situ* α,β-unsaturated imine formation, β-boration, transimination, reduction, oxidation and O-arylation; shown in Scheme 44 for optimisation work on Fluoxetine) which is shown in Scheme 48. Imine **158** was formed in < 9 h (in THF), and was directly transferred to copper-**L**-NaO*t*Bu and $B_2pin_2$ pre-catalyst, under argon. After the addition of methanol, the borylation was allowed to proceed overnight to give

**159**. On completion, four equiv. of methylamine was added (2 M THF solution) to afford **160**, which was subsequently reduced to amine **161**. All traces of methanol were removed *in vacuo* and, after oxidation, work-up and purification, yielded the γ-amino alcohol **162** in 47% (**L** = $PPh_3$) and 57% (**L32**).

Compound **162** is particularly difficult to isolate by column chromatography, eluting over many fractions, even when high proportions of methanol and TEA are added to the DCM eluent. Furthermore, during TLC analysis of **162**, it was difficult to visualise and distinguish from residual $Et_3N$. This can be overcome using *p*-anisaldehyde staining, which shows **162** as a distinctive dark blue spot on the TLC plate, just above the baseline ($R_F$ <0.1 in 9:1, DCM : MeOH).

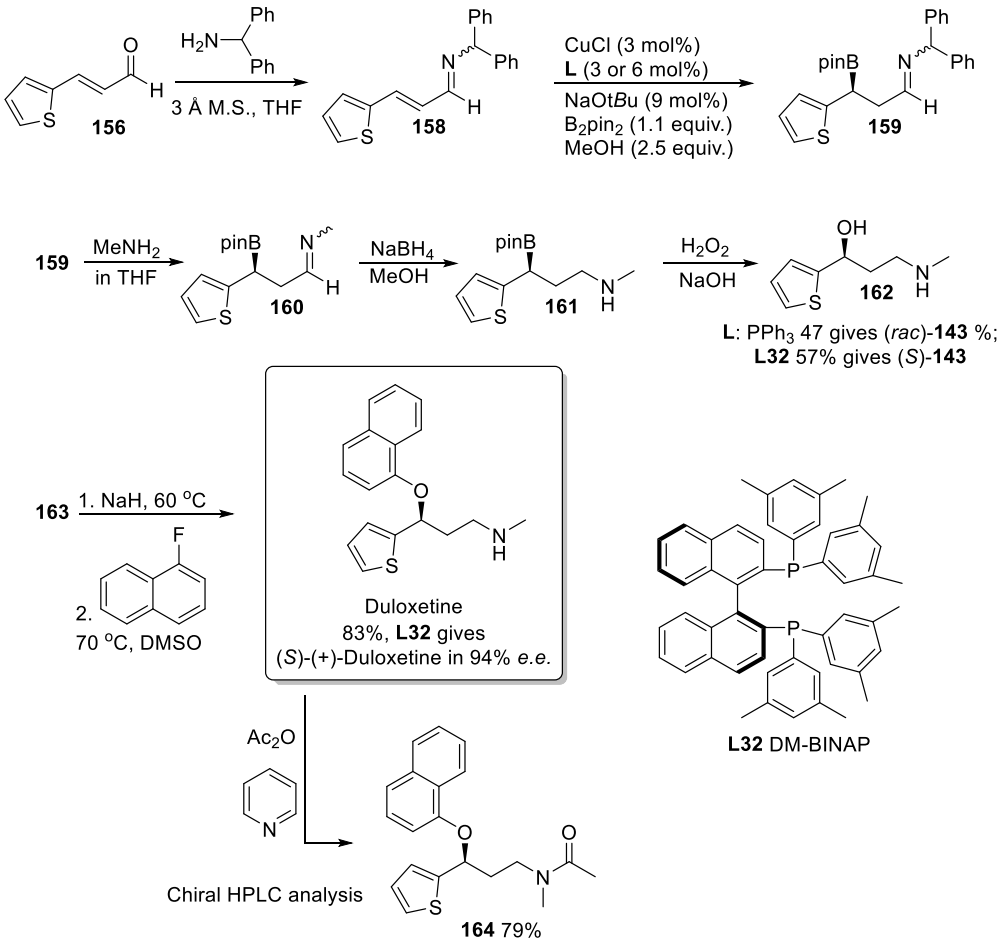


**Scheme 48** Total synthesis of Duloxetine in 47% yield (over six steps), 94% *e.e.*.

Finally, nucleophilic aromatic substitution on **162** was achieved by deprotonation of the **162**–O<u>H</u> (using NaH), and addition of 1-fluoronaphthalene under elevated temperature (70 °C) to yield Duloxetine in high yield (83%).

Derivatisation to the *N*-acetate **164** (79% yield) was required to measure *e.e.* and, indeed, this showed that the Duloxetine was formed in 94% *e.e.* In addition, to confirm the absolute stereochemistry (independently confirmed in section 2.4), the optical rotation of Fluoxetine was measured and found to be $[\alpha]_D^{24}$ = +105.4 (1.0, MeOH). This is consistent with the literature value of (*S*)-Duloxetine in >99% *e.e.*, which was found to be $[\alpha]_D^{20}$ = +117 (1.0, MeOH).[232]

## 2.5.9 Summary

In summary (see Scheme 49), the total synthesis of two pharmaceuticals has been achieved through application of the *in situ* imine formation/borylation methodology. This gave Fluoxetine in 45% yield (96% *e.e.*) and Duloxetine in 47% yield (94% *e.e.*).

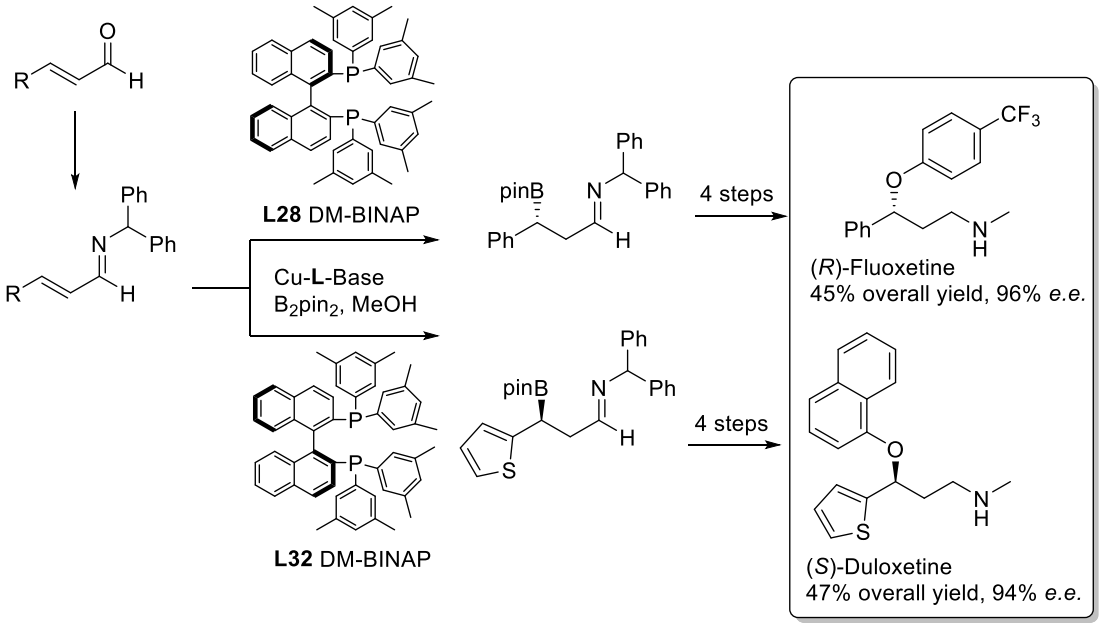


**Scheme 49** Ligand controlled asymmetric induction: **L28** [(*R*)-DM-BINAP] gives (*R*)-Fluoxetine, whereas **L32** [(*S*)-DM-BINAP] gives (*S*)-Duloxetine.

## 2.6 Concluding remarks

The initial aim of this project was to develop a cheap and synthetically simple route to α,β-unsaturated imines. Indeed, this was achieved through classical condensation, which was monitored by *in situ* IR spectroscopy (ReactIR). This not only provided a simple route to such compounds, but this work, in collaboration with other groups, turned into a deeper and more theoretical piece of work which will, hopefully, provide the scientific community with greater insight into the fundamental direct *vs.* conjugate addition pathways of primary amines with enones and enals.

In parallel to this imine study, the one-pot methodology (*in situ* imine formation, borylation, reduction and oxidation) was being developed. Initial hurdles were met; however, after close inspection and analysis, a novel side-reaction was discovered, that is the formation of 1,3-oxazines through the *in situ* oxidation of methanol to formaldehyde/formaldehyde equivalents. Once this had been established, attention was turned to the optimisation of this methodology, which was achieved with great success.

On completion of the optimisation of the one-pot methodology, a research placement was undertaken in Tarragona, Spain (in the research lab of Prof. Elena Fernández). The aim of this placement was, through the use of chiral phosphine ligands, to develop the analogous asymmetric one-pot procedure. However, failure in this endeavour ensued, until the discovery of the competitive 1,2-addition of the of copper-boron nucleophile to aldimines. This later led to a study which would overcome this problem through the use of sterically-bulky *N*-benzhydryl imines. During the remainder of the project, attention was turned towards the enone-based systems. This resulted in a novel base-free borylation protocol whereby the simultaneous addition of both amine and enone to the base-free pre-catalyst resulted, after overnight stirring, to the near quantitative formation of β-boryl imines in high *e.e.* These β-boryl imines have

previously been derivatised within the group(s) to chiral γ-amino alcohols.

Next, the β-boration of *N*-benzhydryl α,β-unsaturated imines was examined which resulted in a highly novel and efficient route to enantioenriched β-boryl imines which, under hydrolysis, yields to β-boryl aldehydes (challenging to obtain from the parent enal, due to competitive direct addition).

Due to such γ-amino alcohols being precursors to drugs, attention was made towards the application of this methodology towards the total synthesis of Duloxetine and Fluoxetine, which proved highly successful.

Although the initial aims of this project was to prepare additional compounds, such as β-amino acids, β-hydroxy acids and γ-hydroxy alcohols, other avenues arose which seemed attractive and, therefore, were explored (as discussed throughout).

## 2.7 Future work

Several problems have been overcome as part of this research, but many still remain. Indeed, Figure 41 highlights two substrate classes that pose challenges. Substrates of the general structure **167** present an increased challenge with regards to asymmetric induction due to the difficulty in achieving enantio-differentiation between the β,β-disubstituents and, in addition, catalytic activity towards selective β-boration. Moreover, when one introduces an addition α-substituent, diastereocontrol becomes an additional factor. To date, varying degrees of control are reported, which predominantly leads to the *anti*-diastereoisomer in this regard. Therefore, that challenge of tuning between *syn*- and *anti*-diastereoselectivity (on protonation) needs to be overcome and that factors which govern this process needs to be studied.

Substrates with the general structure **168** (Figure 41) are challenging targets for asymmetric β-boration. Despite many examples of diastereoselective protonation under this methodology being reported, the author knows of no examples of enantioselective

protonation (where the α-carbon is prochiral and the β-carbon is not), leading to exclusive α-stereocontrol under the β-boration methodology.

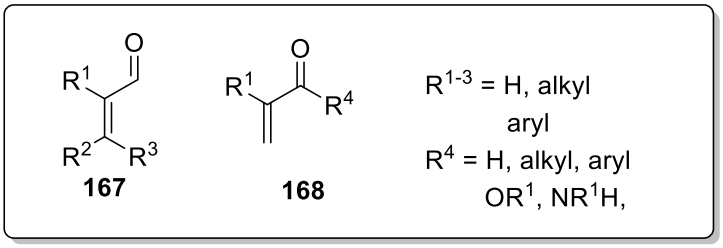


**Figure 41** Challenging targets for future work.

Additional work needs to be undertaken to understand the *in situ* trapping of trace quantities of formaldehyde by presumed methanol oxidation (by γ-amino alcohols), as identified in the late stage oxidation in the one-pot methodology. Indeed, this could lead to novel oxidative procedures.

# Experimental

# 3. Experimental section

## 3.1 General experimental

All reagents were used as received from the supplier without further purification, unless stated. All solvents were used as received from the supplier, except THF (freshly distilled from sodium and benzophenone) and methanol (stored over molecular sieves). Molecular sieves, 3 Å 1-2mm beads, were supplied from Alfa Aesar, and stored at 220 $^{\circ}$C. Reactions were monitored by TLC analysis using POLTFRAM® SIL G/$UV_{254}$ (40 x 80 mm) TLC plates. Flash column chromatography was carried out using Silica gel as supplied from Sigma-Aldrich (230-400 mesh, 40-63 μm, 60 Å) and monitored using TLC analysis.

$^{1}$H NMR spectra were recorded on a Varian Mercury 500 MHz spectrometer, operating at ambient probe temperature unless specified elsewhere. $^{13}$C NMR spectra were recorded on a Varian Mercury 500 MHz instrument, operating at 101 MHz, unless otherwise specified. $^{11}$B NMR was recorded on a Varian Mercurry 400 MHz spectrometer, operating at 128 MHz. Deuterated chloroform $CDCl_3$ was used as solvent for all NMR spectra, unless otherwise specified. NMR peaks are reported as singlet (s), doublet (d), triplet (t), quartet (q), broad (br), combinations thereof, or as a multiplet (m). All chemical shifts (δ) are reported in parts per million (ppm).

Mass spectra for liquid chromatography mass spectrometry (LCMS) were obtained using a Waters (UK) TQD mass spectrometer (low resolution ESI+, electrospray in positive ion mode, ES+), Waters (UK) Xevo QTOF mass spectrometer (low and high resolution ASAP+) and a Waters (UK) LCT premier XE (high resolution ESI+, electrospray in positive ion mode, ES+) unless stated elsewhere.

HPLC analysis was carried out on an Agilent 1100 series instrument, fitted with a Perkin Elmer series 200 degasser. AS-H-CHIRALCEL column (250 x 4.6 mm) fitted with guard cartridge (50 x 4.6 mm), AD-CHIRALCEL column (250 x 4.6 mm) fitted with guard cartridge (50 x 4.6 mm), or OD-CHIRALCEL column (250 x 4.6 mm) fitted with guard cartridge (50 x 4.6 mm) was used to achieve chiral resolution, unless stated elsewhere.

All *in situ* IR spectroscopy experiments (ReactIR) were carried out on the following instrument: ReactIR 15 with MCT detector; ConcIRT window = 1900-900 $cm^{-1}$. Apodization = Happ General. Probe: Prob A DiComp (Diamond) connected *via* KAgX 9.5 mm x 2m Fiber (Silver Halide); Sampling 2500-650 at 8 $cm^{-1}$ resolution; Scan option: auto select, gain 1X.

Melting points were measured using a Gallenkamp Variable Heater (melting point apparatus). Optical rotations were measured using a JASCO P-1020 polarimeter with $[\alpha]_D$ values given in deg $cm^2g^{-1}$.

## 3.2 General reaction procedures

*General methodology for the preparation of α,β-unsaturated imines, monitored by ReactIR (as described in section 2.1-2.4).*

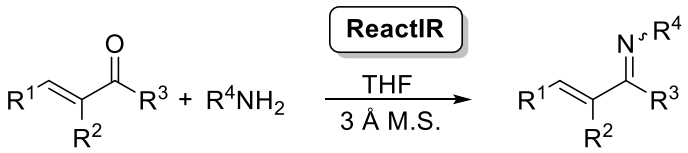


To an oven-dried two-necked flask, fitted with the IR probe (placed at a 45° angle), enone or enal (2.0 mmol) was added to a stirring solution of solvent (8.0 mL) and 3 Å-molecular sieve beads (2.0 g, oven-dried at 250 ºC for >48 h prior to use), under argon at 25 ºC. Once the C=O peak had plateaued (observed through PC-interface), showing maximum intensity, amine (2.0 mmol) was added and the reaction was carried out for 0.5 to 24 h. The *in situ*-formed imine was then utilised without purification by either cannula transfer or using a needle-syringe combination.

*General methodology for in situ $^{1}H$ NMR experiments (as described in section 2.2).*

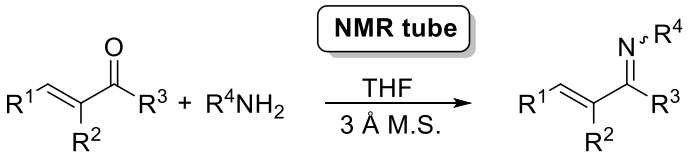


Enal or enone (0.18 mmol) was added to an NMR tube (Norell® Standard Series™ 5 mm x 178 mm NMR tubes) containing Deuterated-solvent (0.7 mL) with/without 3 Å molecular sieve beads (filled 0.7-0.8 mm up the tube, 3 Å molecular sieve beads oven-dried at 250 ºC for >48 h prior to use), and flushed with Argon and sealed. One the acquisition of the first spectrum, amine (0.18 mmol) was added and the next spectrum was acquired in <5 min. Subsequent $^{1}H$ NMR spectra were recorded over time with intermittent shaking of the NMR tube to aid mixing.

*General methodology for the $C_\beta$-selective β-borylation of N-benzhydryl α,β-unsaturated imines (as described in section 2.4).*

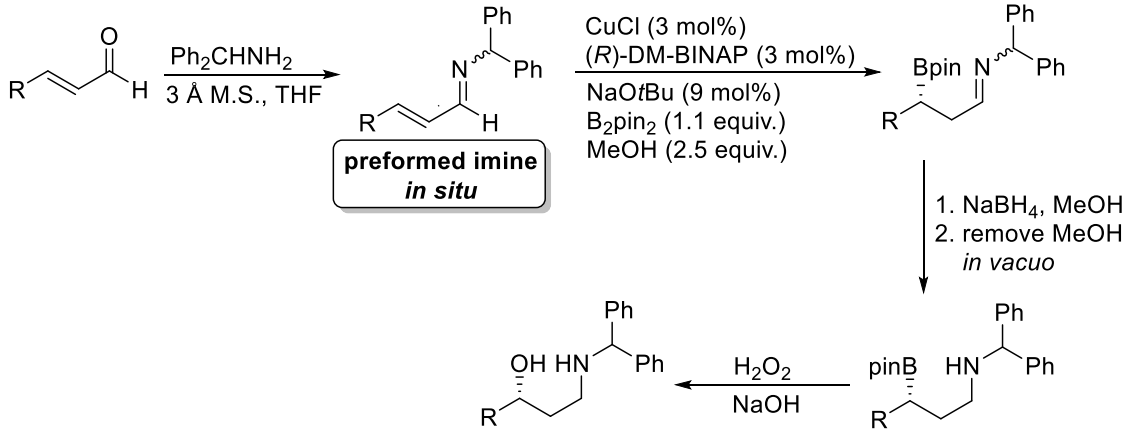


α,β-Unsaturated imine was formed *in situ* from the reaction between benzhydrylamine (2.00 mmol) and enal (2.00 mmol), stirred in THF (8 mL) and oven-dried 3 Å molecular sieve beads (2.0 g) for 6 h. After 6 h, an aliquot of the solution containing the *in situ*-formed imine (2.00 mL, 0.50 mmol) was transferred to a Schlenk-tube (under argon) containing CuCl (1.8 mg, 15 μmol), ligand (30 μmol for monodentate, and 15 μmol for bidentate ligands), NaO*t*Bu (4.3 mg, 45 μmol) and $B_2pin_2$ (0.14 g, 0.55 mmol). After 5 min, MeOH (50 μL, 1.25 mmol) was added to the solution and the reaction was stirred overnight. $NaBH_4$ (57.0 mg, 1.50 mmol) was added, followed by the drop-wise addition of MeOH (1.0 mL). The mixture was stirred for 3 h, followed by the removal of solvent under reduced pressure. THF (5.0 mL) was added to the resulting residue, followed by NaOH (0.30 mL, w/v 20%) and $H_2O_2$ (0.13 mL, w/v 35%), and the solution was heated to reflux for 1 h. After cooling, the resulting solution was partitioned between EtOAc and brine. The aqueous layer was extracted further with EtOAc (3 x EtOAc). The organic phase was separated and dried over $MgSO_4$. After filtration the organic phase was removed under reduced pressure to yield a crude product. Purification by silica gel chromatography (hexane : EtOAc, eluent and silica, 2:1 eluent) allowed for purification of the desired product.

*General methodology for the base-free, copper-BINAP catalyzed β-boration of α,β-unsaturated imines with bis(pinacolato)diboron (as described in section 2.3).*

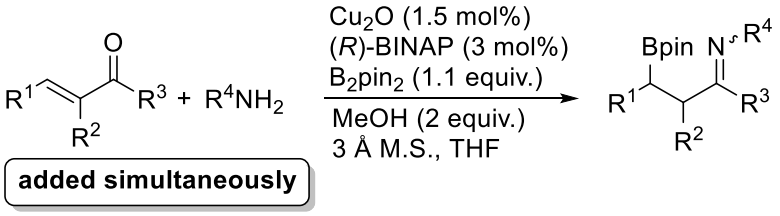


Reaction carried out on a 0.25 mmol scale: Copper(I) salts (1.5-3 mol%), BINAP ligand (3-6 mol%) and 3 Å molecular sieve beads (100 mg) was transferred to a Schlenck tube and dissolved in THF (1 mL) under Argon. After 15 min, bis(pinacolato)diboron (1.1 equiv.) was added to the solution and stirred during 10 min. Then amine (1 equiv.) and enone (1 equiv.) was added simultaneously, followed by MeOH (2.5 equiv.). The reaction mixture was stirred overnight at RT. The reaction products and conversion to the desired β–boryl imine was determined by $^{1}$H NMR and the enantiomeric excess was determined directly for HPLC-UV.[233]

*General methodology γ-amino alcohol synthesis (as described in section 2.1).*

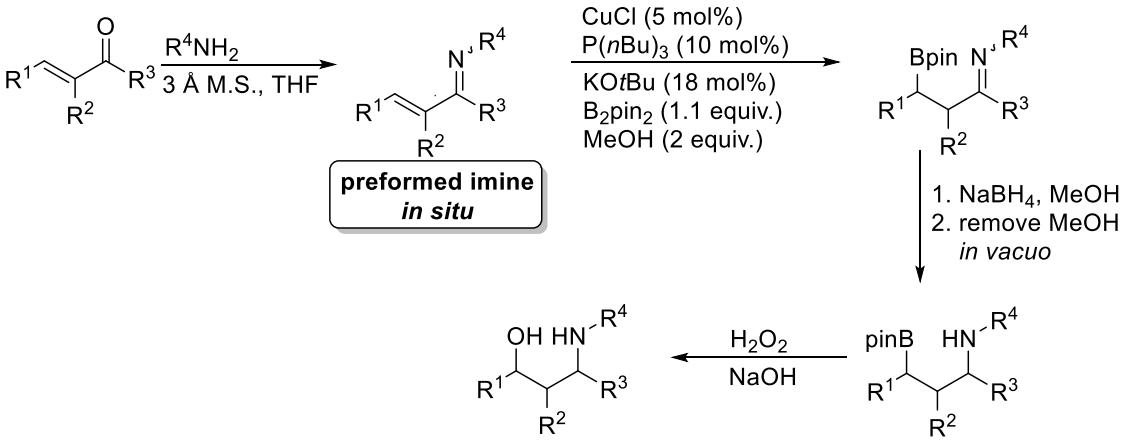


THF (7 mL), 3 Å molecular sieve pellets (2.5 g) were stirred under argon. Benzylamine (1.4 mmol) and α,β-unsaturated aldehyde/ketone (1.4 mmol) were added and stirred for 0-7 h. In a separate vessel, THF (4 mL), CuCl (0.07 mmol), $PPh_3$ (0.14 mmol) and

NaO*t*-Bu (0.21 mmol) were stirred for 30 min. After 30 min, $B_2pin_2$ (1.54 mmol) was added and stirred in the CuCl solution for 10 min. Both solutions were combined and stirred for a further 30 min, after which methanol was added (2.80 mmol) and stirred for 18 h. $NaBH_4$ (4.20 mmol was added and the solution stirred. Methanol (3 mL) was added drop-wise over 10 min. After 3 h, all solvent was removed under reduced pressure. THF (10 mL), NaOH (0.60 mL, 20% w/v solution, 4 mmol), $H_2O_2$ (0.25 mL, 35% w/v solution, *ca.* 4 mmol) was added to the resulting mass and refluxed for 1 h. The resulting solution was cooled and filtered through Celite, further EtOAc was passed through the Celite pad. The resulting solution was partitioned between EtOAc and brine. The aqueous layer was extracted further with EtOAc (3 x EtOAc). The organic phase was separated and dried over $MgSO_4$. After filtration the organic phase was removed under reduced pressure to yield a crude yellow oil. Purification was achieved by silica gel chromatography (hexane:EtOAc, 1:1 and 1% v/v $Et_3N$).

*General methodology (Route A-C) for 1,3-oxazine synthesis (as described in section 2.1).*

*Route A – From the pure γ-amino alcohol.*

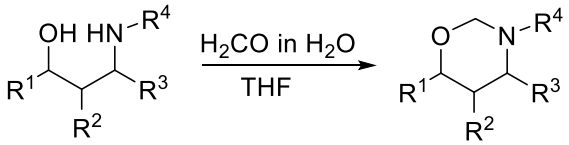


γ-Amino alcohol (0.86 mmol) and formaldehyde solution (75 μL, 37% w/v solution, 1.00 mmol) was stirred in THF (6 mL) for 4.5 h. After 4.5 h, $MgSO_4$ was added, and the organic phase was filtered and removed under reduced pressure to leave a crude oil. Purification was achieved by silica gel chromatography (hexane : EtOAc, 2:1 as eluent).

*Route B – MeOH present during oxidation step.*

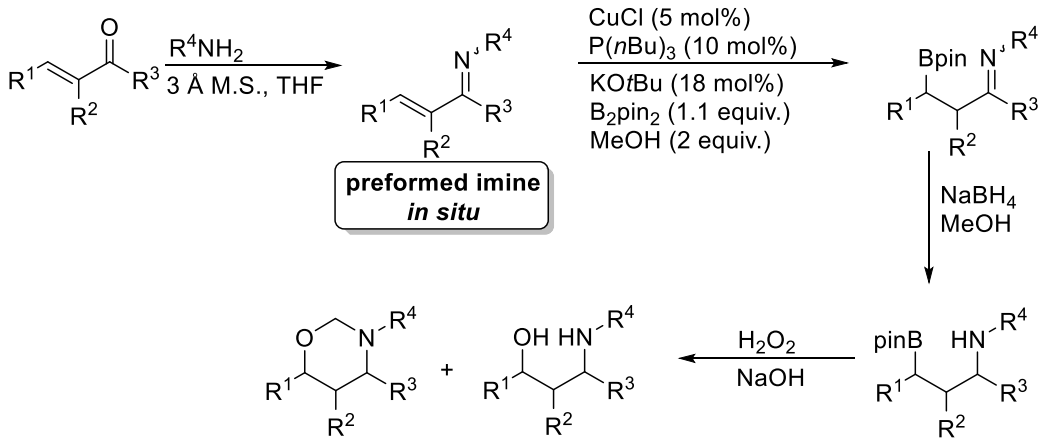


THF (7 mL), 3 Å molecular sieve pellets (2.5 g) were stirred under argon. Benzylamine (1.4 mmol) and α,β-unsaturated aldehyde/ketone (1.4 mmol) were added and stirred for 3 h. In a separate vessel, THF (4 mL), CuCl (0.07 mmol), $PPh_3$ (0.14 mmol) and NaO*t*-Bu (0.21 mmol) were stirred for 30 min. After 30 min, $B_2pin_2$ (1.54 mmol) was added and stirred in the CuCl solution for 10 min. Both solutions were combined and stirred for a further 30 min, after which methanol was added (2.80 mmol) and stirred for 18 h. $NaBH_4$ (4.20 mmol was added and the solution stirred. Methanol (15 mL) was added drop-wise over 10 min. After 3 h, NaOH (4.8 mL, 20% w/v solution, 4 mmol), $H_2O_2$ (2.0 mL, 35% w/v solution, *ca.* 4 mmol) was added drop-wise to the resulting mass and refluxed for 4 h. The resulting solution was cooled and filtered through Celite, further EtOAc was passed through the Celite pad. The resulting solution was partitioned between EtOAc and brine. The aqueous layer was extracted further with EtOAc (3 x EtOAc). The organic phase was separated and dried over $MgSO_4$. After filtration the organic phase was removed under reduced pressure. Purification was achieved by silica gel chromatography (hexane : EtOAc, 5:1 as eluent).

*Route C – MeOH removed before oxidation step.*

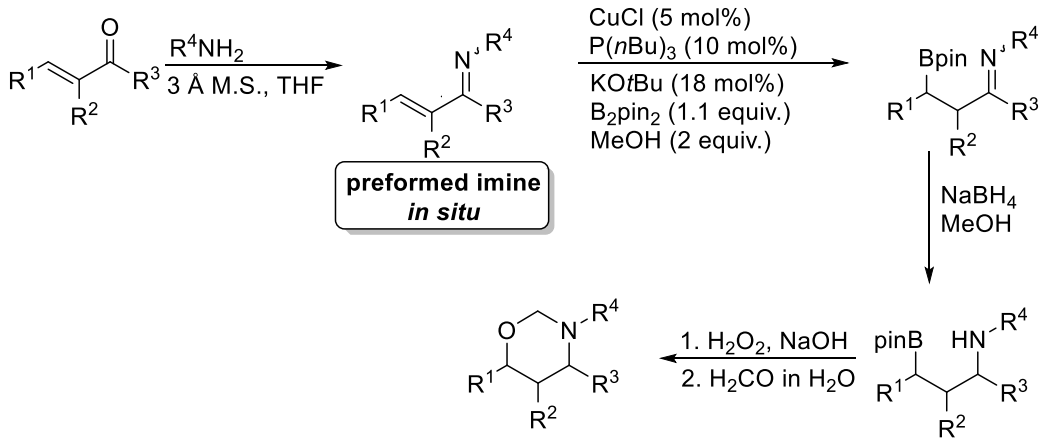


THF (7 mL), 3 Å molecular sieve pellets (2.5 g) were stirred under argon. Benzylamine (1.4 mmol) and α,β-unsaturated aldehyde/ketone (1.4 mmol) were added and stirred for 3 h. In a separate vessel, THF (4 mL), CuCl (0.07 mmol), $PPh_3$ (0.14 mmol) and NaO*t*-Bu (0.21 mmol) were stirred for 30 min. After 30 min, $B_2pin_2$ (1.54 mmol) was added and stirred in the CuCl solution for 10 min. Both solutions were combined and stirred for a further 30 min, after which methanol was added (2.80 mmol) and stirred for 18 h. $NaBH_4$ (4.20 mmol was added and the solution stirred. Methanol (3 mL) was added drop-wise over 10 min. After 3 h, all solvent was removed under reduced pressure. THF (10 mL), NaOH (0.60 mL, 20% w/v solution, 4 mmol), $H_2O_2$ (0.25 mL, 35% w/v solution, *ca.* 4 x $10^{-3}$ mol) was added to the resulting mass and refluxed for 1 h. The resulting solution was cooled and filtered through Celite, further EtOAc was passed through the Celite pad. The resulting solution was partitioned between EtOAc and brine. The aqueous layer was extracted further with EtOAc (3 x EtOAc). The organic phase was separated and dried over $MgSO_4$. After filtration the organic phase was removed under reduced pressure to yield the crude sample. Toluene (2 x 20 mL) was added to the crude sample and removed under pressure (this was repeated twice). After the toluene had been removed, THF (10 mL) and formaldehyde solution (0.12 mL, 37%

w/v solution, 1.00 mmol) were sequentially added to the sample and the solution was stirred under argon overnight (15 h). $MgSO_4$ was added to the reaction, and the solution was filtered. The organics were removed under vacuum to yield a crude sample. Purification was achieved by silica gel chromatography (hexane : EtOAc, 5:1 as eluent).

*General methodology for the Screening of Chiral Ligands for the base-free asymmetric $Cu_2O$/Ligand catalyzed β–boration of α,β–unsaturated imines, formed in situ (as described in section 2.3).*

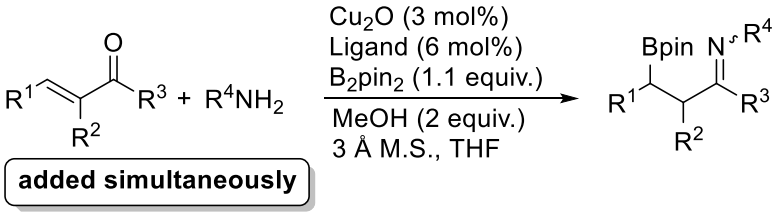


Reactions were carried out in paralle on a 0.25 mmol scale: $Cu_2O$ (3 mol%), chiral diphosphine (6 mol%) and dry THF (1 mL) under argon. The mixtures were stirred for 15 min at room temperature. Bis(pinacolato)diboron (1.1 equiv.) was added and the solution was stirred for 10 min. Then amine (1 equiv.) and the enone (1 equiv.) were added simultaneously to the reaction followed by the addition of MeOH (2.5 equiv.). The reaction mixture was stirred overnight at RT. The products obtained were analyzed by $^1H$ NMR spectroscopy to determine the conversion to the desired β–boryl imine products. The enantiomeric HPLC-UV, otherwise, the enantiomeric excess of the other β–borylimines was determined from the corresponding β–boryl carbonyl derivative obtained by hydrolysis. Purification was carried out by silica gel column chromatography.

*General methodology for the formation of O/N-Diacetate (as described in section 2.4).*

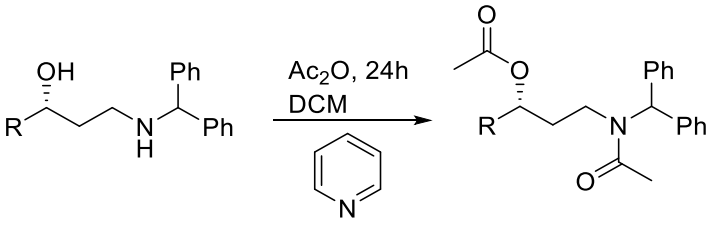


γ-Amino alcohol (0.19 mmol), pyridine (0.5 mL, 6.2 mmol) and acetic anhydride (0.5 mL, 5.3 mmol) were combined in DCM (3.0 mL) and stirred overnight. The resulting solution was diluted in DCM (10.0 mL) and was washed with HCl (3 x 10 mL, w/v 20%) and water (3 x). The organic layer was separated and dried over $MgSO_4$. Filtration followed by the removal of solvent under vacuum yielded a crude off-colourless solid, which was further purified by silica gel chromatography (hexane:EtOAc, eluent and silica, 2:1 eluent) to give the product pure product.

*General methodology for the preparation of pharmaceuticals through the in situ imine formation, borylation, transimination and reduction approached (as described in section 2.5).*

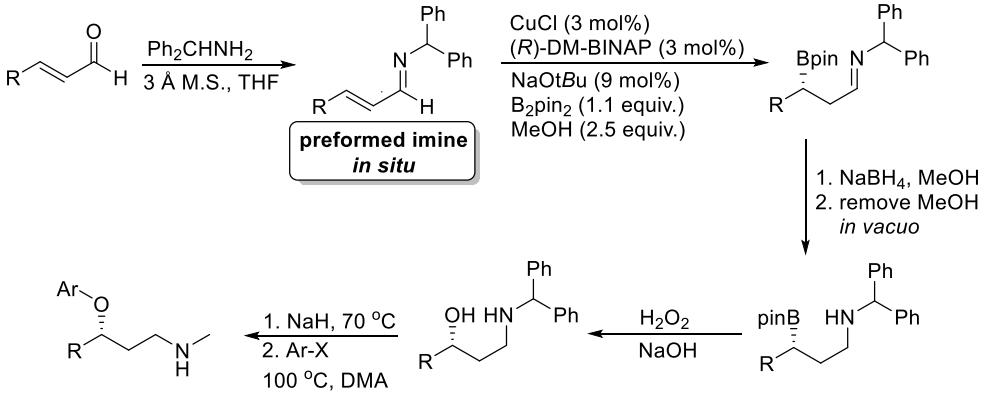


Benzhydrylamine (2.00 mmol) and enal (5.00 mmol) were added to a stirring solution of THF (20 mL) and oven-dried 3 Å molecular sieve pellets (5.0 g) for 6 h, to form the α,β-unsaturated imine *in situ*. After 6 h, an aliquot of the solution containing the *in situ*-

formed imine (16.0 mL, 4.00 mmol) was transferred to a Schlenk-tube (under argon) containing CuCl (12.0 mg, 0.12 mmol), $PPh_3$ (62.9 mg, 0.24 mmol) or (*R/S*)-DM-BINAP (88.2 mg, 0.12 mmol), NaO*t*-Bu (34.6 mg, 0.36 mmol) and $B_2pin_2$ (1.12 g, 4.4 mmol). After 5 min, MeOH (400 µL, 10.0 mmol) was added to the solution and the reaction was stirred overnight. Methylamine (8 mL, 16.0 mmol, 2 M THF solution) was added under argon and the resulting solution was stirred for 1.5 h. $NaBH_4$ (0.46 g, 12.0 mmol) was added, followed by the drop-wise addition of MeOH (8.0 mL). The mixture was stirred for 3 h, followed by the removal of solvent under reduced pressure. THF (20 mL) was added to the resulting residue, followed by NaOH (2.4 mL, w/v 20%) and $H_2O_2$ (1.1 mL, w/v 35%), and the solution was heated to reflux for 1 h. After cooling, the resulting solution was partitioned between EtOAc and brine. The aqueous layer was extracted further with EtOAc (3 x EtOAc). The organic phase was separated and dried over $MgSO_4$. After filtration the organic phase was removed under reduced pressure to yield a crude product. Purification by silica gel chromatography (DCM → DCM : MeOH : $NEt_3$, 5 : 1 : 1%) gave the pure product. The pure γ-amino alcohol (2.00 mmol) was dissolved in dry dimethylacetamide (2.8 mL) and transferred to an oven-dried Schlenk-tube and purged with Argon. NaH (100 mg, 2.2 mmol, 60% in mineral oil) was transferred directly to the solution and heated (70 $^oC$) under Argon for 30-40 min, or until hydrogen evolution had ceased. 4-Chlorobenzotrifluoride (354 µL, 2.4 mmol) was added under argon, and the resulting solution was heated (100 $^oC$) for 3 h. On cooling, the solution was partitioned between toluene and $H_2O$ and washed (3 x $H_2O$). The organic phase was separated and dried over $MgSO_4$. After filtration the organic phase was removed under reduced pressure to yield a crude product. Purification by silica gel chromatography (DCM → DCM:MeOH:$NEt_3$, 5:1:1%) gave the pure product.

## 3.3 Specific procedures and characterisation

### 3.3.1 γ-Amino alcohols

(*R*)-(+)-3-[(Diphenylmethyl)amino]-1-phenylpropan-1-ol. **128**

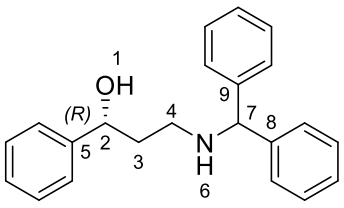


Optimised methodology for synthesis of **128** in 97% enantiomeric excess. α,β-Unsaturated imine **119** was formed *in situ* from the reaction between benzhydrylamine (345 μL, 2.00 mmol) and *trans*-cinnamaldehyde **66** (252 μL, 2.00 mmol), stirred in THF (8 mL) with oven-dried 3 Å molecular sieve beads (2.0 g) for 6 h. After 6 h, an aliquot of the solution containing the *in situ*-formed imine **119** (2.00 mL, 0.50 mmol) was transferred to a Schlenk-tube (under argon) containing CuCl (1.8 mg, 15 μmol), (*R*)-DM-BINAP (11.0 mg, 15 μmol), NaO*t*Bu (4.3 mg, 45 μmol) and $B_2pin_2$ (0.14 g, 0.55 mmol). After 5 min, MeOH (50 μL, 1.25 mmol) was added to the solution and the reaction was stirred overnight. $NaBH_4$ (57.0 mg, 1.50 mmol) was added, followed by the drop-wise addition of MeOH (1.0 mL). The mixture was stirred for 3 h, followed by the removal of solvent under reduced pressure. THF (5.0 mL) was added to the resulting residue, followed by NaOH (0.30 mL, w/v 20%) and $H_2O_2$ (0.13 mL, w/v 35%), and the solution was heated at reflux for 1 h. After cooling, the resulting solution was partitioned between EtOAc and brine. The aqueous layer was extracted further with EtOAc (3 x EtOAc). The organic phase was separated and dried over $MgSO_4$. After filtration the organic phase was removed under reduced pressure to yield a crude product. Purification by silica gel chromatography (hexane:EtOAc, eluent and silica, 2:1 eluent) gave the pure product as a cloudy oil which, on standing overnight,

resulted in the formation of a white solid (79.3 mg, 50%; 97% *e.e.*). *m.p.* 85-87 °C. IR (neat) $\nu_{max}$: 3280, 3026, 2848, 1599, 1492, 1451, 742, 696 $cm^{-1}$. $^{1}H$ NMR (400 MHz, $CDCl_3$): δ 7.33- 7.11 (m, 15H, Ph), 4.84 (dd, *J* = 8.7, 3.1 Hz, 1H, CH-2), 4.71 (s, 1H, $CH_2$-7), 2.85- 2.69 (m, 2H, $CH_2$-4), 1.86 – 1.67 (m, 2H, $CH_2$-3). $^{13}C$ NMR (101 MHz, $CDCl_3$): δ 144.8 (C-5), 143.1 (C-9), 142.8 (C-8), 128.7, 128.7, 128.2, 127.4, 127.3, 127.3, 127.3, 127.0, 125.6, 75.4 (C-2), 67.9 (C-7), 46.8 (C-4), 38.2 (C-3). LRMS (ESI+) 318.2 (100%) $[M+H]^+$, 164.7 (63%). HRMS (ESI+) calculated $[C_{22}H_{23}NO+H]^+$ 318.1858, found 318.1863. $[\alpha]_D^{24}$ = +36.7 (1.3, $HCCl_3$) for the (*R*)-γ-amino alcohol **128** in 97% *e.e.* Anal. Calc. for $C_{22}H_{23}NO$ C, 83.24; H, 7.30; N, 4.41; found C, 80.17; H, 6.95; N, 3.97. X-Ray crystallography was used to confirm this structure. Enantiomeric excess was determined by derivatisation to the analogous *O*/*N*-diacetate **135**.

(*R*)-3-[(Diphenylmethyl)amino]-1-(4-methoxyphenyl)propan-1-ol. **130**

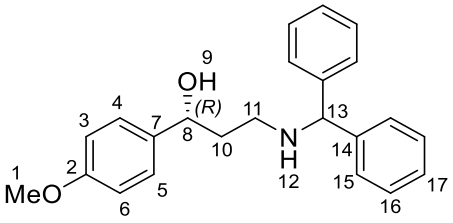


Optimised methodology for synthesis of **130** in 90% enantiomeric excess. α,β-Unsaturated imine **120** was formed *in situ* from the reaction between benzhydrylamine (345 μL, 2.00 mmol) and *trans*-4-methoxycinnamaldehyde **121** (324 mg, 2.00 mmol), stirred in THF (8 mL) and oven-dried 3 Å molecular sieve beads (2.0 g) for 6 h. After 6 h, an aliquot of the solution containing the *in situ*-formed imine **120** (2.00 mL, 0.50 mmol) was transferred to a Schlenk-tube (under argon) containing CuCl (1.8 mg, 15 μmol), (*R*)-DM-BINAP (11.0 mg, 15 μmol), NaO*t*Bu (4.3 mg, 45 μmol) and $B_2pin_2$ (0.14 g, 0.55 mmol). After 5 min, MeOH (50 μL, 1.25 mmol) was added to

the solution and the reaction was stirred overnight. $NaBH_4$ (57.0 mg, 1.50 mmol) was added, followed by the drop-wise addition of MeOH (1.0 mL). The mixture was stirred for 3 h, followed by the removal of solvent under reduced pressure. THF (5.0 mL) was added to the resulting residue, followed by NaOH (0.30 mL, w/v 20%) and $H_2O_2$ (0.13 mL, w/v 35%), and the solution was heated at reflux for 1 h. After cooling, the resulting solution was partitioned between EtOAc and brine. The aqueous layer was extracted further with EtOAc (3 x EtOAc). The organic phase was separated and dried over $MgSO_4$. After filtration the organic phase was removed under reduced pressure EtOAc, eluent and silica, 2:1 eluent) gave the pure product as a cloudy colourless oil (156.2 mg, 90%; 90% *e.e.*). IR (neat) $\nu_{max}$: 3250, 3026, 2836, 1611, 1512, 1452, 1244, 1031, 729 $cm^{-1}$. $^1H$ NMR (400 MHz, $CDCl_3$): δ 7.36-7.11 (m, 12H, Ph), 6.76 (d, *J* = 8.8 Hz, 2H, Ph-3 and 6), 4.79 (dd, *J* = 8.5, 3.2 Hz, 1H, CH-8), 4.71 (s, 1H, CH-13), 3.70 (s, 3H, $CH_3$-1), 2.86-2.66 (m, 2H, $CH_2$-11), 1.83-1.66 (m, 2H, $CH_2$-10). $^{13}C$ NMR (101 MHz, $CDCl_3$): δ 158.7 (C-2), 143.3 (C-7), 142.9 (C-14), 137.1, 129.1, 128.7, 128.5, 128.5, 128.3, 127.4, 127.3, 127.0, 126.9, 113.6 (C-1), 75.0 (C-8), 67.9 (C-13), 59.7 (C-11), 46.9 (C-10). LRMS (ESI+) 348.2 (100%) $[M+H]^+$, 167.0 (18%). HRMS (ESI+) calculated $[C_{23}H_{25}NO_2+H]^+$ 348.1964, found 348.1972. Enantiomeric excess was determined by derivatisation to the analogous *O*/*N*-diaceteate **136**.

(*R*)-1-(4-Chlorophenyl)-3-[(diphenylmethyl)amino]propan-1-ol. **131**

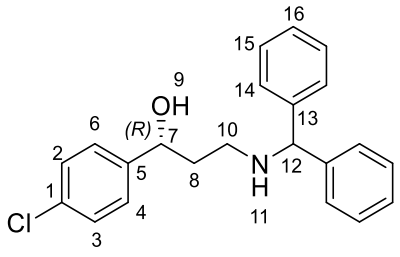

Optimised methodology for synthesis of **131** in 90% enantiomeric excess. α,β-Unsaturated imine **123** was formed *in situ* from the reaction between benzhydrylamine (345 μL, 2.00 mmol) and *trans*-4-chlorocinnamaldehyde **122** (333 mg, 2.00 mmol), stirred in THF (8 mL) and oven-dried 3 Å molecular sieve beads (2.0 g) for 9 h. After 9 h, an aliquot of the solution containing the *in situ*-formed imine **123** (2.00 mL, 0.50 mmol) was transferred to a Schlenk-tube (under argon) containing CuCl (1.8 mg, 15 μmol), (*R*)-DM-BINAP (11.0 mg, 15 μmol), NaO*t*Bu (4.3 mg, 45 μmol) and $B_2pin_2$ (0.14 g, 0.55 mmol). After 5 min, MeOH (50 μL, 1.25 mmol) was added to the solution and the reaction was stirred overnight. $NaBH_4$ (57.0 mg, 1.50 mmol) was added, followed by the drop-wise addition of MeOH (1.0 mL). The mixture was stirred for 3 h, followed by the removal of solvent under reduced pressure. THF (5.0 mL) was added to the resulting residue, followed by NaOH (0.30 mL, w/v 20%) and $H_2O_2$ (0.13 mL, w/v 35%), and the solution was heated to reflux for 1 h. After cooling, the resulting solution was partitioned between EtOAc and brine. The aqueous layer was extracted further with EtOAc (3 x EtOAc). The organic phase was separated and dried over $MgSO_4$. After filtration the organic phase was removed under reduced pressure to yield a crude product. Purification by silica gel chromatography (hexane:EtOAc, eluent and silica, 2:1 eluent) gave the pure product as a colourless oil (103.6 mg, 59%; 90% *e.e.*). IR (neat) $\nu_{max}$: 3250, 3026, 2836, 1611, 1512, 1244, 1031, 729 $cm^{-1}$. $^1H$ NMR (400 MHz, $CDCl_3$): δ 7.36-7.08 (m, 14H, Ph), 4.83 (dd, *J* = 8.7, 3.0 Hz, 1H, CH-7), 4.71 (s, 1H, CH-12), 2.90-2.69 (m, 2H, $CH_2$-10), 1.86-1.59 (m, 2H, $CH_2$-8). $^{13}C$ NMR (101 MHz, $CDCl_3$): 142.3 (C-1), 141.9 (C-5), 141.5 (C-13), 131.5, 128.7, 127.7, 127.5, 127.4, 127.3, 126.6, 126.4, 73.8 (C-7), 66.8 (C-12), 45.7 (C-10), 37.0 (C-8). LRMS (ESI+) 352.2 (100%) $[M+H]^+$, 168.0 (23%). HRMS (ESI+) calculated

$[C_{22}H_{22}NOCl+H]^+$ 352.14669, found 352.14627. Enantiomeric excess was determined by derivatisation to the analogous *O*/*N*-diaceteate **137**.

(*S*)-1-[(Diphenylmethyl)amino]hexan-3-ol. **132**

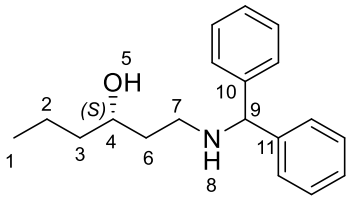


Optimised methodology for synthesis of **132** in 87% enantiomeric excess. α,β-Unsaturated imine **124** was formed *in situ* from the reaction between benzhydrylamine (345 μL, 2.00 mmol) and *trans*-2-hexenal **116** (232 μL, 2.00 mmol), stirred in THF (8 mL) and oven-dried 3 Å molecular sieve beads (2.0 g) for 6 h. After 6 h, an aliquot of the solution containing the *in situ*-formed imine **124** (2.00 mL, 0.50 mmol) was transferred to a Schlenk-tube (under argon) containing CuCl (1.8 mg, 15 μmol), (*R*)-DM-BINAP (11.0 mg, 15 μmol), NaO*t*Bu (4.3 mg, 45 μmol) and $B_2pin_2$ (0.14 g, 0.55 mmol). After 5 min, MeOH (50 μL, 1.25 mmol) was added to the solution and the reaction was stirred overnight. $NaBH_4$ (57.0 mg, 1.50 mmol) was added, followed by the drop-wise addition of MeOH (1.0 mL). The mixture was stirred for 3 h, followed by the removal of solvent under reduced pressure. THF (5.0 mL) was added to the resulting residue, followed by NaOH (0.30 mL, w/v 20%) and $H_2O_2$ (0.13 mL, w/v 35%), and the solution was heated to reflux for 1 h. After cooling, the resulting solution was partitioned between EtOAc and brine. The aqueous layer was extracted further with EtOAc (3 x EtOAc). The organic phase was separated and dried over $MgSO_4$. After filtration the organic phase was removed under reduced pressure to yield a crude product. Purification by silica gel chromatography (hexane:EtOAc, eluent and silica, 2:1 eluent) gave the pure product as colourless oil (83.8 mg, 59%; 87% *e.e.*). IR (neat) $\nu_{max}$:

3290, 3025, 2954, 2928, 2870, 1599, 1492, 1452, 1028, 743, 696 $cm^{-1}$. $^{1}H$ NMR (400 MHz, $CDCl_3$): δ 7.37- 7.08 (m, 10H, Ph), 4.70 (s, 1H, CH-9), 3.78-3.68 (m, 1H, CH-4), 2.88-2.85 (m, 1H, $CH_2$-7), 2.63 (t, *J* = 10.6 Hz, 1H, $CH_2$-7), 1.61-1.45 (m, 2H, $CH_2$-6), 1.47-1.35 (m, 2H, $CH_2$-3), 1.36-1.23 (m, 2H, $CH_2$-2) 0.85 (t, *J* = 6.8 Hz, $CH_3$-1). $^{13}C$ NMR (101 MHz, $CDCl_3$): δ 143.4 (C-10), 142.9 (C-11), 128.7, 128.5, 127.6, 127.3, 127.2, 127.2, 73.2 (C-4), 67.9 (C-9), 47.3 (C-7), 39.9 (C-6), 35.9 (C-3), 18.8 (C-2), 14.2 (C-1). LRMS (ESI+) 284.6 (100%) $[M+H]^+$, 167.3 (86%). HRMS (ESI+) calculated $[C_{19}H_{25}NO+H]^+$ 284.2014, found 284.2012. Enantiomeric excess was determined by derivatisation to the analogous *O*/*N*-diacetate **138**.

(*S*)-1-[(Diphenylmethyl)amino]pentan-3-ol. **133**

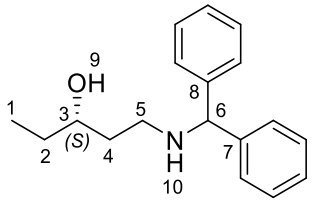


Optimised methodology for synthesis of **133** in 76% enantiomeric excess. α,β-Unsaturated imine **126** was formed *in situ* from the reaction between benzhydrylamine (345 µL, 2.00 mmol) and *trans*-2-pentenal **125** (196 µL, 2.00 mmol), stirred in THF (8 mL) and oven-dried 3 Å molecular sieve beads (2.0 g) for 6 h. After 6 h, an aliquot of the solution containing the *in situ*-formed imine **126** (2.00 mL, 0.50 mmol) was transferred to a Schlenk-tube (under argon) containing CuCl (1.8 mg, 15 µmol), (*R*)-DM-BINAP (11.0 mg, 15 µmol), NaO*t*Bu (4.3 mg, 45 µmol) and $B_2pin_2$ (0.14 g, 0.55 mmol). After 5 min, MeOH (50 µL, 1.25 mmol) was added to the solution and the reaction was stirred overnight. $NaBH_4$ (57.0 mg, 1.50 mmol) was added, followed by the drop-wise addition of MeOH (1.0 mL). The mixture was stirred for 3 h,

followed by the removal of solvent under reduced pressure. THF (5.0 mL) was added to the resulting residue, followed by NaOH (0.30 mL, w/v 20%) and $H_2O_2$ (0.13 mL, w/v 35%), and the solution was heated to reflux for 1 h. After cooling, the resulting solution was partitioned between EtOAc and brine. The aqueous layer was extracted further with EtOAc (3 x EtOAc). The organic phase was separated and dried over $MgSO_4$. After filtration the organic phase was removed under reduced pressure to yield a crude product. Purification by silica gel chromatography (hexane:EtOAc, eluent and silica, 2:1 eluent) gave the pure product as a colourless oil (87.8 mg, 65%; 76% *e.e.*). IR (neat) $\nu_{max}$: 3276, 3025, 2926, 1492, 1452, 1028, 744, 696 $cm^{-1}$. $^1H$ NMR (400 MHz, $CDCl_3$): δ 7.38-7.03 (m, 10H, Ph), 4.70 (s, 1H, CH-6), 3.67-3.59 (m, 1H, CH-3), 2.87 (ddd, *J* = 11.8, 3.6, 1.4 Hz, 1H, $CH_2$-5), 2.63 (dt, *J* = 10.7, 3.3 Hz, 1H, $CH_2$-5), 1.62-1.55 (m, 1H, $CH_2$-4), 1.47-1.41 (m, 1H, $CH_2$-4), 1.45-1.29 (m, 2H, $CH_2$-2), 0.86 (t, *J* = 7.4 Hz, $CH_3$-1). $^{13}C$ NMR (101 MHz, $CDCl_3$): δ 143.4 (C-8), 142.9 (C-7), 129.1, 128.7, 128.4, 127.6, 127.3, 127.1, 67.9 (C-6), 47.2 (C-3), 35.3 (C-5), 30.4 (C-4), 24.9 (C-2), 10.0 (C-1). LRMS (ESI+) 270.2 (93%) $[M+H]^+$, 167.4 (100%). HRMS (ESI+) calculated $[C_{18}H_{22}NO+H]^+$ 270.18524, 270.18558. Enantiomeric excess was determined by derivatisation to the analogous *O*/*N*-diacetate **139**.

(*S*)-(+)-1-[(Diphenylmethyl)amino]butan-2-ol. **134**

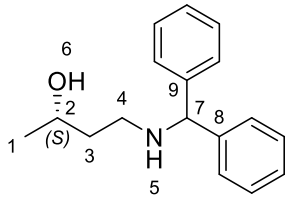


Optimised methodology for synthesis of **134** in 80% enantiomeric excess. α,β-Unsaturated imine **127** was formed *in situ* from the reaction between

benzhydrylamine (345 µL, 2.00 mmol) and crotonaldehyde **59** (166 µL, 2.00 mmol), stirred in THF (8 mL) and oven-dried 3 Å molecular sieve beads (2.0 g) for 6 h. After 6 h, an aliquot of the solution containing the *in situ*-formed imine **127** (2.00 mL, 0.50 mmol) was transferred to a Schlenk-tube (under argon) containing CuCl (1.8 mg, 15 µmol), (*R*)-DM-BINAP (11.0 mg, 15 µmol), NaO*t*Bu (4.3 mg, 45 µmol) and $B_2pin_2$ (0.14 g, 0.55 mmol). After 5 min, MeOH (50 µL, 1.25 mmol) was added to the solution and the reaction was stirred overnight. $NaBH_4$ (57.0 mg, 1.50 mmol) was added, followed by the drop-wise addition of MeOH (1.0 mL). The mixture was stirred for 3 h, followed by the removal of solvent under reduced pressure. THF (5.0 mL) was added to the resulting residue, followed by NaOH (0.30 mL, w/v 20%) and $H_2O_2$ (0.13 mL, w/v 35%), and the solution was heated to reflux for 1 h. After cooling, the resulting solution was partitioned between EtOAc and brine. The aqueous layer was extracted further with EtOAc (3 x EtOAc). The organic phase was separated and dried over $MgSO_4$. After filtration the organic phase was removed under reduced pressure to yield a crude product. Subsequent purification by silica gel chromatography (hexane: EtOAc, eluent and silica, 2:1 eluent) gave the pure product a colourless oil (112.6 mg, 88%; 80% *e.e.*). IR (neat) $\nu_{max}$: 3290, 3026, 2966, 2926, 1492, 1452, 1099, 732, 696 $cm^{-1}$. $^1H$ NMR (400 MHz, $CDCl_3$): δ 7.42-7.17 (m, 10H, Ph) 4.78 (s, 1H, CH-7), 4.02-3.94 (m, 1H, CH-2), 2.95 (ddd, *J* = 11.9, 3.6, 1.4 Hz, 1H, $CH_2$-4), 2.71 (dt, *J* = 10.6, 3.4 Hz, 1H, $CH_2$-4), 1.69-1.47 (m, 2H, $CH_2$-4), 1.17 (d, *J* = 6.2 Hz, 1H, $CH_3$-1). $^{13}C$ NMR (101 MHz, $CDCl_3$): δ 143.3 (C-8), 142.8 (C-9), 128.6, 128.6, 128.4, 127.2, 127.1, 126.9, 69.5 (C-2), 67.9 (C-7), 47.1 (C-4), 37.5 (C-3), 23.4 (C-1). LRMS (ESI+) 256.2 (100%) $[M+H]^+$, 167.3 (68%). HRMS (ESI+) calculated $[C_{17}H_{21}NO+H]^+$ 256.1701, found 256.1697. $[\alpha]_D^{24}$ = +3.6 (1.5, $HCCl_3$) for the (*R*)-γ-amino alcohol **134** in 80% *e.e.*

Enantiomeric excess was determined by derivatisation to the analogous *O*/*N*-diacetate **140**.

(*anti*)-3-(Benzylamine)-1-phenylbutan-1-ol. **64**

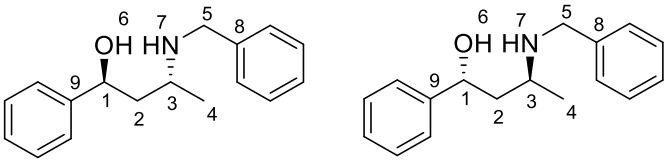


THF (10 mL) and 3 Å molecular sieve pellets (2.5 g) were stirred under argon. Benzylamine (0.15 mL, 1.4 mmol) and (3*E*)-4-phenylbut-3-en-2-one (0.20 g, 1.4 mmol) were added and stirred for 6 h. In a separate vessel, THF (5 mL), CuCl (6.93 mg, 0.07 mmol), P*n*$Bu_3$ (34.5 μL, 0.14 mmol) and NaO*t*-Bu (24.0 mg, 0.25 mmol) were stirred for 30 min. After 30 min, $B_2pin_2$ (0.39 g, 1.54 mmol) was added and stirred in the CuCl solution for 10 min. Both solutions were combined and stirred for a further 30 min, after which methanol was added (0.16 mL, 2.80 mmol) and stirred for 18 h. $NaBH_4$ (0.16 g, 4.20 mmol) was added and the solution stirred. Methanol (3 mL) was added drop-wise over 10 min. After 3 h, all solvent was removed under reduced pressure. THF (10 mL), NaOH (0.60 mL, 20% w/v solution, 4 mmol), $H_2O_2$ (0.25 mL, 35% w/v solution, *ca.* 4 x $10^{-3}$ mol) was added to the resulting mass and refluxed for 1 h. The resulting solution was cooled and filtered through Celite, further EtOAc was passed through the Celite pad. The resulting solution was partitioned between EtOAc and brine. The aqueous layer was extracted further with EtOAc (3 x EtOAc). The organic phase was separated and dried over $MgSO_4$. After filtration the organic phase was removed under reduced pressure to yield a crude dark yellow oil. Purification by silica gel chromatography (hexane:EtOAc, 1% v/v $Et_3N$ in eluent and silica, 4:1 eluent) gave the product as a cloudy colourless oil (0.32 g, 90%). IR (neat) $\nu_{max}$: 3336, 3027, 2971, 2925, 1494, 1448,

1367, 1300, 1142, 1059, 966, 942, 825, 747, 692 $cm^{-1}$. $^{1}H$ NMR (400 MHz, $CDCl_3$): δ 7.33- 7.13 (m, 10H, Ph), 4.84 (dd, *J* = 10.6, 2.0 Hz, 1H, CH-1), 3.92 (d, *J* = 12.5 Hz, 1H, CH-5), 3.71 (d, *J* = 12.5, 1H, CH-5), 3.09 - 2.95 (m, 1H, CH-3), 1.68 (dt, *J* = 14.4, 2.3 Hz, 1H, CH-2 ) 1.52 (dt, *J* = 14.4, 10.8 Hz, 1H, CH-2) 1.14 (d, *J* = 6.3, 3H, CH-4). $^{13}C$ NMR (101 MHz, $CDCl_3$): δ 145.3 (C-9), 139.3 (C-8), 128.6, 128.4, 128.2, 1271.3, 127.0, 125.6, 75.4 (C-1), 54.3 (C-5), 50.9 (C-3), 46.1 (C-2), 21.1 (C-4). LRMS (ASAP+) 256.2 (28%) [$M+H^+$], 134.1.0 (100%). HRMS (TOF ASAP+) calculated [$C_{17}H_{21}NO+H^+$] 256.1701, found 256.1684. All spectroscopic and analytical properties are identical with those reported in the literature.[64]

3-(Benzylamine)-2-methylpropan-1-ol. **69**

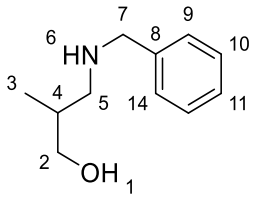


THF (7 mL), 3 Å molecular sieve pellets (2.5 g) were stirred under argon. Benzylamine (0.15 mL, 1.4 mmol) and methacrolein (0.12 mL, 1.4 mmol) were added and stirred for 3 h. In a separate vessel, THF (4 mL), CuCl (6.93 mg, 0.07 mmol), $PPh_3$ (36.72 mg, 0.14 mmol) and NaO*t*-Bu (20.2 mg, 0.21 mmol) were stirred for 30 min. After 30 min, $B_2pin_2$ (0.39g, 1.54 mmol) was added and stirred in the CuCl solution for 10 min. Both solutions were combined and stirred for a further 30 min, after which methanol was added (0.11 mL, 2.80 mmol) and stirred for 18 h. $NaBH_4$ (0.16 g, 4.20 mmol was added and the solution stirred. Methanol (3 mL) was added drop-wise over 10 min. After 3 h, all solvent was removed under reduced pressure. THF (10 mL), NaOH (0.60 mL, 20% w/v solution, 4 mmol), $H_2O_2$ (0.25 mL, 35% w/v solution, *ca.* 4 x $10^{-3}$ mol) was added

to the resulting mass and refluxed for 1 h. The resulting solution was cooled and filtered through Celite, further EtOAc was passed through the Celite pad. The resulting solution was partitioned between EtOAc and brine. The aqueous layer was extracted further with EtOAc (3 x EtOAc). The organic phase was separated and dried over $MgSO_4$. After filtration the organic phase was removed under reduced pressure to yield a crude yellow oil. Purification by silica gel chromatography (EtOAc, 1% v/v $Et_3N$ in eluent and silica) gave the product as a cloudy colourless oil (0.19 g, 64%, >90% purity). IR (neat) $\nu_{max}$: 3302, 2871, 2163, 1495, 1453, 1384, 1104, 1028, 953, 734, 697 $cm^{-1}$. $^1H$ NMR (400 MHz, $CDCl_3$): δ 7.35 - 7.15 (m, 5H, Ph), 3.80 (bs, 1H, NH-6), 3.75 (d, *J* = 13.1 Hz, 1H, $CH_2$-7), 3.65 (d, *J* = 13.2 Hz, 1H, $CH_2$-7), 3.63 (ddd, *J* = 11.8, 3.3, 2.1 Hz, 1H, $CH_2$-2), 3.48 (dd, 11.8, 10.2 Hz, 1H, $CH_2$-2), 3.00 - 2.60 (bs, 1H), 2.83 (ddd, *J* = 11.8, 3.3, 2.1 Hz, 1H, $CH_2$-5), 2.50 (dd, 11.8, 10.2 Hz, 1H, $CH_2$-5), 1.95 – 1.83 (m, 1H, CH-4), 0.73 (d, *J* = 6.9 Hz, 3H, $CH_3$-3). $^{13}C$ NMR (101 MHz, $CDCl_3$): δ 138.3 (C-8), 127.6, 127.5, 127.2, 69.9 (C-2), 55.9 (C-7), 53.1 (C-5), 33.3 (C-4), 14.0 (C-3). LRMS (ASAP+) 180.1 (54%) [$M+H^+$], 162.1 (40%), 120.1 (9%). HRMS (TOF ASAP+) calculated [$C_{11}H_{18}NO+H^+$] 180.1388, found 180.1358.

(*anti*)-4-(Benzylamine)-3-methylbutan-2-ol. **71**

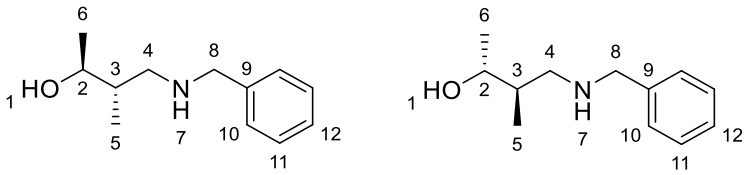


THF (7 mL), 3 Å molecular sieve pellets (2.5 g) were stirred under argon. Benzylamine (0.15 mL, 1.4 mmol) and tiglic aldehyde, (0.14 mL, 1.4 mmol) were added and stirred for 3 h. In a separate vessel, THF (4 mL), CuCl (6.93 mg, 0.07 mmol), P*n*$Bu_3$ (34.5 μL, 0.14 mmol) and NaO*t*-Bu (20.2 mg, 0.21 mmol) were stirred for 30 min. After 30 min,

$B_2pin_2$ (0.39g, 1.54 mmol) was added and stirred in the CuCl solution for 10 min. Both solutions were combined and stirred for a further 30 min, after which methanol was added (0.11 mL, 2.80 mmol) and stirred for 18 h. $NaBH_4$ (0.16 g, 4.20 mmol was added and the solution stirred. Methanol (3 mL) was added drop-wise over 10 min. After 3 h, all solvent was removed under reduced pressure. THF (10 mL), NaOH (0.60 mL, 20% w/v solution, 4 mmol), $H_2O_2$ (0.25 mL, 35% w/v solution, *ca.* 4 x $10^{-3}$ mol) was added to the resulting mass and refluxed for 1 h. The resulting solution was cooled and filtered through Celite, further EtOAc was passed through the Celite pad. The resulting solution was partitioned between EtOAc and brine. The aqueous layer was extracted further with EtOAc (3 x EtOAc). The organic phase was separated and dried over $MgSO_4$. After filtration the organic phase was removed under reduced pressure to yield a crude yellow oil. Purification by silica gel chromatography (hexane:EtOAc, 1% v/v $Et_3N$ in eluent and silica, 1:1 eluent) gave the product as a colourless oil (0.32 g, 70%). IR (neat) $\nu_{max}$: 3444, 2966, 2971, 1452, 1377, 1111, 733 $cm^{-1}$. $^1H$ NMR (400 MHz, $CDCl_3$): δ 7.34-7.07 (m, 5H, Ph), 3.88 (dq, *J* = 10.0, 2.8 Hz, 1H, $CH_2$-2), 3.72 (ABq, *J* = 13.0, 12.7 Hz, 2H, $CH_2$-8), 2.79 – 2.64 (m, 2H, $CH_2$-4), 1.87 – 1.77 (m, 1H, CH-3), 1.03 (d, *J* = 6.5Hz, 3H, $CH_3$-6) 0.80 (d, *J* = 7.16 Hz, 3H, $CH_3$-5). $^{13}C$ NMR (101 MHz, $CDCl_3$): δ 139.4 (C-9), 129.0 (C-10), 128.5 (C-11), 127.2 (C-12), 72.0 (C-2), 54.3 (C-8), 53.4 (C-4), 37.5 (C-3), 18.8 (C-6), 12.7 (C-5). LRMS (ESI+) 194.3 (80%) [$M+H^+$], 194.8 (100%). HRMS (ESI+) calculated [$C_{12}H_{19}NO+H^+$] 194.1545 found, 194.1534.

3-(Benzylamine)-1-propan-1-ol. **67**

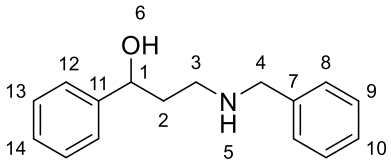

THF (7 mL), 3 Å molecular sieve pellets (2.5 g) were stirred under argon. Benzylamine (0.15 mL, 1.4 mmol) and *trans*-cinnamaldehyde (0.18 mL, 1.4 mmol) were added and stirred for 3 h. In a separate vessel, THF (4 mL), CuCl (6.93 mg, 0.07 mmol), $PPh_3$ (36.72 mg, 0.14 mmol) and NaO*t*-Bu (20.2 mg, 0.21 mmol) were stirred for 30 min. After 30 min, $B_2pin_2$ (0.39 g, 1.54 mmol) was added and stirred in the CuCl solution for 10 min. Both solutions were combined and stirred for a further 30 min, after which methanol was added (0.11 mL, 2.80 mmol) and stirred for 18 h. $NaBH_4$ (0.16 g, 4.20 mmol was added and the solution stirred. Methanol (3 mL) was added drop-wise over 10 min. After 3 h, all solvent was removed under reduced pressure. THF (10 mL), NaOH (0.60 mL, 20% w/v solution, 4 mmol), $H_2O_2$ (0.25 mL, 35% w/v solution, *ca.* 4 x $10^{-3}$ mol) was added to the resulting mass and refluxed for 1 h. The resulting solution was cooled and filtered through Celite, further EtOAc was passed through the Celite pad. The resulting solution was partitioned between EtOAc and brine. The aqueous layer was extracted further with EtOAc (3 x EtOAc). The organic phase was separated and dried over $MgSO_4$. After filtration the organic phase was removed under reduced pressure to yield a crude oil, which formed a white solid on standing. Purification by silica gel chromatography (hexane:EtOAc, 1% v/v $Et_3N$ in eluent and silica, 2:1 eluent) gave the product as a cloudy colourless oil (0.20 g, 58%). IR (neat) $\nu_{max}$: 3250, 3026, 2836, 1603, 1493, 1451, 1438, 1180, 733, 696 $cm^{-1}$. $^1H$ NMR (400 MHz, $CDCl_3$): δ 7.41- 7.09 (m, 10H, Ph), 4.88 (dd, *J* = 8.6, 3.0 Hz, 1H, CH-1), 3.74 (ABq, *J* = 13.0, 5.2 Hz, 2H, $CH_2$-4), 2.94 - 2.80 (m, 2H, $CH_2$-3), 1.88 – 1.67 (m, 2H, $CH_2$-2). $^{13}C$ NMR (101 MHz, $CDCl_3$): δ 145.0 (C-11), 139.2 (C-7), 132.2, 132.1, 131.9, 128.6, 128.4, 128.3, 75.6 (C-1), 53.9 (C-3), 47.8 (C-4), 37.4 (C-2). LRMS (ESI+) 242.6 (100%) $[M+H^+]$, 120.4 (65%). HRMS (ESI+) calculated $[C_{16}H_{19}NO+H^+]$ 242.1545, found

242.1550. All spectroscopic and analytical properties are identical with those reported in the literature.[61]

(*anti*)-3-(benzylamino)-2-methyl-1-phenylpropan-1-ol. **74**

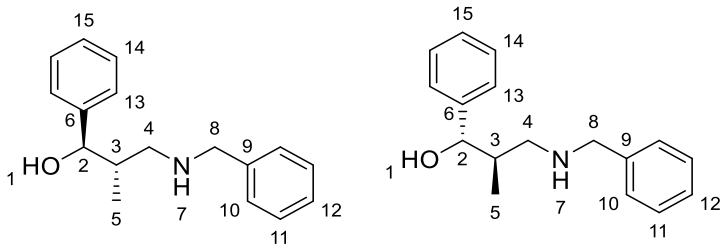


THF (6 mL), 3 Å molecular sieve pellets (2.5 g) were stirred under argon. Benzylamine (101 μL, 1.0 mmol) and α-methylcinnamaldehyde (140 μL, 1.0 mmol) were added and stirred for 7 h. In a separate vessel, THF (3 mL), CuCl (4.95 mg, 0.05 mmol), P*n*$Bu_3$ (24.7 μL, 0.10 mmol) and NaO*t*-Bu (14.4 mg, 0.15 mmol) were stirred for 30 min. After 30 min, $B_2pin_2$ (0.28 g, 1.1 mmol) was added and stirred in the CuCl solution for 10 min. Both solutions were combined and stirred for a further 30 min, after which methanol was added (81.0 μL, 2.0 mmol) and stirred for 18 h. $NaBH_4$ (0.11 g, 3.0 mmol was added and the solution stirred. Methanol (2 mL) was added drop-wise over 10 min. After 3 h, all solvent was removed under reduced pressure. THF (10 mL), NaOH (0.43 mL, 20% w/v solution, 2.86 mmol), $H_2O_2$ (0.18 mL, 35% w/v solution, *ca.* 2.86 mmol) was added to the resulting mass and refluxed for 1 h. The resulting solution was cooled and filtered through Celite, further EtOAc was passed through the Celite pad. The resulting solution was partitioned between EtOAc and brine. The aqueous layer was extracted further with EtOAc (3 x EtOAc). The organic phase was separated and dried over $MgSO_4$. After filtration the organic phase was removed under reduced pressure to yield a yellow oil. Purification by silica gel chromatography (hexane:EtOAc, 1% v/v $Et_3N$ in eluent and silica, 2:1 eluent) gave the product as a white solid (50 mg, 20%). IR

(neat) $\nu_{max}$: 3320, 3062, 2912, 2841, 1602, 1493, 1453, 1040 $cm^{-1}$. $^{1}H$ NMR (400 MHz, $CDCl_3$): δ 7.32-7.06 (m, 10H, Ph), 4.85 (d, *J* = 3.2 Hz, 1H, CH-2), 3.74 (ABq, *J* = 13.0, 10.9 Hz, 2H, $CH_2$-8), 2.76-2.64 (m, 2H, $CH_2$-4), 2.12-2.04 (m, 1H, CH-3), 0.67 (d, *J* = 7.2 Hz, 3H, $CH_3$-5). $^{13}C$ NMR (101 MHz, $CDCl_3$): δ 141.7 (C-6), 138.2 (C-9), 127.8, 127.4, 127.0, 126.9, 126.4, 126.1, 79.7 (C-2), 53.3 (C-8), 52.3 (C-4), 37.5 (C-3), 11.68 (C-5). LRMS (ESI+) 256.3 (100%) $[M+H^+]$, 161.4 (27%). HRMS (ESI+) calculated $[C_{17}H_{21}NO+H^+]$ 256.1701, found 256.1704.

3-(benzylamino)cyclohexan-1-ol (*syn*/*anti* mixture). **76**

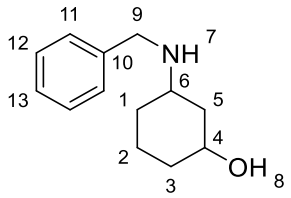


THF (12 mL), 3 Å molecular sieve pellets (3.6 g), CuCl (9.9 mg, 0.1 mmol), P*n*$Bu_3$ (49.3 μL, 0.2 mmol) and NaO*t*-Bu (28.8 mg, 0.3 mmol) were stirred for 30 min under argon. After 30 min, $B_2pin_2$ (0.56 g, 1.1 mmol) was added and stirred for 10 min. Benzylamine (0.22 mL, 2.0 mmol) and cyclohexenone (0.19, 2.0 mmol) was added and stirred for 30 min, after which, methanol was added (0.16 mL, 4.0 mmol) and the resulting solution was stirred for 18 h. $NaBH_4$ (0.23 g, 6.0 mmol was added and the solution stirred. Methanol (4 mL) was added drop-wise over 10 min. After 3 h, all solvent was removed under reduced pressure. THF (15 mL), NaOH (0.86 mL, 20% w/v solution, 5.72 mmol), $H_2O_2$ (0.36 mL, 35% w/v solution, *ca.* 5.72 mmol) was added to the resulting mass and refluxed for 1 h. The resulting solution was cooled and filtered through Celite, further EtOAc was passed through the Celite pad. The resulting solution was partitioned between EtOAc and brine. The aqueous layer was extracted further with

EtOAc (3 x EtOAc). The organic phase was separated and dried over $MgSO_4$. After filtration the organic phase was removed under reduced pressure to yield a dark yellow oil. Toluene (2 x 20 mL) was added to the crude oil and removed under pressure (this was repeated twice). After the toluene had been removed, purification by silica gel chromatography (EtOAc:MeOH, 1% v/v $Et_3N$ in eluent and silica, 9:1 eluent) gave the product as a yellow oil (0.21 g, 51% - mixture diastereoisomers 7:3 *d.r.*).[234] IR (neat) $\nu_{max}$: 3274, 2929, 2854, 1495, 1451, 1125, 1059 $cm^{-1}$. Major diastereoisomer reported: $^1H$ NMR (400 MHz, $CDCl_3$): δ 7.74-7.09 (m, 5H, Ph), 3.83-3.69 (m, 1H, CH-4), 3.81-3.69 (ABq, *J* = 32.2, 12.8 Hz, 2H, $CH_2$-9), 2.86-2.77 (m, 1H, CH-6), 1.91-1.79 (m, 1H), 1.82-1.67 (m, 2H), 1.69-1.46 (m, 4H), 1.47-1.33 (m, 2H), 1.34-1.16 (m, 1H). $^{13}C$ NMR (101 MHz, $CDCl_3$): δ 140.7 (C-10), 128.6 (C-11), 127.9 (C-12), 126.8 (C-13), 68.4 (C-4), 53.6, 51.2 (C-9), 34.3 (C-6), 33.7, 32.0, 31.6, 19.1. LRMS (ESI+) 206.2 (47%) [$M+H^+$], 108.5 (15%). HRMS (ESI+) calculated [$C_{13}H_{19}NO+H^+$] 206.1545, found 206.1533.

(*R*)-3-(Methylamino)-1-phenylpropan-1-ol. **143**

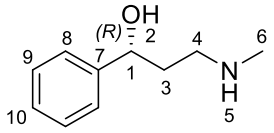


Benzhydrylamine (0.86 mL, 5.00 mmol) and *trans*-cinnamaldehyde **66** (0.63 mL, 5.00 mmol) was added to a stirring solution of THF (20 mL) and oven-dried 3 Å molecular sieve beads (5.0 g) for 6 h, to form the α,β-unsaturated imine **119** *in situ*. After 6 h, an aliquot of the solution containing the *in situ*-formed imine **119** (16.0 mL, 4.00 mmol) was transferred to a Schlenk-tube (under argon) containing CuCl (12.0 mg, 0.12 mmol), $PPh_3$ (62.9 mg, 0.24 mmol) or (*R*)-DM-BINAP (88.2 mg, 0.12 mmol), NaO*t*-Bu (34.6 mg, 0.36 mmol) and $B_2pin_2$ (1.12 g, 4.4 mmol). After 5 min, MeOH (400 μL, 10.0

mmol) was added to the solution and the reaction was stirred overnight. Methylamine (8 mL, 16.0 mmol, 2 M THF solution) was added under argon and the resulting solution was stirred for 1.5 h. $NaBH_4$ (0.46 g, 12.0 mmol) was added, followed by the drop-wise addition of MeOH (8.0 mL). The mixture was stirred for 3 h, followed by the removal of solvent under reduced pressure. THF (20 mL) was added to the resulting residue, followed by NaOH (2.4 mL, w/v 20%) and $H_2O_2$ (1.1 mL, w/v 35%), and the solution was heated to reflux for 1 h. After cooling, the resulting solution was partitioned between EtOAc and brine. The aqueous layer was extracted further with EtOAc (3 x EtOAc). The organic phase was separated and dried over $MgSO_4$. After filtration the organic phase was removed under reduced pressure to yield a crude product. Purification by silica gel chromatography (DCM → DCM:MeOH:$NEt_3$, 5:1:1%) gave the pure product as an off colourless oil, which formed an off colourless solid on standing [356 mg, 54% when using $PPh_3$ and 402 mg, 61% when using (*R*)-DM-BINAP; 96% *e.e.*]. $^1$H NMR (400 MHz, $CDCl_3$): δ 7.40-7.24 (m, 5H), 4.95 (dd, *J* = 8.7, 3.1 Hz, 1H, CH-1), 3.65-3.4 (bs, 1H, NH-5), 2.97-2.83 (m, 2H, $CH_2$-4), 2.46, (s, 3H, $CH_3$-6), 1.93-1.72 (m, 2H, $CH_2$-3); $^{13}$C NMR (101 MHz, $CDCl_3$): δ 145.0 (C-7), 128.2, 127.0, 125.6, 75.4 (C-1), 50.3 (C-4), 36.7 (C-6), 35.9 (C-3); LRMS (ESI+) 166.5 $[M+H]^+$; HRMS (ESI+) Calculated [$C_{10}H_{15}NO$+H] 166.1232, found 166.1228. All spectroscopic and analytical properties are identical with those reported in the literature.[223]

(*S*)-3-(Methylamino)-1-(thiophen-2-yl)propan-1-ol. **162**

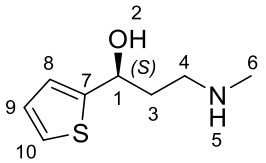

Benzhydrylamine (0.86 mL, 5.00 mmol) and (2*E*)-3-(thiophen-2-yl)prop-2-enal **156** (0.63 mL, 5.00 mmol) was added to a stirring solution of THF (20 mL) and oven-dried 3 Å molecular sieve beads (5.0 g) for 6 h, to form the α,β-unsaturated imine **158** *in situ*. After 6 h, an aliquot of the solution containing the *in situ*-formed imine **158** (12.0 mL, 3.0 mmol) was transferred to a Schlenk-tube (under argon) containing CuCl (9.0 mg, 0.09 mmol), $PPh_3$ (48.0 mg, 0.18 mmol) or (*S*)-DM-BINAP (66.1 mg, 0.09 mmol), NaO*t*-Bu (27.0 mg, 0.27 mmol) and $B_2pin_2$ (0.84 g, 3.3 mmol). After 5 min, MeOH (300 μL, 7.5 mmol) was added to the solution and the reaction was stirred overnight. Methylamine (6 mL, 12.0 mmol, 2 M THF solution) was added under argon and the resulting solution was stirred for 1.5 h. $NaBH_4$ (0.34 g, 9.0 mmol) was added, followed by the drop-wise addition of MeOH (6.0 mL). The mixture was stirred for 3 h, followed by the removal of solvent under reduced pressure. THF (15 mL) was added to the resulting residue, followed by NaOH (1.8 mL, w/v 20%) and $H_2O_2$ (0.84 mL, w/v 35%), and the solution was heated to reflux for 1 h. After cooling, the resulting solution was partitioned between EtOAc and brine. The aqueous layer was extracted further with EtOAc (3 x EtOAc). The organic phase was separated and dried over $MgSO_4$. After filtration the organic phase was removed under reduced pressure to yield a crude product. Purification by silica gel chromatography (DCM → DCM:MeOH:$NEt_3$, 5:1:1%) gave the pure product as an off colourless oil, which formed a pale yellow oil on standing **9b** [241 mg, 47% when using $PPh_3$ and 292 mg, 57% when using (*S*)-DM-BINAP; 94% *e.e.*]. $^1$H NMR (400 MHz, $CDCl_3$): δ 7.20 (dd, *J* = 5.0, 1.2 Hz, 1H, CH-8), 7.06 (dd , *J* = 5.0, 3.4, 1H, CH-10), 6.93-6.91 (m, 1H, CH-9), 5.19 (dd, *J* = 8.4, 3.2 Hz, 1H, CH-1), 4.68-4.32 (bs, 1H, NH-5), 3.02-2.83 (m, 2H, $CH_2$-4), 2.45 (s, 3H, $CH_3$-6), 2.05-1.86 (m, 2H, $CH_2$-3). $^{13}$C NMR (101 MHz, $CDCl_3$): δ 149.7 (C-7), 126.6 (C-10), 123.7 (C-9), 122.3 (C-8), 71.9 (C-1), 50.1 (C-4), 36.8 (C-6), 35.9 (C-3). LRMS (ESI+)

$[M+H]^+$, 171.9. HRMS (ESI+) calculated $[C_8H_{13}NOS+H]^+$ 172.0796, found 172.0829. All spectroscopic and analytical properties are identical with those reported in the literature.[232]

### 3.3.2 1,3-Oxazines

(*R*)-3-(Diphenylmethyl)-6-phenyl-1,3-oxazinane. **129**

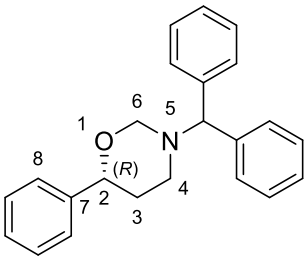


α,β-Unsaturated imine **119** was formed *in situ* from the reaction between benzhydrylamine (0.34 mL, 2.00 mmol) and cinnamaldehyde **66** (252 μL, 2.00 mmol), stirred in THF (8 mL) and oven-dried 3 Å molecular sieve beads (2.0 g) for 6-24 h. After 6-24 h, an aliquot of the solution containing the *in situ*-formed imine **2** (2.00 mL, 0.50 mmol) was transferred to a Schlenk-tube (under argon) containing CuCl (1.8 mg, 15 μmol), (*R*)-DM-BINAP (11.0 mg, 15 μmol), NaO*t*Bu (4.3 mg, 45 μmol) and $B_2pin_2$ (0.14 g, 0.55 mmol). After 5 min, MeOH (50 μL, 1.25 mmol) was added to the solution and the reaction was stirred overnight. $NaBH_4$ (57.0 mg, 1.50 mmol) was added, followed by the drop-wise addition of MeOH (1.0 mL). The mixture was stirred for 3h, with the addition THF (3.0 mL), NaOH (0.30 mL, w/v 20%) and $H_2O_2$ (0.13 mL, w/v 35%). The resulting solution was heated to reflux for 1 h. After cooling, formaldehyde solution (6.0 mmol, w/v 37%) was added, and the solution was stirred for 3h. The resulting solution was partitioned between EtOAc and brine. The aqueous layer was extracted with EtOAc (3 x EtOAc). The organic phase was separated and dried over

$MgSO_4$. After filtration the organic phase was removed under reduced pressure to yield a crude product. Purification by silica gel chromatography (hexane:EtOAc, eluent and silica, 5:1 eluent) gave the pure product as a white, highly insoluable solid (158 mg, 48%; 97% *e.e.*). *m.p.* 90-91 °C. IR (neat) $\nu_{max}$: 2921, 2858, 1492, 1179, 996, 698 $cm^{-1}$. $^1H$ NMR (400 MHz, $CDCl_3$): δ 7.50-7.07 (m, 15H, Ph), 5.08 (s, 1H, CH-5), 4.53 (d, *J* = 10.2 Hz, 1H, $CH_2$-4), 4.48 (d, *J* = 11.3 Hz, 1H, CH-1), 4.32 (d, *J* = 10.2 Hz, 1H, $CH_2$-4), 3.10-2.88 (m, 2H, $CH_2$-3), 2.05-1.95 (q, 1H, $CH_2$-3), 1.43-1.39 (d, *J* = 13.6 Hz, $CH_2$-3). $^{13}C$ NMR (101 MHz, $CDCl_3$): δ 142.7 (C-8), 142.6 (C-6), 142.5 (C-7), 128.7, 128.7, 128.4, 128.2, 127.8, 127.5, 127.2, 125.7, 83.0 (C-5), 79.5 (C-1), 68.1(C-4), 48.2 (C-3), 29.3 (C-2). LRMS (ESI+) 330.1 (100%) $[M+H]^+$, 167.3 (66%). HRMS (ESI+) calculated $[C_{23}H_{23}NO+H]^+$ 330.1858, found 330.1886. Anal. Calc. for $C_{23}H_{23}NO$ C, 83.85; H, 7.04; N, 4.25; found C, 84.02; H, 7.02; N, 4.08. Enantiomeric excess was determined by derivatisation to the analogous *O*/*N*-diacetate **135**. Absolute stereochemistry was confirmed by X-ray crystallography.

(*anti*)-3-Benzyl-4-methyl-6-phenyl-1, 3-oxazinane. **65**

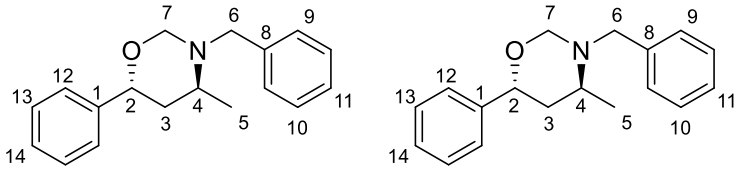


*Route A*

3-(Benzylamine)-1-phenylbutan-1-ol (0.22 g, 0.86 mmol) and formaldehyde solution (75 μL, 37% w/v solution, 1.00 mmol) was stirred in THF (6 mL) for 4.5 h. After 4.5 h, $MgSO_4$ was added, and the organic phase was filtered and removed under reduced

pressure to leave a crude oil. Purification by silica gel chromatography (hexane:EtOAc, 2:1 eluent) gave a colourless oil (0.17 g, 74%).

*Route B*

THF (7 mL), 3 Å molecular sieve pellets (2.5 g) were stirred under argon. Benzylamine (0.15 mL, 1.4 mmol) and (3*E*)-4-phenylbut-3-en-2-one (0.20 g, 1.4 mmol) were added and stirred for 3 h. In a separate vessel, THF (4 mL), CuCl (6.93 mg, 0.07 mmol), $PPh_3$ (36.72 mg, 0.14 mmol) and NaO*t*-Bu (20.2 mg, 0.21 mmol) were stirred for 30 min. After 30 min, $B_2pin_2$ (0.39 g, 1.54 mmol) was added and stirred in the CuCl solution for 10 min. Both solutions were combined and stirred for a further 30 min, after which methanol was added (0.11 mL, 2.80 mmol) and stirred for 18 h. $NaBH_4$ (0.16 g, 4.20 mmol was added and the solution stirred. Methanol (15 mL) was added drop-wise over 10 min. After 3 h, NaOH (4.8 mL, 20% w/v solution, 4 mmol), $H_2O_2$ (2.0 mL, 35% w/v solution, *ca.* 4 x $10^{-3}$ mol) was added drop-wise to the resulting mass and refluxed for 4 h. The resulting solution was cooled and filtered through Celite, further EtOAc was passed through the Celite pad. The resulting solution was partitioned between EtOAc and brine. The aqueous layer was extracted further with EtOAc (3 x EtOAc). The organic phase was separated and dried over $MgSO_4$. After filtration the organic phase was removed under reduced pressure to yield a crude yellow oil. Purification by silica gel chromatography (hexane:EtOAc, 3:1 eluent) gave the product as a colourless oil (0.18 g, 51%). IR (neat) $\nu_{max}$: 3027, 2996, 2859, 1602, 1494, 1452, 1363, 1207 (C-O), 988, 696 $cm^{-1}$. $^1$H NMR (400 MHz, $CDCl_3$): δ 7.40 - 7.10 (m, 10H, Ph), 4.48 (d, *J* = 10.0 Hz, 1H, $CH_2$-7), 4.48 (dd, *J* = 11.3, 2.8 Hz, 1H, CH-2), 4.23 (d, *J* = 10 Hz, 1H, $CH_2$-7), 3.93 (d, *J* = 13.6, 1H, $CH_2$-6), 3.61 (d, *J* = 13.6 Hz, 1H, $CH_2$-6), 3.21 (m, 1H, CH-4), 1.72 (dt, *J* = 13.4, 11.5 Hz, 1H, $CH_2$-3), 1.57 (dt, *J* = 13.4, 2.8 Hz, 1H, $CH_2$-3), 1.18 (d, *J* = 6.6 Hz, 3H, $CH_3$-5). $^{13}$C NMR (101 MHz, $CDCl_3$): δ 141.5 (C-1), 138.3 (C-

8), 128.0, 127.6, 127.4, 127.3, 126.5, 125.9, 124.8, 82.7 (C-7), 78.5 (C-2), 54.3 (C-6), 47.5 (C-4), 36.4 (C-3), 19.3 (C-5). LRMS (ASAP+) 268.2 (14%) [$M+H^+$], 148.1 (100%), 134.1 (38%). HRMS (TOF ASAP+) calculated [$C_{18}H_{21}NO+H^+$] 268.1701, found 268.1708. Anal. Calc. for $C_{18}H_{21}NO$ C, 80.86; H, 7.92; N, 5.24; found C, 79.29; H, 7.84; N, 4.56.

3-Benzyl-5-methyl-1,3-oxazinane. **70**

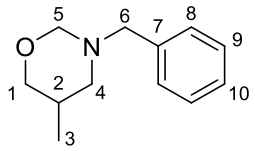


THF (7 mL), 3 Å molecular sieve pellets (2.5 g) were stirred under argon. Benzylamine (0.15 mL, 1.4 mmol) and methacrolein (0.12 mL, 1.4 mmol) were added and stirred for 3 h. In a separate vessel, THF (4 mL), CuCl (7.0 mg, 0.07 mmol), $PPh_3$ (37.0 mg, 0.14 mmol) and NaO*t*-Bu (20.2 mg, 0.21 mmol) were stirred for 30 min. After 30 min, $B_2pin_2$ (0.39g, 1.54 mmol) was added and stirred in the CuCl solution for 10 min. Both solutions were combined and stirred for a further 30 min, after which methanol was added (0.11 mL, 2.80 mmol) and stirred for 18 h. $NaBH_4$ (0.16 g, 4.20 mmol was added and the solution stirred. Methanol (3 mL) was added drop-wise over 10 min. After 3 h, all solvent was removed under reduced pressure. THF (10 mL), NaOH (0.60 mL, 20% w/v solution, 4 mmol), $H_2O_2$ (0.25 mL, 35% w/v solution, *ca.* 4 x $10^{-3}$ mol) was added to the resulting mass and refluxed for 1 h. The resulting solution was cooled and filtered through Celite, further EtOAc was passed through the Celite pad. The resulting solution was partitioned between EtOAc and brine. The aqueous layer was extracted further with EtOAc (3 x EtOAc). The organic phase was separated and dried over $MgSO_4$. After filtration the organic phase was removed under reduced pressure to yield a yellow oil. Toluene (2 x 20 mL) was added to the crude oil and removed under pressure (this was

repeated twice). After the toluene had been removed, THF (10 mL) and formaldehyde solution (0.12 mL, 37% w/v solution, 1.54 mmol) were sequentially added to the sample and the solution was stirred under argon overnight (15 h). $MgSO_4$ was added to the reaction, and the solution was filtered. The organics were removed under vacuum to yield a yellow oil. Purification by silica gel chromatography (hexane:EtOAc, 5:1 eluent) gave the product as a colourless oil (0.20g, 75%). IR (neat) $\nu_{max}$: 2953, 2850, 1453, 1017, 883, 698 $cm^{-1}$. $^1H$ NMR (400 MHz, $CDCl_3$): δ 7.34-7.13 (m, 5H, Ph), 4.35 (d, *J* = 9.6 Hz, 1H, $CH_2$-5), 4.03 (d, *J* = 9.6 Hz, 1H, $CH_2$-5), 3.92 (ddd, *J* = 10.9, 4.3, 1.7 Hz, 1H, $CH_2$-1) 3.75 (ABq, *J* = 13.4, 5.7 Hz, 2H, $CH_2$-6), 3.09 (t, *J* = 10.8 Hz, 1H, $CH_2$-1) 2.89-2.80 (m, 1H, $CH_2$-4), 2.29 (dd, *J* = 12.8, 11.2 Hz, 1H, $CH_2$-4), 2.18-2.04 (m, 1H, $CH_2$-2), 0.63 (d, *J* = 6.6 Hz, 3H, $CH_2$-2). $^{13}C$ NMR (101 MHz, $CDCl_3$): δ 138.6 (C-7), 128.9 (C-8), 128.3 (C-9), 127.1 (C-10), 84.2 (C-5), 74.3 (C-1), 57.2 (C-6), 56.2 (C-4), 25.9 (C-2), 14.7 (C-3). LRMS (ESI+) 192.5 (100%) [$M+H^+$], 180.5 (16%). HRMS (ESI+) calculated [$C_{12}H_{17}NO+H^+$] 192.1388, found 192.1368.

3-Benzyl-6-methyl-1,3-oxazinane. **79**

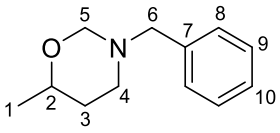


THF (6 mL), 3 Å molecular sieve pellets (1.8 g) were stirred under argon. Benzylamine (0.11 mL, 1.0 mmol) and crotonaldehyde (83 μL, 1.0 mmol) were added and stirred for 3 h. In a separate vessel, THF (3 mL), CuCl (4.95 mg, 0.05 mmol), P*n*$Bu_3$ (24.7 μL, 0.10 mmol) and NaO*t*-Bu (14.0 mg, 0.15 mmol) were stirred for 30 min. After 30 min, $B_2pin_2$ (0.28 g, 1.1 mmol) was added and stirred in the CuCl solution for 10 min. Both solutions were combined and stirred for a further 30 min, after which methanol was

added (81.0 μL, 2.0 mmol) and stirred for 18 h. $NaBH_4$ (0.11 g, 3.0 mmol was added and the solution stirred. Methanol (2 mL) was added drop-wise over 10 min. After 3 h, all solvent was removed under reduced pressure. THF (10 mL), NaOH (0.43 mL, 20% w/v solution, 2.86 mmol), $H_2O_2$ (0.18 mL, 35% w/v solution, *ca.* 2.86 mmol) was added to the resulting mass and refluxed for 1 h. The resulting solution was cooled and filtered through Celite, further EtOAc was passed through the Celite pad. The resulting solution was partitioned between EtOAc and brine. The aqueous layer was extracted further with EtOAc (3 x EtOAc). The organic phase was separated and dried over $MgSO_4$. After filtration the organic phase was removed under reduced pressure to yield a yellow oil. Toluene (2 x 20 mL) was added to the crude oil and removed under pressure (this was repeated twice). After the toluene had been removed, THF (8 mL) and formaldehyde solution (84 μL, 37% w/v solution, 1.1 mmol) were sequentially added to the sample and the solution was stirred under argon overnight (15 h). $MgSO_4$ was added to the reaction, and the solution was filtered. The organics were removed under vacuum to yield a yellow oil. Purification by silica gel chromatography (hexane:EtOAc, 5:1 eluent) gave the product as a colourless oil (0.10 g, 50%). IR (neat) $\nu_{max}$: 2967, 2931, 2853, 1495, 1453, 1082, 993, 735, 698 $cm^{-1}$. $^1H$ NMR (400 MHz, $CDCl_3$): δ 7.35-7.10 (m, 5H, Ph), 4.40 (dd, *J* = 9.7, 2.1 Hz, 1H, $CH_2$-5$_{axial}$) 4.15 (d, *J* = 9.6 Hz, 1H, $CH_2$-5$_{equatorial}$) 3.71 (s, 2H, CH-6), 3.58-3.47 (m, 1H, CH-2), 2.93-2.85 (m, 1H, $CH_{2-4}$), 2.70 (dd, *J* = 12.8, 3.2 Hz, 1H, $CH_2$-4), 1.73-1.62 (m, 1H, $CH_2$-3), 1.29-1.22 (m, 1H, $CH_2$-3), 1.16 (d, *J* = 6.2 Hz, 3H, $CH_3$-1). $^{13}C$ NMR (101 MHz, $CDCl_3$): δ 138.6 (C-7), 129.0 (C-8), 128.3 (C-9), 127.1 (C-10), 84.5 (C-5), 73.6 (C-2), 55.8 (C-6), 49.5 (C-4), 29.5 (C-3), 21.9 (C-1). LRMS (ESI+) 192.5 (100%) [$M+H^+$], 134.4 (13%). HRMS (ESI+) calculated [$C_{12}H_{17}NO+H^+$] 192.1388, found 192.1400.

3-Benzyl-4-methyl-octahydro-2H-1,3-benzoxazine**. 78**

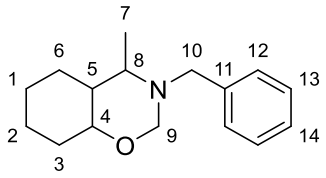


THF (12 mL), 3 Å molecular sieve pellets (3.6 g), CuCl (9.9 mg, 0.1 mmol), P*n*$Bu_3$ (49.3 μL, 0.2 mmol) and NaO*t*-Bu (28.8 mg, 0.3 mmol) were stirred for 30 min under argon. After 30 min, $B_2pin_2$ (0.56 g, 1.1 mmol) was added and stirred for 10 min. Benzylamine (0.22 mL, 2.0 mmol) and 1-Acetyl-1-cyclohexene (0.26, 2.0 mmol) was added and stirred for 30 min, after which, methanol was added (0.16 mL, 4.0 mmol) and the resulting solution was stirred for 18 h. $NaBH_4$ (0.23 g, 6.0 mmol was added and the solution stirred. Methanol (4 mL) was added drop-wise over 10 min. After 3 h, all solvent was removed under reduced pressure. THF (15 mL), NaOH (0.86 mL, 20% w/v solution, 5.72 mmol), $H_2O_2$ (0.36 mL, 35% w/v solution, *ca.* 5.72 mmol) was added to the resulting mass and refluxed for 1 h. The resulting solution was cooled and filtered through Celite, further EtOAc was passed through the Celite pad. The resulting solution was partitioned between EtOAc and brine. The aqueous layer was extracted further with EtOAc (3 x EtOAc). The organic phase was separated and dried over $MgSO_4$. After filtration the organic phase was removed under reduced pressure to yield a dark yellow oil. Toluene (2 x 20 mL) was added to the crude oil and removed under pressure (this was repeated twice). After the toluene had been removed, THF (15 mL) and formaldehyde solution (0.16 mL, 37% w/v solution, 2.1 mmol) were sequentially added to the sample and the solution was stirred under argon overnight (15 h). $MgSO_4$ was added to the reaction, and the solution was filtered. The organics were removed under vacuum to yield a yellow oil. Purification by silica gel chromatography (hexane:EtOAc, 12:1 eluent) gave the product as a colourless oil (0.21 g, 42%). IR (neat) $\nu_{max}$: 2932,

2850, 1494, 1445, 1215, 1099 $cm^{-1}$. $^{1}H$ NMR (400 MHz, $CDCl_3$): δ 7.32-7.11 (m, 5H, Ph), 4.33 (d, *J* = 8.4 Hz, 1H, $CH_2$-9), 3.84 (d, *J* = 14.3, 1H, $CH_2$-10), 3.72 (d, *J* = 8.4, 1H, $CH_2$-9), 3.52 (m, *J* = 2.5, 1H, CH-4), 3.17 (d, *J* = 14.3, 1H, $CH_2$-10), 2.63 (dq, *J* = 6.6, 4.0 Hz, 1H, $CH_3$-8), 1.86-1.78 (m, 1H), 1.77-1.68 (m, 2H), 1.57-1.44 (m, 2H), 1.42-1.35 (m, 2H), 1.27-1.20 (m, 1H). 1.15 (d, *J* = 6.6 Hz, $CH_3$-7). $^{13}C$ NMR (101 MHz, $CDCl_3$): δ 139.9 (C-11), 128.4 (C-12), 128.2 (C-13), 126.7 (C-14), 84.6 (C-9), 59.2 (C-4), 52.3 (C-8), 41.7 (C-5), 31.8, 25.8, 20.9, 20.8, 17.6 LRMS (ESI+) 247.6 (100%) [$M+H^+$], 102.4 (80%). HRMS (ESI+) calculated [$C_{16}H_{23}NO+H^+$] 246.1858, found 246.1852.

(*anti*)-3-Benzyl-5,6-dimethyl-1,3-oxazine**. 72**

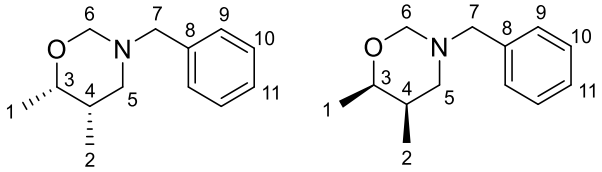


THF (7 mL), 3 Å molecular sieve pellets (2.5 g) were stirred under argon. Benzylamine (0.15 mL, 1.4 mmol) and tiglic aldehyde (0.14 mL, 1.4 mmol) were added and stirred for 3 h. In a separate vessel, THF (4 mL), CuCl (6.93 mg, 0.07 mmol), P*n*$Bu_3$ (34.5 μL, 0.14 mmol) and NaO*t*-Bu (20.2 mg, 0.21 mmol) were stirred for 30 min. After 30 min, $B_2pin_2$ (0.39g, 1.54 mmol) was added and stirred in the CuCl solution for 10 min. Both solutions were combined and stirred for a further 30 min, after which methanol was added (0.11 mL, 2.80 mmol) and stirred for 18 h. $NaBH_4$ (0.16 g, 4.20 mmol was added and the solution stirred. Methanol (3 mL) was added drop-wise over 10 min. After 3 h, all solvent was removed under reduced pressure. THF (10 mL), NaOH (0.60 mL, 20% w/v solution, 4 mmol), $H_2O_2$ (0.25 mL, 35% w/v solution, *ca.* 4 x $10^{-3}$ mol) was added to the resulting mass and refluxed for 1 h. The resulting solution was cooled and filtered

through Celite, further EtOAc was passed through the Celite pad. The resulting solution was partitioned between EtOAc and brine. The aqueous layer was extracted further with EtOAc (3 x EtOAc). The organic phase was separated and dried over $MgSO_4$. After filtration the organic phase was removed under reduced pressure to yield a yellow oil. Toluene (2 x 20 mL) was added to the crude oil and removed under pressure (this was repeated twice). After the toluene had been removed, THF (10 mL) and formaldehyde solution (0.12 mL, 37% w/v solution, 1.54 mmol) were sequentially added to the sample and the solution was stirred under argon overnight (15 h). $MgSO_4$ was added to the reaction, and the solution was filtered. The organics were removed under vacuum to yield a yellow oil. Purification by silica gel chromatography (hexane:EtOAc, 6:1 eluent) gave the product as a colourless oil (0.80g, 28%). IR (neat) $\nu_{max}$: 2976, 1496, 1244, 1107, 742 $cm^{-1}$. $^1H$ NMR (400 MHz, $CDCl_3$): δ 7.34-7.13 (m, 5H, Ph), 4.39 (dd, *J* = 8.3, 1.7 Hz, 1H, $CH_2$-6$_{axial}$), 3.77 (d, *J* = 8.3 Hz, 1H, $CH_2$-6$_{equatorial}$), 3.65 (dq, *J* = 6.6, 3.1 Hz, 1H, CH-3), 3.56 (d, *J* = 13.5 Hz, 1H, $CH_2$-7), 3.39 (d, *J* = 13.5 Hz, 1H, $CH_2$-7), 2.71 (ddd, *J* = 11.8, 3.8, 1.7 Hz, 1H, $CH_2$-5$_{equatorial}$) 2.39 (dd, *J* = 11.8, 3.5 Hz, 1H $CH_2$-5$_{axial}$), 1.66-1.56 (m, 1H, CH-4), 1.1 (d, *J* = 6.6 Hz, 3H, $CH_3$-1), 0.99 (d, *J* = 7.0 Hz, 3H, $CH_3$-2). $^{13}C$ NMR (101 MHz, $CDCl_3$): δ 138.4 (C-8), 128.6 (C-9), 128.3 (C-10), 127.0 (C-11), 84.6 (C-6), 75.3 (C-3), 57.3 (C-5), 57.2 (C-7), 32.5 (C-5), 17.3 (C-1), 12.8 (C-2. LRMS (ESI+) 206.5 (73%) [$M+H^+$], 194.1 (47%). HRMS (ESI+) calculated [$C_{13}H_{19}NO+H^+$] 206.1545, found 206.1549.

### 3.3.3 *O*/*N*-Diacetates

(*R*)-3-[*N*-(Diphenylmethyl)acetamido]-1-phenylpropyl acetate. **135**

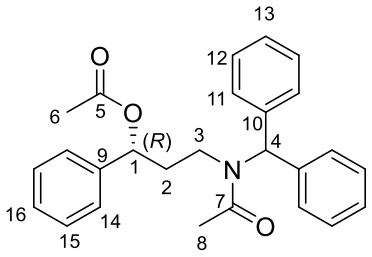


3-[(Diphenylmethyl)amino]-1-phenylpropan-1-ol **128** (79 mg, 0.25 mmol), pyridine (0.5 mL, 6.2 mmol) and acetic anhydride (0.5 mL, 5.3 mmol), were combined in DCM (3.0 mL) and stirred overnight. The resulting solution was diluted in DCM (10.0 mL) and was washed with HCl (3 x 10 mL, w/v 20%) and water (3 x). The organic layer was separated and dried over $MgSO_4$. Filtration followed by the removal of solvent under vacuum yielded a crude off-colourless solid, which was further purified by silica gel chromatography (hexane:EtOAc, eluent and silica, 2:1 eluent) to give the product pure product as a colourless viscous oil (88.3 mg, 88%). IR (neat) $\nu_{max}$: 3030, 2958, 1732, 1644, 1410, 1231, 1028, 697 $cm^{-1}$. $^1H$ NMR (400 MHz, $CDCl_3$) observed as a mixture of rotamers, major rotamer: δ 7.40-6.85 (m, 15H, Ph), 6.13 (s, 1H, CH-4), 5.38-5.18 (m, 1H, CH-1), 3.40-3.09 (m, 2H, $CH_2$-3), 2.09 (s, 3H, $CH_3$-6), 1.89 (s, 3H, $CH_3$-8), 1.51-1.27 (m, 2H, $CH_2$-2). $^{13}C$ NMR (101 MHz, $CDCl_3$): δ170.0 (C-5), 169.6 (C-7), 138.9 (C-9), 138.3 (C-10), 138.0, 128.1, 127.6, 127.5, 127.5, 127.5, 127.2, 127.1, 126.6, 126.4, 125.1, 73.0 (C-1), 64.9 (C-4), 59.6 (C-3), 40.5 (C-6), 33.1 (C-8), 21.3 (C-2). LRMS (ESI+) 402.2 (74%) $[M+H]^+$, 342.2 (100%), 167.1 (56%). HRMS (ESI+) calculated $[C_{26}H_{26}NO_3+H]^+$ 402.2069, found 402.2077. Enantiomeric excess was determined by HPLC using an OD-CHIRALCEL column (250 x 4.6 mm) fitted with guard cartridge (50 x 4.6 mm), 25 $^oC$, 1.0 mL/min, 210 nm, hexane : IPA (90 : 10). $t_R$

(*R*) = 15.1 min; $t_R$ (*S*) = 18.1 min. Absolute stereochemistry determined by preparation of the analogous oxazine **129** and X-ray crystallography of that compound.

(*R*)-3-[*N*-(Diphenylmethyl)acetamido]-1-(4-methoxyphenyl)propyl acetate. **136**

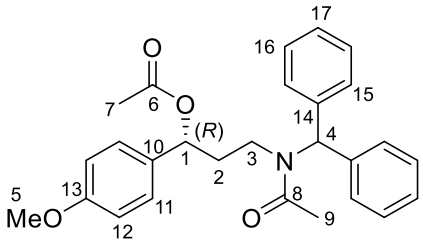


3-[(Diphenylmethyl)amino]-1-(4-methoxyphenyl)propan-1-ol **130** (157 mg, 0.45 mmol), pyridine (0.5 mL, 6.2 mmol) and acetic anhydride (0.5 mL, 5.3 mmol), were combined in DCM (3.0 mL) and stirred overnight. The resulting solution was diluted in DCM (10.0 mL) and was washed with HCl (3 x 10 mL, w/v 20%) and water (3 x water). The organic layer was separated and dried over $MgSO_4$. Filtration followed by the removal of solvent under vacuum yielded a crude off-colourless solid, which was further purified by silica gel chromatography (hexane:EtOAc, eluent and silica, 2:1 eluent) to give the product pure product as a colourless viscous oil (60.2 mg, 31%). IR (neat) $\nu_{max}$: 3027, 1732, 1641, 1541, 1233, 1176, 1030, 730 $cm^{-1}$. $^1H$ NMR (400 MHz, $CDCl_3$) observed as a mixture of rotamers, major rotamer: δ 7.37-7.33 (m, 10H, Ph), 6.88 (d, *J* = 8 Hz, 2H, CH-12), 6.68 (d, *J* = 8 Hz, 2H, CH-11), 6.13 (s, 1H, CH-4), 5.32-5.18 (m, 1H, CH-1), 3.68 (s, 3H, $CH_3$-5), 3.35-3.08 (m, 2H, $CH_2$-3), 2.08 (s, 3H, $CH_3$-7), 1.85 (s, 3H, $CH_3$-9), 1.60-1.28 (m, 2H, $CH_2$-2). $^{13}C$ NMR (101 MHz, $CDCl_3$): δ 171.1 (C-6), 170.1 (C-8), 159.1 (C-13), 141.6 (C-10), 139.5, 139.3, 132.0, 128.8, 128.7, 128.6, 128.6, 128.0, 127.7, 127.5, 127.4, 113.9, 73.8 (C-1), 66.0 (C-4), 57.0 (C-3), 41.6 (C-7), 35.9 (C-9), 23.4 (C-2). LRMS (ESI+) 432.2 (40%) $[M+H]^+$, 328.9 (54%). HRMS (ESI+) calculated $[C_{27}H_{29}NO_4+H]^+$ 432.2175, found 432.2154. Enantiomeric excess was

determined by HPLC using an AD-CHIRALCEL column (250 x 4.6 mm) fitted with guard cartridge (50 x 4.6 mm), 25 $^{o}$C, 1.0 mL/min, 210 nm, hexane : IPA (75 : 25). $t_R$ (*R*) = 8.7 min; $t_R$ (*S*) = 12.9 min.

(*R*)-1-(4-Chlorophenyl)-3-[*N*-diphenylmethyl)acetamido]propyl acetate. **137**

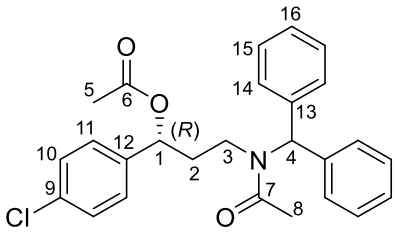


1-(4-Chlorophenyl)-3-[(diphenylmethyl)amino]propan-1-ol **131** (126 mg, 0.36 mmol), pyridine (0.5 mL, 6.2 mmol) and acetic anhydride (0.5 mL, 5.3 mmol), were combined in DCM (3.0 mL) and stirred overnight. The resulting solution was diluted in DCM (10.0 mL) and was washed with HCl (3 x 10 mL, w/v 20%) and water (3 x water). The organic layer was separated and dried over $MgSO_4$. Filtration followed by the removal of solvent under vacuum yielded a crude off-colourless solid, which was further purified by silica gel chromatography (hexane:EtOAc, eluent and silica, 2:1 eluent) to give the product pure product as a colourless viscous oil (70.6 mg, 45%). IR (neat) $\nu_{max}$: 3028, 1735, 1644, 1411, 1230, 1014, 733 cm$^{-1}$. $^{1}$H NMR (400 MHz, $CDCl_3$) observed as a mixture of rotamers, major rotamer: δ 7.31-6.81 (m, 14H, Ph), 6.13 (s, 1H, CH-4), 5.30-5.19 (m, 1H, CH-1), 3.35-3.14 (m, 2H, $CH_2$-3), 2.09 (s, 3H, $CH_3$-5), 1.89 (s, 3H, $CH_3$-8), 1.54-1.23 (m, 2H, $CH_2$-2). $^{13}$C NMR (101 MHz, $CDCl_3$): δ 171.1 (C-6), 170.0 (C-7), 139.0 (C-9), 138.9, 133.4, 129.2, 128.8, 128.7, 128.7, 128.6, 128.5, 128.5, 128.0, 127.5, 73.4 (C-1), 65.9 (C-4), 60.7 (C-3), 41.3 (C-5), 34.0 (C-8), 22.3 (C-2). LRMS (ESI+) 436.0 (40%) $[M+H]^+$, 376.1 (100%). HRMS (ESI+) calculated $[C_{26}H_{26}NO_3Cl+H]^+$ 436.16740, found 436.16806. *e.e.* was determined by HPLC using an AD-CHIRALCEL

column (250 x 4.6 mm) fitted with guard cartridge (50 x 4.6 mm), 25 $^{o}$C, 1.0 mL/min, 210 nm, hexane : IPA (85 : 15). $t_R$ (*R*) = 11.2 min; $t_R$ (*S*) = 15.1 min.

(*S*)-1-[*N*-(Diphenylmethyl)acetamido]hexan-3-yl acetate. **138**

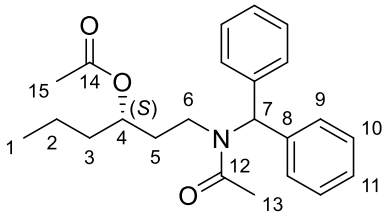


1-[(Diphenylmethyl)amino]hexan-3-ol **132** (85 mg, 0.30 mmol), pyridine (0.5 mL, 6.2 mmol) and acetic anhydride (0.5 mL, 5.3 mmol), were combined in DCM (3.0 mL) and stirred overnight. The resulting solution was diluted in DCM (10.0 mL) and was washed with HCl (3 x 10 mL, w/v 20%) and water (3 x water). The organic layer was separated and dried over $MgSO_4$. Filtration followed by the removal of solvent under vacuum yielded a crude off-colourless solid, which was purified by silica gel chromatography (hexane:EtOAc, eluent and silica, 2:1 eluent) to give the product pure product as a colourless viscous oil (59.5 mg, 70%). IR (neat) $\nu_{max}$: 2958, 2873, 1731, 1644, 1238, 1022, 732, 698 cm$^{-1}$. $^{1}$H NMR (400 MHz, $CDCl_3$) observed as a mixture of rotamers, major rotamer: δ 7.32-7.00 (m, 10H, Ph), 6.14 (s, 1H, CH-7), 4.51-4.35 (m, 1H, CH-4), 3.33-3.14 (m, 2H, $CH_2$-6), 2.10 (s, 3H, $CH_3$-15), 1.84 (s, 3H, $CH_3$-13), 1.31-1.15 (m, 2H, $CH_2$-5), 1.15-1.06 (m, 2H, $CH_2$-3),1.06-0.80 (m, 2H, $CH_2$-2), 0.71(t, *J* = 7.2 Hz, 3H, $CH_3$-1). $^{13}$C NMR (101 MHz, $CDCl_3$): δ 171.1, 170.6, 139.7, 139.1, 129.3, 128.7, 128.6, 128.5, 128.0, 127.9, 72.3, 72.0, 66.0, 41.4, 35.8, 32.0, 22.3, 21.7, 18.3. LRMS (ESI+) 368.1 (17%) $[M+H]^+$, 167.0 (19%). HRMS (ESI+) calculated $[C_{23}H_{29}NO_3+H]^+$ 368.2226, found 368.2202. Enantiomeric excess was determined by HPLC using an AS-H-CHIRALCEL column (250 x 4.6 mm) fitted with guard cartridge (50 x 4.6 mm), 25

$^{o}$C, 1.0 mL/min, 210 nm, hexane : IPA (90 : 10). $t_R$ (*S*) = 12.3 min; $t_R$ (*R*) = 14.7 min.

(*S*)-1-[*N*-(Diphenylmethyl)acetamido]pentan-3-yl acetate. **139**

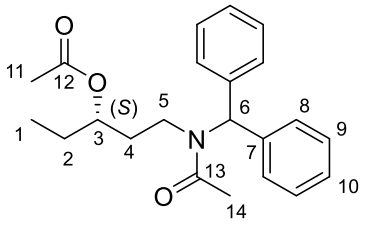


1-[(Diphenylmethyl)amino]pentan-3-ol **133** (56.5 mg, 0.21 mmol), pyridine (0.5 mL, 6.2 mmol) and acetic anhydride (0.5 mL, 5.3 mmol), were combined in DCM (3.0 mL) and stirred overnight. The resulting solution was diluted in DCM (10.0 mL) and was washed with HCl (3 x 10 mL, w/v 20%) and water (3 x). The organic layer was separated and dried over $MgSO_4$. Filtration followed by the removal of solvent under vacuum yielded a crude off-colourless solid, which was further purified by silica gel chromatography (hexane:EtOAc, eluent and silica, 2:1 eluent) to give the product pure product as a colourless viscous oil (63.6 mg, 84%). IR (neat) $\nu_{max}$: 2967, 1734, 1636, 1411, 1239, 1030, 730, 698 cm$^{-1}$. $^{1}$H NMR (400 MHz, $CDCl_3$) observed as a mixture of rotamers, major rotamer: δ 7.34-7.03 (m, 10H, Ph), 6.14 (s, 1H, CH-6), 4.42-4.30 (m, 1H, $CH_2$-5), 3.36-3.15 (m, 2H, $CH_2$-5), 2.10 (s, 3H, $CH_3$-11), 1.85 (s, 3H, $CH_3$-13), 1.28-1.17 (m, 2H, CH-4), 1.16-1.03 (m, 2H, $CH_2$-2), 0.57 (t, *J* = 7.4 Hz, 3H, $CH_3$-1). $^{13}$C NMR (101 MHz, $CDCl_3$): δ 170.7 (C-12), 170.7 (C-13), 139.1 (C-7), 139.0, 128.8, 128.7, 128.6, 128.5, 128.5, 128.0, 73.7 (C-3), 66.0 (C-6), 60.6, (C-11) 41.4 (C-13), 31.5 (C-4), 26.6 (C-2), 21.7 (C-1). LRMS (ESI+) 354.2 (72%) $[M+H]^+$, 167. (88%). HRMS (ESI+) calculated $[C_{22}H_{27}NO_3+H]^+$ 354.20637, found 354.20677. Enantiomeric excess was determined by HPLC using an AS-H-CHIRALCEL column (250 x 4.6 mm) fitted

with guard cartridge (50 x 4.6 mm), 25 $^{o}$C, 1.0 mL/min, 210 nm, hexane : IPA (90 : 10). $t_R$ (*S*) = 13.2 min; $t_R$ (*R*) = 17.2 min.

(*S*)-4-[*N*-(Diphenylmethyl)acetamido]butan-2-yl acetate. **140**

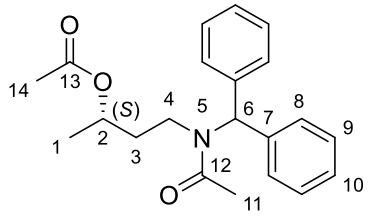


1-[(Diphenylmethyl)amino]butan-2-ol **134** (103 mg, 0.40 mmol), pyridine (0.5 mL, 6.2 mmol) and acetic anhydride (0.5 mL, 5.3 mmol), were combined in DCM (3.0 mL) and stirred overnight. The resulting solution was diluted in DCM (10.0 mL) and was washed with HCl (3 x 10 mL, w/v 20%) and water (3 x). The organic layer was separated and dried over $MgSO_4$. Filtration followed by the removal of solvent under vacuum yielded a crude off-colourless solid, which was further purified by silica gel chromatography (hexane:EtOAc, eluent and silica, 2:1 eluent) to give the product pure product as a colourless viscous oil (67.9 mg, 51%). IR (neat) $\nu_{max}$: 2979, 1731, 1640, 1412, 1241, 733, 698 cm$^{-1}$. $^{1}$H NMR (400 MHz, $CDCl_3$) observed as a mixture of rotamers, major rotamer: δ 7.32-7.04 (m, 10H, Ph), 6.15 (s, 1H, CH-6), 4.53-4.41 (m, 1H, CH-2), 3.36-3.15 (m, 2H, $CH_2$-4), 2.10 (s, 3H, $CH_3$-14), 1.83 (s, 3H, $CH_3$-11), 1.21-1.10 (m, 2H, $CH_2$-3), 0.85 (t, *J* = 6.4 Hz, 3H, $CH_3$-1). $^{13}$C NMR (101 MHz, $CDCl_3$): δ 170.7 (C-13), 170.4 (C-12), 139.6, 139.1, 129.2, 129.1, 128.7, 128.7, 128.5, 128.0, 69.2 (C-2), 66.0 (C-6), 56.97 (C-14), 41.4 (C-11), 33.9 (C-3), 21.7 (C-1). LRMS (ESI+) 362.1 (41%) $[M+Na]^+$ HRMS (ESI+) calculated $[C_{21}H_{25}NO+H]^+$ 340.1913, found 340.1905. Enantiomeric excess was determined by HPLC using an AS-H-CHIRALCEL column

(250 x 4.6 mm) fitted with guard cartridge (50 x 4.6 mm), 25 $^{o}$C, 1.0 mL/min, 210 nm, hexane : IPA (90 : 10). $t_R$ (*S*) = 20.9 min; $t_R$ (*R*) = 27.7 min.

### 3.3.4 Other

(*S*)-3-(Tetramethyl-1,3,2-dioxaborolan-2-yl)hexenal. **142**

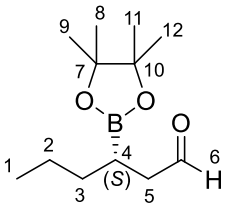


Optimised methodology for synthesis of **142** in 87% enantiomeric excess. α,β-Unsaturated imine **124** was formed *in situ* from the reaction between benzhydrylamine (345 µL, 2.00 mmol) and *trans*-2-hexenal **116** (232 µL, 2.00 mmol), stirred in THF (8 mL) and oven-dried 3 Å molecular sieve beads (2.0 g) for 6 h. After 6 h, an aliquot of the solution containing the *in situ*-formed imine **124** (2.00 mL, 0.50 mmol) was transferred to a Schlenk-tube (under argon) containing CuCl (1.8 mg, 15 µmol), (*R*)-DM-BINAP (11.0 mg, 15 µmol), NaO*t*Bu (4.3 mg, 45 µmol) and $B_2pin_2$ (0.14 g, 0.55 mmol). After 5 min, MeOH (50 µL, 1.25 mmol) was added to the solution and the reaction was stirred overnight. Afterwards, $H_2O$ (4 mL) was added to the solution and stirred for 1 h. The resulting solution was partitioned between EtOAc and brine. The aqueous layer was extracted further with EtOAc (3 x EtOAc). The organic phase was separated and dried over $MgSO_4$. After filtration the organic phase was removed under reduced pressure to yield a crude product. Purification by silica gel chromatography (hexane:EtOAc, eluent and silica, 8:1 eluent) gave the pure product as colourless oil (104.0 mg, 92%; 87% *e.e.*). IR (neat) $\nu_{max}$: 2976, 2927, 1722, 1466, 1379, 1315, 1143, 967 cm$^{-1}$. $^1$H NMR (400 MHz, $CDCl_3$): δ 9.69 (s, 1H, CH-6), 2.57-2.39 (m, 2H, $CH_2$-5), 1.43-1.33 (m, 1H, CH-4) 1.31-1.20 (m, 4H, CH-2/3), 1.18 (s. 6H, $CH_3$-

9/11), 1.16 (s, 6H, $CH_3$-8/12), 0.82 (t, $J$ = 6.8 Hz, 3H, $CH_2$-1). $^{13}$C NMR (101 MHz, $CDCl_3$): δ 203.0 (C-6), 83.2 (C-10/7), 45.8 (C-5), 32.7 (C-6), 24.7 (C-4), 24.6 (C-3), 21.9 (C-2), 14.2 (C-1). $^{11}$B NMR (128 MHz, $CDCl_3$): δ 34.1. LRMS (ESI+) 249.1 (74%) $[M+Na]^+$. HRMS (ESI+) calculated $[C_{12}H_{23}BO_3+H]^+$ 249.1639, found 249.1639. All spectroscopic and analytical properties are identical with those reported in the literature.[235]

(*E*)-Benzyl(2-methylprop-2-en-1-ylidene)amine. **58**

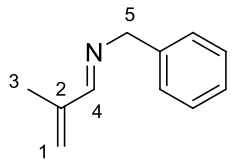


Methacrolein (1.00 mL, 12.15 mmol) and benzylamine (1.43 mL, 13.37 mmol) were weighed out under inert atmosphere and injected into a flask containing 3 Å molecular sieves (beads, 5 g) and dry THF (50 mL). The solution was stirred under argon for 16 h and the resulting solution was filtered over celite. The solvent removed under reduced pressure, after which purification was achieved using Kügelrohr distillation (15 mbar, 117-127 $^{o}$C). This yielded a colourless oil (0.65 g, 34%). IR (neat) $\nu_{max}$: 3027, 2838, 1640 ($C=N_{asym}$), 1618 ($C=N_{sym}$), 1496 (C=C), 1452, 1356, 1156, 1029, 908, 854, 732, 696, 616 cm$^{-1}$. $^1$H NMR (400 MHz, $CDCl_3$): δ 7.95 (s, 1H, CHN-4), 7.36-7.08 (m, 5H, Ph), 5.55 (s, 1H, $CH_2$-$1_{(E)}$), 5.34 (s, 1H, $CH_2$-$1_{(Z)}$), 4.64 (s, 2H,$CH_2$-5), 1.90 (s, 3H, $CH_3$-3). $^{13}$C NMR (101 MHz, $CDCl_3$): δ 165.01, 143.87, 139.44, 128.42, 127.86, 126.89, 124.30, 64.64, 17.14. LRMS (GC EI) 159.1 (18 %) [$M^+$], 91.0 (100 %), 82.1 (4 %), 65.1 (24 %), 51.1 (7%), 39.1 (22 %). HRMS (TOF ASAP+) calculated [$C_{11}H_{13}N+H^+$] 160.1126, found 160.1139. All spectroscopic observations were as reported in the literature.[131]

(*E*)-Benzyl[(2*E*)-but-2-en-1-ylidene]amine. **56**

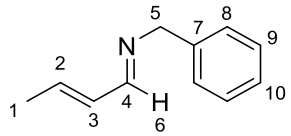


Benzylamine (3.37 mL, 30.95 mmol) and potassium carbonate (1.50 g, 22.00 mmol) was added to flask of dry THF (10 mL) under argon. The reaction mixture was cooled to -10 $^{o}$C and stirred for 15 min. Crotonaldehyde (2.57 mL, 30.95 mmol) was added and the solution and stirred for a further 1 h at 263 $^{o}$C, and then allowed to warm to ambient temperature for a further 3 h. The mixture was filtered and the solvent removed under reduced pressure. Kugelrohr distillation (10 mbar, 70 - 80 $^{o}$C) gave off the first fraction, followed by a pale yellow oil (0.35 g, 7%). $^{1}$H NMR (400 MHz, $CDCl_3$): δ 7.89 (d, *J* = 8 Hz, 1H, CH-6), 7.43 – 7.00 (m, 5H, Ph), 6.27-6.10 (m, 2H, CHCH-2/3), 4.54 (s, 2H, $CH_2$-5), 1.82 (d, *J* = 6 Hz, 3H, $CH_3$-1). All spectroscopic and analytical properties are identical with those reported in the literature.[131]

(*E*)-Benzyl[(2*E*)-2-methylbut-2-en-1-ylidene]amine. **57**

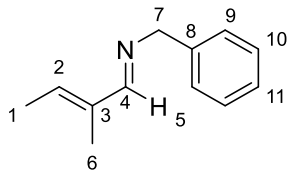


Tiglic aldehyde (0.29 mL, 2.97 mmol) and benzylamine (0.33 mL, 2.97 mmol) were added to a flask containing 3 Å molecular sieve beads (15 g) and dry THF (20 mL). The solution was stirred under argon for 16 h and the resulting solution was filtered over celite. The solvent removed under reduced pressure, after which purification was achieved using Kügelrohr distillation (10 mbar, over a temperature range of 143 to 150 $^{o}$C) to yield a colourless oil (0.11 g, 21%). $^{1}$H NMR (400 MHz,

$CDCl_3$): δ 7.88 (s, 1H, CHN-5), 7.31-7.18 (m, 5H, Ph), 6.07 (q, *J* = 7 Hz, 1H, CH-2), 4.64 (s, 2H, $CH_2$-7), 1.88 (s, 3H, $CH_3$-6), 1.81 (d, *J* = 7 Hz, 3H, $CH_3$-1). $^{13}$C NMR (101 MHz, $CDCl_3$): δ 166.7 (C-4), 139.9 (C-2), 136.9 (C-8), 136.7 (C-3), 128.4 (C-9), 127.8 (C-10), 126.8 (C-11), 64.6 (C-7), 14.2 (C-6), 11.32 (C-1). All spectroscopic and analytical properties are identical with those reported in the literature.[131]

(*E*)-Benzyl[(3*E*)-4-phenylbut-3-en-2-ylidene]amine. **62**

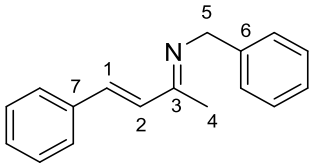


(*E*)-4-Phenyl-3-buten-2-one (1.50 g, 10.27 mmol) and benzylamine (1.25 mL, 11.30 mmol) were added to a flask containing 3 Å molecular sieve beads (5 g) and dry THF (15 mL). The solution was stirred under argon for 16 h and the resulting solution was filtered over Celite. The solvent removed under reduced pressure, after which purification was achieved using Kügelrohr distillation (10 mbar, over a temperature range of 143 - 150 $^{o}$C) to yield a yellow oil (0.53 g, 22%). $^1$H NMR (400 MHz, $CDCl_3$): δ 7.50 – 7.17 (m, 10H, Ph), 7.45 (d, *J* = 16 Hz, 1H, CH-1), 6.65 (d, *J* = 16 Hz, 1H, CH-2), 3.80 (s, 2H, $CH_2$-5), 2.30 (s, 3H, $CH_3$-4). All spectroscopic and analytical properties are identical with those reported in the literature.[64]

(*E*)-(Diphenylmethyl)[(2*E*)-3-phenylprop-2-en-1-ylidene]amine **119**

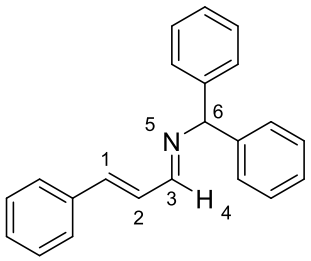


Crystallisation of **119** was achieved by dissolving **119** in IPA:toluene (20:1) and allowing for slow evaporation through a capillary tube (fitted in the top of a sealed vial). This resulted in the formation of pale yellow, crystalline needles with the following properties: $^{1}$H NMR (400 MHz, $CDCl_3$): δ 8.22 (d, *J* = 8.4 Hz, 1H, CH-4), 7.53-7.21 (m, 15H, Ph), 7.10 (unsymmet. dd, *J* = 16.0, 8.4 Hz, 1H, CH-2), 7.00 (unsymmet. d, *J* = 16.0 Hz, 1H, CH-1), 5.52 (s, 1H, CH-6). $^{13}$C NMR (101 MHz, $CDCl_3$): δ 162.9 (C-3), 143.6, 142.4, 135.7 (C-1), 129.2, 128.8, 128.5, 128.4, 127.7, 127.3, 127.0, 78.2 (C-6). LRMS (ESI+) 298.2 (99%) $[M]^+$; HRMS (ESI+) Calculated $[C_{22}H_{19}N+H]^+$ 298.1596, found 298.1583. X-ray crystallography was used to confirm this structure. All spectroscopic and analytical properties are identical with those reported in the literature.[236]

(*R*)-(+)-*N*-Methyl-3-phenyl-3-[4-(trifluoromethyl)phenoxy]propan-1-amine

(**Fluoxetine**).

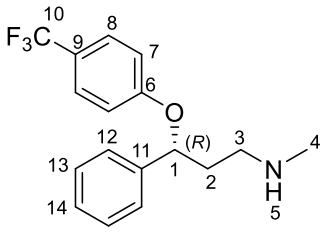


3-(Methylamino)-1-phenylpropan-1-ol **143** (330 mg, 2.00 mmol) was dissolved in dry dimethylacetamide (2.8 mL) and transferred to an oven-dried Schlenk-tube and purged with Argon. NaH (100 mg, 2.2 mmol, 60% in mineral oil) was transferred directly to the

solution and heated (70 °C) under Argon for 30-40 min, or until hydrogen evolution had ceased. 4-Chlorobenzotrifluoride (354 µL, 2.4 mmol) was added under argon, and the resulting solution was heated (100 °C) for 3 h. On cooling, the solution was partitioned between toluene and $H_2O$ and washed (3x $H_2O$). The organic phase was separated and dried over $MgSO_4$. After filtration the organic phase was removed under reduced pressure to yield a crude product. Purification by silica gel chromatography (DCM → DCM:MeOH:$NEt_3$, 5:1:1%) gave the pure product as a yellow oil **154**, (458 mg, 74%; 96% *e.e.*). $^1$H NMR (400 MHz, $CDCl_3$): δ 7.43 (d, *J* = 8.6 Hz, 2H, CH-8), 7.39-7.24 (m, 5H, Ph), 6.90 (d, *J* = 8.6 Hz, 2H, CH-7), 5.31 (dd, *J* = 8.2, 4.7 Hz, 1H, CH-1), 2.79-2.69 (m, 2H, $CH_2$-3), 2.43, (s, 3H, $CH_3$-4), 2.26-1.95 (m, 2H, $CH_2$-2). $^{13}$C NMR (101 MHz, $CDCl_3$): δ 160.5 (C-10), 141.0 (C-6), 128.8 (C-9), 127.9, 126.8, 126.7, 125.8, 115.8, 78.6 (C-1), 48.2 (C-3), 38.6 (C-4), 29.7 (C-2). LRMS (ESI+) 309.3 (57%) $[M]^+$; HRMS (ESI+) Calculated $[C_{17}H_{18}NOF_3+H]^+$ 310.1419, found 310.1411. $[\alpha]_D^{22}$ = +3.5 (1.0, $HCCl_3$) for the (*R*)-Fluoxetine in 96% *e.e.* Enantiomeric excess was determined by derivatisation to the analogous acetate **152**. All spectroscopic and analytical properties are identical with those reported in the literature.[223]

(*S*)-(+)-Methyl[3-(naphthalene-1-yloxy)-3-(thiophen-2-yl)propyl]amine (**Duloxetine**).

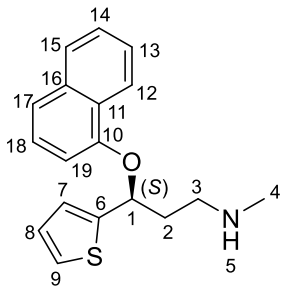


3-(Methylamino)-1-(thiophen-2-yl)propan-1-ol **162** (150 mg, 0.87 mmol) was dissolved in dry DMSO (3.0 mL) and transferred to an oven-dried Schlenk-tube and purged with Argon. NaH (43.5 mg, 0.96 mmol, 60% in mineral oil) was transferred directly to the

solution and heated (60 °C) under Argon for 1.5 h, or until hydrogen evolution had ceased. 1-Fluoronaphthalene (154 µL, 1.2 mmol) was added under argon, and the resulting solution was heated (70 °C) for 1.5 h. On cooling, the solution was partitioned between toluene and $H_2O$ and washed (3x $H_2O$). The organic phase was separated and dried over $MgSO_4$. After filtration the organic phase was removed under reduced pressure to yield a crude product. Purification by silica gel chromatography (DCM → DCM:MeOH:$NEt_3$, 5:1:1%) gave the pure product (Duloxetine) as a yellow oil (214 mg, 83%; 94% *e.e.*). $^1$H NMR (400 MHz, $CDCl_3$): δ 8.38-8.33 (m, 1H, Aryl), 7.80-7.76 (m, 1H, Aryl), 7.51-7.46 (m, 2H, Aryl), 7.39 (d, *J* = 8.3 Hz, 1H), 7.29 (d, *J* = 7.9 Hz, 1H), 7.21 (dd, *J* = 5.0, 1.2 Hz, 1H, CH-9), 7.06 (d, *J* = 3.5 Hz, 1H, CH-7), 6.94 (dd, *J* = 5.0, 3.5 Hz, 1H, CH-8), 6.86 (d, *J* = 7.2 Hz, 1H), 5.79 (dd, *J* = 7.7, 5.3 Hz, 1H, CH-1), 2.88-2.79 (m, 2H, $CH_2$-3), 2.51-2.40 (m, 2H, $CH_2$-2), 2.44 (s, 3H, $CH_3$-4). $^{13}$C NMR (101 MHz, $CDCl_3$): δ 153.4 (C-6), 145.3 (C-10), 134.6 (C-9), 127.5, 126.6, 126.3, 126.2, 125.7, 125.2, 124.7, 124.5, 122.1, 122.1, 120.6, 107.0, 74.8 (C-1), 48.4 (C-3), 39.1 (C-4), 36.6 (C-2). LRMS (ESI+) $[M+H]^+$, 298.0. HRMS (ESI+) calculated $[C_{18}H_{19}NOS+H]^+$ 298.1266, found 298.1263. $[\alpha]_D^{22}$ = +105.4 (1.0, MeOH) (*S*)-Duloxetine in 94% *e.e.* Enantiomeric excess was determined by derivatisation to the analogous acetylated compound **164**. All spectroscopic and analytical properties are identical with those reported in the literature.[232]

Methyl *N*-(diphenylmethyl)-*N*-{3-phenyl-3-[4-(trifluoromethyl)phenoxy]propyl} carbamate. **147**

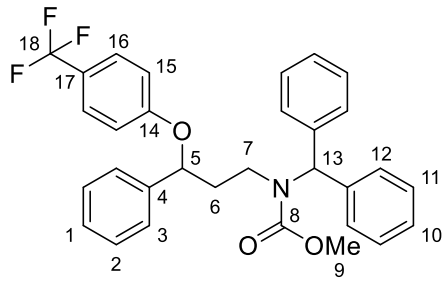


3-[(Diphenylmethyl)amino]-1-phenylpropan-1-ol **128** (0.65 g, 2.05 mmol) was dissolved in dry DMA (2.8 mL) and transferred to an oven-dried Schlenk-tube and purged with Argon. NaH (100 mg, 2.26 mmol, 60% in mineral oil) was transferred directly to the solution and heated (70 $^{o}$C) under Argon for 30 min, or until hydrogen evolution had ceased. 4-Chlorobenzotrifluoride (354 µL, 2.46 mmol) was added under argon, and the resulting solution was heated (110 $^{o}$C) for 3 h. On cooling, the solution was partitioned between toluene and $H_2O$ and washed (3x $H_2O$). The organic phase was separated and dried over $MgSO_4$. After filtration the organic phase was removed under reduced pressure to yield a crude product yellow product. To the crude oil, DCM (4 mL) was added and the reaction was stirred under argon. $K_2CO_3$ (1.4 g, 10.2 mmol) was dissolved in $H_2O$ (4 mL) and added to the stirring solution, followed by the addition of methyl chloroformate (205 µL, 2.67 mmol). After 1.5 h, the solution was partitioned between EtAcO and $H_2O$ and washed (3x $H_2O$). The organic phase was separated and dried over $MgSO_4$. After filtration the organic phase was removed under reduced pressure to yield a crude product yellow product. Purification by silica gel chromatography (Hexane:EtAcO → EtAcO, 5:1 → 1) gave the pure product as a yellow oil (0.809 g, 76%). Mixture of rotamers observed, major reported as: $^{1}$H NMR (400 MHz, $CDCl_3$): δ 7.46-7.21 (m, 17H, Ph), 6.75 (d, *J* = 8.6 Hz, 2H, CH-16), 6.68-6.59 (bs, 1H, CH-13), 5.53 (dd, *J* = 8.6, 4.4 Hz, 1H, CH-5), 3.70 (s, 3H, $CH_3$-9), 3.60-3.48

(m, 2H, $CH_2$-7), 1.75-1.47 (m, 2H, $CH_2$-6). LRMS (ESI+) $[M+H]^+$, 520.5 (5%), HRMS (ESI+) calculated $[C_{31}H_{28}NO_3+H]^+$ 520.2100, found 520.2125.

(2*E*)-*N*-Methoxy-*N*-methyl-3-(thiophen-2-yl)prop-2-enamide. **155**

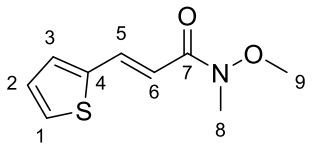


(2*E*)-3-(Thiophen-2-yl)prop-2-enoic acid **153** (4.0 g, 26.0 mmol) and dimethylformamide (200 µL, 2.6 mmol) was dissolved in DCM (70 mL) and stirred under argon. Oxalyl chloride (2.5 mL, 26.0 mmol) was added and the solution was refluxed for 4 h and allowed to cool to room temperature. All the solvent was removed *in vacuo* to yield a brown solid. THF (50 mL) was added to the resulting solid and stirred under argon. *N*,*O*-Dimethylhydroxylamine (2.54 g, 26.0 mmol) and triethylamine (3.6 mL, 26.0 mmol) were added and the solution was allowed to stir overnight. After, the reaction was quenched by the addition of $H_2O$ (50 mL). the resulting solution was partitioned between EtAcO (250 mL) and the organic layer was washed with $H_2O$ (3 x 30 mL). The organic layer was separated and dried over $MgSO_4$. After filtration the organic phase was removed under reduced pressure to yield pure yellow oil (4.36 g, 85%). $^1$H NMR (400 MHz, $CDCl_3$) observed as a mixture of rotamers, major rotamer: δ 7.83 (d, *J* = 15.5 Hz, 1H, CH-5), 7.34 (d, *J* = 5.1H, 1H, CH-1), 7.04 (dd, *J* = 5.1, 3.6 Hz, 1H, CH-2), 7.25 (d, *J* – 3.6 Hz, 1H, CH-3), 6.02 (d, *J* = 15.5 Hz, 1H, CH-6), 3.76 (s, 3H, $CH_3$-8), 3.30 (s, 3H, $CH_3$-9). $^{13}$C NMR (101 MHz, $CDCl_3$): δ 166.8 (C-7), 142.8 (C-1), 140.4 (C-4), 136.0 (C-3), 130.6 (C-2), 127.6 (C-6), 61.9 (C-8), 32.6 (C-9). LRMS (ESI+) 197.3 (53%) $[M+]^+$, HRMS (ESI+) calculated $[C_9H_{11}NO_2+H]^+$ 198.0589, found 198.0611.

Benzyl[(2*E*)-but-2-en-1-yl]amine. **59a**

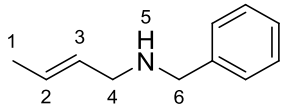


Crotonaldehyde (41.4 μL, 0.50 mmol) and benzylamine (54.6 μL, 0.50 mmol) were added to a stirring solution of THF (3.5 mL) and 3 Å molecular sieve pellets (1.0 g). The resulting mix was stirred under argon overnight (15 h). To the stirring solution, $NaBH_4$ (38 mg, 1.0 mmol) was added, followed by the drop-wise addition of methanol (2 mL). This solution was stirred for a further 2 h, after which, the solution was filtered through Celite. The resulting solution was partitioned between EtOAc and brine. The aqueous layer was extracted further with EtOAc (3 x EtOAc). The organic phase was separated and dried over $MgSO_4$. Purification by silica gel chromatography (hexane:EtOAc, 3:1 eluent) gave a yellow oil (37.8 mg, 47%).[1]H NMR (400 MHz, $CDCl_3$): δ 7.31- 7.10 (m, 5H, Ph), 5.60-5.43 (m, 2H, CH=CH-2/3), 3.70 (s, 2H, $CH_2$-6), 3.13 (d, *J* = 6.0 Hz, 2H, $CH_2$-4), 1.62 (d, *J* = 4.4 Hz, 3H, $CH_3$-1). 13C NMR (101 MHz, $CDCl_3$): δ 140.4, 129.6, 128.4, 128.1, 127.4, 126.7, 53.4, 51.3, 17.7 All spectroscopic and analytical properties are identical with those reported in the literature.[237]

Benzyl[(2*E*)-2-methylbut-2-en-1-yl]amine. **61a**

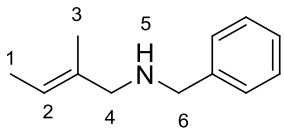


Tiglic aldehyde (48.3 μL, 0.50 mmol) and benzylamine (54.6 μL, 0.5o mmol) were added to a stirring solution of THF (3.5 mL) and 3 Å molecular sieve pellets (1.0 g). The resulting mix was stirred under argon overnight (15 h). To the stirring solution, $NaBH_4$ (38 mg, 1.0 mmol) was added, followed by the drop-wise addition of methanol

(2 mL). This solution was stirred for a further 2 h, after which, the solution was filtered through Celite. The resulting solution was partitioned between EtOAc and brine. The aqueous layer was extracted further with EtOAc (3 x EtOAc). The organic phase was separated and dried over $MgSO_4$. Purification by silica gel chromatography (EtOAc, 1% v/v $Et_3N$ in eluent and silica) gave a colourless oil (77.4 mg, 88%). IR (neat) $\nu_{max}$: 2915 (N-H), 1495, 1452 (C=$C_{Ar}$), 1116, 1028, 733, 696 $cm^{-1}$. $^1H$ NMR (400 MHz, $CDCl_3$): δ 7.38- 7.03 (m, 5H, Ph), 5.38-5.29 (m, 1H, CH-2), 3.66 (s, 2H, $CH_2$-5), 3.09 (s, 2H, $CH_2$-4), 1.59 (s, 3H, $CH_3$-3), 1.55 (dq, *J* = 6.7, 1.0 Hz, 3H, $CH_3$-1). 13C NMR (101 MHz, $CDCl_3$): δ 140.7, 134.2, 128.3, 128.2, 126.8, 120.4, 57.1, 53.0, 46.6, 14.5, 13.2 LRMS (ESI+) 176.2 (100%) [$M+H^+$], 115.2 (17%). HRMS (ESI+) calculated [$C_{12}H_{17}N+H^+$] 176.1439, found 176.1460. All spectroscopic and analytical properties are identical with those reported in the literature.[238]

Benzyl[(2*E*)-3-phenylprop-2-en-1-yl]amine. **66a**

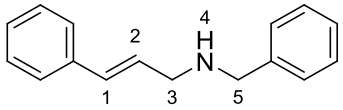


Cinnamaldehyde (0.18 mL, 1.4 mmol) and benzylamine (0.15, 1.4 mmol) were added to a stirring solution of THF (8 mL) and 3 Å molecular sieve pellets (2.5 g). The resulting mix was stirred under argon overnight (15 h). To the stirring solution, $NaBH_4$ (0.16 g, 4.2 mmol) was added, followed by the drop-wise addition of methanol (5 mL). This solution was stirred for a further 2 h, after which, the solution was filtered through Celite. The resulting solution was partitioned between EtOAc and brine. The aqueous layer was extracted further with EtOAc (3 x EtOAc). The organic phase was separated and dried over $MgSO_4$. This resulted in the formation of a colourless oil (0.23 g, 74%). The resulting oil was sufficiently pure to characterise without further purification. IR

(neat) $\nu_{max}$: 3026 (N-H), 2818,1599 (C=C), 1494, 1456 (C=$C_{Ar}$), 966, 732, 692 $cm^{-1}$. $^{1}H$ NMR (400 MHz, $CDCl_3$): δ 7.33- 7.13 (m, 10H, Ph), 6.47 (d, *J* = 15.9 Hz, 1H, CH-1), 6.25 (dt, *J* = 15.9, 6.23 Hz, 1H, CH-2), 3.77 (s, 2H, $CH_2$-5), 3.38 (dd, *J* = 6.28, 1.4 Hz, $CH_2$-3). $^{13}C$ NMR (101 MHz, $CDCl_3$): δ 188.6, 140.2, 137.2, 131.5, 129.4, 128.7, 128.6, 128.5, 128.4, 53.3, 51.2. LRMS (ESI+) 224.3 (100%) [$M+H^+$], 116.9 (38%). HRMS (ESI+) calculated [$C_{14}H_{17}N+H^+$] 224.1439, found 224.1473. All spectroscopic and analytical properties are identical with those reported in the literature.[239]

(2*E*)-3-(Thiophen-2-yl)prop-2-enal. **156**

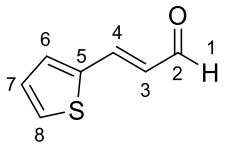


(2*E*)-3-(Thiophen-2-yl)prop-2-enoic acid (3.0 g, 19.5 mmol) was dissolved in THF (80 mL) and cooled to -78 °C under argon. DIBAL-H (58.5 mL, 1 M THF) was added slowly over 1 hour, and the resulting solution was allowed to react overnight, warming to room temperature. The resulting solution was quenched with saturated potassium sodium tartrate solution (aqueous) and allowed to stir for 1 h. After, the resulting solution was partitioned between EtOAc and the aqueous layer was extracted with EtOAc (3 x EtOAc). The organic phase was separated and dried over $MgSO_4$. After filtration the organic phase was removed under reduced pressure to yield a crude allylic product [(2*E*)-3(thiophen-2-yl)prop-2-en-1-ol)]. In a separate vessel, DMSO (42.9 mmol, 3.0 mL) and DCM (40 mL) were combined under argon and cooled (to -78°C). Oxalyl chloride (21.5 mmol, 1.8 mL) was added and the reaction mixture was stirred for 10 min. The crude allylic alcohol [(2*E*)-3(thiophen-2-yl)prop-2-en-1-ol)] was added (in DCM, 12 mL) to the -78 °C solution, and allowed to stir for 10 min. Triethylamine

(97.5 mmol, 13.6 mL) was subsequently added, and the solution allowed to warm to room temperature over 1.5 h. After, the resulting solution was partitioned quenched with water and partitioned between EtOAc and the aqueous layer was extracted with EtOAc (3 x EtOAc). The organic phase was separated and dried over $MgSO_4$. After filtration the organic phase was removed under reduced pressure to yield a crude brown oil. Purification by silica gel chromatography (hexane:EtAcO, 9:1) gave **156** as a yellow oil (996 mg, 37%).$^1$H NMR (400 MHz, $CDCl_3$): δ 9.63 (d, *J* = 7.7 Hz, 1H, CH-1), 7.58 (d, *J* = 15.6 Hz, 1H, CH-4), 7.51 (d, *J* = 5.0 Hz, 1H, CH-6), 7.37 (d, J = 3.7 Hz, 1H, CH-8), 7.11 (dd, *J* = 5.1, 3.6 Hz, 1H, CH-7), 6.52 (dd, *J* = 15.6, 7.7 Hz, 1H, CH-3). $^{13}$C NMR (101 MHz, $CDCl_3$): δ 192.9 (C-2), 144.4 (C-4), 139.3 (C-5), 132.0 (C-8), 130.4 (C-6), 128.5 (C-7), 127.4 (C-3). LRMS (ESI+) $[M+H]^+$, 138.8. HRMS (ESI+) calculated $[C_7H_6OS+H]^+$ 139.0218, found 139.0246. All spectroscopic and analytical properties are identical with those reported in the literature.[240]

(*R*)-*N*-Methyl-*N*-{3-phenyl-3-[4-trifluoromethyl] phenoxyl}propyl}acetamido. **152**

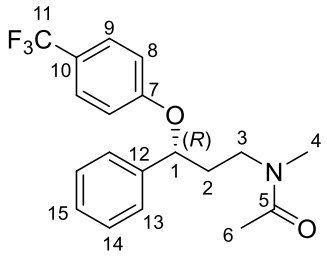


Fluoxetine (200 mg, 0.65 mmol), DCM (4 mL), acetic anhydride (1 mL) and pyridine (1 mL) were combined and allowed to stir over night. The resulting solution was diluted in DCM (30 mL) and washed with HCl (3 x 10 mL, w/v 20%) and $H_2O$ (3 x). The organic layer was separated and dried over $MgSO_4$. Filtration followed by the removal of solvent under vacuum yielded a yellow oil. Purification by silica gel chromatography (hexane : DCM, 1:1 → DCM : MeOH, 9 : 1) gave **13b** as a yellow oil (220 mg, 96%).

IR (neat) $\nu_{max}$: 3052, 2928, 1636, 1578, 1396, 1093, 771 $cm^{-1}$. NMR spectra shows **152** as a mixture of rotamers, major peaks given as the following: $^{1}H$ NMR (400 MHz, $CDCl_3$): δ 7.42 (d, *J* = 8.5 Hz, 2H, CH-9), 7.38-7.27(m, 5H, Ph), 6.89 (d, *J* = 8.4 Hz, 2H, CH-8), 5.21 (dd, *J* = 8.6, 4.3 Hz, 1H, CH-1) 3.63-3.51 (m, 2H, $CH_2$-3), 2.97 (s, 3H, $CH_3$-4), 2.25-2.09 (m, 2H, $CH_2$-2), 2.04 (s, 3H, $CH_3$-6). $^{13}C$ NMR (101 MHz, $CDCl_3$): δ 170.6 (C-5), 160.3 (C-11), 140.7 (C-7), 129.1, 128.3, 126.9, 126.8, 125.7, 125.5, 115.6, 78.4 (C-1), 47.1 (C-4), 37.4 (C-3), 36.6 (C-6), 21.1 (C-2). LRMS (ESI+) $[M+H]^+$, 351.9. HRMS (ESI+) calculated $[C_{19}H_{2O}NO_2F_3+H]^+$ 352.1524 found 352.1515. Enantiomeric excess was determined by HPLC using an AS-H CHIRALCEL column (250 x 4.6 mm) fitted with guard cartridge (50 x 4.6 mm), 25 $^{o}C$, 1.0 mL/min, 210 nm, hexane : IPA (9 : 1). $t_R$ (*R*) = 23.6 min; $t_R$ (*S*) = 31.9 min.

(*S*)-*N*-Methyl-*N*-[3-(naphthalene-1-yloxy)-3-(thiophen-2-yl)propyl]acetamido. **164**

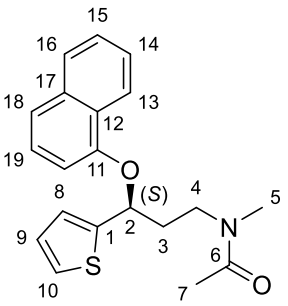


Duloxetine **2** (166 mg, 0.56 mmol), DCM (3 mL), acetic anhydride (1 mL) and pyridine (1 L) were combined and allowed to stir over night. The resulting solution was diluted in DCM (30 mL) and washed with HCl (3 x 10 mL, w/v 20%) and $H_2O$ (3 x). The organic layer was separated and dried over $MgSO_4$. Filtration followed by the removal of solvent under vacuum yielded a crude yellow oil. Purification by silica gel chromatography (Hexane : DCM, 1 : 1 → DCM : MeOH, 9 : 1) gave **164** as a yellow oil (150 mg, 79%). IR (neat) $\nu_{max}$: 2931, 1636, 1516, 1323, 1245, 1108, 835 $cm^{-1}$. NMR

spectra shows **164** as a mixture of rotamers, major peaks given as the following: $^{1}$H NMR (400 MHz, $CDCl_3$): δ 8.40-8.30 (m, 1H, Aryl), 7.84-7.81 (m, 1H, Aryl), 7.56-7.51 (m, 2H, Aryl), 7.44 (d, *J* = 8.6 Hz, 1H, Aryl), 7.30 (d, *J* = 8.0 Hz, 1H), 7.21 (dd, *J* = 5.0, 1.2 Hz, 1H, CH-10), 7.11 (d, *J* = 3.8 Hz, 1H, CH-8), 6.97 (dd, *J* = 5.0, 3.5 Hz, 1H, CH-9), 6.87 (d, *J* = 8.5 Hz, 1H), 5.74 (dd, *J* = 8.0, 4.9 Hz, 1H, CH-2), 3.82-3.61 (m, 2H, $CH_2$-4), 3.00 (s, 3H, $CH_3$-5) 2.57-2.45 (m, 2H, $CH_2$-3), 2.06 (s, 3H, $CH_3$-7). $^{13}$C NMR (101 MHz, $CDCl_3$): δ 170.7 (C-6), 153.1 (C-1), 144.8 (C-11), 134.6, 127.7, 126.8, 126.5, 126.1, 125.7, 127.5, 124.9, 124.8, 122.0, 121.1, 106.9, 74.5 (C-2), 45.1 (C-4), 36.7 (C-5), 33.3 (C-7), 21.9 (C-3). LRMS (ESI+) $[M+Na]^+$, 361.3. HRMS (ESI+) calculated $[C_{20}H_{21}NO_2S+H]^+$ 340.1371, found 340.1377. Enantiomeric excess determined by HPLC using an AS-H CHIRALCEL column (250 x 4.6 mm) fitted with guard cartridge (50 x 4.6 mm), 25 $^{o}$C, 1.0 mL/min, 210 nm, hexane : IPA (85 : 15). $t_R$ (*S*) = 29.2 min; $t_R$ (*R*) = 38.2 min.

## References


1 E. L. Muetterties, *The Chemistry of Boron and Its Compounds* (John Wiley & Sons Inc., New York, 1967).

2 C. M. Crudden, B. W. Glasspoole and C. J. Lata, *Chem. Commun.*, 2009, 6704-6716.

3 The Nobel Prize in Chemistry 1979. Last accessed on Janruary 2015: http://www.nobelprize.org/nobel_prizes/chemistry/laureates/1979/

4 H. C. Brown, *Hydroboration* (W. A. Benamin, Inc., New York, 1962).

5 N. Miyaura, K. Yamada and A. Suzuki, *Tetrahedron Lett*., 1979, **36**, 3437-3440.

6 G. A. Molander and L. Jean-Gérard, *J. Org. Chem*., 2009, **74**, 1297-1303.

7 E. Fernández, M. W. Hooper, F. I. Knight and J. M. Brown, *Chem. Commun.*, 1997, 173-174.

8 S. N. Mlynarski, A. S. Karns and J. P. Morken, *J. Am. Chem. Soc*., 2012, **134**, 16449-16451.

9 J. L. Stymiest, V. Bagutski, R. M. French and V. K. Aggarwal, *Nature*, 2008, **456**, 778-782.

10 D. A. Evans, T. C. Crawford, R. C. Thomas and J. A. Walker, *J. Org. Chem.*, 1976, **41**, 3947-3943.

11 H. C. Brown, M. W. Rathke and M. M. Rogic, *J. Am. Chem. Soc.*, 1968, **90**, 5038-5040.

12 H. C. Brown, C. F. Lane, *J. Am. Chem. Soc.*, 1970, **92**, 6660-6661.

13 H. C. Brown, W. R. Heydkamp, E. Breuer and W. S. Murphy, *J. Am. Chem. Soc.*, 1964, **86**, 3565-3566.

14 D. S. Matteson, *Stereodirected Synthesis with Organoboranes* (Springer-Verlag, Berlin, 1995).

15 E. Hupe, I. Marek and P. Knochel, *Org. Lett*. 2002, **4**, 2961-2863.

16 R. P. Sonawane, V. Jheengut, C. Rabalakos, R. Larouche-Gauthier, H. K. Scott and V. K. Aggarwal, *Angew. Chem. Int.* Ed., 2011, **50**, 3760-3763.

17 J. Cid, H. Gulyás, J. J. Carbó and E. Fernández, *Chem. Soc. Rev.*, 2012, **41**, 3558-3570.

18 F. J. Lawlor, N. C. Norman, N. L. Pickett, E. G. Robins, P. Nguyen, G. Lesley, T. B. Marder, J. A. Ashmore and J. C. Green, *Inorg. Chem.*, 1998, **37**, 5282-5288.

19 Y. G. Lawson, M. J. G Lesley, N. C. Norman, C. R. Rice and T. B. Marder, *Chem. Commun.,* 1997, 2051-2052.

20 T. B. Marder and N. C. Norman, *Top. Catal.*, 1998, **5**, 63-73.

21 D. Männig and H. Nöth, *Angew. Chem. Int. Engl.*, 1985, **24**, 878-879.

22 D. A. Evans and G. C. Fu, *J. Org. Chem*., 1990, **55**, 5678-5680.

23 R. T. Baker, P. Nguyen, T. B. Marder and S. A. Westcott, *Angew. Chem. Int. Ed.,* 1995, **34**, 1336-1338.

24 T. Ishiyama, M. Yamamoto and N. Miyaura, *Chem. Commun.,* 1997, 689-690.

25 N. Miyaura and A. Suzuki, *Chem. Rev.,* 1995, **95**, 2457-2483.

26 N. J. Bell, N. R. Cameron, A. J. Cox, S. O. Evans, T. B. Marder, M. A. Duin, C. J. Elsevier, X. Baucherel, A. A. D. Tulloch and J. R. P. Tooze, *Chem. Commun.*, 2004, 1854-1855.

27 H. Ito, H. Yamanaka, J. Tateiwa and A. Hosomi, *Tetrahedron Lett.,* 2000, **41**, 6821-6825.

28 K. Takahashi, T. Ishiyama and N. Miyaura, *Chem. Lett.*, 2000, 982-983.

29 K. Takahashi, T. Ishiyama and N. Miyaura, *J. Organomet. Chem.,* 2001, **625**, 47-53.

30 H. Ito, T. Ishizuka, H. Ito, J. Tateiwa, M. Sonoda and A. Hosomi, T. *J. Am. Chem. Soc.*, 1998, **120**, 11196-11197.

31 Y. Segawa, M. Yamashita and K. Nozaki, *Science*, 2006, **314**, 113-115.

32 G. W. Kabalka, B. C. Das and S. Das, *Tetrahedron Lett*., 2002, **43**, 2323-2325.

33 G. W. Kabalka, Z. Wu and M. Yao, *Appl. Organometal. Chem.,* 2008, **22**, 516-522.

34 S. Mun, J. -E. Lee and J. Yun, *Org. Lett.,* 2006, **8**, 4887-4889.

35 D. Kim, B. -M. Park and J. Yun, *Chem. Commun.*, 2005, 1755-1757.

36 G. Hughes, M. Kimura and S. L. Buchwald, *J. Am. Chem. Soc.*, 2003, **125**, 11253-11258.

37 M. N. Cheemala (2007), *Synthesis of New Chiral Phosphine Ligands and Their Applications in Asymmetric Catalysis,* Ph.D. Thesis, der Ludwig-Maximilians-Universität-Münche, Germany. Available online at: http://edoc.ub.uni-muenchen.de/7383/1/Cheemala_NarasimhaMurthy.pdf (last accessed on Janruary 2015).

38 J.–E. Lee and J. Yun, *Angew. Chem. Int. Ed.*, 2008, **47**, 145-147.

39 M. J. Geier, V. Lillo, S. A. Westcott and E. Fernández, *Org. Biomol. Chem.*, 2009, **7**, 4674-4676.

40 J. K. Park, H. H. Lackey, M. D. Rexford, Kovnir, K., M. Shatruk and D. T. McQuade, *Org. Lett.*, 2010, **12**, 5008-5011.

41 V. Lillo, A. Prieto, A. Bonet, M. M. Díaz-Requejo, J. Ramírez, P. J. Pérez and E. Fernández, *Organometallics.*, 2009, **28**, 659-662.

42 H. Chea, H.–S. Sim and J. Yun, *Adv. Synth. Catal.*, 2009, **351**, 855-858.

43 T. Shiomi, T. Adachi, K. Toribatake, L. Zhou and H. Nishiyama, *Chem. Commun.*, 2009, 5987-5989.

44 K. Hirano, H. Yorimitsu and K. Oshima, *Org. Lett.*, 2007, **9**, 5031-5033.

45 K. Toribatake, L. Zhou, A. Tsuruta and H. Nishiyama, *Tetrahedron*, 2013, **69**, 3551-3560.

46 G. A. Molander and S. A. Mckee, *Org. Lett.*, 2011, **13**, 4684-4687.

47 G. A. Molander, S. R. Wisniewski and M. Hosseini-Sarvari, *Adv. Synth. Catal.*, 2013, **355**, 3037-3057.

48 X. Feng, H.–S. Sim and J. Yun, *Chem. Eur. J.*, 2009, **15**, 1939-1943.

49 I.–H. Chen, L. Yin, W. Itano, M. Kanai and M. Shibasaki, *J. Am. Chem. Soc*., 2009, **131**, 11664-11665.

50 X. Feng and J. Yun, *Chem. Eur. J.*, 2010, **16**, 13609-13609.

51 A. R. Burns, J. S. González and H. W. Lam, *Angew. Chem. Int. Ed.*, 2012, **51**, 10827-10831.

52 I.–H. Chen, M. Kanai and M. Shibasaki, *Org. Lett*., 2010, **12**, 4098-4101.

53 E. Hartmann, D. J. Vyas and M. Oestreich, *Chem. Commun*., 2011, **47**, 7917-7932.

54 D. A. Colby, R. G. Bergman and J. A. Ellman, *J. Am. Chem. Soc*., 2008, **130**, 3645-3651.

55 D. A. Colby, R. G. Bergman and J. A. Ellman, *J. Am. Chem. Soc*., 2006, **128**, 5604-5605.

56 J. W. Rigoli, S. A. Moyer, S. D. Pearce and J. M. Schomaker, *Org. Biomol. Chem.*, 2012, **10**, 1746-1749.

57 A. Bonet, C. Solé, H. Gulyás and E. Fernández, *Curr. Org. Chem.*, 2010, **14**, 2531-2548.

58 T. Kochi, T. P. Tang and J. A. Ellman, *J. Am. Chem. Soc.*, 2002, **124**, 6518-6519.

59 C. Solé and E. Fernández, *Chem. Asian J.*, 2009, **4**, 1790- 1793.

60 C. Solé, A. Whiting, H. Gulyás, E. Fernández, *Adv. Synth. Catal.*, 2011, **353**, 376-384.

61 D. Liu, W. Gao, C. Wang, X. Zhang, *Angew. Chem. Int. Ed*., 2005, **44**, 1687-1689.

62 H. E. Sailes, J. P. Watts and A. Whiting, *J. Chem. Soc., Perkin Trans. 1*, 2000, 3362-3374.

63 H. E. Sailes, J. P. Watts and A. Whiting, *Tetrahedron Lett.*, 2000, **41**, 2457–2461.

64 C. Solé, A. Tatla, J. A. Mata, A. Whiting, H. Gulyás and E. Fernández, *Chem. Eur. J.*, 2011, **17**, 14248-14257.

65 B. List, *Angew. Chem. Int. Ed.*, 2010, **49**, 1730-1734.

66 B. List, R. A. Lerner and C. F. Barbas III, *J. Am. Chem. Soc.*, 2000, **122**, 2395-2396.

67 K. A. Ahrendt, C. J. Borths and D. W. C. MacMillan, *J. Am. Chem. Soc.*, 2000, **122**, 4243-4244.

68 S. Bertelsen and K. A. Jørgensen, *Chem. Soc. Rev.*, 2009, **38**, 2178-2189.

69 K. S. Lee, A. R. Zhugralin and A. H. Hoveyda, *J. Am. Chem. Soc*., 2009, **131**, 7253-7255.

70 D. S. Laitar, P. Müller and J. P. Sadighi, *J. Am. Chem. Soc.*, 2005, **127**, 17196-17197.

71 D. S. Laitar, E. Y. Tsui and J. P. Sadighi, *Organometallics*, 2006, **25**, 2405–2408.

72 A. Bonet, H. Gulyás and E. Fernández, *Angew. Chem. Int. Ed.*, 2010, **49**, 5130-5134.

73 H. Wu, S. Radomkit, J. M. O'Brien and A. H. Hoveyda, *J. Am. Chem. Soc.*, 2012, **134**, 8277-8285.

74 J. A. Schiffner, K. Müther and M. Oestreich, *Angew. Chem. Int. Ed.*, 2010, **49**, 1194-1196.

75 A. Bonet, C. Solé, H. Gulyás and E. Fernández, *Chem. Asian J.*, 2011, **6**, 1011-1014.

76 I. Ibrahem, P. Breistein and A. Córdova, *Chem. Eur. J.*, 2012, **18**, 5175-5179.

77 I. Ibrahem, P. Breistein and A. Córdova, *Angew. Chem. Int. Ed.*, 2011, **50**, 12036 -12041.

78 C. J. Li, *Chem. Rev.*, 2005, **105**, 3095-3165.

79 S. Kobayashi, P. Xu, T. Endo, M. Ueno and T. Kitanosono, *Angew. Chem. Int. Ed*., 2012, **51**, 12763-12766.

80 S. B. Thorpe, J. A. Calderone and W. L. Santos, *Org. Lett.*, 2012, **14**, 1918-1921.

81 T. Kitanosono, P. Xu and S. Kobayashi, *Chem. Commun*., 2013, **49**, 8184-8186.

82 T. Kitanosono, P. Xu and S. Kobayashi, *Chem. Asian J.*, 2014, **9**, 179-188.

83 T. B. Marder and N. C. Norman, *Top. Catal*., 1998, **5**, 63-73.

84 M. Yamashita, *Bull. Chem. Soc. Jpn.*, 2011, **84**, 983-999.

85 G. Palau-Lluch and E. Fernández, *Adv. Synth. Catal.*, 2013, **355**, 1464-1470.

86 L. Dang, Z. Lin and T. B. Marder, *Chem. Commun.*, 2009, 3987-3995.

87 L. Dang, Z. Lin an d T. B. Marder, *Organometallics*, 2007, **26**, 2824-2832.

88 L. Dang, Z. Lin and T. B. Marder, *Organometallics*, 2008, **27**, 4443-4454.

89 B. Liu, M. Gao, L. Dang, H. Zhao, T. B. Marder and Z. Lin, *Organometallics*., 2012, **31**, 3410-3425.

90 J. Cid, J. J. Carbó and E. Fernández, *Chem. Eur. J.*, 2012, **18**, 12794-12802.

91 C. Kleeberg, A. G. Crawford, A. S. Batsanov, P. Hodgkinson, D.C. Apperley, M. S. Cheung, Z. Y. Lin and T. B. Marder, *J. Org. Chem*., 2012, **77**, 785–789.

92 J. S. Johnson and D. A. Evans, *Acc. Chem. Res.*, 2000, **33**, 325-335.

93 C. Pubill-Ulldemolins, A. Bonet, H. Gulyás, C. Bo and E. Fernández, *Org. Biomol. Chem*., 2012, **10**, 9677-9682.

94 D. Basavaiah and G. Veeraraghavaiah, *Chem. Soc. Rev.*, 2012, **41**, 68-78.

95 N. Khiar, A. Salvador, A. Chelouan, A. Alcudia and I. Fernández, *Org. Biomol. Chem.*, 2012, **10**, 2366-2368.

96 M. Poliakoff and P. Licence, *Nature*, 2007, **450**, 810-812.

97 K. C. Nicolaou, Z. Yang, G.–Q. Shi, J. L. Gunzner, K. A. Agrios and P. Gärtner, *Nature*., 1998, **392**, 264-269.

98 E. J. Ariëns, *Eur. J. Clin. Pharmacol*., 1984, **26**, 663-668.

99 D. Seeback and J. L. Matthews, *Chem. Commun*., 1997, 2015-2022.

100 J. Patel, G. Clavé, P. –Y. Renard, and X. Franck, *Angew. Chem. Int. Ed.*, 2008, **47**, 4224-4227.

101 D. J. Ager, I. Prakash and D. R. Schaad, *Chem. Rev.*, 1996, **96**, 835-875.

102 J. C. Barrish and W. C. Still, *J. Am. Chem. Soc*., 1983, **105**, 2487-2489.

103 M. Suginome, L. Uehlin and M. Murakami, *J. Am. Chem. Soc.*, 2004, **126**, 13196-13197.

104 H. Geng, W. Zhang, J. Chen, G. Hou, L. Zhou, Y. Zou, W. Wu and X. Zhang, *Angew. Chem. Int. Ed.*, 2009, **48**, 6052 -6054.

105 S. G. Davies, N. M. Garrido, D. Kruchinin, O. Ichihara, L. J. Kotchie, P. D. Price, A. J. Price-Mortimer, A. J. Russell and A. D. Smith, *Tetrahedron: Asymmetry*, 2006, **17**, 1793-1811.

106 F. S. Messiha, *Neurosci. Biobehav. Rev*., 1993, **4**, 385-396.

107 C. Hiemke and S. Härtter, *Pharmacology & Therapeutics*., 2000, **85**, 11-28.

108 C. J. Harmer, N. C. Shelly, P. J. Cowen and G. M. Goodwin, *Am. J. Psychiatry*., 2004, **161**, 1256-1263.

109 M. J. Staquet, *Curr. Med. Res. Opin*., 1980, **6**, 475-477.

110 D. T. Wong, K. W. Perry and F. P. Bymaster, *Nat. Rev. Drug. Discov.*, 2005, **4,** 764-774.

111 IMS Health MIDAS, *Top 20 Global Products 2012*, IMS Health, Danbury, Conneticut, United States, 2012. http://www.imshealth.com/deployedfiles/ims/Global/Content/Corporate/Press%20Room/Top-Line%20Market%20Data%20&%20Trends/Top_20_Global_Products_2012_2.pdf (last accessed on November 2013).

112 C. M. Perry and L. J. Scott, *Drugs*, 2000, **60**, 139-179.

113 M. E. Thase, A. R. Entsuah and R. L. Rudolph, *Br. J. Psychiatry*., 2001, **178**, 234-24.

114 S. C. Bergmeier, *Tetrahedron*, 2000, **56**, 2561-2576.

115 M. K. Ghorai, K. Das, D. Shukla, *J. Org. Chem.*, 2007, **72**, 5859-5862.

116 P. Etayo and A. Vidal-Ferran, *Chem. Soc. Rev.*, 2013, **42**, 728-754.

117 A. J. A. Cobb, D. M. Shaw, D. A. Longbottom, J. B. Gold and S. V. Ley, *Org. Biomol. Chem.*, 2005, **3**, 84-96.

118 S. G. Davies, A. M. Fletcher, P M. Roberts and J. E. Thomson, *Tetrahedron: Asymmetry*, 2012, **23**, 1111-1153.

119 S. G. Davies, A. D. Smith and P. D. Price, *Tetrahedron: Asymmetry*, 2005, **16**, 2833-2891.

120 E. Abraham, E. A. Brock, J. I. Candela-Lena, S. G. Davies, M. Georgiou, R. L. Nicholson, J. H. Perkins, P. M. Roberts, A. J. Russell, E. M. Sánchez-Fernández, P. M. Scott, A. D. Smith and J. E. Thomson, *Org. Biomol. Chem.*, 2008, **6** 1665-1673.

121 S. G. Davies, N. Mujtaba, P. M. Roberts and A. D. Smith, J. E. Thomson, *Org. Lett.*, 2009, **9**, 1959-1962.

122 S. G. Davies and I. A. S. Walters, *J. Chem. Soc. Perkin Trans. 1*, 1994, 1129-1139.

123 S. Jayakumar, M. P. S. Ishar and M. P. Mahajan, *Tetrahedron*, 2002, **58**, 379-471.

124 P. Buonora, J. C. Olsen and T. Oh, *Tetrahedron.*, 2001, **57**, 6099-6138.

125 M. J. Schnermann and D. L. Boger, *J. Am. Chem. Soc.*, 2005, **127**, 15704-15705.

126 D. L. Boger, D. R. Soenen, C. W. Boyce, M. P. Hedrick and Q. J. Jin, *Org. Chem.*, 2000, **65**, 2479-2483.

127 J. W. Rigoli, S. A. Moyer, S. D. Pearce and J. M. Schomaker, *Org. Biomol. Chem.*, 2012, **10**, 1746-1749.

128 F. Palacios, J. Vicario and D. Aparicio, *J. Org. Chem.*, 2006, **71**, 7690-7696.

129 F. Basuli, H.Aneetha, J. C. Huffman and D. J. Mindiola *J. Am. Chem. Soc*., 2005, **127**, 17992-17993.

130 *Ylides and imines of phosphorus*; Johnson, A. W., Kahsa, W. S., Starzewski, K. A. D., Dixon, D. A., Eds.; Wiley: New York, 1993.

131 D. A. Colby, R. G. Bergman and J. A. Ellman, *J. Am. Chem. Soc*., 2008, **130**, 3645-3651.

132 D. A. Colby, R. G. Bergman and J. A. Ellman, *J. Am. Chem. Soc., 2006*, **128**, 5604-5605.

133 A. S. Kiselyov, *Tetrahedron Letters*, 1995, **36**, 9297-9300.

134 A. F. Abdel-Magid, K. G. Carson, B. D. Harris, C. A. Maryanoff and R. D. Shah, *J. Org. Chem.*, 1996, **61**, 3849-3862.

135 C. F. Carter, H. Lange, S. V. Ley, I. R. Baxendale, B. Wittkamp, J. G. Goode and N. L. Gaunt, *Org. Process Res. Dev.*, 2010, **14**, 393-404.

136 Molecular Sieves, http://www.sigmaaldrich.com/chemistry/chemical-synthesis/learning-center/technical-bulletins/al-1430/molecular-sieves.html, (last accessed on April 2014).

137 M. C. Durrant, D. M. Davies and M. E. Deary, *Org. Biomol. Chem.*, 2011, **9** 7249-7254.

138 M. E. Deary, M. C. Durrant and D. M. Davies, *Org. Biomol. Chem*., 2013, **11**, 309-317.

139 D. M. Davies, M. E. Deary, K. Quill and R. A. Smith, *Chem. Eur. J.*, 2005, **11**, 3552-3558.

140 S. Velusamy and T. Punniyamurthy, *Tetrahedron Lett.*, 2003, **44**, 8955-8957.

141 S. Velusamy, A. Srinivasan and T. Punniyamurthy, *Tetrahedron Lett.*, 2006, **47**, 923-926.

142 M. D. Thomas, *J. Am. Chem. Soc.*, 1920, **42**, 867–882.

143 K. Hashimoto, Y. Hanada, Y. Minami and Y. Kera, *Applied Catalysis A: General.*, 1996, **141**, 57-69.

144 R. Newton and B. F. Dodge, *J. Am. Chem. Soc*., 1933, **55**, 4747–4759.

145 A. W. Hoffman, *Justus Liebigs Ann. Chem.*, 1868, **145**, 357-361.

146 R. Newton and B. F. Dodge, *J. Am. Chem. Soc*., 1934, **56**, 1287–1291.

147 G. Bertoli, C. Cimarelli, E. Marcantoni, G. Palmieri and M. Petrini, *J. Org. Chem.*, 1994, **59**, 5328-5335.

148 S. Asrof Ali, S. M. A. Hashmi and M. I. M. Wazeer, *Spectrochimica Acta Part A*, 1999, **55**, 1445-1452.

149 A. R. Katritzky, V. J. Baker, F. M. S. Brito-Palma, R. C. Patel, G. Pfister-Guillouzo and C. Guimon, *J. Chem. Soc., Perkin Trans. 2*, 1980, 91-95.

150 N. S. Karthikeyan, G. Ramachandran, R. S. Rathore and K. I. Sathiyanarayanan, *Asian J. Org. Chem*., 2012, **1**, 173-179.

151 P. Perlmutter, *Conjugate Addition Reactions in Organic Synthesis*, Tetrahedron Organic Chemistry, Pergamon, Oxford, 7th edn, 1992.

152 B. E. Rossiter and N. M. Swingle, *Chem. Rev.*, 1992, **92**, 771-806.

153 A. G. Csáky, G. de la Herrán and M. C. Murcia, *Chem. Soc. Rev*., 2010, **39**, 4080-4102.

154 L. Pardo, R. Osman, H. Weinstein and J. R. Rabinowitz, *J. Am. Chem. Soc.*, 1993, **115**, 8263-8269.

155 P. H. Phua, S. P. Mathew, A. J. P. White, J. G. de Vries, D. G. Blackmond and K. K. Hii, *Chem. Eur. J*., 2007, **13**, 4602-4613.

156 C. F. Bernasconi, *Tetrahedron*., 1989, **45**, 4017-4090.

157 Smith, Ian J. (2003) *Some kinetic and equilibrium studies of the reactions of carbonyl compounds with amines and/or sulfite*, Durham theses, Durham University. Available at Durham E-Theses Online: http://etheses.dur.ac.uk/3733/ (accessed last on Janrurary 2015).

158 J. H. Atherton, K. H. Brown and M. R. Crampton, *J. Chem. Soc., Perkin Trans. 2*, 2000, **5**, 941-946.

159 J. Hine, J. C. Craig, J. G. Underwood II and F. A. Via, *J. Am. Chem. Soc.*, 1970, **92**, 5194–5199.

160 J. Hine and F. A. Via, *J. Am. Chem. Soc.*, 1972, **94**, 190–194.

161 J. Hine and Y. Chou, *J. Org. Chem.*, 1981, **46**, 649–652.

162 J. M. Sayer and W. P. Jencks, *J. Am. Chem. Soc.*, 1977, **99**, 464–474.

163 R. V. Hoffman, R. A. Bartsch and B. Rae Cho, *Acc. Chem. Res.*, 1989, **22**, 211-217.

164 F. P. Cossío, J. M. Odriozola, M. Oiarbide and C. Palomo, *J. Chem. Soc., Chem. Commun.*, 1989, 74-76.

165 C. Palomo, I. Ganboa and L. Dembkowski, A. Kot, *J. Org. Chem*., 1998, **63**, 6398-6400.

166 C. Palomo, J. M. Aizpurua, I. Ganboa and M. Oiarbide, *Eur. J. Org. Chem*., 1999, 3223-3235.

167 Y. Lu and B. A. Arndtsen, *Org. Lett.*, 2009, **11**, 1369-1372.

168 F. P. Cossío, C. Alonso, M. Ayerbe, B. Lecea, G. Rubiales and F. Palacios, *J. Org. Chem.*, 2006, **71**, 2839–2847.

169 G. Barker, J. L. McGrath, A. Klapars, D. Stead, G. Zhou, K. R. Campos and P. O'Brien, *J. Org. Chem.*, 2011, **76**, 5936–5953.

170 D. Stead, G. Carbone, P. O'Brien, K. R. Campos, I. Coldham and A. Sanderson, *J. Am. Chem. Soc.*, 2010, **132**, 7260-7261.

171 C. Lamberti, A. Zecchina, E. Groppo and S. Bordiga, *Chem. Soc. Rev.*, 2010, **39**, 4951-5001.

172 J. Clayden, N. Greeves, S. Warren, P. Wothers, *Organic Chemistry* (Oxford University Press., Oxford, 2001).

173 Brown, Kathryn Helen (1999) *Kinetic studies on the reaction of formaldehyde with amines in the presence of sulfite*, Durham theses, Durham University. Available at Durham E-Theses Online:http://etheses.dur.ac.uk/4972/ (accessed last on Janruary 2015).

174 R. Benhallam, T. Zair, A. Jarid and M. Ibrahim-Ouali, *J. Mol. Struct. (THEOCHEM)*, 2003, **626**, 1-17.

175 S. Romo, N. S. Antonova, J. J. Carbó and J. M. Poblet, *Dalton Trans.*, 2008, 5166-5172.

176 C. Barba, D. Carmona, J. I. García, M. P. Lamata, J. A. Mayoral, L. Salvatella and F. Viguri, *J. Org. Chem.*, 2006, **71**, 9831–9840.

177 R. J. Loncharich, F. K. Brown and K. N. Houk, *J. Org. Chem.*, 1989, **54**, 1129-1134.

178 V. A. Bataev, O. S. Bokareva and I. A. Godunov, *J. Mol. Struct. (THEOCHEM)*, 2009, **913**, 254–264.

179 J. R. Durig, S. C. Brown, V. F. Kalasinsky and W. O. George, *Spectrochim. Acta A*, 1976, **32**, 807-813.

180 D. S. Wilcox, A. J. Shirar, O. L. Williams, B. C. Dian, *Chem. Phys, Lett.*, 2011, **508**, 10-16.

181 A. C. Fantoni, W. Caminati and R. Meyer, *Chem. Phys. Lett.*, 1987, **133**, 27-33.

182 J. R. During and T. S. Little, *J. Chem. Phys.*, 1981, **75**, 3660-3668.

183 A. D. J. Calow and A. Whiting, *Org. Biomol. Chem*., 2012, **10**, 5485-5497.

184 L. Zhao, Y. Ma, W. Duan, F. He, J. Chen and C. Song, *Org. Lett.*, 2012, **14**, 5780–5783.

185 L. Zhao, Y. Ma, W. Duan, F. He, J. Chen and C. Song, *J. Org. Chem.*, 2013, **78**, 1677–1681.

186 M. Nielsen, D. Worgull, T. Zweifel, B. Gschwend, S. Bertelsen and K. A. Jørgensen, *Chem. Commun.*, 2011, **47**, 632-649.

187 A. C. Ferretti, J. S. Mathew, I. Ashworth, M. Purdy, C. Brennan and D. G. Blackmond, *Adv. Synth. Catal*., 2008, **350**, 1007-1012.

188 B. P. Carrow and J. F. Hartwig, *J. Am. Chem. Soc.*, 2011, **133**, 2116-2119.

189 D. S. Laitar, E. Y. Tsui and J. P. Sadighi, *J. Am. Chem. Soc.*, 2006, **128**, 11036-11037.

190 A. Bonet, V. Lillo, J. Ramírez, M. M. Díaz-Requejo and E. Fernández, *Org. Biomol. Chem.*, 2009, **7**, 1533-1535.

191 H. D. Flack, *Acta Chim. Slov.*, 2008, **55**, 689-691.

192 P. Aslanidis, P. J. Cox, S. Divanidis and P. Karagiannidis, *Inorg. Chim. Act.*, 2004, **357**, 1063-1076.

193 A. Alexakis, N. Krause and S. Woodward, *Copper-Catalyzed Asymmetric Synthesis* (Wiley VCH., 2014).

194 W. Tang and X. Zhang, *Chem. Rev.*, 2003, **103**, 3029-3069.

195 A. J. Deeming, D. M. Speel and M. Stchedroff, *Organometallics*, 1997, **16**, 6004-6009.

196 Q. –L. Zhou, *Privileged Chiral Ligands and Catalysts*, (Wiley VCH., 2011).

197 G. Trabesinger, A. Albinati, N. Feiken, R. W. Kunz, P. S. Pregosin and M. Tschoerner, *J. Am. Chem. Soc.*, 1997, **119**, 6315–6323.

198 R. Noyori and T. Ohkuma, *Angew. Chem. Int. Ed*., 2001, **40**, 40-73.

199 D. T. Wong, J. S. Horng, F. P. Bymaster, K. L. Hauser and B. B. Molloy, *Life Sci.*, 1974, **15**, 471-479.

200 D. T. Wong, F. P. Bymaster and E. A. Engleman, *Life Sci.*, 1995, **57**, 411-441.

201 L. Sghendo and J. Mifsud, *J. Pharm. Pharmacol*., 2012, **64**, 317-325.

202 C. J. Wenthur, M. R. Bennett and C. W. Lindsley, *ACS Chem. Neurosci*., 2014, **5**, 14-23.

203 M. Srebnik, P. V. Ramachandran and H. C. Brown, *J. Org. Chem.*, 1988, **53**, 2916–2920.

204 Y. Gao and K. B. Sharpless, *J. Org. Chem.*, 1988, **53**, 4081–4084.

205 E. J. Corey and G. A. Reichard, *Tetrahedron Lett*., 1989, **30**, 5207-5210.

206 M. Iwata, R. Yazaki, N. Kumagai and M. Shibasaki, *Tetrahedron: Asymmetry*, 2010, **21**, 1688-1694.

207 R. Noyori, *Angew. Chem. Int. Ed.*, 2002, **41**, 2008-2022.

208 R. Noyori, T. Ohkuma, M. Kitamura, H. Takaya, N. Sayo, H. Kumobayashi and S. Akutagawa, *J. Am. Chem. Soc.*, 1987, **109**, 5856-5858.

209 T. Ohkuma, D. Ishii, H. Takeno and R. Noyori, *J. Am. Chem. Soc*., 2000, **122**, 6519-6511.

210 H.–L. Huang, L. T. Liu, S.–F. Chen and H. Ku, *Tetrahedron: Asymmetry*, 1998, **9**, 1637–1640.

211 R. C. Bernotas and R. V. Cube, *Synth. Commun*., 1990, **8**, 1209-1212.

212 S. Rajagopal and A. F. Spatola, *Appl. Catal., A*, 1997, **152**, 69-81.

213 R. J. Rahaim and R. E. Maleczka, *Org. Lett.*, 2011, **13**, 584–587.

214 S. Rajagopal and A. F. Spatola, *Appl. Catal., A*, 1997, **152**, 69–81.

215 S. Ram and L. D. Spicer, *Synth. Commun.*, 1987, **4**, 415-418.

216 B. Yan, N. Nguyen, L. Liu, G. Holland, B. Raju, *J. Comb. Chem*., 2000, **2**, 66-74.

217 A. A. Haddach, A. Kelleman and M. V. Deaton-Rewolinski, *Tetrahedron Letters*, 2002, **43**, 399-402.

218 R. Gigg and R. J. Conant, *J. Chem. Soc., Chem. Commun.*, 1983, 465-466.

219 G. A. Russell and A. G. Bemis, *J. Am. Chem. Soc*., 1966, **88**, 5491-5497.

220 G. A. Russell, A. J. Moye, E. G. Janzen, S. Mak, E. R. Talaty, *J. Org. Chem.*, 1967, **32**, 137–146.

221 G. K. Cantrell and T. Y. Meyer, *Organometallics*, 1997, **25**, 5381-5383

222 M. Ciaccia, R. Cacciapaglia, P. Mencarelli, L. Mandolini and S. Di Stefano, *Chem. Sci*., 2013, **4**, 2253-2261.

223 G. Wang, X. Liu and G. Zhao, *Tetrahedron: Asymmetry*, 2005, **10**, 1873-1879.

224 A. Y. Khan and M. Macaluso, *Neuropsychiatr. Dis. Treat.*, 2009, **5**, 23-31.

225 S. Nahm and S. M. Weinreb, *Tetrahedron Letters*, 1981, **39**, 3815-3818.

226 T. Q. Dinh and R. W. Armstrong, *Tetrahedron Letters*, 1996, **8**, 1161-1164.

227 H. Tokuyama, S. Yokoshima, T. Yamashita and T. Fukuyama, *Tetrahedron Letters*, 1998, **39**, 3189-3192.

228 D. C. Beshore and A. B. Smith, III, *J. Am. Chem. Soc*., 2007, **129**, 4148-4149.

229 B. Qu and D. B. Collum, *J. Org. Chem.*, 2006, **71**, 7117-7119.

230 D. B. Dess and J. C. Martin, *J. Org. Chem*., 1983, **48**, 4155-5156.

231 K. Omura and D. Swern, *Tetrahedron*, 1978, **34**, 1651-1660.

232 J. Deeter, J. Frazier, G. Staten, M. Staszak and L. Weigel, *Tetrahedron Letters*, 1990, **31**, 7101–7104.

233 A. D. J. Calow, C. Solé, A. Whiting and E. Fernández, *ChemCatChem*, 2013, **5**, 2233-2239.

234 P. Bernardelli, M. Bladon, E. Lorthiois, A. C. Manage, F. Vergne and R. Wrigglesworthb, *Tetrahedron: Asymmetry*, 2004, **12**, 1451–1455.

235 M. Gao, S. B. Thorpe, C. Kleeberg, C. Slebodnick, T. B. Marder and W. L. Santos, *J. Org. Chem*., 2011, **76**, 3997–4007.

236 A. M. Seayad, B. Ramalingam, K. Yoshinaga, T. Nagata and C. L. L. Chai, *Org. Lett.*, 2010, **12**, 264–267.

237 J. Blid, P. Brandt and P. Somfai, *J. Org. Chem.*, 2004, **69**, 3043-3049.

238 R. I. McDonald and S. S. Stahl, *Angew. Chem. Int. Ed.*, 2010, **49**, 5529-5532.

239 R. Takeuchi, N. Ue, K. Tanabe, K. Yamashita and N. Shiga, *J. Am. Chem. Soc.*, 2001, **123**, 9525-9534.

240 E. Kim, M. Koh, J. Ryu and S. B. Park, *J. Am. Chem. Soc*., 2008, **170**, 12206-12207.

# Appendix 1

Oxazine (*rac*)-(*anti*)-**65**
H & **C**

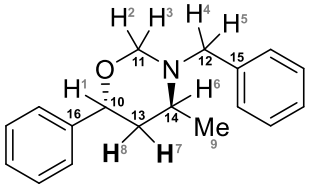


*COSY Spectrum of **65**.*

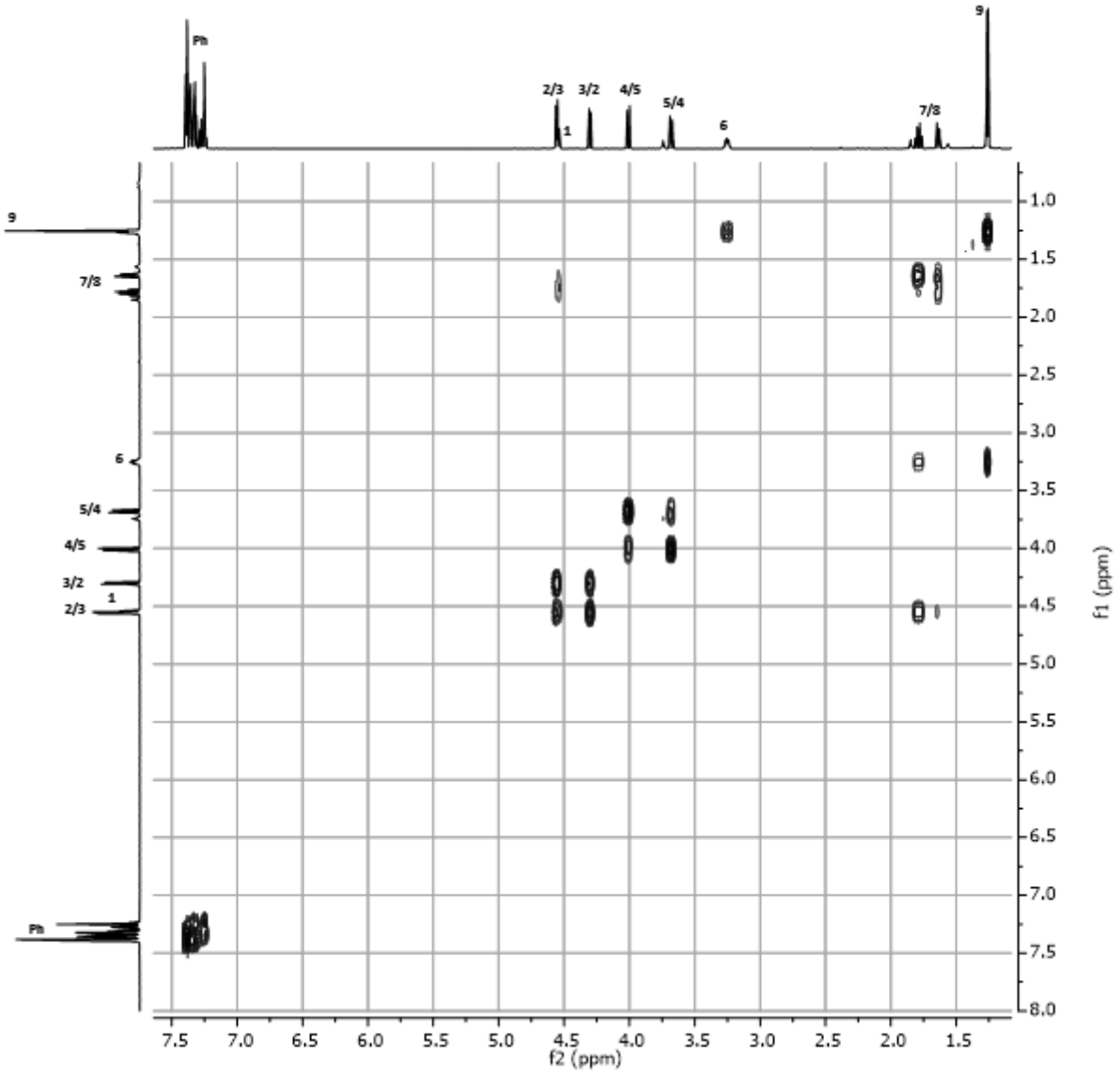

*HSQC Spectrum of **65**.*

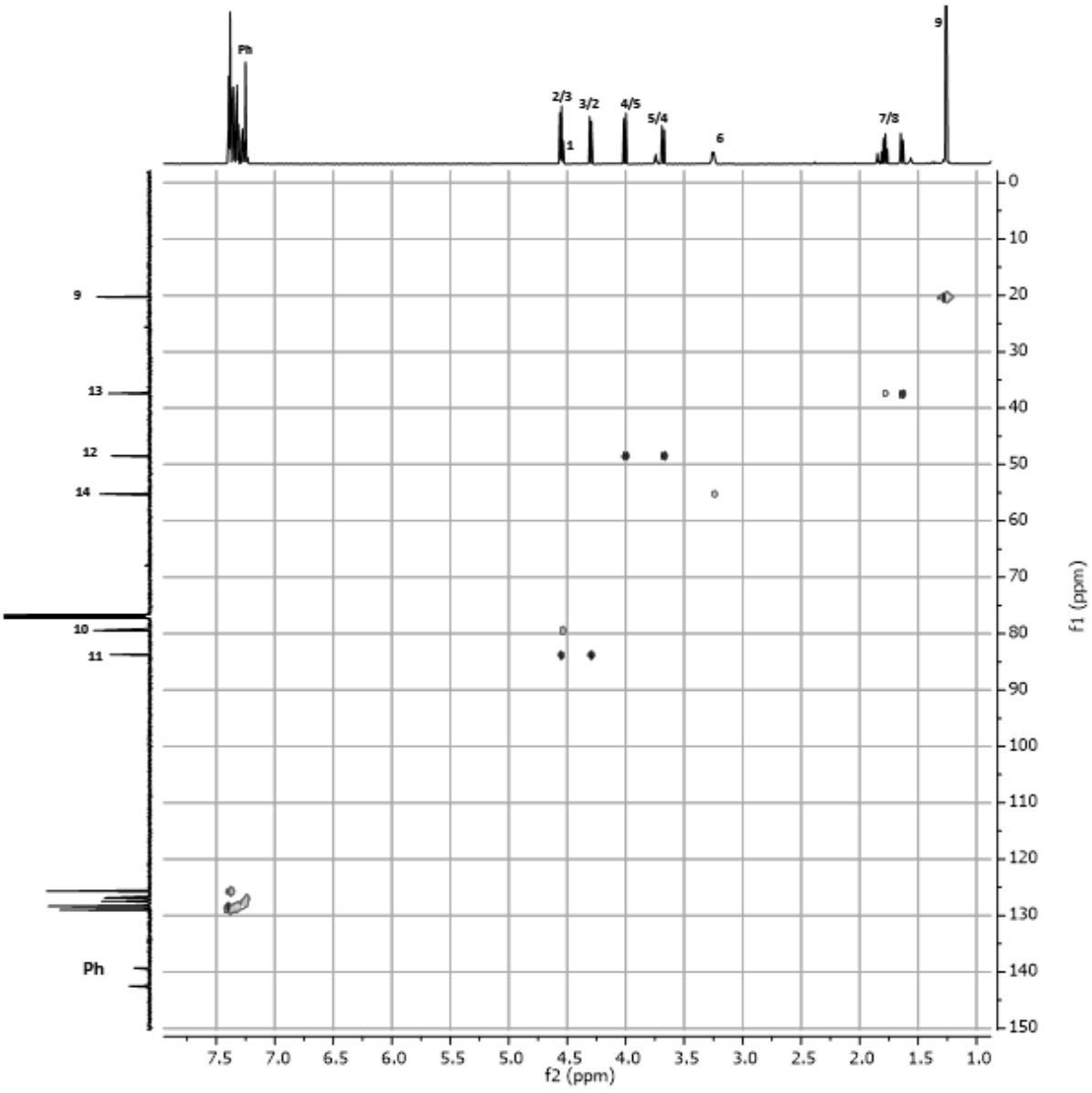

*HMBC Spectrum of* ***65****.*

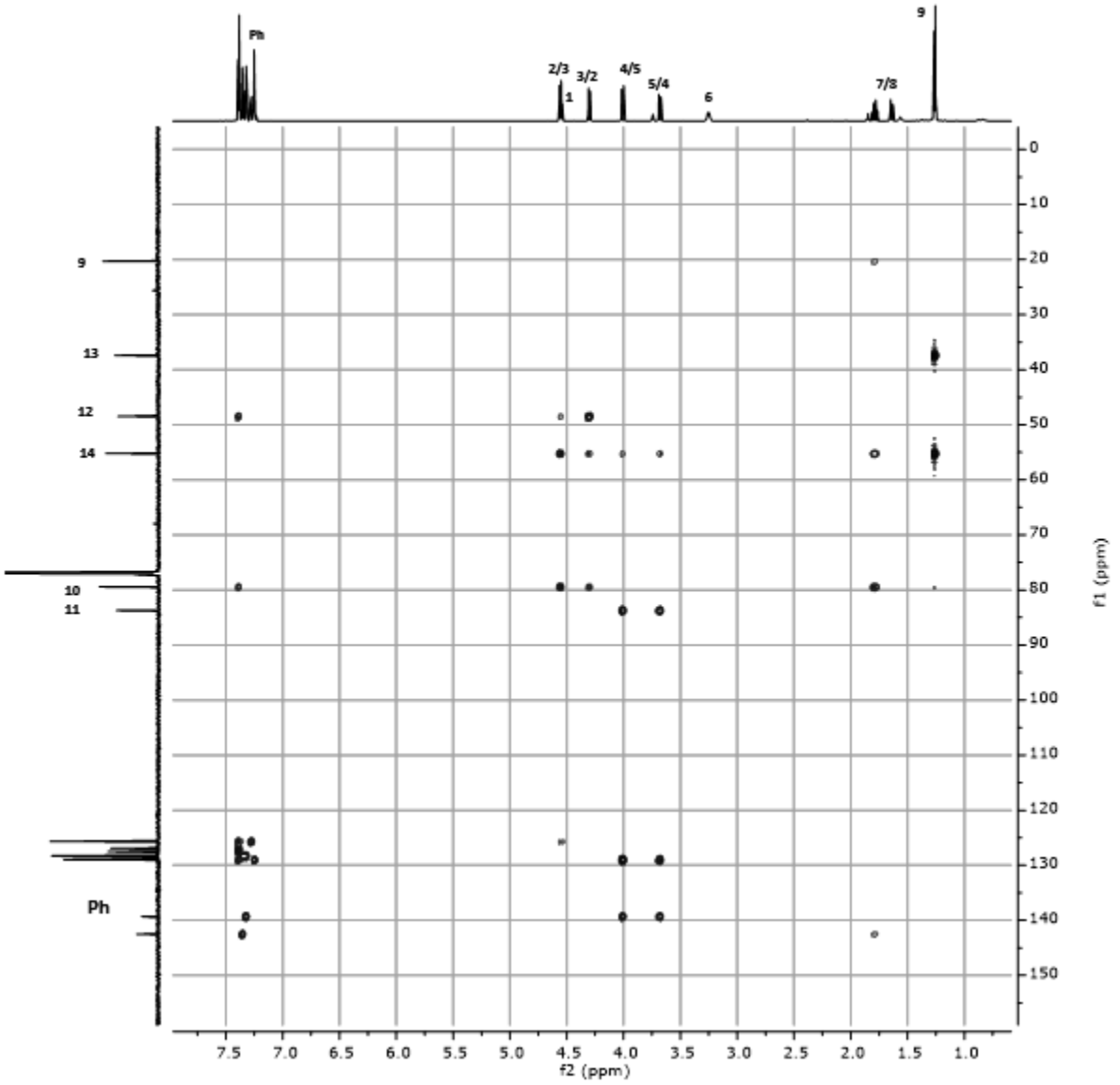

*NOESY Spectrum of **65**.*

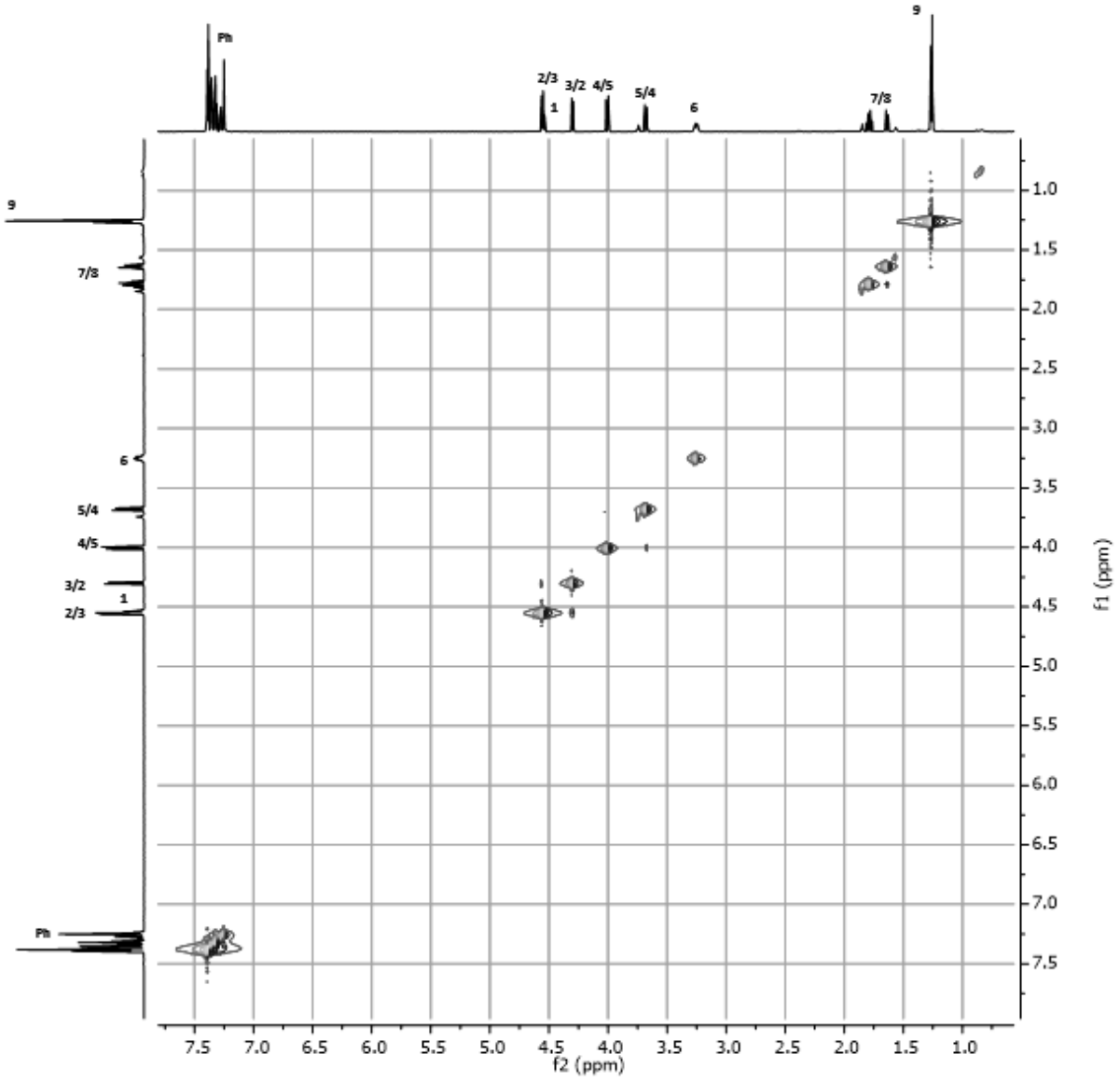

## Appendix 2

All X-ray crystallographic structures were acquired by Dr Andrei S. Batsanov, Durham University (2012-2014).

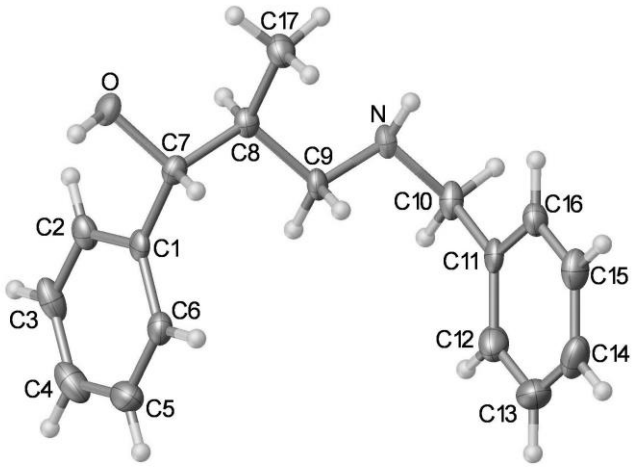


**Table 30** Crystal data and structure refinement for **74**.

| | |
|---|---|
| Identification code | 12srv128 (**74**) |
| Empirical formula | $C_{17}H_{21}NO$ |
| Formula weight | 255.35 |
| Temperature/K | 120 |
| Crystal system | monoclinic |
| Space group | $P2_1/c$ |
| a/Å | 13.1529(9) |
| b/Å | 13.0660(7) |
| c/Å | 9.0291(6) |
| α/° | 90.00 |
| β/° | 108.679(8) |
| γ/° | 90.00 |
| Volume/Å$^3$ | 1469.97(16) |
| Z | 4 |
| $\rho_{calc}$mg/mm$^3$ | 1.154 |
| m/mm$^{-1}$ | 0.071 |
| F(000) | 552.0 |
| Crystal size/mm$^3$ | 0.56 × 0.18 × 0.03 |
| 2Θ range for data collection | 5.7 to 49.98° |
| Index ranges | $-15 \leq h \leq 15$, $-15 \leq k \leq 15$, $-8 \leq l \leq 10$ |
| Reflections collected | 9045 |
| Independent reflections | 2586[R(int) = 0.0564] |
| Data/restraints/parameters | 2586/0/181 |
| Goodness-of-fit on $F^2$ | 1.107 |
| Final R indexes [I>=2σ (I)] | $R_1$ = 0.0652, $wR_2$ = 0.1485 |

| | |
|---|---|
| Final R indexes [all data] | $R_1$ = 0.0837, $wR_2$ = 0.1569 |
| Largest diff. peak/hole / e Å$^{-3}$ | 0.26/-0.20 |

**Table 31** Fractional Atomic Coordinates (×10$^4$) and Equivalent Isotropic Displacement Parameters (Å$^2$×10$^3$) for **74**. $U_{eq}$ is defined as 1/3 of of the trace of the orthogonalised $U_{IJ}$ tensor.

| Atom | *x* | *y* | *z* | U(eq) |
|---|---|---|---|---|
| O | 343.3(14) | 1516.2(14) | 4050(2) | 25.1(5) |
| N | 1160.6(18) | 4648.2(16) | 1735(2) | 22.8(5) |
| C1 | 2155(2) | 1717.5(18) | 3952(3) | 20.4(6) |
| C2 | 2031(2) | 991(2) | 2778(3) | 26.3(6) |
| C3 | 2902(2) | 492(2) | 2584(3) | 35.2(7) |
| C4 | 3922(3) | 706(2) | 3569(4) | 40.1(8) |
| C5 | 4060(2) | 1427(2) | 4747(4) | 36.9(7) |
| C6 | 3180(2) | 1927(2) | 4933(3) | 27.2(6) |
| C7 | 1179.6(19) | 2247.4(19) | 4161(3) | 20.6(6) |
| C8 | 708(2) | 3088.0(19) | 2961(3) | 20.7(6) |
| C9 | 1574(2) | 3857.1(18) | 2932(3) | 21.3(6) |
| C10 | 1994(2) | 5346(2) | 1578(3) | 26.6(6) |
| C11 | 2637(2) | 5895.6(19) | 3055(3) | 23.7(6) |
| C12 | 3741(2) | 5821(2) | 3618(4) | 35.0(7) |
| C13 | 4330(2) | 6336(2) | 4958(4) | 44.4(8) |
| C14 | 3816(3) | 6937(2) | 5759(4) | 39.8(8) |
| C15 | 2711(2) | 7009(2) | 5220(3) | 32.5(7) |
| C16 | 2128(2) | 6498(2) | 3885(3) | 26.9(6) |
| C17 | -230(2) | 3615(2) | 3301(3) | 28.1(6) |

**Table 32** Anisotropic Displacement Parameters (Å$^2$×10$^3$) for **74**. The Anisotropic displacement factor exponent takes the form: $-2\pi^2[h^2a^{*2}U_{11}+...+2hka\times b\times U_{12}]$

| Atom | $U_{11}$ | $U_{22}$ | $U_{33}$ | $U_{23}$ | $U_{13}$ | $U_{12}$ |
|---|---|---|---|---|---|---|
| O | 28.3(10) | 19.7(10) | 26.5(10) | 3.2(8) | 7.5(8) | -6.6(8) |
| N | 30.8(13) | 12.6(11) | 25.3(12) | 2.0(9) | 9.5(10) | 1.6(10) |
| C1 | 27.3(14) | 12.7(13) | 21.3(13) | 5.5(10) | 8.1(11) | -1.3(10) |
| C2 | 34.5(15) | 18.9(14) | 24.5(14) | 5.1(11) | 7.8(12) | 3.2(12) |
| C3 | 54(2) | 21.4(15) | 32.1(16) | 4.2(12) | 15.9(15) | 12.8(14) |
| C4 | 45.7(19) | 33.6(18) | 46.5(19) | 13.8(15) | 22.5(16) | 17.6(15) |
| C5 | 26.7(15) | 32.1(17) | 48.2(19) | 10.1(15) | 6.5(14) | 2.2(13) |
| C6 | 30.6(15) | 17.2(13) | 32.5(15) | 2.3(12) | 8.1(12) | -1.8(11) |
| C7 | 23.5(13) | 17.9(13) | 19.7(13) | -1(1) | 5.7(11) | -3.3(11) |
| C8 | 25.5(14) | 16.4(13) | 20.3(13) | 0.4(10) | 7.5(11) | 0.3(11) |
| C9 | 28.6(14) | 11.5(12) | 22.7(13) | 0.3(10) | 6.4(11) | 0.6(10) |
| C10 | 40.6(16) | 16.0(13) | 27.8(15) | 0.6(11) | 17.2(13) | -1.7(12) |
| C11 | 32.9(15) | 10.9(12) | 29.2(14) | 3.4(11) | 12.8(12) | -2.4(11) |

| | | | | | | |
|---|---|---|---|---|---|---|
| C12 | 33.5(16) | 23.3(15) | 51.8(19) | -1.0(14) | 18.7(14) | 0.6(13) |
| C13 | 27.0(16) | 34.2(18) | 62(2) | 5.2(16) | 0.7(15) | -2.4(14) |
| C14 | 50(2) | 24.2(16) | 36.0(17) | -1.3(13) | 1.5(15) | -11.8(14) |
| C15 | 46.7(18) | 19.7(14) | 32.8(16) | -3.4(12) | 15.0(14) | -2.2(13) |
| C16 | 31.7(15) | 16.6(13) | 31.8(15) | 0.1(12) | 9.4(12) | 0.9(12) |
| C17 | 30.5(15) | 21.8(14) | 34.1(15) | 1.3(12) | 13.5(12) | 3.1(12) |

**Table 33** Bond Lengths for **74**.

| Atom | Atom | Length/Å | Atom | Atom | Length/Å |
|---|---|---|---|---|---|
| O | C7 | 1.436(3) | C7 | C8 | 1.528(3) |
| N | C9 | 1.468(3) | C8 | C9 | 1.525(3) |
| N | C10 | 1.468(3) | C8 | C17 | 1.529(3) |
| C1 | C2 | 1.393(4) | C10 | C11 | 1.512(4) |
| C1 | C6 | 1.383(4) | C11 | C12 | 1.381(4) |
| C1 | C7 | 1.522(3) | C11 | C16 | 1.397(4) |
| C2 | C3 | 1.377(4) | C12 | C13 | 1.384(4) |
| C3 | C4 | 1.380(4) | C13 | C14 | 1.382(5) |
| C4 | C5 | 1.388(4) | C14 | C15 | 1.380(4) |
| C5 | C6 | 1.386(4) | C15 | C16 | 1.377(4) |

**Table 34** Bond Angles for **74**.

| Atom | Atom | Atom | Angle/° | Atom | Atom | Atom | Angle/° |
|---|---|---|---|---|---|---|---|
| C10 | N | C9 | 113.4(2) | C9 | C8 | C7 | 110.50(19) |
| C2 | C1 | C7 | 120.4(2) | C9 | C8 | C17 | 111.2(2) |
| C6 | C1 | C2 | 118.3(2) | N | C9 | C8 | 112.0(2) |
| C6 | C1 | C7 | 121.2(2) | N | C10 | C11 | 115.7(2) |
| C3 | C2 | C1 | 121.3(3) | C12 | C11 | C10 | 121.1(2) |
| C2 | C3 | C4 | 119.9(3) | C12 | C11 | C16 | 118.1(2) |
| C3 | C4 | C5 | 119.5(3) | C16 | C11 | C10 | 120.8(2) |
| C6 | C5 | C4 | 120.2(3) | C11 | C12 | C13 | 121.1(3) |
| C1 | C6 | C5 | 120.7(3) | C14 | C13 | C12 | 120.2(3) |
| O | C7 | C1 | 110.2(2) | C15 | C14 | C13 | 119.4(3) |
| O | C7 | C8 | 107.52(19) | C16 | C15 | C14 | 120.3(3) |
| C1 | C7 | C8 | 113.9(2) | C15 | C16 | C11 | 121.0(3) |
| C7 | C8 | C17 | 110.6(2) | | | | |

**Table 35** Hydrogen Bonds for **74**.

| D | H | A | d(D-H)/Å | d(H-A)/Å | d(D-A)/Å | D-H-A/° |
|---|---|---|---|---|---|---|
| O | H0 | $N^{1}$ | 0.92(4) | 1.86(4) | 2.771(3) | 168(4) |
| N | H1 | $O^{2}$ | 0.88(3) | 2.38(3) | 3.078(3) | 137(3) |

$^{1}$+X,$^{1/2}$-Y,$^{1/2}$+Z; $^{2}$-X,$^{1/2}$+Y,$^{1/2}$-Z

**Table 36** Hydrogen Atom Coordinates (Å×$10^4$) and Isotropic Displacement Parameters (Å$^2$×$10^3$) for **74**.

| Atom | *x* | *y* | *z* | U(eq) |
|---|---|---|---|---|
| H0 | 570(30) | 1190(30) | 5010(50) | 80(13) |
| H1 | 650(20) | 5000(20) | 1930(30) | 38(9) |
| H2 | 1346 | 840 | 2111 | 32 |
| H3 | 2803 | 11 | 1792 | 42 |
| H4 | 4513 | 370 | 3445 | 48 |
| H5 | 4746 | 1575 | 5413 | 44 |
| H6 | 3279 | 2409 | 5725 | 33 |
| H7 | 1391 | 2553 | 5207 | 25 |
| H8 | 436 | 2769 | 1926 | 25 |
| H9A | 1853 | 4181 | 3949 | 26 |
| H9B | 2161 | 3499 | 2728 | 26 |
| H10A | 1656 | 5855 | 793 | 32 |
| H10B | 2487 | 4959 | 1193 | 32 |
| H12 | 4095 | 5419 | 3088 | 42 |
| H13 | 5074 | 6277 | 5321 | 53 |
| H14 | 4211 | 7289 | 6653 | 48 |
| H15 | 2359 | 7405 | 5761 | 39 |
| H16 | 1384 | 6555 | 3530 | 32 |
| H17A | -744 | 3098 | 3403 | 42 |
| H17B | -587 | 4082 | 2442 | 42 |
| H17C | 38 | 4004 | 4278 | 42 |

**Experimental**

Single crystals of $C_{17}H_{21}NO$ **74**. A suitable crystal was selected and on a Gemini diffractometer. The crystal was kept at 120 K during data collection. Using Olex2 [1], the structure was solved with the XS [2] structure solution program using Direct Methods and refined with the XL [3] refinement package using Least Squares minimisation.


1. O. V. Dolomanov, L. J. Bourhis, R. J. Gildea, J. A. K. Howard and H. Puschmann, OLEX2: a complete structure solution, refinement and analysis program. *J. Appl. Cryst.* (2009). **42**, 339-341.
2. XS, G.M. Sheldrick, *Acta Cryst.* (2008). **A64**, 112-122.
3. XL, G.M. Sheldrick, *Acta Cryst.* (2008). **A64**, 112-122.


Crystal structure determination of **74**.

**Crystal Data.** $C_{17}H_{21}NO$, *M* =255.35, monoclinic, *a* = 13.1529(9) Å, *b* = 13.0660(7) Å, *c* = 9.0291(6) Å, *β* = 108.679(8)°, *V* = 1469.97(16) Å$^3$, *T* = 120, space group $P2_1/c$ (no. 14), *Z* = 4, μ(Mo Kα) = 0.071, 9045 reflections measured, 2586 unique ($R_{int}$ = 0.0564)

which were used in all calculations. The final $wR_2$ was 0.1569 (all data) and $R_1$ was 0.0652 (I>2\s(I)).

This report has been created with Olex2, compiled on 2012.07.17 svn.r2416.

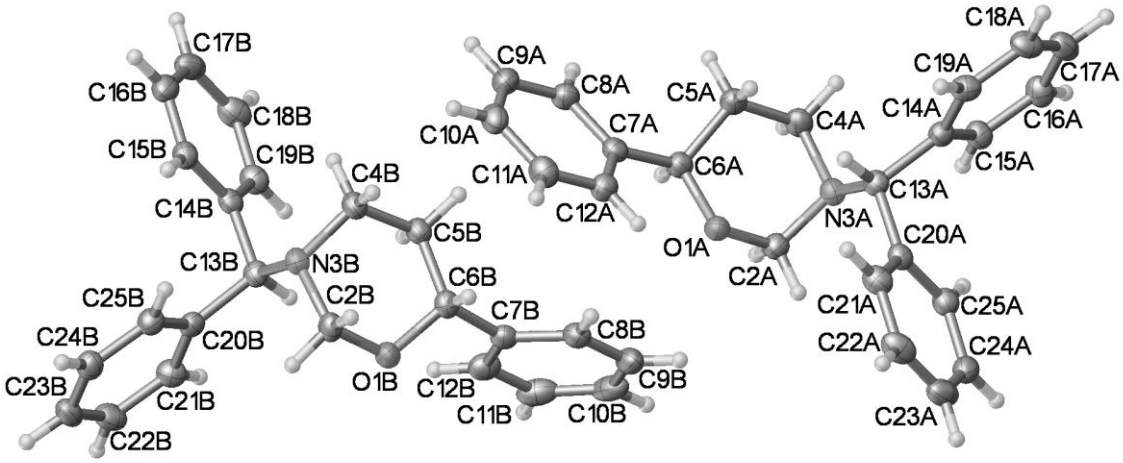


**Table 37** Crystal data and structure refinement for **129**.

| | |
|---|---|
| Identification code | 13srv136 (**129**) |
| Empirical formula | $C_{23}H_{23}NO$ |
| Formula weight | 329.42 |
| Temperature/K | 120 |
| Crystal system | triclinic |
| Space group | P1 |
| a/Å | 6.0216(3) |
| b/Å | 9.2574(4) |
| c/Å | 16.7185(8) |
| α/° | 79.272(8) |
| β/° | 80.758(10) |
| γ/° | 89.418(10) |
| Volume/Å$^3$ | 903.60(8) |
| Z | 2 |
| $\rho_{calc}$mg/mm$^3$ | 1.211 |
| m/mm$^{-1}$ | 0.567 |
| F(000) | 352.0 |
| Crystal size/mm$^3$ | 0.3 × 0.2 × 0.2 |
| 2Θ range for data collection | 5.452 to 134.674° |
| Index ranges | $-6 \le h \le 6$, $-10 \le k \le 11$, $-19 \le l \le 19$ |
| Reflections collected | 19622 |
| Independent reflections | 5382[R(int) = 0.0272] |
| Data/restraints/parameters | 5382/3/452 |

| | |
|---|---|
| Goodness-of-fit on $F^2$ | 1.035 |
| Final R indexes [I>=2σ (I)] | $R_1$ = 0.0242, $wR_2$ = 0.0650 |
| Final R indexes [all data] | $R_1$ = 0.0242, $wR_2$ = 0.0651 |
| Largest diff. peak/hole / e Å$^{-3}$ | 0.12/-0.12 |
| Flack parameter | 0.090(36) |

**Table 38** Fractional Atomic Coordinates (×10$^4$) and Equivalent Isotropic Displacement Parameters (Å$^2$×10$^3$) for **129**. $U_{eq}$ is defined as 1/3 of of the trace of the orthogonalised $U_{IJ}$ tensor.

| **Atom** | ***x*** | ***y*** | ***z*** | **U(eq)** |
|---|---|---|---|---|
| O1A | 6348(2) | 7176.0(13) | 3534.1(8) | 26.6(3) |
| N3A | 4983(3) | 9272.0(17) | 2661.6(10) | 26.9(4) |
| C2A | 5088(4) | 7693(2) | 2883.7(12) | 27.3(5) |
| C4A | 4004(4) | 9846(2) | 3407.0(13) | 31.1(5) |
| C5A | 5190(4) | 9290(2) | 4139.4(13) | 30.9(5) |
| C6A | 5311(4) | 7618(2) | 4281.4(12) | 26.9(4) |
| C7A | 6576(3) | 6980.8(19) | 4971.0(12) | 25.9(4) |
| C8A | 5681(4) | 7098(2) | 5778.1(12) | 31.8(5) |
| C9A | 6813(4) | 6534(2) | 6423.3(13) | 34.1(5) |
| C10A | 8842(4) | 5843(2) | 6272.4(12) | 34.3(5) |
| C11A | 9738(4) | 5720(2) | 5473.8(13) | 34.5(5) |
| C12A | 8616(3) | 6291(2) | 4822.4(12) | 30.2(4) |
| C13A | 7147(3) | 10015(2) | 2257.0(12) | 24.6(4) |
| C14A | 6766(3) | 11629(2) | 1924.7(12) | 25.2(4) |
| C15A | 4852(4) | 12103(2) | 1591.0(13) | 28.8(5) |
| C16A | 4605(4) | 13572(2) | 1264.1(13) | 32.2(5) |
| C17A | 6265(4) | 14597(2) | 1267.2(14) | 35.2(5) |
| C18A | 8162(4) | 14143(2) | 1603.7(14) | 34.3(5) |
| C19A | 8418(4) | 12668(2) | 1928.0(13) | 29.9(5) |
| C20A | 8275(3) | 9250.7(19) | 1572.3(12) | 25.0(4) |
| C21A | 10352(4) | 8613(2) | 1619.5(14) | 31.5(5) |
| C22A | 11382(4) | 7890(2) | 1003.6(15) | 37.6(5) |
| C23A | 10350(4) | 7800(2) | 336.5(14) | 38.7(6) |
| C24A | 8286(4) | 8441(2) | 281.1(13) | 34.4(5) |
| C25A | 7254(4) | 9171(2) | 890.8(13) | 29.0(5) |
| O1B | 4956(2) | 804.5(14) | 5984.9(8) | 29.4(3) |
| N3B | 5053(3) | 992.4(17) | 7401.6(10) | 25.5(4) |
| C2B | 6124(4) | 467(2) | 6678.3(12) | 28.7(5) |
| C4B | 4891(4) | 2605(2) | 7179.4(13) | 28.0(5) |
| C5B | 3719(4) | 3075(2) | 6431.1(12) | 27.6(4) |

| | | | | |
|---|---|---|---|---|
| C6B | 4832(3) | 2368(2) | 5715.1(12) | 26.8(4) |
| C7B | 3569(3) | 2634(2) | 4995.9(12) | 26.8(4) |
| C8B | 4354(4) | 3652(2) | 4290.3(12) | 31.0(5) |
| C9B | 3117(5) | 3966(2) | 3652.6(14) | 39.4(6) |
| C10B | 1067(4) | 3268(2) | 3717.2(14) | 43.0(6) |
| C11B | 285(4) | 2221(3) | 4407.0(14) | 41.4(5) |
| C12B | 1538(3) | 1901(2) | 5043.6(13) | 32.9(4) |
| C13B | 2875(3) | 224(2) | 7762.7(12) | 25.0(4) |
| C14B | 1671(3) | 951.4(19) | 8450.4(12) | 25.1(4) |
| C15B | 2637(4) | 1044(2) | 9142.0(12) | 27.9(5) |
| C16B | 1562(4) | 1767(2) | 9742.5(13) | 34.0(5) |
| C17B | -499(4) | 2405(2) | 9669.1(14) | 36.2(5) |
| C18B | -1489(4) | 2301(2) | 8990.4(15) | 36.5(5) |
| C19B | -416(4) | 1576(2) | 8388.3(13) | 30.5(5) |
| C20B | 3228(3) | -1400(2) | 8076.3(11) | 25.6(4) |
| C21B | 1633(4) | -2431(2) | 8016.3(13) | 30.8(5) |
| C22B | 1827(4) | -3908(2) | 8342.8(14) | 36.0(5) |
| C23B | 3632(4) | -4380(2) | 8735.0(13) | 34.6(5) |
| C24B | 5254(4) | -3369(2) | 8785.2(13) | 31.4(5) |
| C25B | 5062(4) | -1889(2) | 8455.2(12) | 27.9(5) |

**Table 39** Anisotropic Displacement Parameters ($Å^2 \times 10^3$) for **129**. The Anisotropic displacement factor exponent takes the form: $-2\pi^2[h^2a^{*2}U_{11}+...+2hka \times b \times U_{12}]$

| **Atom** | **$U_{11}$** | **$U_{22}$** | **$U_{33}$** | **$U_{23}$** | **$U_{13}$** | **$U_{12}$** |
|---|---|---|---|---|---|---|
| O1A | 31.6(8) | 23.8(6) | 24.6(7) | -5.7(5) | -4.1(6) | 3.8(6) |
| N3A | 27.3(10) | 25.2(8) | 27.1(9) | -2.8(7) | -3.9(7) | 1.2(7) |
| C2A | 30.4(12) | 26.6(10) | 25(1) | -4.7(8) | -4.7(9) | -1.5(8) |
| C4A | 32.1(12) | 28.4(10) | 31.0(11) | -4.7(8) | -0.8(9) | 6.4(9) |
| C5A | 37.8(13) | 27.7(10) | 26.4(10) | -6.3(8) | -1.7(9) | 5.1(9) |
| C6A | 29.1(12) | 24.9(9) | 25.4(10) | -4.2(8) | -1.2(8) | 1.0(8) |
| C7A | 29.1(11) | 20.7(9) | 27.8(9) | -4.7(7) | -3.8(8) | -1.7(8) |
| C8A | 37.3(13) | 27.8(10) | 30(1) | -7.2(8) | -2.3(9) | 4.2(9) |
| C9A | 46.9(14) | 29.5(10) | 26(1) | -6.1(8) | -5.5(9) | 0.7(9) |
| C10A | 41.7(13) | 30.2(10) | 32.1(11) | -2.5(8) | -13.0(9) | -1.8(9) |
| C11A | 32.1(12) | 32.2(10) | 39.0(11) | -3.7(8) | -8.4(9) | 4.0(9) |
| C12A | 32.1(12) | 30.4(10) | 27.3(10) | -4.9(8) | -3.0(8) | 0.0(8) |
| C13A | 24.2(12) | 25.1(10) | 25.3(10) | -4.4(8) | -6.7(8) | 0.9(8) |
| C14A | 25.9(11) | 25.9(10) | 23.8(10) | -5.8(8) | -2.5(8) | 0.6(8) |
| C15A | 27.8(12) | 26.3(10) | 31.2(11) | -3.2(8) | -4.1(9) | -0.6(9) |
| C16A | 29.0(13) | 30.4(10) | 35.3(11) | -2.2(9) | -4.2(9) | 6.3(9) |

| | | | | | | |
|---|---|---|---|---|---|---|
| C17A | 39.4(14) | 24.4(10) | 37.9(12) | -4.7(9) | 3.9(10) | 2.8(9) |
| C18A | 33.3(13) | 27.9(10) | 41.5(12) | -10.5(9) | -0.3(10) | -6.5(9) |
| C19A | 27.9(12) | 31.1(10) | 32.5(11) | -10.8(9) | -4.7(9) | 0.2(9) |
| C20A | 25.0(12) | 21.4(9) | 27.5(10) | -2.2(8) | -3.6(9) | -1.4(8) |
| C21A | 27.6(12) | 28.8(10) | 38.9(12) | -5.9(9) | -7.8(9) | 0.7(9) |
| C22A | 27.7(13) | 30.3(11) | 52.4(14) | -8.4(10) | 1.7(10) | 3.6(9) |
| C23A | 46.1(15) | 27.6(11) | 38.3(12) | -8.9(9) | 9.1(11) | -4.9(10) |
| C24A | 48.2(15) | 27.6(10) | 26.8(11) | -3.9(8) | -5.5(10) | -5(1) |
| C25A | 30.8(12) | 26.3(10) | 29.7(11) | -3.3(8) | -6.5(9) | -0.1(8) |
| O1B | 37.7(9) | 23.8(7) | 25.9(7) | -3.8(5) | -4.2(6) | 4.4(6) |
| N3B | 26.3(10) | 23.3(8) | 25.6(8) | -1.5(6) | -3.6(7) | -0.6(7) |
| C2B | 30.9(12) | 27.6(10) | 25.7(10) | -0.1(8) | -5.0(9) | 5.1(9) |
| C4B | 31.3(12) | 23.7(10) | 28.7(10) | -2.3(8) | -6.6(9) | -1.3(8) |
| C5B | 32.5(12) | 22.5(9) | 27.7(10) | -3.1(8) | -6.6(9) | -0.1(8) |
| C6B | 27.3(12) | 25.3(9) | 26.4(10) | -1.4(8) | -3.9(8) | 0.1(8) |
| C7B | 29.0(11) | 24.4(9) | 27.3(9) | -7.8(7) | -2.5(8) | 4.7(8) |
| C8B | 38.5(12) | 24.8(10) | 30.9(10) | -7.4(8) | -6.6(9) | 3.5(8) |
| C9B | 62.9(17) | 27.5(11) | 30.6(11) | -7.4(8) | -14.1(11) | 10(1) |
| C10B | 54.9(15) | 44.2(13) | 41.3(12) | -23.3(10) | -24.8(10) | 22.5(11) |
| C11B | 31.6(12) | 51.1(13) | 50.8(13) | -29.3(11) | -11.4(10) | 8.9(10) |
| C12B | 29.9(11) | 35.6(10) | 33.7(10) | -12.4(8) | 0.0(8) | 1.4(8) |
| C13B | 24.4(12) | 26.2(10) | 25.3(10) | -4.1(8) | -7.3(8) | 0.2(8) |
| C14B | 26.0(11) | 20.2(9) | 28.2(10) | -2.2(7) | -4.3(9) | -2.7(8) |
| C15B | 29.8(12) | 25.2(9) | 28.0(11) | -1.6(8) | -6.6(9) | -1.3(8) |
| C16B | 45.1(15) | 28.2(11) | 28.4(11) | -4.4(9) | -5.1(10) | -6.8(10) |
| C17B | 42.3(14) | 26.9(10) | 36.0(12) | -9.3(9) | 8.1(10) | -3(1) |
| C18B | 28.0(12) | 31.2(11) | 48.3(13) | -8.1(10) | 1.1(10) | 1.0(9) |
| C19B | 27.7(13) | 28.2(10) | 35.7(12) | -4.6(9) | -7.1(9) | 1.1(9) |
| C20B | 28.0(12) | 25.9(10) | 22.0(9) | -5.4(7) | -0.9(8) | 0.8(8) |
| C21B | 28.0(12) | 31.2(10) | 33.7(11) | -7.9(9) | -4.5(9) | 1.1(9) |
| C22B | 37.7(14) | 27.7(10) | 41.5(12) | -10.0(9) | 1.2(10) | -5.5(10) |
| C23B | 43.9(14) | 21.9(10) | 34.1(12) | -2.7(8) | 2.1(10) | 3.1(9) |
| C24B | 33.7(13) | 30.6(10) | 28.3(11) | -3.5(8) | -3.1(9) | 5.8(9) |
| C25B | 28.5(13) | 28.7(10) | 26.6(10) | -5.5(8) | -4.5(9) | -0.8(9) |

**Table 40** Bond Lengths for **129**.

| Atom | Atom | Length/Å | Atom | Atom | Length/Å |
|---|---|---|---|---|---|
| O1A | C2A | 1.432(2) | O1B | C2B | 1.435(2) |
| O1A | C6A | 1.433(2) | O1B | C6B | 1.439(2) |

| | | | | | |
|---|---|---|---|---|---|
| N3A | C2A | 1.443(2) | N3B | C2B | 1.441(3) |
| N3A | C4A | 1.479(3) | N3B | C4B | 1.476(2) |
| N3A | C13A | 1.480(3) | N3B | C13B | 1.481(3) |
| C4A | C5A | 1.521(3) | C4B | C5B | 1.526(3) |
| C5A | C6A | 1.525(3) | C5B | C6B | 1.528(3) |
| C6A | C7A | 1.509(3) | C6B | C7B | 1.505(3) |
| C7A | C8A | 1.394(3) | C7B | C8B | 1.385(3) |
| C7A | C12A | 1.387(3) | C7B | C12B | 1.389(3) |
| C8A | C9A | 1.386(3) | C8B | C9B | 1.382(3) |
| C9A | C10A | 1.382(3) | C9B | C10B | 1.379(4) |
| C10A | C11A | 1.382(3) | C10B | C11B | 1.382(3) |
| C11A | C12A | 1.392(3) | C11B | C12B | 1.388(3) |
| C13A | C14A | 1.523(3) | C13B | C14B | 1.520(3) |
| C13A | C20A | 1.521(3) | C13B | C20B | 1.522(3) |
| C14A | C15A | 1.392(3) | C14B | C15B | 1.391(3) |
| C14A | C19A | 1.392(3) | C14B | C19B | 1.389(3) |
| C15A | C16A | 1.384(3) | C15B | C16B | 1.381(3) |
| C16A | C17A | 1.386(3) | C16B | C17B | 1.383(3) |
| C17A | C18A | 1.381(3) | C17B | C18B | 1.382(3) |
| C18A | C19A | 1.389(3) | C18B | C19B | 1.384(3) |
| C20A | C21A | 1.385(3) | C20B | C21B | 1.389(3) |
| C20A | C25A | 1.392(3) | C20B | C25B | 1.391(3) |
| C21A | C22A | 1.391(3) | C21B | C22B | 1.386(3) |
| C22A | C23A | 1.377(3) | C22B | C23B | 1.384(3) |
| C23A | C24A | 1.381(3) | C23B | C24B | 1.382(3) |
| C24A | C25A | 1.388(3) | C24B | C25B | 1.390(3) |

**Table 41** Bond Angles for **129**.

| Atom | Atom | Atom | Angle/° | Atom | Atom | Atom | Angle/° |
|---|---|---|---|---|---|---|---|
| C2A | O1A | C6A | 110.26(14) | C2B | O1B | C6B | 111.12(14) |
| C2A | N3A | C4A | 108.20(15) | C2B | N3B | C4B | 107.85(15) |
| C2A | N3A | C13A | 114.63(16) | C2B | N3B | C13B | 112.15(15) |
| C4A | N3A | C13A | 112.15(15) | C4B | N3B | C13B | 114.06(16) |
| O1A | C2A | N3A | 114.80(15) | O1B | C2B | N3B | 114.36(17) |
| N3A | C4A | C5A | 112.70(17) | N3B | C4B | C5B | 112.33(16) |
| C4A | C5A | C6A | 110.01(16) | C4B | C5B | C6B | 110.16(17) |
| O1A | C6A | C5A | 109.32(15) | O1B | C6B | C5B | 109.91(15) |
| O1A | C6A | C7A | 109.42(15) | O1B | C6B | C7B | 108.01(15) |
| C7A | C6A | C5A | 113.39(16) | C7B | C6B | C5B | 112.57(17) |

| | | | | | | | |
|---|---|---|---|---|---|---|---|
| C8A | C7A | C6A | 119.18(18) | C8B | C7B | C6B | 120.98(18) |
| C12A | C7A | C6A | 121.73(16) | C8B | C7B | C12B | 118.77(18) |
| C12A | C7A | C8A | 119.09(18) | C12B | C7B | C6B | 120.20(17) |
| C9A | C8A | C7A | 120.48(19) | C9B | C8B | C7B | 120.9(2) |
| C10A | C9A | C8A | 120.22(19) | C10B | C9B | C8B | 119.9(2) |
| C11A | C10A | C9A | 119.60(19) | C9B | C10B | C11B | 120.0(2) |
| C10A | C11A | C12A | 120.5(2) | C10B | C11B | C12B | 119.9(2) |
| C7A | C12A | C11A | 120.12(17) | C11B | C12B | C7B | 120.43(19) |
| N3A | C13A | C14A | 110.02(16) | N3B | C13B | C14B | 110.10(15) |
| N3A | C13A | C20A | 110.74(15) | N3B | C13B | C20B | 110.70(16) |
| C20A | C13A | C14A | 110.97(15) | C14B | C13B | C20B | 110.98(15) |
| C15A | C14A | C13A | 122.35(17) | C15B | C14B | C13B | 121.47(18) |
| C15A | C14A | C19A | 118.49(19) | C19B | C14B | C13B | 120.11(18) |
| C19A | C14A | C13A | 119.13(19) | C19B | C14B | C15B | 118.39(19) |
| C16A | C15A | C14A | 120.73(19) | C16B | C15B | C14B | 120.6(2) |
| C15A | C16A | C17A | 120.3(2) | C15B | C16B | C17B | 120.6(2) |
| C18A | C17A | C16A | 119.5(2) | C18B | C17B | C16B | 119.3(2) |
| C17A | C18A | C19A | 120.24(19) | C17B | C18B | C19B | 120.3(2) |
| C18A | C19A | C14A | 120.7(2) | C18B | C19B | C14B | 120.9(2) |
| C21A | C20A | C13A | 120.13(18) | C21B | C20B | C13B | 119.54(19) |
| C21A | C20A | C25A | 118.66(19) | C21B | C20B | C25B | 118.34(19) |
| C25A | C20A | C13A | 121.21(18) | C25B | C20B | C13B | 122.06(17) |
| C20A | C21A | C22A | 120.6(2) | C22B | C21B | C20B | 121.1(2) |
| C23A | C22A | C21A | 120.4(2) | C23B | C22B | C21B | 120.1(2) |
| C22A | C23A | C24A | 119.4(2) | C24B | C23B | C22B | 119.4(2) |
| C23A | C24A | C25A | 120.5(2) | C23B | C24B | C25B | 120.4(2) |
| C24A | C25A | C20A | 120.4(2) | C24B | C25B | C20B | 120.62(19) |

**Table 42** Hydrogen Atom Coordinates (Å×$10^4$) and Isotropic Displacement Parameters (Å$^2$×$10^3$) for **129**.

| **Atom** | ***x*** | ***y*** | ***z*** | **U(eq)** |
|---|---|---|---|---|
| H2A1 | 3534 | 7285 | 3053 | 33 |
| H2A2 | 5766 | 7304 | 2389 | 33 |
| H41A | 2393 | 9551 | 3556 | 37 |
| H42A | 4098 | 10934 | 3281 | 37 |
| H51A | 4360 | 9597 | 4639 | 37 |
| H52A | 6730 | 9723 | 4033 | 37 |
| H6A | 3740 | 7204 | 4425 | 32 |
| H8A | 4285 | 7569 | 5887 | 38 |
| H9A | 6193 | 6622 | 6971 | 41 |

| | | | | |
|---|---|---|---|---|
| H10A | 9617 | 5454 | 6715 | 41 |
| H11A | 11129 | 5243 | 5369 | 41 |
| H12A | 9248 | 6208 | 4275 | 36 |
| H13A | 8163 | 9959 | 2679 | 30 |
| H15A | 3702 | 11410 | 1587 | 35 |
| H16A | 3292 | 13880 | 1037 | 39 |
| H17A | 6098 | 15604 | 1039 | 42 |
| H18A | 9297 | 14843 | 1613 | 41 |
| H19A | 9734 | 12366 | 2154 | 36 |
| H21A | 11081 | 8670 | 2077 | 38 |
| H22A | 12806 | 7456 | 1044 | 45 |
| H23A | 11051 | 7301 | -82 | 46 |
| H24A | 7567 | 8383 | -178 | 41 |
| H25A | 5842 | 9618 | 843 | 35 |
| H2B1 | 7664 | 899 | 6515 | 34 |
| H2B2 | 6263 | -614 | 6821 | 34 |
| H41B | 6424 | 3051 | 7060 | 34 |
| H42B | 4049 | 2980 | 7655 | 34 |
| H51B | 3808 | 4159 | 6263 | 33 |
| H52B | 2110 | 2773 | 6577 | 33 |
| H6B | 6394 | 2785 | 5526 | 32 |
| H8B | 5761 | 4141 | 4244 | 37 |
| H9B | 3679 | 4662 | 3170 | 47 |
| H10B | 192 | 3507 | 3288 | 52 |
| H11B | -1109 | 1721 | 4445 | 50 |
| H12B | 1003 | 1175 | 5515 | 39 |
| H13B | 1915 | 309 | 7321 | 30 |
| H15B | 4048 | 605 | 9202 | 33 |
| H16B | 2245 | 1827 | 10210 | 41 |
| H17B | -1228 | 2910 | 10081 | 43 |
| H18B | -2911 | 2729 | 8937 | 44 |
| H19B | -1116 | 1505 | 7926 | 37 |
| H21B | 389 | -2119 | 7747 | 37 |
| H22B | 718 | -4598 | 8297 | 43 |
| H23B | 3755 | -5389 | 8968 | 42 |
| H24B | 6508 | -3689 | 9047 | 38 |
| H25B | 6194 | -1206 | 8489 | 33 |

## Experimental

Single crystals of $C_{23}H_{23}NO$ [**129**]. A suitable crystal was selected and on a Bruker APEX2 microsource diffractometer. The crystal was kept at 120 K during data collection. Using Olex2 [1], the structure was solved with the XS [2] structure solution program using Direct Methods and refined with the ShelXL-2012 [3] refinement package using Least Squares minimisation.


1. O. V. Dolomanov, L. J. Bourhis, R. J. Gildea, J. A. K. Howard and H. Puschmann, OLEX2: a complete structure solution, refinement and analysis program. J. Appl. Cryst. (2009). **42**, 339-341.
2. XS, G.M. Sheldrick, Acta Cryst. (2008). **A64**, 112-122.
3. SHELXL-2012, G.M. Sheldrick, Acta Cryst. (2008). **A64**, 112-122.


## Crystal structure determination of 129.

**Crystal Data** for $C_{23}H_{23}NO$ ($M$ =329.42): triclinic, space group P1 (no. 1), $a$ = 6.0216(3) Å, $b$ = 9.2574(4) Å, $c$ = 16.7185(8) Å, $\alpha$ = 79.272(8)°, $\beta$ = 80.758(10)°, $\gamma$ = 89.418(10)°, $V$ = 903.60(8) Å$^3$, $Z$ = 2, $T$ = 120 K, μ(Cu Kα) = 0.567 mm$^{-1}$, *Dcalc* = 1.211 g/mm$^3$, 19622 reflections measured (5.452 ≤ 2Θ ≤ 134.674), 5382 unique ($R_{int}$ = 0.0272) which were used in all calculations. The final $R_1$ was 0.0242 (I > 2σ(I)) and $wR_2$ was 0.0651 (all data).

This report has been created with Olex2, compiled on Apr 23 2013 17:54:37.

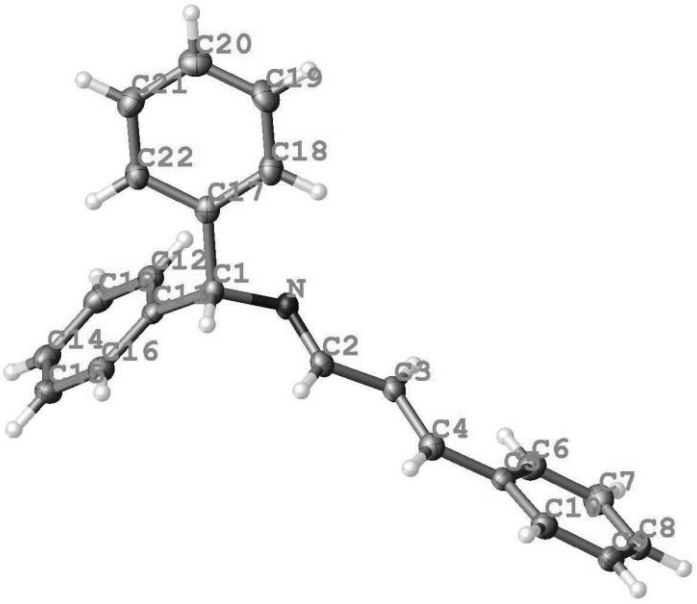

**Table 43 Crystal data and structure refinement for 119.**

| | |
|---|---|
| Identification code | **119** |
| Empirical formula | $C_{22}H_{19}N$ |
| Formula weight | 297.38 |
| Temperature/K | 120 |
| Crystal system | monoclinic |
| Space group | $P2_1/c$ |
| a/Å | 5.4941(2) |
| b/Å | 24.8448(10) |
| c/Å | 12.4135(5) |
| α/° | 90 |
| β/° | 102.044(4) |
| γ/° | 90 |
| Volume/Å$^3$ | 1657.15(12) |
| Z | 4 |
| $\rho_{calc}$g/cm$^3$ | 1.192 |
| μ/mm$^{-1}$ | 0.069 |
| F(000) | 632.0 |
| Crystal size/mm$^3$ | 0.4 × 0.1 × 0.08 |
| Radiation | MoKα (λ = 0.71073) |
| 2Θ range for data collection/° | 3.734 to 55.728 |
| Index ranges | $-6 \le h \le 6$, $-30 \le k \le 32$, $-15 \le l \le 15$ |
| Reflections collected | 11019 |
| Independent reflections | 3426 [$R_{int}$ = 0.0288, $R_{sigma}$ = 0.0269] |
| Data/restraints/parameters | 3426/0/208 |
| Goodness-of-fit on $F^2$ | 1.059 |
| Final R indexes [I>=2σ (I)] | $R_1$ = 0.0397, $wR_2$ = 0.0903 |
| Final R indexes [all data] | $R_1$ = 0.0495, $wR_2$ = 0.0961 |
| Largest diff. peak/hole / e Å$^{-3}$ | 0.22/-0.20 |

**Table 44** Fractional Atomic Coordinates (×10$^4$) and Equivalent Isotropic Displacement Parameters (Å$^2$×10$^3$) for **119**. $U_{eq}$ is defined as 1/3 of of the trace of the orthogonalised $U_{IJ}$ tensor.

| **Atom** | ***x*** | ***y*** | ***z*** | **U(eq)** |
|---|---|---|---|---|
| N | 2825.9(19) | 3983.4(4) | 1787.8(8) | 22.0(2) |
| C11 | 3333(2) | 4028.4(5) | 3766.2(9) | 19.9(3) |
| C4 | 6747(2) | 3525.8(5) | -12.4(10) | 23.8(3) |
| C2 | 4719(2) | 3928.4(5) | 1355.0(9) | 21.5(3) |
| C5 | 7106(2) | 3155.8(5) | -888.6(10) | 21.2(3) |
| C3 | 4803(2) | 3547.0(5) | 475.2(9) | 22.2(3) |
| C1 | 3117(2) | 4361.3(5) | 2723.2(9) | 20.6(3) |
| C16 | 5476(2) | 4054.0(5) | 4586.7(10) | 24.1(3) |
| C13 | 1704(2) | 3354.9(5) | 4828.9(11) | 26.0(3) |
| C21 | -1509(3) | 5411.6(5) | 3300.0(11) | 28.9(3) |

| | | | | |
|---|---|---|---|---|
| C14 | 3857(2) | 3383.4(5) | 5641.4(10) | 27.4(3) |
| C12 | 1442(2) | 3676.7(5) | 3897.9(10) | 23.0(3) |
| C17 | 993(2) | 4767.1(5) | 2550.4(10) | 20.8(3) |
| C6 | 5732(2) | 2682.1(5) | -1135.2(10) | 25.7(3) |
| C7 | 6158(3) | 2340.3(5) | -1952.9(11) | 30.5(3) |
| C19 | -2129(3) | 5297.6(5) | 1348.1(11) | 30.7(3) |
| C9 | 9351(2) | 2926.9(6) | -2308.1(11) | 28.9(3) |
| C10 | 8925(2) | 3272.3(5) | -1491(1) | 25.5(3) |
| C8 | 7981(3) | 2460.5(6) | -2540.6(11) | 30.2(3) |
| C22 | 344(2) | 5024.5(5) | 3447.4(10) | 24.9(3) |
| C15 | 5741(2) | 3734.0(6) | 5523.6(10) | 27.8(3) |
| C18 | -264(2) | 4912.3(5) | 1498.7(10) | 26.2(3) |
| C20 | -2764(3) | 5548.8(5) | 2247.4(11) | 29.5(3) |

**Table 45** Anisotropic Displacement Parameters ($Å^2×10^3$) for 119. The Anisotropic displacement factor exponent takes the form: $-2\pi^2[h^2a^{*2}U_{11}+2hka^*b^*U_{12}+\ldots]$.

| Atom | $U_{11}$ | $U_{22}$ | $U_{33}$ | $U_{23}$ | $U_{13}$ | $U_{12}$ |
|---|---|---|---|---|---|---|
| N | 24.3(5) | 22.9(5) | 18.6(5) | -1.5(4) | 4.2(4) | -0.7(4) |
| C11 | 21.4(6) | 19.5(6) | 19.7(6) | -2.5(5) | 6.4(5) | 2.3(5) |
| C4 | 25.9(7) | 22.4(6) | 23.0(6) | 0.8(5) | 4.6(5) | -1.1(5) |
| C2 | 23.3(6) | 22.5(6) | 18.1(6) | 3.1(5) | 2.5(5) | -1.1(5) |
| C5 | 21.0(6) | 22.5(6) | 19.5(6) | 3.3(5) | 3.0(5) | 3.8(5) |
| C3 | 23.9(6) | 23.6(6) | 17.8(6) | 1.9(5) | 1.7(5) | 1.1(5) |
| C1 | 21.9(6) | 21.4(6) | 18.8(6) | -2.5(5) | 4.5(5) | -4.2(5) |
| C16 | 20.6(6) | 28.0(7) | 24.1(6) | -0.1(5) | 5.7(5) | -0.5(5) |
| C13 | 25.5(7) | 23.9(6) | 31.8(7) | 1.9(5) | 12.9(5) | 0.9(5) |
| C21 | 35.4(8) | 24.8(7) | 27.9(7) | -1.8(5) | 10.2(6) | 1.4(6) |
| C14 | 30.7(7) | 29.1(7) | 24.7(6) | 6.8(5) | 11.2(5) | 11.1(6) |
| C12 | 20.7(6) | 24.5(6) | 23.8(6) | -1.1(5) | 4.8(5) | 0.3(5) |
| C17 | 22.8(6) | 18.3(6) | 21.9(6) | 0.2(5) | 5.8(5) | -5.7(5) |
| C6 | 27.2(7) | 22.7(6) | 28.7(7) | 3.7(5) | 9.2(5) | 1.5(5) |
| C7 | 35.7(8) | 22.0(6) | 33.2(7) | -1.7(5) | 5.6(6) | 1.5(6) |
| C19 | 39.0(8) | 26.6(7) | 24.0(7) | 7.5(5) | 1.3(6) | 1.9(6) |
| C9 | 23.8(7) | 41.9(8) | 22.1(6) | 3.5(6) | 7.3(5) | 6.1(6) |
| C10 | 22.4(6) | 29.5(7) | 24.5(6) | 1.5(5) | 4.6(5) | -1.5(5) |
| C8 | 33.7(7) | 33.7(7) | 22.2(7) | -3.1(5) | 3.9(5) | 10.1(6) |
| C22 | 29.8(7) | 24.7(6) | 19.3(6) | 0.1(5) | 2.9(5) | -0.2(5) |
| C15 | 21.8(6) | 36.8(7) | 24.3(6) | 2.8(5) | 3.5(5) | 6.2(6) |
| C18 | 35.9(7) | 23.2(6) | 20.0(6) | 1.9(5) | 7.1(5) | -1.6(5) |
| C20 | 31.4(7) | 20.5(6) | 36.6(8) | 6.1(5) | 7.1(6) | 2.9(5) |

**Table 46** Bond Lengths for **119**.

| Atom | Atom | Length/Å | Atom | Atom | Length/Å |
|---|---|---|---|---|---|
| N | C2 | 1.2737(15) | C13 | C12 | 1.3878(17) |

| | | | | | |
|---|---|---|---|---|---|
| N | C1 | 1.4757(15) | C21 | C22 | 1.3847(18) |
| C11 | C1 | 1.5200(16) | C21 | C20 | 1.3866(19) |
| C11 | C16 | 1.3882(17) | C14 | C15 | 1.3838(19) |
| C11 | C12 | 1.3932(17) | C17 | C22 | 1.3936(17) |
| C4 | C5 | 1.4684(17) | C17 | C18 | 1.3911(17) |
| C4 | C3 | 1.3343(17) | C6 | C7 | 1.3803(18) |
| C2 | C3 | 1.4538(16) | C7 | C8 | 1.3893(19) |
| C5 | C6 | 1.3969(18) | C19 | C18 | 1.3861(19) |
| C5 | C10 | 1.3981(17) | C19 | C20 | 1.3856(19) |
| C1 | C17 | 1.5231(17) | C9 | C10 | 1.3851(18) |
| C16 | C15 | 1.3912(17) | C9 | C8 | 1.379(2) |
| C13 | C14 | 1.3867(19) | | | |

**Table 47** Bond Angles for **119**.

| Atom | Atom | Atom | Angle/° | Atom | Atom | Atom | Angle/° |
|---|---|---|---|---|---|---|---|
| C2 | N | C1 | 115.86(10) | C15 | C14 | C13 | 119.90(12) |
| C16 | C11 | C1 | 120.23(11) | C13 | C12 | C11 | 120.57(12) |
| C16 | C11 | C12 | 118.80(11) | C22 | C17 | C1 | 120.51(11) |
| C12 | C11 | C1 | 120.91(11) | C18 | C17 | C1 | 121.31(11) |
| C3 | C4 | C5 | 127.19(12) | C18 | C17 | C22 | 118.10(12) |
| N | C2 | C3 | 122.92(11) | C7 | C6 | C5 | 120.86(12) |
| C6 | C5 | C4 | 122.68(11) | C6 | C7 | C8 | 120.34(13) |
| C6 | C5 | C10 | 118.10(11) | C20 | C19 | C18 | 120.38(12) |
| C10 | C5 | C4 | 119.20(11) | C8 | C9 | C10 | 120.38(12) |
| C4 | C3 | C2 | 121.35(12) | C9 | C10 | C5 | 120.81(12) |
| N | C1 | C11 | 107.49(9) | C9 | C8 | C7 | 119.50(12) |
| N | C1 | C17 | 110.87(9) | C21 | C22 | C17 | 121.13(12) |
| C11 | C1 | C17 | 113.67(9) | C14 | C15 | C16 | 119.87(12) |
| C11 | C16 | C15 | 120.79(12) | C19 | C18 | C17 | 120.93(12) |
| C14 | C13 | C12 | 120.06(12) | C19 | C20 | C21 | 119.29(12) |
| C22 | C21 | C20 | 120.17(12) | | | | |

**Table 48** Torsion Angles for **119**.

| A | B | C | D | Angle/° | A | B | C | D | Angle/° |
|---|---|---|---|---|---|---|---|---|---|
| N | C2 | C3 | C4 | 175.25(12) | C16 | C11 | C1 | C17 | -118.56(12) |
| N | C1 | C17 | C22 | 156.10(11) | C16 | C11 | C12 | C13 | -0.48(18) |
| N | C1 | C17 | C18 | -27.26(15) | C13 | C14 | C15 | C16 | -0.44(19) |
| C11 | C1 | C17 | C22 | 34.87(15) | C14 | C13 | C12 | C11 | 0.33(18) |
| C11 | C1 | C17 | C18 | -148.48(11) | C12 | C11 | C1 | N | -58.94(14) |
| C11 | C16 | C15 | C14 | 0.29(19) | C12 | C11 | C1 | C17 | 64.15(14) |
| C4 | C5 | C6 | C7 | -178.85(12) | C12 | C11 | C16 | C15 | 0.17(18) |
| C4 | C5 | C10 | C9 | 178.67(11) | C12 | C13 | C14 | C15 | 0.14(19) |
| C2 | N | C1 | C11 | -106.54(12) | C6 | C5 | C10 | C9 | -0.03(18) |

| | | | | | | | | | |
|---|---|---|---|---|---|---|---|---|---|
| C2 | N | C1 | C17 | 128.66(11) | C6 | C7 | C8 | C9 | -0.6(2) |
| C5 | C4 | C3 | C2 | 178.55(11) | C10 | C5 | C6 | C7 | -0.20(18) |
| C5 | C6 | C7 | C8 | 0.5(2) | C10 | C9 | C8 | C7 | 0.4(2) |
| C3 | C4 | C5 | C6 | -17.1(2) | C8 | C9 | C10 | C5 | -0.1(2) |
| C3 | C4 | C5 | C10 | 164.24(12) | C22 | C21 | C20 | C19 | -0.5(2) |
| C1 | N | C2 | C3 | 175.88(10) | C22 | C17 | C18 | C19 | -0.73(18) |
| C1 | C11 | C16 | C15 | -177.18(11) | C18 | C17 | C22 | C21 | 0.37(18) |
| C1 | C11 | C12 | C13 | 176.85(11) | C18 | C19 | C20 | C21 | 0.1(2) |
| C1 | C17 | C22 | C21 | 177.12(11) | C20 | C21 | C22 | C17 | 0.23(19) |
| C1 | C17 | C18 | C19 | -177.45(11) | C20 | C19 | C18 | C17 | 0.5(2) |
| C16 | C11 | C1 | N | 118.35(12) | | | | | |

**Table 49** Hydrogen Atom Coordinates (Å×$10^4$) and Isotropic Displacement Parameters (Å$^2$×$10^3$) for **119**.

| Atom | *x* | *y* | *z* | U(eq) |
|---|---|---|---|---|
| H4 | 8016 | 3773 | 229 | 29 |
| H2 | 6109 | 4142 | 1613 | 26 |
| H3 | 3474 | 3313 | 248 | 27 |
| H1 | 4679 | 4559 | 2768 | 25 |
| H16 | 6750 | 4288 | 4509 | 29 |
| H13 | 436 | 3120 | 4908 | 31 |
| H21 | -1913 | 5580 | 3908 | 35 |
| H14 | 4034 | 3167 | 6264 | 33 |
| H12 | -9 | 3657 | 3357 | 28 |
| H6 | 4516 | 2596 | -743 | 31 |
| H7 | 5219 | 2028 | -2111 | 37 |
| H19 | -2959 | 5388 | 639 | 37 |
| H9 | 10567 | 3010 | -2702 | 35 |
| H10 | 9862 | 3585 | -1341 | 31 |
| H8 | 8276 | 2228 | -3087 | 36 |
| H22 | 1169 | 4935 | 4157 | 30 |
| H15 | 7181 | 3756 | 6070 | 33 |
| H18 | 153 | 4749 | 888 | 31 |
| H20 | -4018 | 5807 | 2146 | 35 |

**Crystal structure determination of 119**

**Crystal Data** for $C_{22}H_{19}N$ (*M* =297.38 g/mol): monoclinic, space group $P2_1/c$ (no. 14), *a* = 5.4941(2) Å, *b* = 24.8448(10) Å, *c* = 12.4135(5) Å, *β* = 102.044(4)°, *V* = 1657.15(12) Å$^3$, *Z* = 4, *T* = 120 K, μ(MoKα) = 0.069 mm$^{-1}$, *Dcalc* = 1.192 g/cm$^3$, 11019 reflections measured (3.734° ≤ 2Θ ≤ 55.728°), 3426 unique ($R_{int}$ = 0.0288, $R_{sigma}$ = 0.0269) which were used in all calculations. The final $R_1$ was 0.0397 (I > 2σ(I)) and $wR_2$ was 0.0961 (all data).

**Refinement model description**

Number of restraints - 0, number of constraints - unknown.
Details:
1. Fixed Uiso
At 1.2 times of:
All C(H) groups
2.a Ternary CH refined with riding coordinates:
C1(H1)
2.b Aromatic/amide H refined with riding coordinates:
C4(H4), C2(H2), C3(H3), C16(H16), C13(H13), C21(H21), C14(H14), C12(H12), C6(H6), C7(H7), C19(H19), C9(H9), C10(H10), C8(H8), C22(H22), C15(H15), C18(H18), C20(H20)

This report has been created with Olex2, compiled on 2014.09.19 svn.r3010 for OlexSys. Please let us know if there are any errors or if you would like to have additional features.

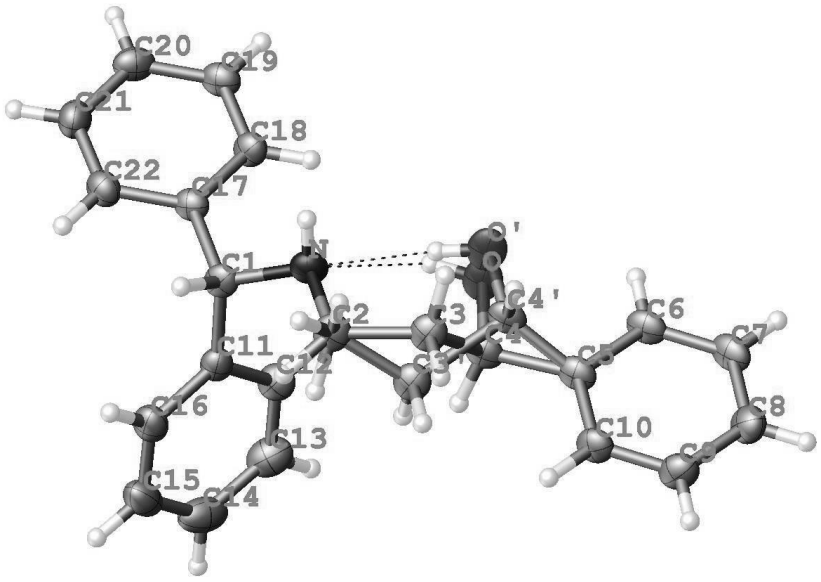


**Table 50** Crystal data and structure refinement for **128**.

| | |
|---|---|
| Identification code | **128** |
| Empirical formula | $C_{22}H_{23}NO$ |
| Formula weight | 317.41 |
| Temperature/K | 120.0 |
| Crystal system | monoclinic |
| Space group | $P2_1$ |
| a/Å | 10.1649(6) |
| b/Å | 5.9781(2) |
| c/Å | 14.3522(9) |
| α/° | 90 |
| β/° | 102.548(6) |
| γ/° | 90 |

| | |
|---|---|
| Volume/Å$^3$ | 851.31(9) |
| Z | 2 |
| $\rho_{calc}$g/cm$^3$ | 1.238 |
| $\mu$/mm$^{-1}$ | 0.075 |
| F(000) | 340.0 |
| Crystal size/mm$^3$ | 0.567 × 0.1335 × 0.0932 |
| Radiation | MoK$\alpha$ ($\lambda$ = 0.71073) |
| 2$\Theta$ range for data collection/° | 4.106 to 54.99 |
| Index ranges | $-13 \leq h \leq 13$, $-7 \leq k \leq 7$, $-18 \leq l \leq 18$ |
| Reflections collected | 13064 |
| Independent reflections | 3905 [$R_{int}$ = 0.0715, $R_{sigma}$ = 0.0688] |
| Data/restraints/parameters | 3905/3/234 |
| Goodness-of-fit on $F^2$ | 1.074 |
| Final R indexes [I>=2$\sigma$ (I)] | $R_1$ = 0.0631, $wR_2$ = 0.1483 |
| Final R indexes [all data] | $R_1$ = 0.0716, $wR_2$ = 0.1553 |
| Largest diff. peak/hole / e Å$^{-3}$ | 0.32/-0.26 |
| Flack parameter | 0.4(10) |

**Table 51** Fractional Atomic Coordinates (×10$^4$) and Equivalent Isotropic Displacement Parameters (Å$^2$×10$^3$) for **128**. $U_{eq}$ is defined as 1/3 of of the trace of the orthogonalised $U_{IJ}$ tensor.

| **Atom** | ***x*** | ***y*** | ***z*** | **U(eq)** |
|---|---|---|---|---|
| N | -126(3) | -4629(5) | -1561.0(19) | 30.0(6) |
| C1 | -742(3) | -5113(5) | -2564(2) | 26.9(6) |
| C2 | 883(3) | -6334(6) | -1144(2) | 32.2(7) |
| C5 | 3643(3) | -2966(5) | 582(2) | 29.6(7) |
| C6 | 3711(3) | -968(5) | 1095(2) | 30.9(7) |
| C7 | 4800(3) | -524(5) | 1838(2) | 34.6(7) |
| C8 | 5843(3) | -2029(6) | 2088(3) | 36.8(8) |
| C9 | 5784(3) | -4045(6) | 1579(2) | 36.8(8) |
| C10 | 4701(3) | -4493(6) | 844(2) | 31.4(7) |
| C11 | 285(3) | -4860(5) | -3187(2) | 27.9(6) |
| C12 | 1079(3) | -2935(6) | -3147(2) | 33.3(7) |
| C13 | 1975(4) | -2705(7) | -3737(3) | 42.7(9) |
| C14 | 2089(4) | -4380(8) | -4388(3) | 47.5(10) |
| C15 | 1307(4) | -6297(8) | -4436(2) | 43.5(9) |
| C16 | 421(3) | -6529(6) | -3832(2) | 35.7(8) |
| C17 | -1956(3) | -3622(5) | -2932(2) | 26.5(6) |
| C18 | -2097(3) | -1523(5) | -2528(2) | 29.4(7) |
| C19 | -3227(3) | -215(6) | -2875(2) | 32.2(7) |
| C20 | -4212(3) | -939(6) | -3624(2) | 34.5(7) |
| C21 | -4073(3) | -2993(7) | -4047(2) | 35.0(7) |
| C22 | -2956(3) | -4321(6) | -3698(2) | 32.1(7) |

| | | | | |
|---|---|---|---|---|
| O | 1631(3) | -1564(4) | -445(2) | 38.6(7) |
| C3 | 1757(3) | -5584(6) | -194(3) | 31.1(8) |
| C4 | 2538(4) | -3432(6) | -281(3) | 29.6(7) |
| O' | 1280(40) | -1940(60) | -100(30) | 38.6(7) |
| C3' | 2240(40) | -5430(70) | -730(30) | 31.1(8) |
| C4' | 2300(40) | -3400(40) | 190(30) | 29.6(7) |

**Table 52** Anisotropic Displacement Parameters ($Å^2×10^3$) for **128**. The Anisotropic displacement factor exponent takes the form: $-2\pi^2[h^2a^{*2}U_{11}+2hka^*b^*U_{12}+\ldots]$.

| Atom | $U_{11}$ | $U_{22}$ | $U_{33}$ | $U_{23}$ | $U_{13}$ | $U_{12}$ |
|---|---|---|---|---|---|---|
| N | 33.3(14) | 20.0(14) | 37.0(14) | 4.1(11) | 8.5(11) | 7.3(11) |
| C1 | 30.7(15) | 11.6(13) | 37.8(16) | 1.0(12) | 5.8(12) | 1.8(12) |
| C2 | 37.1(16) | 14.3(14) | 43.5(18) | 5.1(13) | 4.9(13) | 4.1(13) |
| C5 | 39.8(17) | 13.7(14) | 37.8(17) | 2.4(12) | 13.6(13) | 2.0(13) |
| C6 | 41.7(17) | 13.2(15) | 41.4(18) | 2.0(12) | 16.7(14) | 1.9(13) |
| C7 | 46.6(18) | 15.8(16) | 45.4(19) | -3.6(13) | 18.3(15) | -5.0(14) |
| C8 | 34.9(17) | 27.0(18) | 48(2) | -5.1(15) | 8.1(14) | -6.8(14) |
| C9 | 35.5(16) | 22.7(17) | 52(2) | 0.5(15) | 8.8(14) | 3.7(14) |
| C10 | 37.4(16) | 15.7(15) | 42.0(17) | -1.3(13) | 10.4(13) | 2.5(13) |
| C11 | 28.4(14) | 20.4(15) | 32.6(15) | 0.5(13) | 1.8(11) | 4.4(12) |
| C12 | 37.7(17) | 20.4(15) | 41.4(18) | 2.3(13) | 7.7(14) | 0.9(13) |
| C13 | 39.8(18) | 31(2) | 58(2) | 12.6(17) | 11.9(16) | 0.9(16) |
| C14 | 39.1(18) | 63(3) | 42.6(19) | 16(2) | 12.8(15) | 16(2) |
| C15 | 45.1(19) | 47(2) | 36.9(19) | -7.4(17) | 5.3(14) | 14.8(18) |
| C16 | 37.7(17) | 25.1(17) | 42.0(18) | -6.0(15) | 3.6(13) | 4.6(14) |
| C17 | 30.8(15) | 15.6(14) | 34.6(16) | 1.5(12) | 10.3(12) | -0.7(12) |
| C18 | 31.4(15) | 17.6(15) | 38.5(17) | -1.6(13) | 6.0(12) | -0.5(12) |
| C19 | 37.8(16) | 18.9(15) | 42.1(18) | 1.6(14) | 13.6(13) | 1.8(14) |
| C20 | 34.3(16) | 31.8(19) | 38.1(17) | 9.7(14) | 9.5(13) | 9.5(14) |
| C21 | 34.1(17) | 35.1(18) | 33.5(17) | -2.1(14) | 2.4(13) | -1.6(14) |
| C22 | 37.7(16) | 24.3(16) | 34.9(16) | -3.3(13) | 9.1(13) | -2.4(14) |
| O | 43.8(17) | 12.7(13) | 54(2) | 3.7(13) | -1.0(13) | 9.1(12) |
| C3 | 37.1(17) | 15.9(17) | 39(2) | 6.3(13) | 6.5(14) | 2.1(13) |
| C4 | 38.3(18) | 14.9(16) | 37(2) | 2.9(14) | 11.3(15) | 6.6(14) |
| O' | 43.8(17) | 12.7(13) | 54(2) | 3.7(13) | -1.0(13) | 9.1(12) |
| C3' | 37.1(17) | 15.9(17) | 39(2) | 6.3(13) | 6.5(14) | 2.1(13) |
| C4' | 38.3(18) | 14.9(16) | 37(2) | 2.9(14) | 11.3(15) | 6.6(14) |

**Table 53** Bond Lengths for **128**.

| Atom | Atom | Length/Å | Atom | Atom | Length/Å |
|---|---|---|---|---|---|
| N | C1 | 1.469(4) | C11 | C16 | 1.388(5) |
| N | C2 | 1.478(4) | C12 | C13 | 1.378(5) |

| | | | | | |
|---|---|---|---|---|---|
| C1 | C11 | 1.522(4) | C13 | C14 | 1.392(6) |
| C1 | C17 | 1.521(4) | C14 | C15 | 1.388(6) |
| C2 | C3 | 1.524(5) | C15 | C16 | 1.386(5) |
| C2 | C3' | 1.48(4) | C17 | C18 | 1.402(4) |
| C5 | C6 | 1.397(4) | C17 | C22 | 1.390(4) |
| C5 | C10 | 1.398(4) | C18 | C19 | 1.390(4) |
| C5 | C4 | 1.506(5) | C19 | C20 | 1.370(5) |
| C5 | C4' | 1.39(3) | C20 | C21 | 1.390(5) |
| C6 | C7 | 1.386(5) | C21 | C22 | 1.387(5) |
| C7 | C8 | 1.378(5) | O | C4 | 1.435(4) |
| C8 | C9 | 1.404(5) | C3 | C4 | 1.531(5) |
| C9 | C10 | 1.375(5) | O' | C4' | 1.34(4) |
| C11 | C12 | 1.400(5) | C3' | C4' | 1.78(5) |

**Table 54 Bond Angles for 128.**

| Atom | Atom | Atom | Angle/° | Atom | Atom | Atom | Angle/° |
|---|---|---|---|---|---|---|---|
| C1 | N | C2 | 111.8(2) | C12 | C13 | C14 | 120.2(4) |
| N | C1 | C11 | 110.8(2) | C15 | C14 | C13 | 119.8(3) |
| N | C1 | C17 | 111.4(2) | C16 | C15 | C14 | 119.7(4) |
| C17 | C1 | C11 | 110.2(2) | C15 | C16 | C11 | 121.2(4) |
| N | C2 | C3 | 112.2(3) | C18 | C17 | C1 | 122.0(3) |
| N | C2 | C3' | 114.5(15) | C22 | C17 | C1 | 119.8(3) |
| C6 | C5 | C10 | 118.0(3) | C22 | C17 | C18 | 118.2(3) |
| C6 | C5 | C4 | 122.3(3) | C19 | C18 | C17 | 120.4(3) |
| C10 | C5 | C4 | 119.5(3) | C20 | C19 | C18 | 120.6(3) |
| C4' | C5 | C6 | 107.8(14) | C19 | C20 | C21 | 119.7(3) |
| C4' | C5 | C10 | 128.4(10) | C22 | C21 | C20 | 120.1(3) |
| C7 | C6 | C5 | 120.6(3) | C21 | C22 | C17 | 120.9(3) |
| C8 | C7 | C6 | 121.1(3) | C2 | C3 | C4 | 112.7(3) |
| C7 | C8 | C9 | 118.8(3) | C5 | C4 | C3 | 113.3(3) |
| C10 | C9 | C8 | 120.2(3) | O | C4 | C5 | 109.2(3) |
| C9 | C10 | C5 | 121.3(3) | O | C4 | C3 | 110.0(3) |
| C12 | C11 | C1 | 121.4(3) | C2 | C3' | C4' | 115(3) |
| C16 | C11 | C1 | 120.0(3) | C5 | C4' | C3' | 107(3) |
| C16 | C11 | C12 | 118.6(3) | O' | C4' | C5 | 129(2) |
| C13 | C12 | C11 | 120.6(3) | O' | C4' | C3' | 109(3) |

**Table 55** Hydrogen Bonds for **128**.

| D | H | A | d(D-H)/Å | d(H-A)/Å | d(D-A)/Å | D-H-A/° |
|---|---|---|---|---|---|---|
| O | H0 | N | 0.86(4) | 2.12(5) | 2.805(4) | 136(4) |
| O' | H0' | N | 0.82 | 2.04 | 2.78(4) | 149.6 |

**Table 56** Hydrogen Atom Coordinates (Å×$10^4$) and Isotropic Displacement Parameters (Å$^2$×$10^3$) for **128**.

| **Atom** | ***x*** | ***y*** | ***z*** | **U(eq)** |
|---|---|---|---|---|
| H1N | -760(30) | -4790(70) | -1260(20) | 33(9) |
| H1 | -1058 | -6702 | -2607 | 32 |
| H2AA | 1467 | -6651 | -1597 | 39 |
| H2AB | 414 | -7738 | -1046 | 39 |
| H2BC | 962 | -7428 | -1647 | 39 |
| H2BD | 553 | -7149 | -639 | 39 |
| H6 | 3004 | 96 | 933 | 37 |
| H7 | 4827 | 841 | 2180 | 42 |
| H8 | 6589 | -1709 | 2596 | 44 |
| H9 | 6495 | -5103 | 1742 | 44 |
| H10 | 4671 | -5867 | 507 | 38 |
| H12 | 999 | -1776 | -2710 | 40 |
| H13 | 2516 | -1399 | -3699 | 51 |
| H14 | 2700 | -4211 | -4799 | 57 |
| H15 | 1378 | -7445 | -4880 | 52 |
| H16 | -103 | -7854 | -3860 | 43 |
| H18 | -1416 | -993 | -2014 | 35 |
| H19 | -3318 | 1196 | -2591 | 39 |
| H20 | -4986 | -43 | -3853 | 41 |
| H21 | -4743 | -3487 | -4575 | 42 |
| H22 | -2873 | -5729 | -3987 | 39 |
| H0 | 960(40) | -1790(90) | -920(30) | 44(12) |
| H3A | 2405 | -6789 | 59 | 37 |
| H3B | 1177 | -5342 | 268 | 37 |
| H4 | 2959 | -3585 | -846 | 35 |
| H0' | 847 | -2269 | -630 | 58 |
| H3'A | 2603 | -4748 | -1248 | 37 |
| H3'B | 2835 | -6688 | -465 | 37 |
| H4' | 1998 | -4262 | 700 | 35 |

**Table 57** Atomic Occupancy for **128**.

| **Atom** | ***Occupancy*** | **Atom** | ***Occupancy*** | **Atom** | ***Occupancy*** |
|---|---|---|---|---|---|
| H2AA | 0.93 | H2AB | 0.93 | H2BC | 0.07 |
| H2BD | 0.07 | O | 0.92 | H0 | 0.92 |
| C3 | 0.92 | H3A | 0.92 | H3B | 0.92 |
| C4 | 0.92 | H4 | 0.92 | O' | 0.08 |
| H0' | 0.08 | C3' | 0.08 | H3'A | 0.08 |
| H3'B | 0.08 | C4' | 0.08 | H4' | 0.08 |

Crystal structure determination of **128**.

**Crystal Data** for $C_{22}H_{23}NO$ ($M$ =317.41 g/mol): monoclinic, space group $P2_1$ (no. 4), $a$ = 10.1649(6) Å, $b$ = 5.9781(2) Å, $c$ = 14.3522(9) Å, $\beta$ = 102.548(6)°, $V$ = 851.31(9) Å$^3$, $Z$ = 2, $T$ = 120.0 K, μ(MoKα) = 0.075 mm$^{-1}$, *Dcalc* = 1.238 g/cm$^3$, 13064 reflections measured (4.106° ≤ 2Θ ≤ 54.99°), 3905 unique ($R_{int}$ = 0.0715, $R_{sigma}$ = 0.0688) which were used in all calculations. The final $R_1$ was 0.0631 (I > 2σ(I)) and $wR_2$ was 0.1553 (all data).

**Refinement model description**

Number of restraints - 3, number of constraints - unknown.
Details:
1. Others
Fixed Sof: H2AA(0.93) H2AB(0.93) H2BC(0.07) H2BD(0.07) O(0.92) H0(0.92) C3(0.92) H3A(0.92) H3B(0.92) C4(0.92) H4(0.92) O'(0.08) H0'(0.08) C3'(0.08) H3'A(0.08) H3'B(0.08) C4'(0.08) H4'(0.08)
Fixed Uiso: H1(0.032) H2AA(0.039) H2AB(0.039) H2BC(0.039) H2BD(0.039) H6(0.037) H7(0.042) H8(0.044) H9(0.044) H10(0.038) H12(0.04) H13(0.051) H14(0.057) H15(0.052) H16(0.043) H18(0.035) H19(0.039) H20(0.041) H21(0.042) H22(0.039) H3A(0.037) H3B(0.037) H4(0.035) H0'(0.058) H3'A(0.037) H3'B(0.037) H4'(0.035)Fixed X: H1(-0.1058) H2AA(0.1467) H2AB(0.0414) H2BC(0.0962) H2BD(0.0553) H6(0.3004) H7(0.4827) H8(0.6589) H9(0.6495) H10(0.4671) H12(0.0999)H13(0.2516) H14(0.27) H15(0.1378) H16(-0.0103) H18(-0.1416) H19(-0.3318) H20(- 0.4986) H21(-0.4743) H22(-0.2873) H3A(0.2405) H3B(0.1177) H4(0.2959) H0'(0.0847) H3'A(0.2603) H3'B(0.2835) H4'(0.1998)Fixed Y: H1(-0.6702) H2AA(-0.6651) H2AB(-0.7738) H2BC(-0.7428) H2BD(-0.7149) H6(0.0096) H7(0.0841) H8(-0.1709) H9(-0.5103) H10(-0.5867) H12(-0.1776) H13(-0.1399) H14(-0.4211) H15(-0.7445) H16(-0.7854) H18(-0.0993) H19(0.1196) H20(-0.0043) H21(-0.3487) H22(-0.5729) H3A(-0.6789) H3B(-0.5342) H4(-0.3585) H0'(-0.2269) H3'A(-0.4748) H3'B(-0.6688) H4'(-0.4262)
Fixed Z: H1(-0.2607) H2AA(-0.1597) H2AB(-0.1046) H2BC(-0.1647) H2BD(-0.0639) H6(0.0933) H7(0.218) H8(0.2596) H9(0.1742) H10(0.0507) H12(-0.271) H13(-0.3699) H14(-0.4799) H15(-0.488) H16(-0.386) H18(-0.2014) H19(-0.2591) H20(-0.3853) H21(-0.4575) H22(-0.3987) H3A(0.0059) H3B(0.0268) H4(-0.0846) H0'(-0.063) H3'A(-0.1248) H3'B(-0.0465) H4'(0.07)

This report has been created with Olex2, compiled on 2014.09.19 svn.r3010 for OlexSys. Please let us know if there are any errors or if you would like to have additional features.

## Appendix 3

**Table 58** Examining the potential oxidation of 2-phenylethanol using boric acid, hydrogen peroxide and copper chloride.

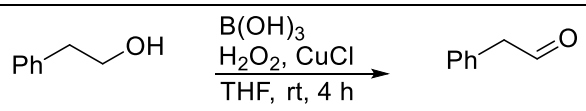


| Entry | $B(OH)_3$ (eq.) | $H_2O_2$ (eq.) | CuCl (%) | 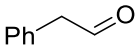 (%)[a] |
|---|---|---|---|---|
| 1 | 1 | 3 | 10 | 4 |
| 2 | 1 | 3 | - | <1 |
| 3 | 1 | - | 10 | 0 |
| 4 | - | 3 | 10 | 3 |
| 5 | - | 3 | - | 0 |
| 6 | 1 | - | - | 0 |
| 7 | - | - | 10 | 0 |

1 mmol scale, typical conditions: 2-Phenylethanol was added to a stirring solution of $B(OH)_3$ and CuCl in THF (2 mL). Hydrogen peroxide solution (35% w/v) was added, and the solution was allowed to stir for 4 h (open to air). [a] Conversion to phenylacetaldehyde was determined by removing the solvent *in vacuo* and running $^1$H NMR analysis on the crude sample.

**Table 59** Examining the potential oxidation of 2-phenylethanol using boric acid, hydrogen peroxide and copper chloride – addition of base.

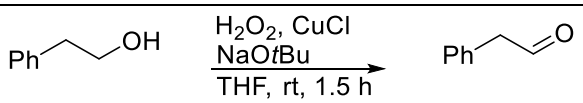


| Entry | NaO*t*Bu (eq.) | $H_2O_2$ (eq.) | CuCl (%) | 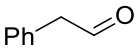 (%)[a] |
|---|---|---|---|---|
| 1 | 1 | 3 | 10 | <<1% |
| 2 | 1 | 3 | 100 | <<1% |
| 3[b] | 1 | 3 | 10 | <<1% |

1 mmol scale, typical conditions: 2-Phenylethanol was added to a stirring solution of NaO*t*Bu and CuCl in THF (2 mL). Hydrogen peroxide solution (35% w/v) was added, and the solution was allowed to stir for 1.5 h (open to air). [a]Conversion to phenylacetaldehyde was determined by removing the solvent *in vacuo* and running $^1$H NMR analysis on the crude sample. [b] Entry 3 was run under reflux in THF (6 mL).

## Appendix 4

*Durham lectures and seminars – attended.*

- 'Green Chemistry and biorefinery - from waste to wealth' - Prof James Clark, *The University of York* (19th October 2011).
- 'Getting a chemical handle on protein modification' Dr Ed Tate, *Imperial College London*, (26th October 2011).
- 'Hetero(arenes) as activating groups in asymmetric catalysis' - Dr Hon Wai Lam, *The University of Edinburgh* (8th November 2011).
- 'Developing tools for molecular imaging of copper in biology' - Dr Elizabeth New, *The University of Sydney* (22nd November 2011).
- 'New copper catalysed reactions' - Dr Matthew Gaunt, *University of Cambridge* (1st February 2012).
- 'Chemistry of biohydrogen' - Prof Fraser Armstrong, *University of Oxford* (8th February 2012).
- 'Chiral Metal compounds in catalysis and medicine' - Dr Peter Scott, *University of Warwick* (28th February 2012).
- 'Chemistry and business a rollercoaster' - Dr Tony Flinn, *Industry* (13th March 2012).
- 'Tech at Shasun; ABP an overview' - Dr Paul Quigley, *Industry* (13th March 2012).
- 'An odyssey in simple chemistry' - Prof Steve Davies, *University of Oxford* (25th of April 2012).
- 'Probe, excite, measure, redox' - Prof David Parker, *Durham University* (1st May 2012).
- 'Functionalising hydrocarbons using Fe Catalysts' - Dr Peter Rutledge, *The University of Sydney* (8th May 2012).
- 'Catalysts by Design. A Case Study of Arylamine Synthesis' - Prof John Hartwig, *University of California, Berkley* (14th May 2012).

- ‘Selective Functionalization of Aryl and Alkyl C-H Bonds’ - Prof John Hartwig, *University of California, Berkley* (15th May 2012).
- ‘Making Sense of Copper-Catalyzed Coupling Reactions’ - Prof John Hartwig, *University of California, Berkley* (16th May 2012).
- ‘Diamines are forever: Asymmetric synthesis of nitrogen heterocycles’ – Prof Peter O’Brien, *The University of York* (22nd May 2012).
- ‘Phosphate trimester hydrolysis’ – Prof Tony Kirby, *The University of Cambridge* (10th of September 2012.
- ‘Enzymatic dynamic kinetic resolution and directed evolution techniques for the synthesis of chiral intermediates’ – Prof Jan E. Bäckvall, *Stockholm University* (U.RiV-October 2012)
- ‘A stereochemical model for additions to aldehydes next to a quaternary centre, with applications in the total synthesis of (-)-Luminactin D’ – Prof Bruno Lindau, The *University of Southampton* (20th of February 2013).
- ‘Making peptides’ – Dr Rachael Slater, *Almac* (12th of march 2013)
- ‘Fluoropyridine as a building block in peptide chemistry’ Dr Chris Coxon, *Durham University* (12th of March 2013).
- ‘A trio of challenges in the reactivity, stereocontrol and regiocontrol in asymmetric catalysis’ – Dr Matt Clarke, *The University of St. Andrews* (25th of March 2013).
- ‘MS-from membrane protein complexes to drug discovery’ – Prof Carol Robinson, *The University of Oxford* (8th of May 2013).
- ‘Preventing and curing infectious disease: carbohydrates and continuous flow synthesis’ – Prof Peter M. Seeberger, *Max-Planck Institute* (14th of May 2013).
- ‘Automated oligosaccharide synthesis as a basis for chemical glycomics’ – Prof Peter M. Seeberger, *Max-Planck Institute* (15th of May 2013).
- ‘Carbohydrate-based nanotechnology’ – Prof Peter M. Seeberger, *Max-Planck Institute* (16th of May 2013).
- ‘Atom-efficient entry to complex chemical space’ – Prof Joe Sweeney, *The University of Huddersfield* (16th October 2013)
- ‘Trifluoroethanol, the magic solvent in the search for new cancer therapies’ – Prof Bernard T. Golding, *Newcastle* University (23th October 2013).

- ‘Borenium cations: versatile reagents for the borylation of π-nucleophiles’ – Dr Mike J. Inglenson, *The University of Manchester* (29th October 2013).
- ‘Cats and dogma’, Prof Guy. C. Lloyd-Jones, *The University of Edinburgh* (12th February 2014).
- ‘Photochemical synthesis, reactivity and kinetics of tricyclic azidines’, Dr Jonathan Knowles, *The University of Bristol* (11th March 2014).
- ‘Switchable solvents’, Prof P. G. Jessop, *Queen’s University* (12th March 2014).
- ‘Assembly line synthesis’, Prof Vrinda Aggarwal, *The University of Bristol* (7th May 2014).
- ‘Liquid crystals: nature’s delicate and prosperous state of matter’, Prof John W. Goodby, *The University of York* (14th May 2014).
- ‘Designing friendly catalysts for controlled radical polymerizations’, Dr P. M. Shaver, *The University of Edinburgh* (16th May 2014).
- ‘Glycopolymers and glyconanoparticles’, Prof Neil Cameron, *Durham University* (16th May 2014).
- ‘Controlled polymer synthesis with olefin metathesis reaction’, Prof Robert Grubbs (Nobel Prize 2005), *The California Institute of Technology* (16th May 2014).
- ‘Design and synthesis of smart polymer materials for applications in bionanotechnology and biomedicine’, Prof Brigitte Voit, *Leibniz Institute of Polymer Research Dresden, TU Dresden, Germany* (29th May 2014).
- ‘Organo-Lanthanide molecular nanomagnets’, Dr Richard A. Layfield, *The University of Manchester* (2nd of September 2014).
- ‘Medicinal Inorganic Chemistry of Biomedical Imaging Probes’, Prof Peter Caravan, *Harvard Medical School and Massachusetts General Hospital* (11th of September).
- ‘Boronate complexes: old dogs with new tricks’, Dr Amadeu Bonet, *The University of Bristol* (23rd of September 2014).

*Courses attended*

- GD188 - ‘Getting published in science’ (14th February 2012).

- GD229 - ‘Thesis writing in Science and English’ (9th March 2012).
- ‘Practical NMR spectroscopy’ AMK (Year 1).
- ‘Problems in organic synthesis’ EJG (Year 1).
- ‘Liquid crystals’ LOP (Year 1).
- ‘Problems in organic chemistry’ EJG (Year 2).
- ‘pKa and kinetics in organic chemistry - a practical guide’ AMOD (Year 2).
- Problems in organic chemistry’ EJG (Year 3).

*Conferences presentations*

- **Organic Division Poster Symposium 2014** The Royal Society of Chemistry, London, 12/14. Gave a poster presentation with the title *An asymmetric route to γ-amino alcohols, with application towards the synthesis of top-selling pharmaceuticals.*
- **Challenges in Catalysis Symposium** The Royal Society of Chemistry, London, 11/14. Gave a poster presentation with the title *In situ imine formation-borylation: a protocol for the synthesis of γ-amino alcohols.*
- **Northern Sustainable Chemistry Meeting (NORSC)** The University of Huddersfield, 10/14. Gave an oral presentation with the title *In situ imine formation-borylation and the catalytic asymmetric synthesis of γ-amino alcohols.*
- **Durham Gala Postgraduate Symposium** Durham University, 06/14. Gave an oral presentation with the title *Asymmetric borylation of α,β-unsaturated imines: a route to γ-amino alcohols*.
- **Northern Sustainable Chemistry Meeting (NORSC)** The University of Hull, 04/14. Gave a poster presentation with the title *An in situ imine formation/β-borylation approach to the synthesis of γ-amino alcohols.*
- **EuroBoron6** Poland, 09/13. Gave an oral presentation with the title *A One-Pot, Multistep, Borylation Protocol For the Synthesis of γ-amino alcohols*.
- **RSC Organic Section North East Regional Meeting** The University of Huddersfield, 03/13. Gave a poster presentation with the title *Novel transformation of α,β-unsaturated aldehydes and ketones into γ-amino alcohols or 1,3-oxazines via a four or five step, one-pot sequence*.

*Conferences attended (where I did not present)*

- NORSC Network Seminar Day (25th October 2011, York).
- Stereochemistry at Sheffield 'Modern Aspects of Stereochemistry' (10th January 2012, Sheffield).
- RSC Organic Section North East Regional Meeting (28th March 2012, York).
- NEPIC - NORSC (24th April 2012, Durham).
- NEPIC-NORSC Sustainable Chemistry for Industry Event Durham Postgraduate Symposium (24th April, 2012, Ramside Hall, Durham).
- Durham Postgraduate Symposium (13th June, 2012, Durham University).
- North West Organic Chemistry (3rd July, 2012, Liverpool).